Delivery of pDNA to human skin facilitated by microneedle arrays: potential for DNA vaccination

Marc Pearton BSc

A thesis submitted to Cardiff University in accordance with the requirements for the degree of

DOCTOR OF PHILOSOPHY

Drug Delivery Department

Welsh School of Pharmacy

August 2007

ProQuest LLC
789 East Eisenhower Parkway
P.O. Box 1346
Ann Arbor, MI 48106-1346

Declaration

This work has not previously been accepted in substance for any degree and is not concurrently submitted in candidature for any degree.

Signed..... (Candidate) Date.16/8/07.....

Statement 1

This thesis is being submitted in partial fulfilment of the requirements for the degree of PhD.

Signed..... (Candidate) Date.16/8/07.....

Statement 2

This thesis is the result of my own independent work/investigation, expect where otherwise stated. Other sources are acknowledged by explicit references.

Signed..... (Candidate) Date.16/8/07.....

Statement 3

I hereby give consent for my thesis, if accepted, to be available for photocopying and inter-library loan, and for the title and summary to be made available to outside organisations.

Signed..... (Candidate) Date.16/8/07.....

Acknowledgements

I would like to take this opportunity to thank my supervisors, Dr James Birchall, Dr Chris Allender and Dr Keith Brain first for the opportunity to undertake this PhD and for the direction and advice provided throughout.

I would also like to acknowledge our collaborators at the Tyndall National Institute (TNI), Dr Antony Morrisey and Nicole Wilke, who were responsible for supplying the microneedles.

I am also grateful Dr Antoine Hann for his help and advice during the electron microscopy studies.

I have also received help from people throughout the Welsh School of Pharmacy including Dr Mark Gumbleton and the rest of the PCB group, Dr Allan Cosslett, Dr Dirk Schmaljohann and all the technical staff. Also I would like to acknowledge Sion who I was fortunate enough to share the lab with for most of my PhD studies.

Additionally, I would like to thank Zoe Young for help in compiling my thesis.

I would also like to acknowledge the BBSRC for the studentship.

Finally, I would like to thank Vicky, Harry, Milly and my mum for their continued encouragement and support.

Abbreviations

A	Adenine
Ab	Antibody
ADA	adenosine deaminase
AAV	Adeno-associated virus
Ag	Antigen
APC	Antigen presenting cell
ATP	Adenosine triphosphate
BMZ	Basement membrane zone
BSA	Bovine serum albumin
C	Cytosine
cDNA	Complementry DNA
DC	Dendritic cell
DMSO	Dimethylsulfoxide
DNA	Deoxyribonucelic acid
DOTAP	1,2-dioleoyl-3-triammonium-tropane
ds	Double stranded
FBS	Foetal bovine serum
FDA	Food and drug administration
HSV	Herpes simplex virus
EB	Epidermolysis bullosa
EDTA	Ethylenediaminetetraacetic acid
EPU	Epidermal proliferation units
EMEA	European Medicines Agency
G	Guanine
GAGs	Glycosaminoglycans
GCV	Ganciclovir
GTAC	Gene Therapy Advisory Committee
GFP	Green fluorescent protein
H&E	Haematoxylin and eosin

HCl	Hydrochloric
hr	Hour
IDC	Interdigitating dendritic cell
KOH	Potassium hydroxide
LB	Lamellar bodies
LC	Langerhans cell
LPD	Lipid-polycation-pDNA
LVV	lentiviral vector
MHRA	Medicine & Healthcare Product Regulatory Agency
mRNA	Messenger RNA
MHC I	Major histocompatability type I complex
MHC II	Major histocompatability type II complex
min	Minute
MW	Molecular weight
N	Newtons
NLS	Nuclear localization signal
OTC	Ornithine transcarbamylase
OCT	Optimal cutting temperature
PBS	Phosphate buffered saline
PCS	Photon Correlation Spectroscopy
pDNA	Plasmid DNA
PEG	Polyethylene glycol
PLGA	Poly (lactic-co-glycolic acid)
RAC	Recombinant DNA Advisory Committee
RNA	Ribonucleic acid
RNAi	Ribonucleic acid interference
ROP	Ring opening polymerisation
SALT	Skin associated lymphoid tissue
SB	Stratum basale
SC	Stratum corneum
sd	Standard deviation

SDP	Size distribution processor
SEM	Scanning electron microscope
sec	Second
SG	Stratum granulsum
SL	Stratum lucidum
SS	Stratum spinosum
T	Thymine
TA	Transient amplifying cells
TBE	Tris-borate EDTA
TE	Tris-EDTA
TEM	Transmission electron microscope
TK	Thymidine Kinase
TNF	Tumor necrosis factor
TNI	Tyndall National Institute
UK	United Kingdom
USA	United States of America
UV	Ultra violet
X-gal	4-bromo-5-chloro-3-indoyl-β-D-galactopyrosanide
X-SCID	X-linked severe combined immunodeficiency

Summary

The skin presents an attractive target for the delivery and expression of plasmid DNA (pDNA). Potential therapeutic benefits from cutaneous gene therapy approaches include the correction or alleviation of inherited skin disorders (genodermatoses) and genetic vaccination. The skin is a particularly suitable portal for genetic vaccination due to its innate immunogenic capabilities. However, delivery of pDNA to the epidermis is severely constrained by the stratum corneum (SC), low transfection efficiency and rapid loss of pDNA associated with epidermal cells.

Microfabricated microneedles are employed as a means of penetrating the SC for macromolecular delivery. Solid silicon microneedles with different heights and tip morphologies were made by careful manipulation of the etching process, along with hollow silicon microneedles and solid polymer microneedles. To address the low transfection efficiency and rapid loss of pDNA in skin, hydrogels formed from "smart" polymers were investigated to provide sustained release "reservoirs" of pDNA.

Gene delivery studies were performed in freshly maintained *ex vivo* human skin; delivery formulations of reporter plasmid (pCMVβ and pEGFP-N1) and a therapeutic plasmid (pCMV.M) were applied to skin prior to microneedle application and maintenance in an optimized organ culture system. The results indicate that it is possible to deliver and express genes in the epidermis using microneedles. However, morphology of microneedles, their application protocol, and pDNA formulation all contribute to the efficiency of trans-gene expression.

Content

Content

CHAPTER 1: Introduction

1.1 A brief history of therapeutic nucleic acid delivery

During 1953 Watson and Crick elucidated the structure of Deoxyribonucleic acid (DNA), the molecule of life (Watson and Crick 1953). One of the consequences that stemmed directly from this discovery was the realization that the "language" of life, the genetic code, is digital in nature. The information stored within DNA is encrypted in the sequence of nitrogenous bases, adenine (A), thymine (T), cytosine (C) and guanine (G), which form the iconic double helix structure. Because of the digital nature of the code and its universal occurrence, it is possible to "cut and splice" genes within and between species. This phenomena lead to the idea of genetic cures for certain diseases. A patient suffering a condition, caused by a defective gene, could have the faulty gene removed or "masked" and a correctly functioning copy inserted to compensate.

The first people to envisage the potential of this technology were Edward Tatum and Joshua Lederberg in the 1960's. Lederberg, in 1966, queried:

For the sake of argument, suppose we could mimic with human cells what we know in bacteria, the useful transfer of DNA extracted from one cell line to the chromosomes of another cell. Suppose we could even go one step further and sprinkle some specified changes of genotype over that DNA. What use could we make of this technology in the production as opposed to the experimental phase?

Repair genetic-metabolic disease?

(Lederberg 1966)

It was inevitable that such novel approaches would provoke concerns regarding ethical implications and how society could be affected (Nirenberg 1967). Nevertheless, in the 1970's human genetic engineering or gene therapy, as it became known, came of age. In 1970 the first experiments involving human patients were conducted by Stanfield Rogers

(Terheggen 1975). The experiment involved three girls afflicted with argininemia, an autosomal recessive condition that which resulted in severe and progressive neurological syndrome (Freidmann 2001). Two were administered the Shope papilloma virus, which previously had been shown to reduce blood levels of arginine because it carried a gene encoding the enzyme argininase (Rogers 1966). The results of this study did not improve the health of the two girls and the experiment was criticised and deemed premature (Terheggen 1975; Freidmann 2001). It was believed by some that the "tools" required to perform gene therapy properly were not and probably never would be available. Yet, as these views were being voiced sequence specific restriction endonucleases were being described for the first time (Danna and Nathans 1971; Nathans and Smith 1975), Beckwith and Shapiro successfully isolated a gene for the first time (Shapiro *et al* 1969) and Paul Berg successfully spliced exogenous genes into the SV40 viral genome (Jackson *et al* 1972). In 1976 the first guidelines were devised by the Recombinant DNA Advisory Committee (RAC) and subsequently published. The tools, knowledge and framework were beginning to emerge. Nevertheless, ethical concerns were still prevalent, Erwin Chargaff stated in 1976:

Have we the right to counteract, irreversibly, the evolutionary wisdom of millions of years?...I am one of the few people old enough to remember that extermination camps in Nazi Germany began as an experiment in genetics

(Chargaff 1976)

During the early 1980's both *Drosophila melanogaster* and the mouse were the subject of attempted "genetic cures" by gene therapy. A mutant strain of *Drosophila*, which displayed a white-eyed phenotype, was the recipient of a copy of the normal gene. The result was a reversion back to the wild type, red eye phenotype. This was achieved by

splicing the gene into a transposon called the P factor (Spradling and Rubin 1982). The study conducted in the mouse was not considered as successful, mainly because expression of the delivered gene was not controlled properly. The study involved the delivery of a rat growth hormone gene to a strain of mouse that had a defect resulting in reduced levels of their own growth hormone, the consequence was a dwarf phenotype called *little*. Upon introduction of the rat growth hormone gene the mice grew rapidly, however, because the gene was expressed at high levels, the level of growth hormone was elevated above normal levels and the mice took on a "gigantic" phenotype (Hammer *et al* 1984). Nevertheless, the potential was clearly and dramatically apparent. Such studies added weight to the argument that gene therapy could be employed to cure genetic diseases in man.

As researchers began to consider treatment in humans it was proposed that the bone marrow would be a suitable target tissue because at that time it was the only tissue that could be removed from a patient, cultured *in vitro*, before transfer back into the patient. Disorders of the blood, as a result, were seen as attractive gene therapy targets, with β-thalassemia ranked as a primary candidate. It was anticipated that when the bone marrow was being cultured, a retroviral vector engineered to contain a correct copy of a defective gene, could be introduced and used to transfect the bone marrow cells.

The very first clinical trial on a human patient took place in 1989, though in this case no attempt to alleviate an illness was made, the delivered gene was a reporter, which just confirmed the presence and location of expression. Also in this year Rosenberg *et al*

used a retroviral vector to deliver a neomycin resistance gene to tumor-infiltrating lymphocytes of patients with advanced melanoma followed by infusion back into the patients (Kasid *et al* 1990). Less than a year later an attempt to treat an actual inherited disease, adenosine deaminase (ADA) deficient severe combined immunodeficiency (SCID), was undertaken. The clinical trial began in 1990 with the patient a 4 year old girl receiving an infusion of her own T-lymphocytes that had been treated with a retroviral vector containing a correct copy of the ADA gene (Blaese *et al* 1995). Then during 1991 another ADA patient, a 9 year old girl, received the similar treatment. Both patients showed improvements, though the technique was not completely satisfactory. Nevertheless, more clinical trial applications were being submitted and the range of targets intended for treatment increased. During 1992, Jim Wilson undertook the first trial where an internal organ, the liver, was the target for gene therapy. The condition was Familial Hypercholesterolemia, and the therapy involved isolating liver cells, transfection was performed with a retroviral vector containing the complementary DNA (cDNA) for the LDLr gene, while in culture, followed by infusion back into the patient (Wilson *et al* 1995). Another important development occurred in this year, with the first clinical trial of a non-viral based gene delivery vector. The study was conducted by Gary Nabel, who injected a DNA/liposome complex (the DNA encoding the HLA-B7 gene) directly into the tumours of cancer patients (Nabel *et al* 1992). The first total cure of a human disease in a mammalian model was demonstrated in 1993. The study involved the delivery of the human β-glucuronidase gene, spliced into a retroviral vector, delivered into bone marrow cells extracted from and subsequently returned to a MPS VII mouse (Marechal *et al* 1993). The remaining years of the 1990's saw many more clinical trails,

with the spectrum of possible vectors and disease targets increasing. However, there was still much criticism concerning ethics, and the lack of therapeutic progress. Nonetheless, therapies were becoming more adventurous, the close of the decade saw the first phase III clinical trial, involving retroviral vectors encoding the thymidine kinase gene (from Herpes simplex virus) attempting to treat brain tumours (Rainov 2000).

In 1999 one particular incident had a momentous impact on the field of gene therapy. Jesse Gelsinger a patient suffering ornithine transcarbamylase deficiency (OTC) had been involved in a clinical trail at the University of Pennsylvania; he was receiving an intrahepatic infusion of an adenoviral vector when he suddenly died of multiple organ failure. The death was attributed directly to the gene therapy trial (Editorial 2000). This forced the U.S. Food and Drug Administration (FDA) to suspend all gene therapy clinical trials. The death was due to an immune response, by the patient, to the adenoviral vector. This led to calls for changes and an increase in safety when adenoviral vectors were used. In 2002 another setback occurred during a French clinical trial. In this instance children suffering from X-linked severe combined immunodeficiency (X-SCID) were involved in a gene therapy trail at the Necker hospital, Paris. The therapy involved delivery of a retroviral vector containing the gene γc (gamma-c), in X-SCID this gene is mutated but in normal cells it encodes a subunit of a receptor which binds several interleukins, including interleukin-7 (IL-7). Interleukin is required to convert blood stem cells into precursors of T-cells (Kaiser 2003). As a result those unfortunate enough to suffer the condition cannot generate a cell mediated immune response and also lack T-helper cells, which are essential for generating an antibody-mediated immune response. Consequently, the

patients have no defence against infection; their non-existent immune system forces them to spend their lives enclosed in a sterile bubble, the reason why the condition has been called "bubble boy syndrome". Initially progress in the trials was promising; all patients responded and with the news that a teams in the UK, USA and Italy had recently succeeded in treating X-SCID patients, resulting in them developing fully functional immune systems (Wilkinson 2003) hopes were high that the trial would be a complete success. However, as the trial progressed it became apparent that one of the patients began to develop leukaemia-like symptoms. Not long after other patients began to display similar leukaemia-like symptoms (Wilkinson 2003; Selkirk 2004). A total of three patients developed the symptoms, with one unfortunately proving fatal. Nevertheless, 14 of the patients that received the gene therapy treatment responded and are now able to live outside of the bubbles, no longer requiring periodic immunoglobulin (IG) infusions, and have responded to normal childhood immunizations like tetanus and polio. The reason why some of the patients developed cancer is a result of the viral vector inserting itself randomly into the host genome of the patient, insertional mutagenesis, which can result in activation of oncogenes. In the case of the X-SCID patients it is believed that activation of the gene *lmo2* resulted in the oncogenic phenotype (Croft and Krimsky 2005). Insertional mutagenesis is a problem associated with the use of viral vectors, simply because over evolutionary time they have become extremely efficient at random insertion into host cell genomes. As will become apparent, it is because of the safety issues associated with viral vectors that recently there has been a growth of interest in non-viral gene delivery vectors.

1.2 Current status of therapeutic gene delivery

When assessing the current state of therapeutic gene therapy it is important to consider that many of the therapeutic practises that are performed today, including blood transfusions, surgery and tissue transplantation caused deaths when they were first introduced, however, each constitutes a vital weapon in the armoury of the clinician today (Nathwani *et al* 2004). As of June 2005 ninety six clinical trails have been approved in the UK. Of these the vast majority, 73%, are for cancer therapy, then single gene disorders with 13% and vascular disease receiving 7%. Clinical gene therapy proposals, in the UK, are assessed by the Gene Therapy Advisory Committee (GTAC) with; licenses to conduct trails are issued by the Medicines and Healthcare Products Regulatory Agency (MHRA). However, to date in the UK no gene therapy protocol has developed into a licensed treatment and would require marketing licences from the European Medicines Agency (EMEA) to do so.

Worldwide the number of clinical trails rose steadily throughout the nineties, reaching a peak of 116 in 1999; this was followed by a decline due to unexpected events described previously, to 7 in 2007 (Figure 1.1). The vast majority of clinical trails are still in early phases (Figure 1.2) with cytokine and antigen genes by far the most common strategies, both constituting 20% of current delivery protocols (Figure 1.3).

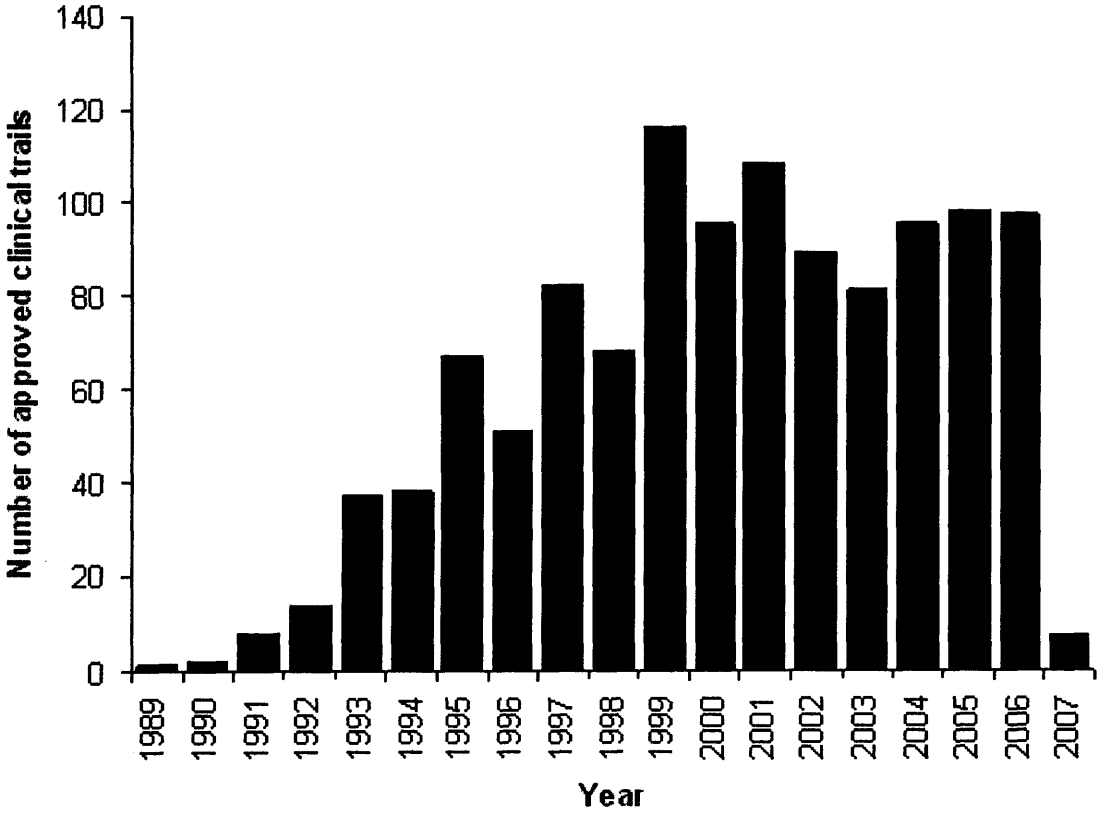

Figure 1.1 The number of yearly approved clinical trails from 1989 to 2007 (adapted from http://www.wiley.co.uk/genetherapy/clinical/).

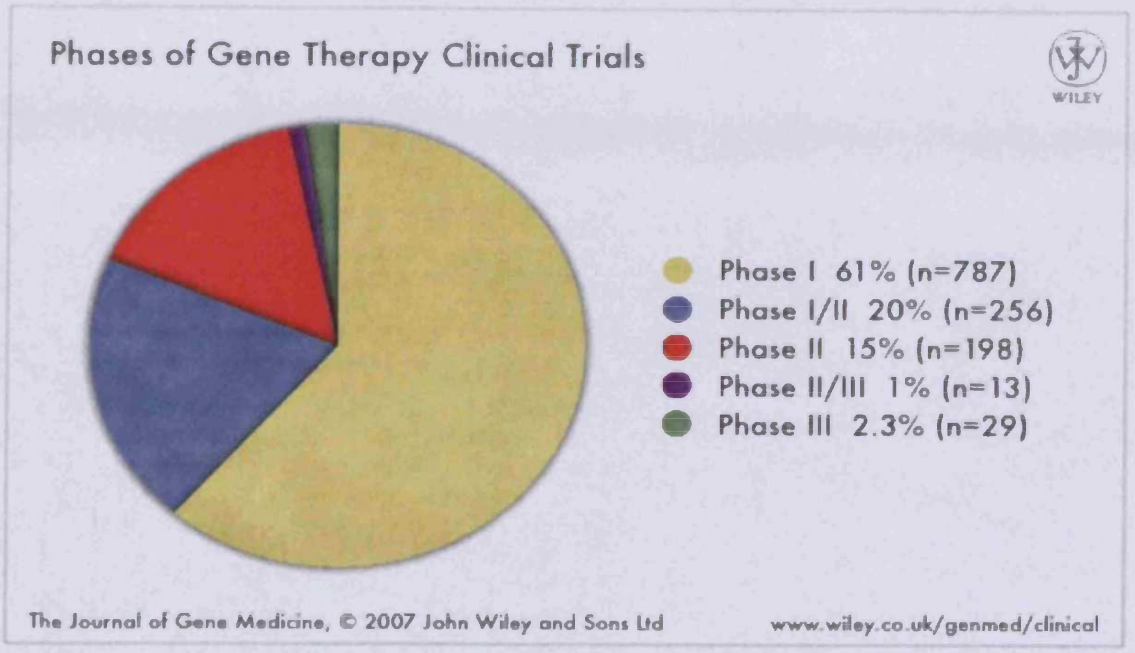

Figure 1.2 Phases of gene therapy protocols in current clinical trails (from http://www.wiley.co.uk/genetherapy/clinical/)

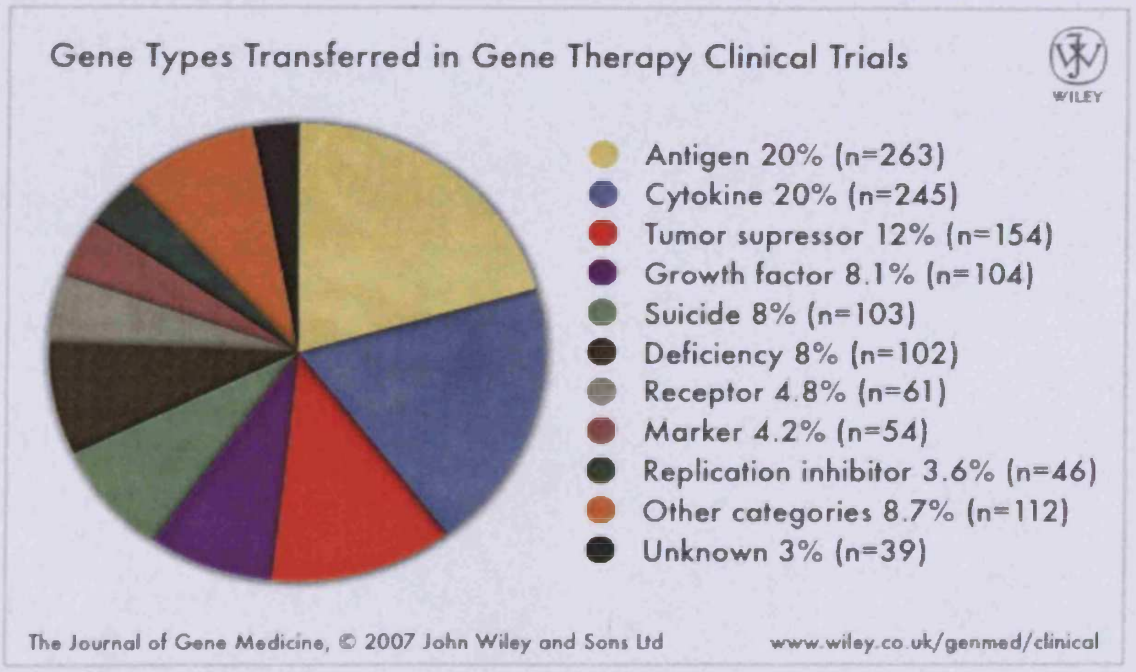

Figure 1.3 Current gene delivery strategies and targets (from http://www.wiley.co.uk/genetherapy/clinical/)

It is probably fair to say that early gene therapy trails were performed prematurely as a result some of the aforementioned setbacks could have been avoided. Nevertheless, the potential for this therapy still remains, more so than ever. In the not to distant future the therapeutic targets will further increase and the effectiveness of treatment will likewise, finally fulfilling the promises made all those decades ago.

1.3 Approaches to therapeutic gene delivery

Therapeutic genes are delivered by means of a vector. The vector contains components that ensure expression will occur once the transgene is inside the target cell. Current vectors fall into one of two categories, non-viral or viral. Viruses, by their very nature, are highly efficient at transferring genetic material into cells. However, in a therapeutic context the virus must first be modified so that virulence genes and genes that control replication are inactivated or removed. Many kinds of virus have been tailored for use as therapeutic vectors; some of the more common ones are listed in Table 1.1, along with some of the advantages and disadvantages.

Table 1.1 Advantages and disadvantages of common viral vectors currently utilized for delivery of therapeutic genes.

Viral vector	Advantages	Disadvantages
Retro viruses	Stable integration giving long term expression. Well characterised.	Random insertion into genomes. Limited insertion size. Can only infect dividing cells.
Lentivirus	Can infect non-dividing cells.	Difficulties in production.
Adenovirus	Infects both dividing and non-dividing cells. Does not integrate into genome. Transient expression.	Can result in severe immune responses. Limited insertion size. Transient expression limits therapeutic applications.
Adeno-associated virus (AAV)	Integrates into genome at specific location. Goes not initiate an immune response.	Limited production of viral stock.
Herpes simplex virus (HSV)	Large insertional size. Long term expression.	Viral toxicity issues.

Fears over viral vectors are not unwarranted; they have resulted in adverse effects, including a number of high profile instances. Because of the inherent safety issues associated with many viral vectors there has been a steady rise in interest in non-viral vectors. Non-viral vectors have an improved safety record over viral vectors; they elicit no immune response and do no integrate into the genome of the host. Additionally, non-viral vectors are easy to mass produce, store and manipulate, they can also deliver relatively large fragments of DNA. As no genomic integration occurs the delivered transgene is only transient expressed, which can be the desired goal for certain therapies, but for conditions where long term expression is required the lack of a hosts immune response ensures that the vector can be re-administered. However, the major draw back with non-viral vectors is low levels of expression. The reasons for this are still not fully understood and will no doubt turn out to be complex in nature. Consequently, there is much effort being made to try and improve the intra-cellular stability and longevity of non-viral vectors and also the means by which the vectors are delivered. Advantages and disadvantages of viral and non-viral vectors are summarised in Table 1.2.

Examples of non-viral vectors include plasmid DNA (pDNA), DNA complexed with cationic lipids (Raghavachari *et al* 2002; Tranchat *et al* 2004), anionic lipids (Lasch *et al* 2003), cationic peptides (Maruyama 2004), and polymers (Gary *et al* 2007). The rationale for complexing DNA is principally protection; as the human body can be extremely hostile to DNA (Azzoni *et al* 2007) but also in targeting the vector to certain cell types or locations within the body (Wen *et al* 2007).

Table 1.2 Notable advantages and disadvantages of viral and non-viral gene delivery vectors.

Viral gene delivery	**Non-Viral gene delivery**
Advantages	
High gene delivery rates	Large DNA fragments can be delivered
Potential for long term gene expression	Cheap to prepare
Viruses exist to transduce dividing cells and non-dividing cells	Easy to manipulate
	Low toxicity and immunogenicity
	Transient expression
Disadvantages	
Only small DNA fragments can be delivered	Low gene delivery rates
Potential oncogenes activation	Results not reproducible
Some can cause sever immune responses	

Expression from a plasmid delivered *in vivo* was first demonstrated by Wolff *et al* in 1990, where a mouse received an intramuscular injection of a solution of plasmid (Wolff *et al* 1990). Since then pDNA has become an accepted method of delivering genes. Currently, viral vectors still predominate; adenovirus and retroviruses comprise 25 and 24% of the total respectively. However, pDNA is the third most common method current clinical trails, totaling around 17% (Figure 1.4). Many tissues have since been shown capable of uptake and expression pDNA, for example, the skin (Meykadeh *et al* 2005), the thyroid (Sikes *et al* 1994), synovial cells (Yovandich *et al* 1995), and the stomach (Takehara *et al* 1996).

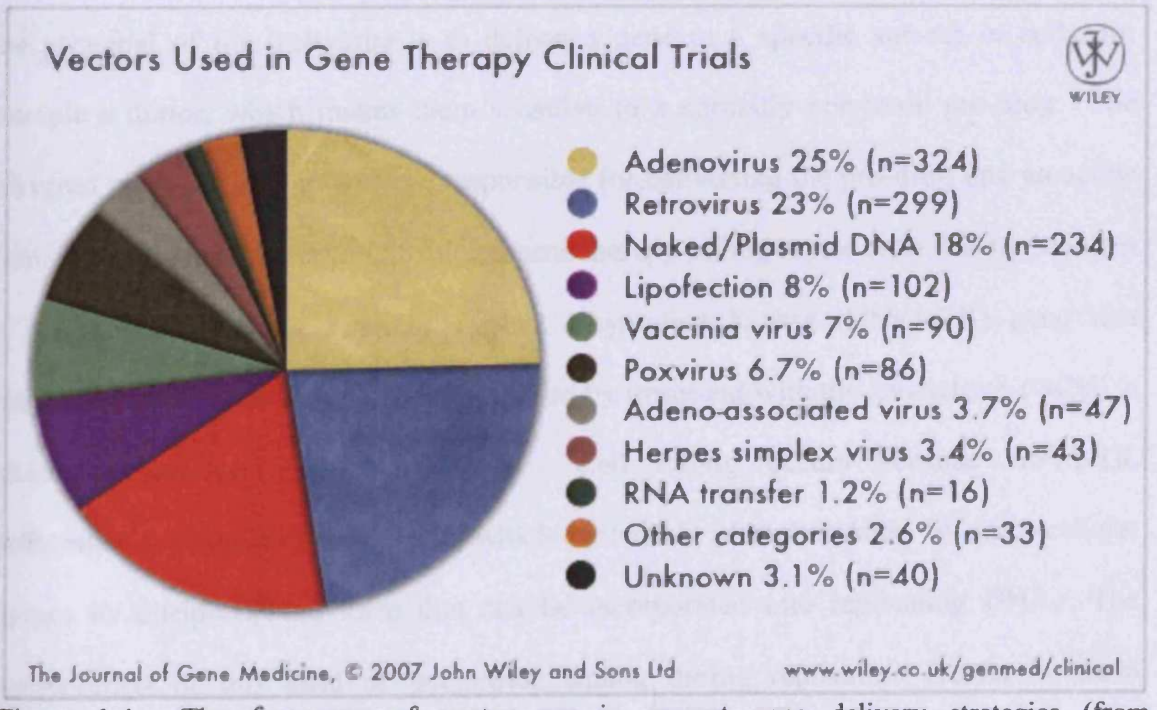

Figure 1.4 The frequency of vector use in current gene delivery strategies (from http://www.wiley.co.uk/genetherapy/clinical/)

1.4 Strategies for therapeutic nucleic acid delivery

The types of therapeutic applications that gene delivery strategies could potentially benefit are diverse. Some of the more common applications are briefly discussed below.

1.4.1 Single gene disorders

Certain disease states are a consequence of mutations in single genes, for example cystic fibrosis, where the symptoms result from a single mutation in the CFTR gene. It is proposed that delivering a correct copy of the gene to an afflicted individual will eliminate or reduce the symptoms of the disease.

1.4.2 Suicide gene therapy

The principal of the technique is to deliver a gene to a specific sub-set of cells, for example a tumor, which makes them sensitive to a normally non-toxic pro-drug. The delivered gene encodes an enzyme responsible for converting the pro-drug into an active form. The first demonstration of suicide gene therapy killing tumor cells was by Moolten in 1986, where Herpes Simplex Type 1 Thymidine Kinase (HSV1-TK) gene was transduced into mouse sarcoma cells followed by treatment with the ganciclovir (GCV), a nucleoside analogue (Moolten 1986). Cell killing occurs because HSV1-TK preferentially phosphorylates GCV, which in turn is phosphorylated by intra-cellular kinases to a triphosphate form that can be incorporated into replicating DNA. The incorporation of this kind of nucleoside analog during replication results in chain termination and single strand breaks and ultimately cell death. As mammalian thymidine kinase does not phosphorylate GCV there is no disruption to DNA replication in the

absence of HSV-TK and therefore non-targeted cells survive. Interestingly, it is possible to kill the an entire tumor using this method when only 10-70% of the tumor cell population receives the suicide gene, the phenomena is called the "bystander effect" though precise mechanisms of why this occurs are not fully elucidated (Freeman *et al* 1993; Pope *et al* 1997).

1.4.3 Tissue repair/regeneration

The ability to manipulate the innate biological repair mechanisms is of considerable therapeutic benefit in a number of different contexts. For example, the ability to increase the speed of wound healing would benefit patients following invasive surgery, those with extensive wound, e.g. burns victims and also those with impaired wound healing e.g. the elderly. Initial work conducted in animal models has suggested that there is potential for this technology to be successful (Cutroneo 2002).

1.4.4 Vaccination and immunomodulatory

Conventional vaccination involves the delivery of antigens in the form of live viruses or microbes, attenuated viruses or microbes, sub-unit and toxoid vaccines. Some of the disadvantages of the conventional methods include their time consuming and expensive production methods, risk of reversion back to an infective form and controlled storage. In contrast genetic or DNA vaccination requires the DNA sequence that encodes the antigen be delivered. Upon expression the antigen will be recognized by the immune system subsequently causing an immune response. DNA vaccination offers a number of distinct advantages over the conventional methods including no risk of adverse infection, poly-immunisation through multiple antigens encoded in a single vector, generation of

both humoral and cell mediated immune responses, cost effective and large scale production and improved stability. Another approach, principally proposed for cancer therapy, is the delivery of genes that encode genes that modulate the immune system in some way, for example tumor necrosis factor (TNF) or interleukin 1 (IL-1) both of which have been shown to have a role in anti-tumor immunity (Lei *et al* 2000).

1.4.5 Cell cycle regulation and apoptosis

The molecular mechanisms that underpin the mammalian cell cycle are well characterized. It is well established that cell cycle progression and apoptosis are intimately linked. Consequently, cancer typically arises when there are problems with the cell cycle or apoptotic "machinery", for example the tumor suppressor gene p53. p53 is expressed in response to DNA damage and upregulates cell cycle arrest and DNA repair genes but can also force apoptosis if damage is extensive. Because of the central role p53 plays it has been given the name "guardian of the cell cycle". It has been shown that p53 is mutated in nearly 50% of cancers (Bowen and Farhana 2000). Consequently, p53 could be a potential candidate for gene delivery strategies for certain cancers, both forcing cell cycle arrest and therefore limiting cancer progression or to force apoptosis within tumors directly.

1.4.6 Antisense

Following expression a gene is transcribed into messenger RNA (mRNA), however transcription utilizes only one of the two strands of complementary DNA, the "sense" strand. If fragments or complete copies of the un-transcribed strand, the "antisense" strand, are delivered to cells expressing the gene, the antisense strand can bind to the

complementary mRNA transcript preventing translation. Therefore, if there is a disease which has a strong genetic component then antisense technology can be employed to reduce expression of the target gene and potentially elevate the symptoms.

1.4.7 RNA interference (RNAi)

The phenomenon of RNAi was first described by Andrew Fire *et al.* in 1998 and has since been touted as a powerful therapeutic strategy (Fire *et al* 1998). RNAi prevents expression of specific genes, including genes associated with disease. The process requires the delivery of short double-stranded RNA (dsRNA) molecules with matching sequence to the genomic gene that is to be silenced.

1.5 Selecting a suitable target for therapeutic gene delivery

In order for a therapeutic gene delivery strategy to be successful, careful consideration of the therapeutic goal and the target tissue must be made, for example:

- Does the condition result from mutation(s) in specific gene(s)?
    - This might not be applicable for all applications, e.g. DNA vaccination.
- What gene is to be delivered?
    - Typical gene therapy applications would require a correct copy of the mutated gene.
    - Applications like DNA vaccination require a sequence that can elicit an immune response upon expression
- The biology of the both the disorder and the effect of delivering exogenous nucleic acid.
- Will the addition of the gene have the desired consequences?
    - In certain situations it will not, e.g. if the disorder stems from a dominant negative mutation.
- Is it possible to produce a sufficient immune response to achieve vaccination using delivered nucleic acids?
- Is it possible to deliver the gene to the target tissue?
    - Certain tissues/organs are easily assessable, for example the skin, blood or the lungs.
    - Other tissue/organs are extremely difficult to target, e.g. the brain.

vaccination, mentioned in section 1.4.4, technically DNA vaccination should be easier to achieve than many other forms of gene delivery. For example, the population of cells that need to uptake and express the transgene would be considerably less than that required to alleviate an inherited single disorder, like cystic fibrosis. Additionally, the DNA sequence of any protein antigen is extremely easy to produce and manipulated to change its antigenic properties. Non-viral vectors are well suited for DNA vaccination, particularly those based on plasmids. pDNA has intrinsic immunostimulatory, CpG motifs (regions of a linear DNA molecule where a cytosine nucleotide occurs next to a guanine nucleotide separated by a phosphate group) that can enhance the immune response (Uwiera *et al* 2001). Other plasmids can be delivered in conjunction expressing co-stimulatory molecules like cytokines or the co-stimulatory molecules themselves that can modify the generated immune response (Cui *et al* 2005). There is a considerable reduction in the risk of random genomic integration. Also pDNA can be re-applied to boost immunization, in contrast to viral vectors. Furthermore, pDNA is easy to amplify, purify, manipulate and store, factors that are of concern particularly in third world countries and western countries immersed in a climate of bio-weapons and concerns of pandemic disease. Wolf *et al* have demonstrated that pDNA is expressed in muscle cells (Wolff *et al* 1990), however, due to low levels of immunogenic cells and co-stimulatory factors associated with muscles (Pasquini *et al* 1997), a far better target tissue would be the skin (Birchall *et al* 2005). In addition to this being the most accessible organ, permitting direct access and convenience in monitoring it also contains a powerful immune surveillance system.

1.6 Major features of the human Integument: gross morphology of the skin

Our bodies are virtually covered by our skin, thus making the skin the largest organ of the body, composing an estimated 10% of our body mass (Williams 2003). The architecture of the skin is complex but can be divide it into three broad layers, the epidermis, dermis and hypodermis (Figure 1.5). The outer most layer of the epidermis, the stratum corneum (SC) is in contact with the physical environment, it is formed by a tightly regulated pathway of differentiation which results in a tough, watertight barrier. This contrasts with the other extreme of the skin, the hypodermis which encounters a completely different environment as it is close proximity to our internal organs. This is the reason why the skin has such an important role is homeostasis and immune surveillance. It is important to also understand the dynamic nature of the skin. The skin is continually changing, the SC surface is constantly being lost but at the same time it is continuously being replenished from below, the result of a tightly regulated form of differentiation by keratinocytes. Immune cells are constantly moving into and out of the skin responding to and preparing for encounters with foreign antigens.

The hypodermis is the lowermost region of the skin, the composition of which includes, loose connective tissue, fat, blood and lymphatic vessels, the roots of hair follicles, nerves, and sheets of muscle (panniculus carnosus) (Williams 2003). The dermis is generally between 1 and 4 mm in depth composed of an amalgamation of cells, fibres and extracellular matrix (mucopolysaccharides), all of which are supported by a rich blood supply. Fibroblasts compose a large proportion of the dermis and are responsible for the synthesis and excretion of collagen and elastin, which provide mechanical strength,

support and elasticity to the skin. Additionally, other cell types found in the dermal region include histiocytes (immobile macrophage), lymphocytes (involved in immune responses), mast cells (produce heparin and histamine during inflammatory response) and dermal dendritic cells (Antigen presentation). Where the dermis and epidermis meet there typically exist numerous undulations ensuring that a high surface area of contact is maintained between the two layers, indicating a close functional relationship.

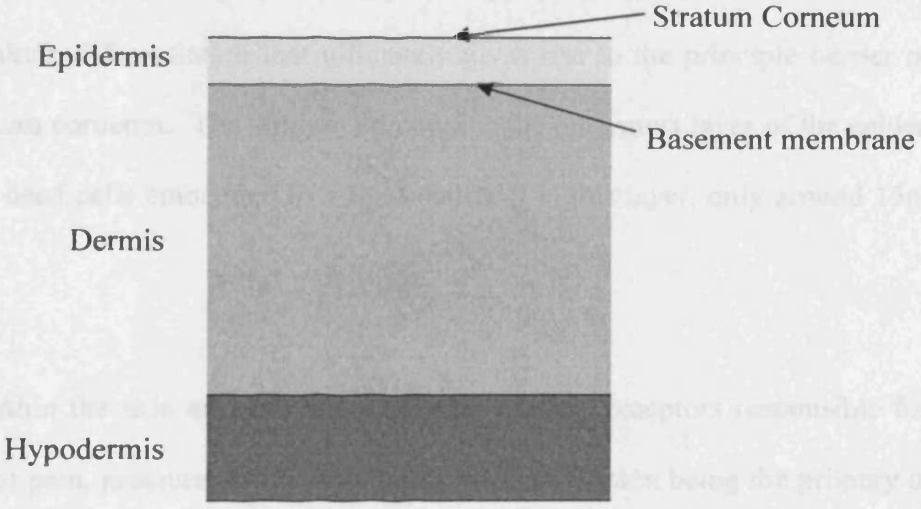

Figure 1.5 A schematic representation of the three distinct layers that constitute the human skin.

The epidermis, as already mentioned, has considerable self renewal capabilities because of the physical disruption that it is likely to encounter due to its proximity with the external environment. The mitotically active cells are located deepest in the epidermis, in a region called the basal layer; it is in this layer that the stem cells are located. As mitosis occurs, the daughter cells move away from the basal layer and undergo as series of tightly regulated cellular differentiations, ultimately ending in programmed cell death. However, it is this terminal differentiation that ultimately gives rise to the principle barrier of the skin, the stratum corneum. The stratum corneum is the outermost layer of the epidermis, composed of dead cells embedded in a lipid matrix it is this layer, only around 15nm in depth.

Embedded within the skin are also many somatic sensory receptors responsible for the discernment of pain, pressure, touch, and temperature. The skin being the primary organ involved in thermoregulatory homeostasis achieves this by vasoconstriction, to maintain body heat, or vasodilation and sweating to reduce body heat. Two type of sweat gland exist within the human skin, apocrine, associated with hair apparatus and eccrine, not associated with hair apparatus. A general characteristic of mammals is the possession of fur or hair, and humans are no exception. Each hair has associated with it an erector pili muscle, sebaceous glad, which produces sebum, together termed a pilosbaceous unit. One final major feature of our skin is the presence of nails that are located at the ends of our fingers and toes. These structures are principally composed of keratin and have a major role in protection. The complexity of the skin is shown in Figure 1.6.

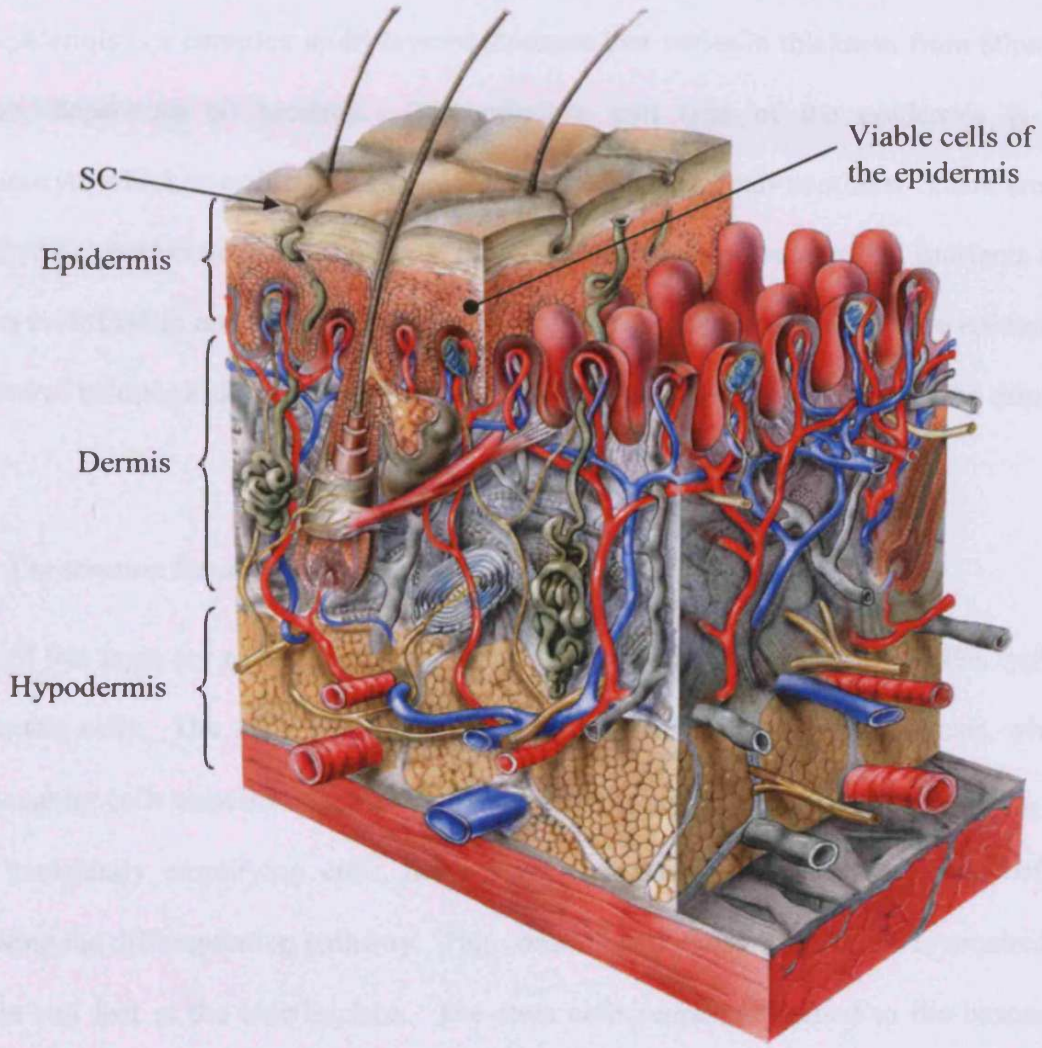

Figure 1.6 A schematic highlighting the complexity of the human skin (httpwww.scf-online.comenglish27_efrontpage27_e.htm)

This brief overview of the main features of the human skin and its components provide a flavor of the complexity involved in delivering therapeutic nucleic acids to skin. However, to appreciate completely the reason why this organ is suited to nucleic acid based therapies a more detailed examination is required.

1.7 A closer look at the epidermis

The epidermis is a complex multi-layered structure that varies in thickness from 60μm to 800μm, depending on location. The principle cell type of the epidermis is the keratinocyte which is estimated to comprise 95% of the total cell numbers. There are no blood vessel perforating the epidermis, therefore keratinocytes require O_2, nutrients and wastes to diffuse in and out of the underlying capillary beds respectively. The epidermis consists of histologically distinct layers; each will be considered starting with the deepest layer.

1.7.1 The stratum basale (basal layer; SB)

Cells of this layer are metabolically active and contain all sub-cellular organelles typical of somatic cells. The SB contain the only epidermal cells that undergo mitosis, where one daughter cells remains attached to the basement membrane, epidermal stem cells, the other transiently amplifying cells, move away and divide a number of times before following the differentiation pathway. This constant cell division in the SB is required to replace cell lost at the skin surface. The stem cells remains attached to the basement membrane by means of hemidesmosomes, and their pluripotent potential is maintained due to the microenvironment or niche that they resides (Díaz-Flores *et al* 2006), the niche concept is outlined in Figure 1.7. The location of stem cells was controversial, some groups claiming residence within rete ridges (Webb *et al* 2004), while other claim that they were found over the tips of dermal papilla (Ma *et al* 2004), others maintained that they were to be found in both locations (Ghazizadeh and Taichman 2005). Recently Ghazizadeh and Taichman have shown that epidermal stem cells are not associated with any distinct region in the basal layer. They used a lentiviral vector (LVV) to stability

transduce keratinocytes with Green fluorescent protein (GFP), only the stem cell are capable of maintaining the marker over an extended period of time. All transiently amplifying cells and differentiating cells will, with time, be lost, consequently so will the transduced gene. As well as showing the dispersed nature of the epidermal stem cells, it also showed that spatially distinct units consisting of a single stem cell and all its progeny forming a column, perpendicular to the skin surface, an epidermal proliferation unit (EPU) (Ghazizadeh and Taichman 2001). This phenomenon has also been observed in the mouse but was not confirmed in humans until this study (Ghazizadeh and Taichman 2005).

In addition to keratinocytes other cell types are found within the SB, these including melanocytes, which produce melanin giving skin it colour, Merkel cells, which are associated with sensory nerve ending (Shimohira-Yamasaki *et al* 2006) and Langerhans cells, the principle antigen presenting cells of the skin.

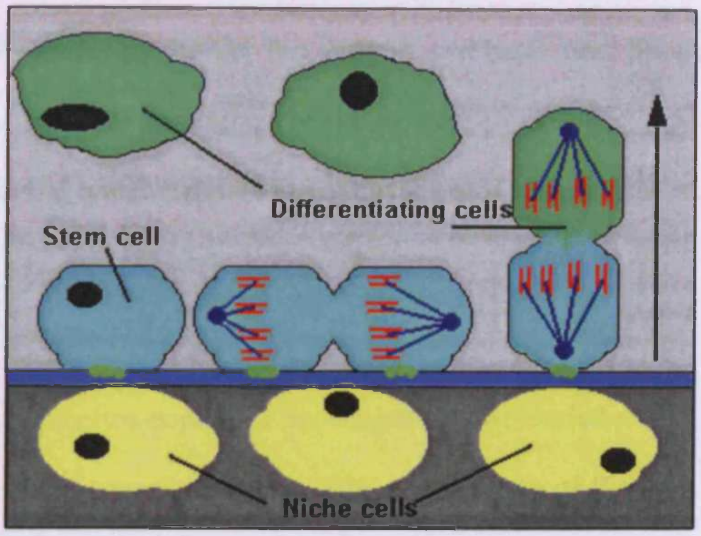

Figure 1.7 The niche concept and differentiation. Stem cells reside in close approximation to niche cells which continually stimulate and consequently cause the stem cell to remain in an undifferentiated state. During division of the stem cell the daughter cell can loose contact with the niche cell and no longer receives stimulation from it, this is the trigger for differentiation.

1.7.2 The stratum spinosum (spinous layer; SS)

This layer is immediately above the SB and together they are referred to as the Malpighian layer. Generally, this layer is composed of keratinocytes typically 2 to 6 cells deep that begin to change in morphology from columnar to polygonal. It is in the SS layer that specific lipid markers of keratinocyte differentiation begin to appear, the epidermal lamellar bodies (LB). Further differential keratin expression is also observed which aggregate to form tonofilaments that attach to desmosomes, the primary cause adhesion between these cells. It is because of the many desmosomes in this layer that give the layer its characteristic "spiny" appearance.

1.7.3 The stratum granulsum (granular layer; SG)

Typically 1 to 3 cells deep, with a flatter more compact morphology. Enzyme mediated degradation of the organelles begins but protein synthesis and lipogenesis continue. Additionally, many granular structures begin to appear in the cytoplasm, containing keratohyalin and eleidin, which become larger as they move toward the skin surface.

1.7.4 The stratum lucidum (SL)

Degradation of the organelles continues the nucleus is dismantled at this stage, however, protein synthesis and lipogenesis increase. The morphology of the cells become further flattened and compacted as differentiation proceeds.

1.7.5 The stratum corneum (horny layer; SC)

The SC represents the final stage of keratinocyte differentiation. The layer is typically 10μm thick and composed of 10 to 15 dead, terminally differentiated cells, sometimes called corneocytes. The cells are embedded in a lipid matrix, giving rise to the "brick and mortar" model of SC structure (Figure 1.8). Typically it takes approximately 14 days for a cell in the SB to enter the SC, where it is retained for a further 14 days before being shed (Williams 2003). The primary protein within the corneocytes is α-keratin, which constitutes around 70% followed by β-keratin, 10%, proteinaceous cell envelope, ~5%, with enzymes and other proteins ~15% (Steinert and Marekov 1995). The corneocytes are anchored in the lipid matrix by envelope protein through glutamate moieties. The lipid matrix is a composite and varies between individuals and body site. Lipids of the SC include, ceramides, cholesterol, fatty acids, cholesterol sulphate and sterol/wax esters,

with phospholipids virtually absent. Water is also a component of SC integrity, where it acts as a plasticizer preventing damage that could result from mechanical stress (Verdier-Sévrain and Bonté 2007).

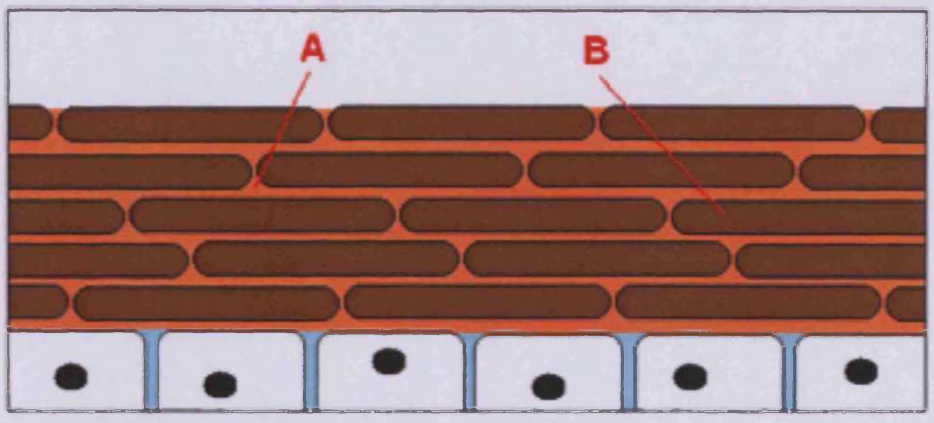

Figure 1.8 The "bricks and mortar" model for SC structure as proposed by Peter Elias (Elias 1981). Within the extracellular lipid matrix (A) are terminally differentiated cells called corneocytes (B).

1.8 The immune system in the skin

Because the skin is the barrier between our biological interior and the physical environment, it continuously comes into contact with a verity of foreign objects and antigens. Consequently, a powerful immune surveillance system has evolved the skin-associated lymphoid tissue (SALT). Keratinocytes are a component of the SALT because they can synthesis cytokines, which modulate immune responses (Soumelis *et al* 2002). The SALT also contains dendritic cells (DCs), professional antigen presenting cells (APCs) able to initiate T-cell immune responses. Located in both the dermis (dermal DCs) and epidermis (Langerhans cells), it has been estimated that DCs are able to intake and process 4 times their own volume of the surrounding extracellular liquid in 1 hour (Roitt 1988). There is estimated to be in human skin between 912-1806 (mean ± SD1394 ±321) immature Langerhans cells per mm^2 of epidermis and at a ratio of 1:53 to other epidermal cells, thus constituting 1.86% of the total epidermal cells (Bauer *et al* 2001), they are typically located at a depth of 15μm, approximately 3μm above the epidermal-dermal junction (Mulholland *et al* 2006) where it has been estimated that although the constitute on 2% of total epidermal cells they comprise around 20% of the total surface area because of there many cellular projections. LCs exists in close proximity to keratinocytes, principally in the SB region of the epidermis, by means of E-cadherin. Once an antigen is encountered it is taken up and processed, E-cadherin expression is reduced from the cell surface and the cell migrates out of the epidermis into the lymph where it travels as a veiled cell (McKeever et al 1992; Cyster 1999). Once it reaches a lymph node it fully matures and becomes an interdigitating dendritic cell (IDC) (McKeever et al 1992). IDCs present the processed antigen, with the necessary co-

stimulatory molecules to naïve T-cells, which recognize the antigen-MHC complex resulting in an immune response (Cyster 1999).

The accessibility of the skin and the presence of the SALT therefore make the skin an ideal target tissue for vaccination and DNA vaccination.

1.9 Barriers to delivering genes to the skin

While the skin is an attractive site for therapeutic gene delivery, in particular DNA vaccination, there are a number of obstacles that need to be overcome in order for expression to occur. Many of these barriers are common to non-viral gene delivery approaches in general and can be physical, chemical or biological in nature but all represent considerable limiting factors that must be faced and overcome in order for the technology to function correctly. It is probably a combination of these barriers that cause the much lower efficiency observed with of non-viral gene delivery compared to viral delivery. Viruses have had far longer, evolutionary, to "learn" to surmount these obstacles. Similarly, cells have evolved these barriers as ways of reducing viruses and other genetic sequences from getting into the sanctuary of the nucleus where they exploit the host cell's replication machinery. This evolutionary arms race has, on the one hand, produced an excellent delivery vehicle, the virus, but on the other made non-viral gene delivery that much more difficult.

The principle barriers that need to be overcome for the non-viral vector are shown schematically in Figure 1.9. Firstly, the vector (a non-viral gene delivery complex or naked DNA) must have the ability to defy interactions with components of the extra-

cellular matrix as well as have the ability to avoid degradation by extracellular nucleases. This barrier is critical as delivery formulations generally are deposited in the extracellular milieu; therefore, stability outside of cells but within the body is imperative. One component of extracellular matrix that can result in reduced cellular uptake of DNA cationic lipid complexes are a group called glycosaminoglycans (GAGs). GAGs can exist in the extra cellular matrix but can also be associated with the cell surface. One such GAG, heparin sulphate, has been shown to drastically reduce uptake of DNA cationic lipid complexes (Ruponen *et al* 2003; Ruponen *et al* 2001). The vector must then recognize and complex to the cell surface so that endocytosis can occur. It has been proposed that keratinocytes internalize pDNA by macropinocytosis with two DNA binding proteins, ezrin and moesin, involving in uptake and intracellular trafficking internalized DNA (Basner-Tschakarjan *et al* 2004). If the vector is taken up by endocytosis, it must remain stable within the endosome but ultimately escape into the cytoplasm before fusion with lysosomes. Also, gene delivery complexes like lipid:peptide:DNA (LPD) at some point, though precisely when is not clear, must dissociate to free the DNA component. Both naked DNA and DNA released from a complex must also remain stable within the cytoplasm and avoid degradation by intracellular nucleases. These enzymes appear to degrade cytoplasmic plasmid DNA relatively quickly, ensuring an apparent half-life of 50-90 minutes following micro-injection of pasmid DNA (Lechardeur *et al* 1999). The vector DNA must then move either passively or transported actively toward the nucleus where it must compromise the nuclear envelope. It is important to note that precisely how these events actually happen is not completely understood at present.

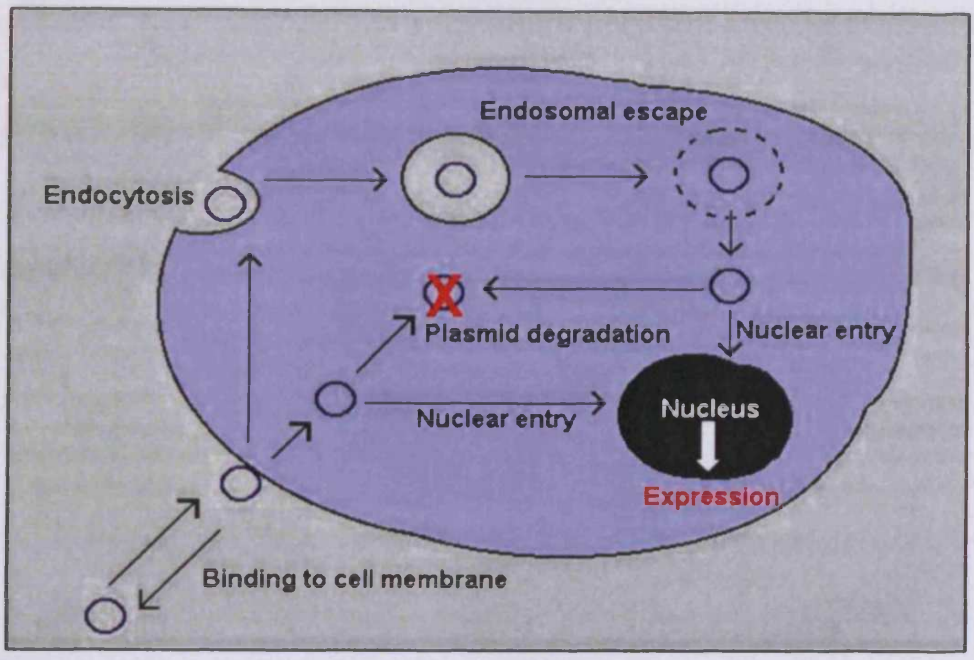

Figure 1.9 A diagram showing the main barriers that need to be overcome during non-viral gene delivery (adapted from Banks *et al* 2003).

While these barriers are common to the majority of non-viral gene delivery approaches, the skin has another particular obstacle, the SC. As already mentioned the SC is a considerable physical barrier, in particular to the passage of large molecules, like plasmid DNA. Consequently there has been much effort exerted to address this.

1.10 Methods to surmount the SC barrier

Most topically applied therapeutics cannot pass the SC barrier in pharmacological useful quantities. Consequently, application generally requires other components that aid their transport across the SC. A common method of increasing the permeability of the SC is hydration. Hydration of the SC can be achieved by preventing trans-epidermal water loss, frequently by occluding the skin surface. The consequence is an increase in water

content of the SC, which permits an increase in flux of the delivered substance across it. The flux of both hydrophilic and lipophilic substances has been increased by hydration of the SC (Behl *et al* 1980). Another commonly employed method is the use of chemical penetration enhancers. When applied to the skin they affect components of the SC resulting in reduced barrier function (Trommer and Neubert 2006). Common penetration enhancers include dimethylsulfoxide (DMSO), Azone (1-dodecylazacycloheptan-2-one) and pyrrolidones (Williams and Barry 2004). Another strategy is to manipulate the active or the delivery formulation. For example, the use of prodrugs which are not active when applied but have characteristics that make them pass the SC but once across are enzymatically acted upon which converts them to a pharmacologically active substance (Barry 2004).

Vesicles, such as liposomes, formed mainly from phospolipids have also been used as delivery vehicles for many substances. Liposomes are hollow, spherical lipid spheres that have an aqueous central volume which can trap hydrophilic molecules. The first demonstration of liposomes use as a vehicle for topically applied drugs was made in 1980 by Mezei and Gulasekharam. They showed that triamcinolone acetonide delivered in a liposome formulation accumulated in the epidermis at 4-5 time's greater concentration than if it were delivered without the liposomes (Mezei and Gulasekharam 1980). Liposomes have been investigated for delivering macromolecules such as pDNA (Birchall *et al* 2000) and antigens with a view to vaccinate (Babiuk *et al* 2000). However, although liposomes have been shown to be capacble of crossing the SC there is considerable scope for improvement. One problem with normal liposomes is that they

are typically 100-400nm in diameter and this is simply too big travel within the lipid component of the SC. To address this, a new class of highly deformable, elastic liposomes called transfersomes have been developed which can pass through pores approximately 20nm in diameter (Benson 2006). These vehicles have been shown to deliver a wide range of therapeutics across the SC and deep into the skin (Cevec 2004).

In contrast to using chemical means, manipulations of formulations or delivery vehicles, there exists a whole plethora of Physical disruption methods developed to increase permeation the SC. Among the most basic and simplistic methods are SC abrasion, with an abrasive substrate like sand paper and tape stripping, which involves the sequential removal of the SC by repeated application and removal of an adhesive tape or glue to the same region of skin until the SC integrity is severely compromised (Spruit and Malten 1966). Other methods of SC ablation utilize lasers (Jacques *et al* 1987) and radio waves (Birchall *et al* 2006), the latter demonstrating the ability to deliver functional DNA. The use of photomechanic waves is a further method that utilizes laser, though in an indirect manner. A solution of the substance to be delivered is applied to the skin surface, followed by a layer, typically polystyrene, which is targeted by the laser. As the laser is directed at the target material stress waves are generated in the underlying solution which propagates into the SC. This method has successfully delivered particles of 20nm across mouse SC (Lee *et al* 1998).

The use of ultrasound to enhance delivery of substances across the SC is called phonophoresis or sonophoresis. An ultrasounic probe applied to the skin results in

enhanced delivery because as the sound waves encounter a different medium, like the SC, they lose a lot of energy, this results in direct disruption of the barrier (Wu *et al* 1998) and also the formation of cavities in cell membranes which can facilitate the uptake of the delivered substances (Merino *et al* 2003).

Magnetophoresis is another novel approach, here the drug to be delivered either has innate, or is conjugated too a molecule that displays diamagnetic properties, Therefore if such a substance is applied to the skin and subject to a magnetic field it should be forced across the SC. This has been demonstrated using benzoic acid, which has diamagnetic properties, applied to rat skin followed by a magnetic field (Murthy 1999). Clearly this technique is limited to molecules with particular properties and does not provide a platform for ubiquitous drug delivery.

Electrically assisted methods include iontophoresis and electroporation. Iontophoresis requires the delivery of a substance that has a charge, again somewhat restricting suitable drug candidates. This is applied to the skin followed by an electrode of the same charge. Another electrode is placed elsewhere on the skin. When a small current is applied the electrode, being the same charge as the delivery molecule forces it into the skin through electrostatic repulsion. While inotophoresis uses a small, continuous electric current, electroporation generally uses pulses of much higher voltages (10-1000 V). Electrophoration causes aqueous pores to form within cell membranes, it is also able to form pores in the lipid component of the SC (Prausnitz *et al* 1993). Electroporation has successfully transferred DNA into rat skin (Dujardin *et al* 2001; Dujardin and Preat 2004)

Biolistic delivery, utilizing the gene gun, fires gold particles with a radius of approximately 0.5-2μm coated in the delivery substance (Kendall *et al* 2004) into target tissue. First developed to deliver genes into plants, the gene gun has been extensively used to perform the same task with respect to mammalian tissue, including excised human skin (Kendall *et al* 2004; Kent *et al* 2001). The gold particles are accelerated within the gene gun to a sufficient velocity that upon leaving the device, penetrate the SC, taking the delivery substance with them (Liu *et al* 2007). Biolistic delivery is currently being investigated as a means of delivering DNA vaccines to the skin (Kendall *et al* 2004; Mulholland *et al* 2006; Kendall 2006).

Finally, a relatively recent innovation has been proposed as a means of enhancing permeation of the SC, which consist of arrays of micro-projections called microneedles, which are the subject of the following chapter.

1.11 Thesis aims and objectives

1.11.1 Thesis aims

To determine weather arrays of silicon microneedles are capable of facilitating delivery of pDNA to human skin, with an ultimate view toward DNA vaccination.

1.11.2 Thesis objectives

- Characterisation of microneedle arrays.
- Investigate ability of microneedle arrays to disrupt the SC and deliver exogenous materials to the underlying viable epidermis of human *ex vivo* skin.
- Determine optimal methods of applying microneedles to human *ex vivo* skin.
- Confirm *ex vivo* skin maintained in organ culture remains genetically viable.
- Demonstrate that reporter pDNA can successfully be delivered and subsequently expressed in human *ex vivo* skin when applied in conjunction with microneedles.
- Investigate weather simple modifications to application procedures can improve expression from reporter pDNA when delivered to human *ex vivo* skin.
- Explore the potential of using hydrogel sustained release systems in conjunction with microneedle to deliver pDNA to human *ex vivo* skin.
- Preparation, characterisation and formation of stocks of a therapeutic plasmid encoding the small and middle forms of the HBsAg (pCMV.M).
- Transfect cells *in vitro* to confirm expression of the antigen from the plasmid.
- Demonstrate that microneedle can facilitate delivery of HBsAg to ex *vivo* skin.
- To show that microneedle can successfully deliver a therapeutic plasmid (pCMV.M) to *ex vivo* skin where it is expressed.

CHAPTER 2: Microfabricated microneedles, characterisation and ability to disrupt the stratum corneum

2.1 Introduction

We have seen that the skin has many features that make it an attractive target for the delivery of therapeutic and prophylactic agents. However, the outermost layer of the skin, the stratum corneum (SC) represents a considerable barrier to the passage of such medicaments. The previous chapter contains an overview of some of the methods developed to address the SC barrier problem. This chapter aims to discuss microneedles, as one such approach, in more detail and demonstrate that microneedles are particularly suited for application in human skin, causing sufficient disruption to enhance transdermal delivery of macromolecules.

Most microneedles, defined as projections with micron-sized dimensions, are manufactured in the form of an array, and are specifically designed with the intension of creating channels through the SC for the passage of therapeutic agents in a minimally invasive manner. The concept was first conceived during the 1970s (Gerstel and Place 1976), however, at this time the technology did not exist to create devices on such small scales, for that reason it was not until advances in microelectromechanical systems (MEMS) technology that the ability to put theory into practice arose (Henry *et al* 1998; Prausnitz *et al* 2004). The first study demonstrating an enhancement in drug delivery facilitated by microneedles was conducted in 1998, performed by a group led by Mark Prausnitz. The study involved the application of a 20 X 20 array of solid silicon microneedles with heights of 150μm to cadaver skin; this was followed by a solution of calcein, a model small molecule. The result was dramatic; microneedles enhanced the flux of calcein across the SC by three orders of magnitude (Henry *et al* 1998). Since then microneedle facilitated delivery has been demonstrated for both low molecular weight drugs, macromolecules

and nanoparticles of around 100nm diameter (Henry *et al* 1998, Chabri *et al* 2004, Martanto *et al* 2004, Matriano *et al* 2002, Sivamani *et al* 2005, Coulman *et al* 2006). Microneedle facilitated drug delivery has also been shown to have biological effects. For example, Streptozotocin treated hairless mice display a diabetic phenotype, microneedle application followed by an insulin solution reduced blood glucose levels in these mice by 80% (Martanto *et al* 2004). Additionally, Mikazta *et al* have shown that using a similar device, they term a microenhancer array (MEA), which is applied in a lateral, scrapping motion, they are able to increase reporter gene expression 2,800 fold compared to controls, and when a plasmid, encoding a fragment of the Hepatitis B surface antigen (HBsAg) is applied, it results in a stronger, less variable immune response, requiring fewer immunizations for complete seroconversion (Mikszta *et al* 2002). It has also been demonstrated that drugs can be successfully coated onto microneedle tips in sufficient quantities for a biological response, for example Desmopressin, has been coated onto microneedle arrays and delivered by a Macroflux™ delivery system (see below) to hairless guinea pigs, this study showed pharmacological concentrations of the drug was delivered in 5 minutes. (Cormier *et al* 2004).

Since microneedles were first produced the field has developed rapidly and now there are numerous groups around the world investigating the potential of microneedles. To date microneedles have been manufactured from numerous materials and by different processes with materials used including silicon (Chabri *et al* 2004, Henry *et al* 1998), glass (McAllister *et al* 2000; McAllister *et al* 2003), metal (McAllister *et al* 2003) and polymers (Park *et al* 2005; Park *et al* 2006). While silicon is still possibly the most common substrates for microneedle manufacture, interest in other materials

has arisen because silicon is brittle, expensive, requires time consuming steps in its use and has questions regarding its biocompatibility (Park *et al* 2005). Consequently, microneedles have been made out of stainless steel sheets, with the microneedle shape cut with a laser and the needles pushed out of plane so they are at a 90° angle to the base (Martanto *et al* 2004). ALZA Corporation manufactured developed a titanium microneedle delivery system, which has since become a separate company called Macroflux™. This system has been shown to enhance transdermal flux of ovalbumin (Matriano *et al* 2002) and antisense oligonucleotides (Lin *et al* 2001) into hairless guinea pigs and, as already mentioned, desmopressin (Cormier *et al* 2004).

Similarly, polymers, which are cheap, strong, easily mass produced and can be manufactured out of a range of biocompatible materials, are currently receiving much attention. Many polymers are biodegradable, for example, polylactic acid (PLA), polyglycolic acid (PGA) and polylactic acid-co-glycolic acid (PLGA); consequently microneedles manufactured from these polymers would cause little concern if breakages occurred while being applied to a patient. Recently, microneedles manufactured from PGA and PLGA have been described by Park *et al* and shown to have sufficient mechanical strength to puncture the SC for the delivery of calcein and bovine serum albumin (BSA) (Park *et al* 2005). In a follow up to this study PLGA polymer microneedles were shown to encapsulate calcein and BSA during manufacturing. It is proposed that such microneedles, containing the therapeutics within their structure, could be administered in the form of a patch, where the microneedles would penetrate the SC and the polymer microneedle matrix would start to break down in the biological milieu, subsequently releasing the drug over an extended period. In this study the drugs were shown to be effectively encapsulated

directly into the microneedle matrix or by a double encapsulation process, where the drug was first encapsulated into either carboxymethylcellulaose or poly-L-lactide, and subsequently encapsulated into the needle matrix. The microneedles were shown to retain sufficient mechanical strength for SC penetration and subsequently released the drugs into cadaver skin over a period of days to weeks, depending on the encapsulation method (Park *et al* 2006).

Much of the early work, and work presently being undertaken, is performed using solid microneedles; however, hollow microneedles represent a means of infusing therapeutics into patients (McAllister *et al* 2003). This technique has been shown feasible by Davies *et al*, where arrays containing 16 hollow microneedles with heights of 500μm, each containing a channel though its core were inserted into hairless diabetic mice. Insulin was then passed though the microneedles infusing with the body of the mouse. The result was a reduction of blood glucose by 47% compared to pre-treatment values (Davis *et al* 2005). It has also been proposed that hollow microneedles could be used to retrieve extracellular fluids form patients for analysis (Mukerjee *et al* 2004). One group of people which could benefit from such a technology are diabetic's who need to self-monitor their glucose levels. A large proportion of this group neglects self-monitoring, mainly because of the pain and general inconvenience associated with current methods of analyisng glucose in blood. For reasons that will become apparent, microneedles are proposed as a less invasive, patient friendly way of monitoring components of blood or interstitial fluids (ISF) (Wang *et al* 2005). Moreover, because of the overall reduction of size, it has been proposed that in the near future microneedle based monitoring devices will be able to be worn by patients, probably in the form of a patch, permitting real-time, continuous

measurements of metabolites in bodily fluids (Friedl 2005). Such potentials have attracted interest from the military (Friedl 2005) and industry. For examples Nanopass Technologies and Silex Microsystems have created the Micropyramid™, 3M have developed the microstructered transdermal system (MTS™) and BD produce the Microinfusor™ (Fig 2.1).

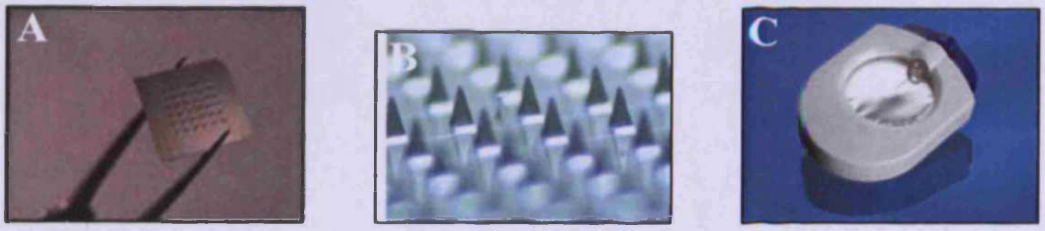

Figure 2.1 some current industrial developed systems based on microneedle technology:

(A) The Micropyramid™ (http://medgadget.com/archives/2007/02/micropyramid_te.html)
(B) The MTS™ (http://solutions.3m.com/wps/portal/3M/en_WW/DDS/DrugDeliverySystems/techsolutions/mts/)
(C) The microinfusor™ (http://catalog.bd.com/bdCat/displayTop3Categories.doCustomer?categoryID=0)

While an increase in permeability of the SC is certainly advantageous it is not the only reason microneedles are attractive for therapeutic transdermal delivery. Because of their restricted dimensions, when microneedles are applied to the skin surface they puncture the SC, penetrate the viable epidermis but do not reach the dermis. This is significant, as the dermis is the region of the skin that houses nerve endings and blood vessels (Figure 2.2). As a result, microneedle application should be effectively, free of pain and result in negligible extravasation (Prausnitz 2004). Consequently, it is likely that patient's perceptions of microneedles will be more favorable compared to current needle and syringe methods, particularly for patients that suffer needle-phobia, a widespread and common affliction (Hamilton 1995). Vindication of this has been shown in a recent study assessing both the general public and professional clinician's perceptions of microneedles as therapeutic instruments (Clemo *et al* 2006[A&B]).

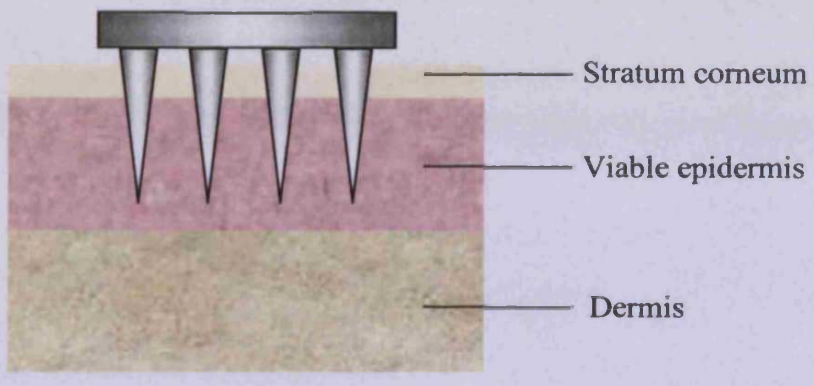

Figure 2.2 A schematic representation of the microneedle concept. Through their design microneedles have the ability to penetrate the SC and viable epidermis but not reach into the dermis where the nerve ending and blood vessels are located.

The microneedles used throughout this study were manufactured by collaborators at the Tyndall National Institute (TNI), Cork, Ireland. Solid microneedles were manufactured from both silicon and polymers. Three different types of silicon microneedles were investigated during this study, two solid designs and one hollow design. The two solid silicon microneedle types were fabricated in different ways. The first method, dry-etching, results in microneedles that are similar in morphology to the original microneedles used by Henry *et al* (1998), where reactive gases are utilized to shape them from the silicon wafer. The second method, called wet-etching, relies on the used of solutions, rather than gases, to "sculpt" the microneedles from the silicon substrate. Hollow silicon microneedles that can conduct fluids were also briefly investigated as were polymer microneedles.

2.1.1 Techniques utilized

Characterisation and integrity of microneedle arrays was achieved by light microscopy and scanning electron microscopy (SEM). Light microscopy is mainly used as a quick method to confirm integrity of microneedle arrays before, during and after experiments. Detailed analysis of microneedle morphology was achieved by SEM, which was also utilized to observe punctures in full thickness skin and heat separated epidermal sheet resulting from microneedle application. At high magnifications, SEM is able to give great resolution of a samples surface compared to light microscopy, which is limited by the wave nature of light. It also has a greater depth of field ensuring that much of the sample is in focus at any one time. Consequently this technique was ideal for examining microneedle arrays and microneedle treated human skin surfaces.

Water is continually lost through the skin surface, more so during strenuous exercise, and this is termed transepidermal water loss (TEWL). Microneedle application to human skin, results in comprehensive disruption to the SC, and subsequently an increase in water flux across the SC will be observed. Measuring TEWL as a means of assessing skin barrier integrity has recently been confirmed in human and rodents both *in vivo* and *ex vivo* (Fluhr *et al* 2006). Therefore, applying microneedles to skin and recording the TEWL will provide an indication of microneedle functionality with respect to a compromise of the SC barrier. There are a number of methods and devices available to measure TEWL, these include the open chamber method, the closed-cup method and ventilated chamber method. During this study TEWL measurements will be made using a coupled hygrometer and thermistor in an open chamber system.

2.1.2 Microneedle application

While interest in microneedle mediated drug delivery to the skin is increasing, little work is being conducted on optimizing the application procedure. This is clearly an important factor that must be addressed if microneedles are to make an impact in a clinical setting. Prausnitz's group have investigated application forces and arrived at a value of approximately 10N, which ensures 95% of microneedles, in a particular array, will penetrate the SC (Henry *et al* 1998). In contrast Davis *et al* report that a force in the range of 0.1-3 N is required. However, there are a number of factors that will ultimately affect the force applied to the microneedle array in order to puncture the SC, for example tip sharpness and diameter (Davis *et al* 2004). Accordingly, these issues will influence experiments conducted for this thesis, as *ex vivo* human skin will be used. Therefore, a means of applying microneedles in a reproducible and consistent manor is required and consequently will be investigated during this chapter. Furthermore, the mechanical properties of *ex vivo* human skin is different compared to human skin *in situ*, as a result different ways of manipulating the skin for microneedle application will be observed. In order to assess which methods of microneedle application and skin manipulation are suitable TEWL measurements will be compared and where appropriate SEM will be utilized.

2.2 Aims and objectives

2.2.1 Aims

The aims of this chapter are to fully characterise microneedles and to demonstrate that they have the capabilities to disrupt the SC.

2.2.3 Objectives

- Characterize the morphology of microneedle arrays
- Demonstrate that arrays of microneedles manufactured from silicon and polymers are robust enough for application to human skin
- To determine the best method of holding *ex vivo* skin in position for microneedle application
- Establish a suitable method for microneedle application
- Show that microneedle application to human skin results in disruption to the SC.

2.3 Materials and Methods

2.3.1 Materials

Reagents used during the course of these studies were of analytical grade and purchased from Fisher Scientific (Loughborough, UK), unless otherwise stated.

Glutaraldehyde solution (50%) was purchased from Sigma (Gillingham, UK).

All water used during these studies was deionized and obtained from an Elga reservoir (High Wycombe, UK).

2.3.2 Microneedle manufacture

All microneedles utilizes throughout this work were fabricated by collaborators at the Tyndall National Institute (TNI), Cork. The following are brief overviews of the fabrication processes for each of the different microneedle arrays used.

2.3.3 Dry-etch microneedle manufacture

A P-type silicon wafer is cleaned and polished on one side, before a photoresist layer is spun onto its surface. A mask layer is then applied which has a high resolution dot array pattern on its surface, exposure to ultra-violet (UV) light results in wavelength specific chemical reactions occurring in the exposed regions. The resist layer is then developed by immersion in an alkaline solution which results in removal of the UV exposed regions. The wafer is then subject to a combination of anisotropic BOSCH deep reactive ion-etching (DRIE), which forms high aspect ratio holes and cavities in silicon, and isotropic-etching, which results in more rounded surfaces, with Fluorine Sulphur Hexafluoride (SF_6) and Oxygen (O_2) gases. The resultant microneedle arrays are then cleaned, with acetone, and completely dried under nitrogen before being coated in platinum. A schematic of the steps involved is shown in Figure 2.3.

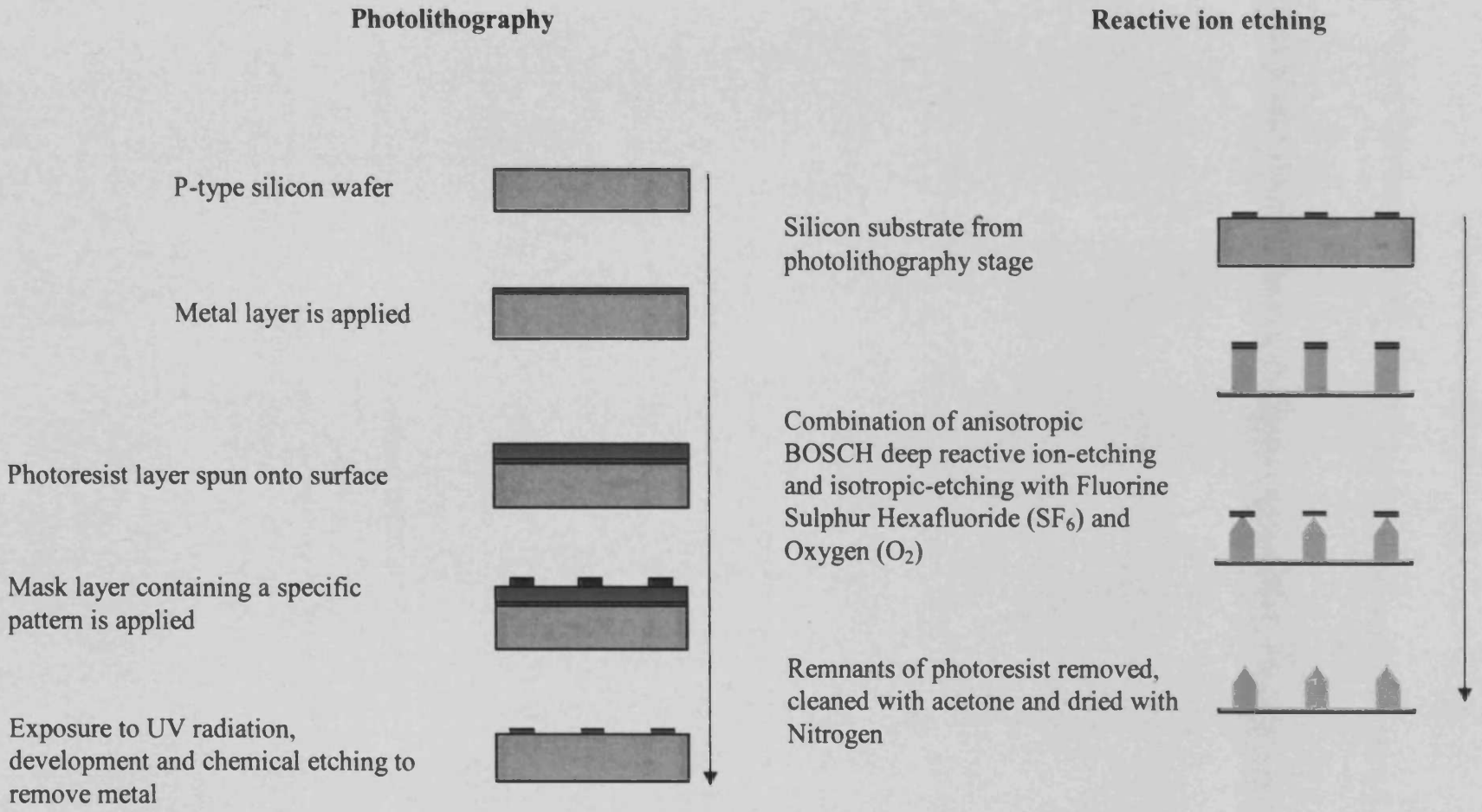

Figure 2.3 An outline of the principal steps involved in the manufacture of silicon microneedle arrays formed by dry-etch processes.

2.3.4 Hollow microneedle manufacture

The fabrication of a hollow microneedle device can be split into two separate but parallel processes. Firstly, microneedle are manufactured by a dry-etch process as previously described (wet-etch microneedles can also be used). The formed microneedles are then protected by coating them with metal. DRIE is used on the back side of the array, forming high resolution cylindrical channels through the array, continuing through each of the microneedles on the other side. The mask layer and metal coat are then etched away. Simultaneously, another wafer is undergoing controlled DRIE to etch away part of the central region of the wafer. The two wafers are then bonded together with accurate alignment and flexible capillary tubes are attached, before being coated in platinum Figure 2.4 shows this process diagrammatically.

2.3.5 Wet-etch microneedle manufacture

A standard P-type silicon wafer, 10cm diameter and 525μm thick, is coated on one of its surfaces with an oxide layer, which is subsequently coated by a further layer of nitride; both layers are applied by Low Pressure Chemical Vapor Deposition (LPCVD). Plasma etching is utilizes to lithographically create a mask pattern in the oxide-nitride layer. The wafer is then immersed in a 29% potassium hydroxide at 79°C with constant agitation, for a specific period of time, depending on the morphology of the needles required. Any remaining mask material is then removed and the microneedle array coated in platinum. A diagram of the steps involved is shown in Figure 2.5 and a more in depth review of the process is described by Wilkes *et al* 2005.

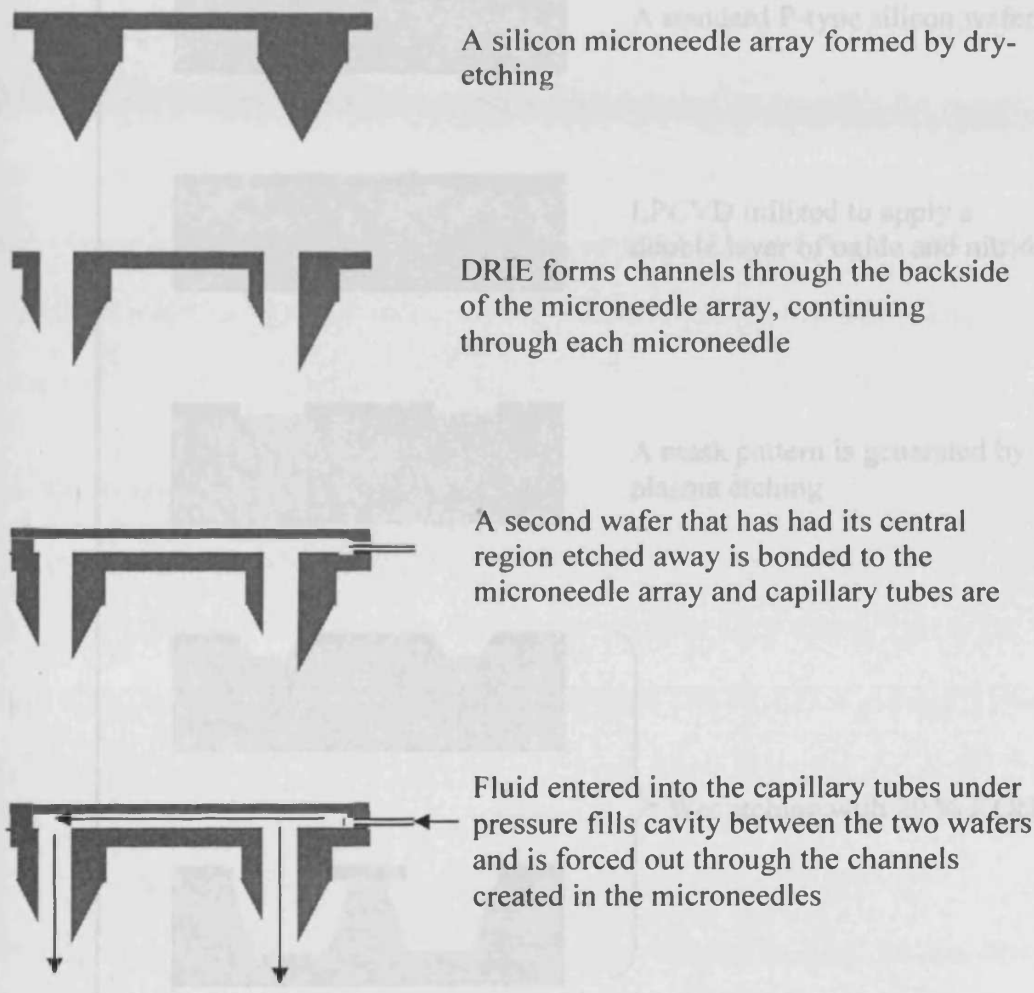

Figure 2.4 The formation of a hollow microneedle array

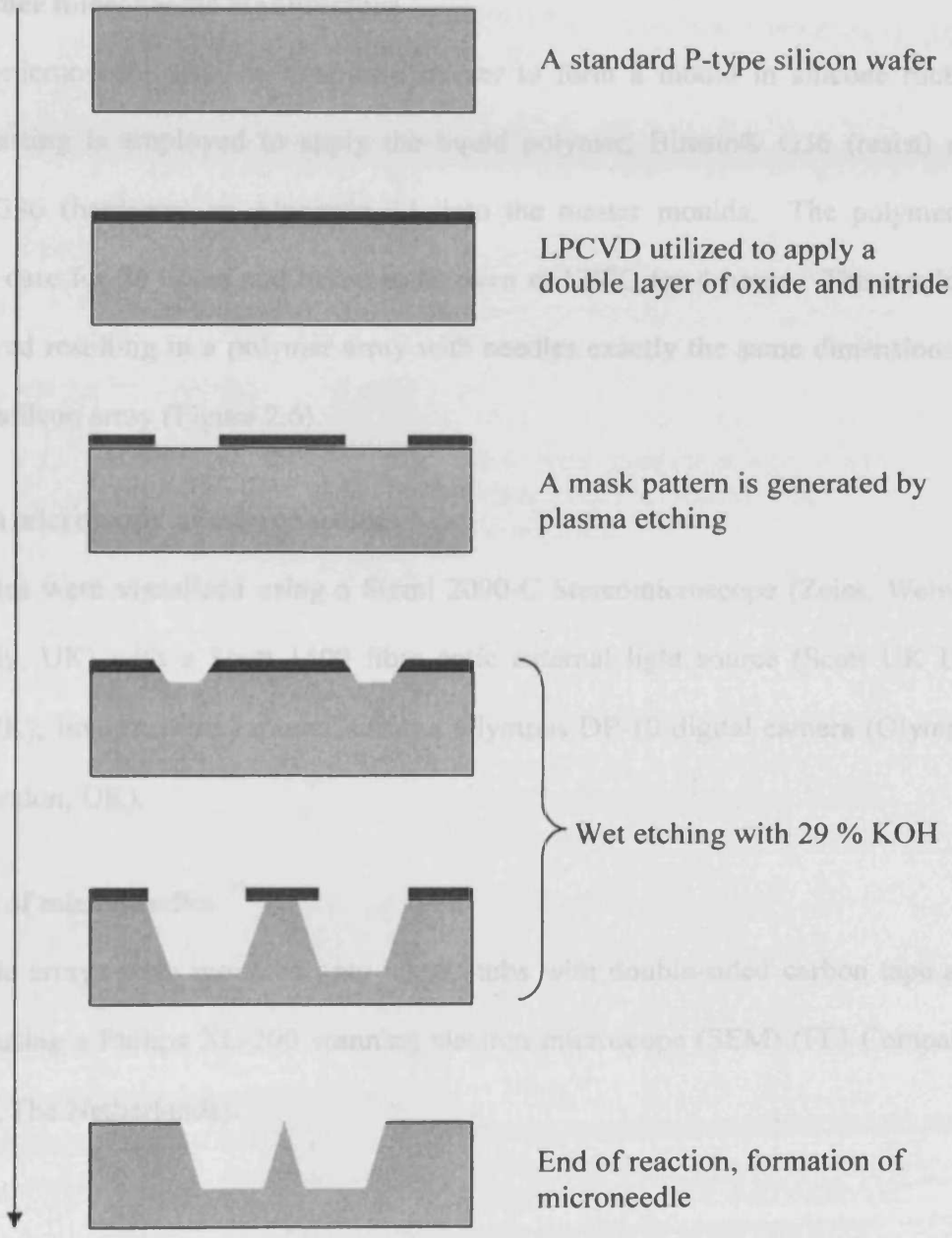

Figure 2.5 Schematic representation of the microneedle formation by wet-etch process (diagram adapted from Wilke *et al* 2005).

2.3.6 Polymer microneedle manufacture

A silicon microneedle array is used as a master to form a mould in silicone rubber. Vacuum casting is employed to apply the liquid polymer, Biresin® G36 (resist) and Biresin® G36 (hardener) or Alparesin 12, into the master moulds. The polymer is allowed to cure for 24 hours and baked in an oven at 120°C for 4 hours. The mould is then removed resulting in a polymer array with needles exactly the same dimensions as the master silicon array (Figure 2.6).

2.3.7 Light microscopy of microneedles

Microneedles were visualized using a Stemi 2000-C Stereomicroscope (Zeiss, Welwyn Garden City, UK) with a Scott 1500 fibre optic external light source (Scott UK Ltd, Stafford, UK); images were captured using a Olympus DP-10 digital camera (Olympus Optical, London, UK).

2.3.8 SEM of microneedles

Microneedle arrays were mounted onto metal stubs with double-sided carbon tape and visualized using a Philips XL-200 scanning electron microscope (SEM) (FEI Company, Eindhoven, The Netherlands).

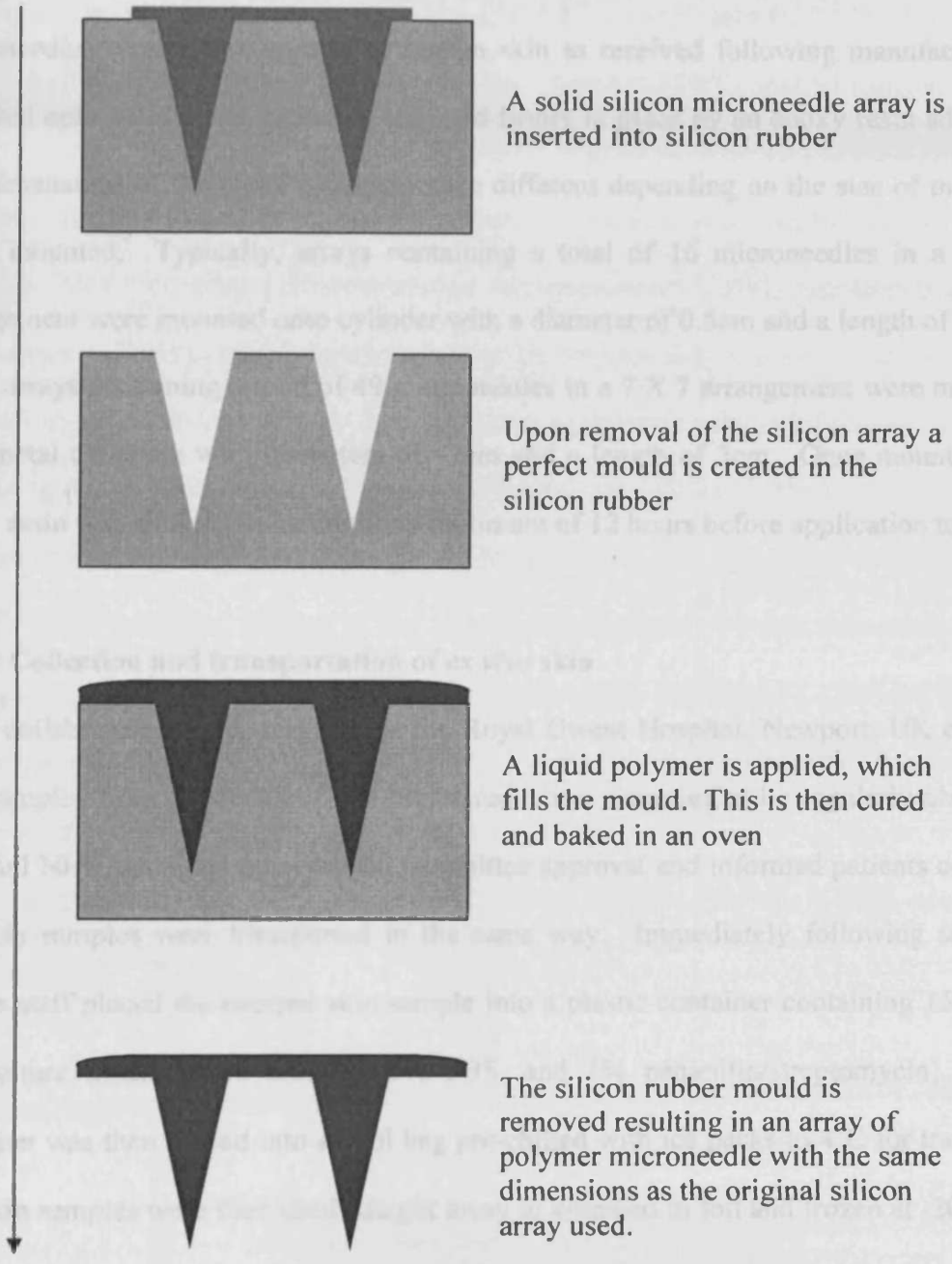

Figure 2.6 The steps involved in the formation of a polymer microneedle array

2.3.9 Mounting microneedles for application to the skin

Microneedles were either applied to human skin as received following manufacture or mounted onto solid metal cylinders and held firmly in place by an epoxy resin adhesive. The dimensions of the metal cylinders were different depending on the size of the array being mounted. Typically, arrays containing a total of 16 microneedles in a 4 X 4 arrangement were mounted onto cylinder with a diameter of 0.5cm and a length of 2.5cm. Other arrays containing a total of 49 microneedles in a 7 X 7 arrangement were mounted onto metal cylinders with diameters of ~1cm and a length of 3cm. Once mounted, the epoxy resin was allowed to harden for a minimum of 12 hours before application to skin.

2.3.10 Collection and transportation of *ex vivo* skin

Close collaborations with surgeons at the Royal Gwent Hospital, Newport, UK enabled skin samples from mastectomy and breast reduction surgeries to be regularly obtained; with full NHS Trust and local ethical committee approval and informed patients consent. All skin samples were transported in the same way. Immediately following surgery, theatre staff placed the excised skin sample into a plastic container containing 150ml of full culture media (94% DMEM, 5% FBS, and 1% penicillin/streptomycin). This container was then placed into a cool bag pre-chilled with ice packs to 4°C for transport. The skin samples were then used straight away or wrapped in foil and frozen at -20°C for use at a later date.

2.3.11 SC disruption by mounted microneedle and unmounted microneedles determined by transepidermal water loss (TEWL) measurements.

Frozen human skin sample (♀ 57 years of age), stored at -20°C, was allowed to defrost for 2 hours, blotted dry and allowed to equilibrate with local environment for a further 30 minutes. After removal of all subcutaneous fat the skin was pinned flat on a cork dissecting board ensuring sufficient tension was generated. TEWL measurements were made using a TEWL probe connected to a DermaLab skin analysis system (Cortex Technology, Hadsund, Denmark). An unmounted microneedle array (260μm) height, containing 49 microneedles in a 7 X 7 arrangement was applied to the skin surface with constant pressure applied to the back of the array with an index finger for 5 seconds. The TEWL probe was then applied to the microneedle treated area and the measurement recorded (Figure 2.7) An identical microneedle array was mounted onto a metal cylinder (~1cm diameter and 3cm length) as described previously, was applied to the skin in a downward motion so that all needles come into contact with the skin surface at the same time. Constant pressure was applied for 5 seconds followed by the TEWL probe and value recorded.

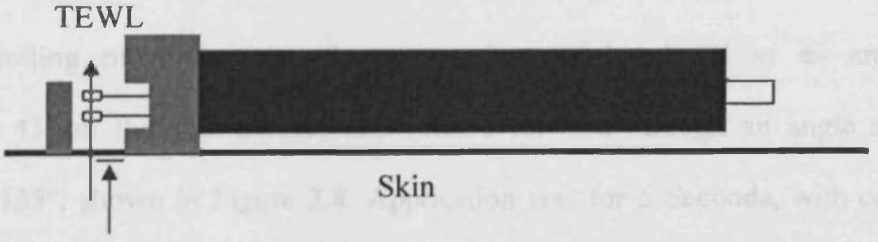

Figure 2.7 A diagrammatic representation of the TEWL probe used to determine SC integrity. The end of the probe is attached to an open cylindrical chamber that contains the hygrosensor coupled to a thermistor. Diagram adapted from Pinnagoda *et al* 1990

2.3.12 Determination of optimal way of securing *ex vivo* human skin for microneedle application

Frozen human skin sample (♀ 62 years of age) was removed from -20°C storage and allowed to defrost and equilibrate as described previously. The skin sample was then cut into two equal pieces of approximately 4 cm by 6 cm. One of these samples was pinned on a flat cork dissecting board while the other was pinned on a semi-circular cork support, in both cases sufficient tension was generated in the skin (Figure 2.8). A mounted microneedle array (260μm) height, containing 49 needles in a 7 X 7 arrangement, was applied to the skin, pinned on both supports, in a downward motion so that all needles come into contact with the skin surface at the same time, with constant pressure being applied for a total of 5 seconds, followed by TEWL determination.

2.3.13 Determination of optimal way of applying microneedle to *ex vivo* human skin

Frozen human skin sample (♀ 60 years of age) was removed and allowed to defrost and equilibrate as described previously. The skin sample was pinned over a semi-circular cork support with sufficient tension generated in the sample. Mounted microneedles (260μm height), containing 49 needles in a 7 X 7 arrangement, were applied to the skin surface, either in a downward motion (Figure 2.8) so that the each needle comes into contact with the skin surface at the same time. Alternatively, microneedles were applied in a single rolling motion, where the mounted array is placed at an angle of approximately 45° to the skin surface and rotated forward through an angle of 90°, finishing at a 135°, shown in Figure 2.8. Application was for 5 Seconds, with constant pressure applied constantly. TEWL measurements were made after each application.

2.3.14 Effect of different needle heights and SC disruption

Frozen human skin sample (♀ 66 years of age) was removed from -20°C storage and allowed to equilibrate as described previously. The skin sample was then pinned over a semi-circular cork support as previously described. Three different microneedle arrays containing 49 needles in a 7 X 7 arrangement, with heights of 80μm, 180μm and 260μm were mounted onto metal cylinders (1cm diameter and 3cm length). The different arrays were applied to different regions of the skin in a single rolling motion, for 5 seconds with constant pressure being applied. TEWL measurements were made after each application.

2.3.15 Comparison of polymer and silicon microneedles ability to disrupt the SC

Frozen human skin (♀ 59 years of age) was removed from -20°C storage and allowed to defrost and equilibrate as described previously. The sample was pinned over a semi circular cork support as previously described. Mounted silicon and polymer microneedles containing 49 needles in a 7 X 7 arrangement with heights of 280μm were applied to the skin in a single rolling motion, for a total of 5 seconds with constant pressure being applied. TEWL was determined after each application. One way analysis of variance (ANOVA) and Tukey's *post hoc* analysis were calculated using MINITAB 13 software (Minitab Ltd., Coventry, UK).

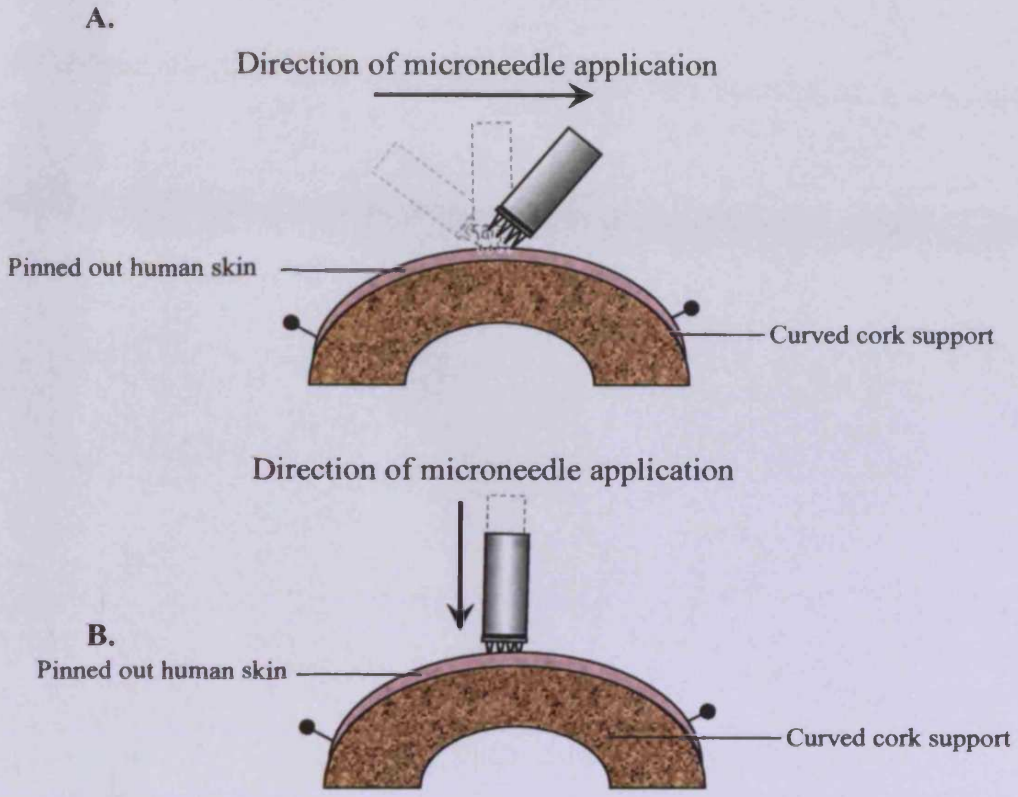

Figure 2.8 The application of a mounted microneedle array mounted onto a metal rod applied in a "single rolling motion" (A) and applied flat (B). Application of a mounted microneedle array, in a single rolling motion, involves the array making contact with the skin surface at an angle of ~45°, then passing through 90° finally to ~135°. The rolling causes localized tension to be generated in the skin aiding microneedle penetration. The skin is curved to maintain sufficient tension and a better representation of the *in vivo* state.

2.3.15 Microneedle treatment of full thickness skin and preparation for SEM

Frozen human *ex vivo* human skin (♀ 64 years of age) was removed from -20°C storage and allowed to defrost for approximately 1 hour. All subcutaneous fat was removed and the sample pinned over a semi-circular cork support, ensuring tension is generated in the sample. A microneedle array containing 16 microneedles (250μm height) in a 4 X 4 arrangement mounted on a metal cylinder with a diameter of ~0.5cm and a length of ~2cm was applied to the skin in a single rolling motion. Treated regions of skin were excised with a scalpel and trimmed to ~0.7cm^2. All samples were fixed in 2ml of 2% glutaraldyhyde at 4°C for 2 hours, before being

dehydrated in an ethanol gradient (2ml of 40%, 50%, 60% 70%, 80%, 90%, and 100% each for 30mins). All samples were further washed a total of 4 times in 2ml 100% ethanol before complete dehydration was achieved using a CPD030 critical point dryer (Bal-Tec, Balzers, Lichenstein). Each sample was mounted onto a metal stub with double sided carbon tape and sputter coated in gold (EM Scope, Kent, UK) before observation with a Philips XL-20 SEM (Philips, Eindhoven, Netherlands).

2.3.16 Microneedle treatment of heat separated epidermal membrane and preparation for SEM

Ex vivo human skin sample (♀ 64 years of age) had all the subcutaneous fat removed and dissected into areas of ~2cm^2. The skin samples were placed into a water bath heated to 60°C for 55 seconds; the epidermis is carefully removed from the dermis using forceps. The heat separated epidermal sheets were placed back onto the dermis and a microneedle array with a total of 16 microneedles (250μm height) in a 4 X 4 arrangement, was applied in a single rolling motion. The heat separated epidermal sheets were fixed in 2% glutaraldehyde and dehydrated in an alcohol gradient (2ml of 70%, 80%, 90% and 100% each for 30 minutes). The heat separated epidermal sheets were then mounted onto a metal stub with double sided carbon tape and sputter coated with gold (EM Scope, Kent, UK) and observed with a Philips XL-20 SEM (Philips, Eindhoven, Netherlands).

2.3.17 SEM study of microneedles *in situ* penetrating heat separated epidermal sheets

Heat separated epidermal sheet were prepared from *ex vivo* skin (♀ 61 years of age) and treated with a 4 X 4 microneedle array with a total of 16 microneedles (250μm height), as described previously (Chapter 2; Section 2.3.16). However, instead of

removing the array from the epidermal sheet, it was allowed to remain *in situ*. The array and epidermal sheet was then subject to fixation and dehydration as described and visualized by a Philips XL-20 SEM (Philips, Eindhoven, Netherlands).

2.3.18 Microneedle robustness test

Mounted silicon and polymer microneedle arrays (both with heights of 260μm) containing 49 needles in a 7 X 7 arrangement was visualized with a Philips XL-20 SEM (Philips, Eindhoven, Netherlands) to ensure all individual needle of each array was intact. Human skin (♀ 59 years of age) was removed from -20°C storage and allowed to defrost for approximately 1 hour. The sub-cutaneous fat was removed and the skin pinned over a semi-circular curved cork support. Microneedle arrays were then applied in a single rolling motion to different parts of the skin a total of 10 times. The arrays were then visualized again by SEM (Philips XL-20 SEM (Philips, Eindhoven, Netherlands) to determine weather all the microneedle were still intact.

2.4 Results and discussion

2.4.1 Dry-etch microneedle characterisation

Dry-etch microneedles were produced on a silicon wafer and cut into arrays of ~2 by 1cm^2. When observed by light microscopy the array was shown to consist of 240 solid microneedles in total, arranged 15 X 16 (Figure 2.9 A). When observed at higher magnification the uniformity of the microneedle within the arrays begins to emerge, appearing in straight lines parallel to one another (Figure 2.9 B). At still higher magnifications the morphology of individual microneedles starts to become clear. Each needle is composed of a cylindrical body that rises from the silicon wafer base, which tapers into a sharp conical tip (Figure 2.9 C). The results from SEM showed that the microneedles were spaced equally, with a tip to tip measurement of adjacent microneedles ~150μm (Figure 2.10 A). Individual microneedles were approximately 250μm in height, with a diameter, of the cylindrical body, of around 150μm (Figure 2.10 B).

2.4.2 Wet-etch microneedle characterisation

Early batches of wet-etch microneedles were much smaller and contained fewer microneedles compared too dry-etch arrays, the dimension of a typical array being 3mm^2. Observation by light microscopy revealed that there was much variation in microneedle morphology between individual arrays (Figure 2.11). However, a common feature of the wet-etch process is that the resultant microneedles are all angular, with a pyramidal morphology. Wet-etch microneedles can be split into three arbitrary groups, determined by there tip morphology. The first group consisted of microneedle arrays that are squat in

appearance with a tip that has a large flat surface, which were termed "blunt" or "frustum tipped" microneedles (Figure 2.11 A & B). The second group, classed as intermediate, was much more Pyramidal in appearance, they still possessed a flat surface but it was considerably smaller than observed with the frustum tipped microneedles (Figure 2.11 C & D). The final group consisted of arrays with extremely sharp tips (Figure 2.11 E & F), and was accordingly called "sharp". SEM illustrates the differences between the microneedle morphologies in greater detail (Figure 2.12 and Figure 2.13). The frustum type microneedle array consists of a total 16 microneedles in a 4 X 4 arrangement. The array is composed of uniform microneedle equally spaced, approximately 750μm between adjacent tips (Figure 2.12 C). The intermediate array contained a total of 9 microneedles arranged 3 X 3, with a distance between tips of ~1mm (Figure 2.12 B). The sharp tip arrays were identical as the frustum tipped arrays in terms of spacing only the difference was the extremely sharp to each needle (Figure 2.13). Later batches were all sharp tipped arrays but were larger than the first batch, typically containing 49 microneedles in a 7 X 7 arrangement on an array that measures $0.8mm^2$.

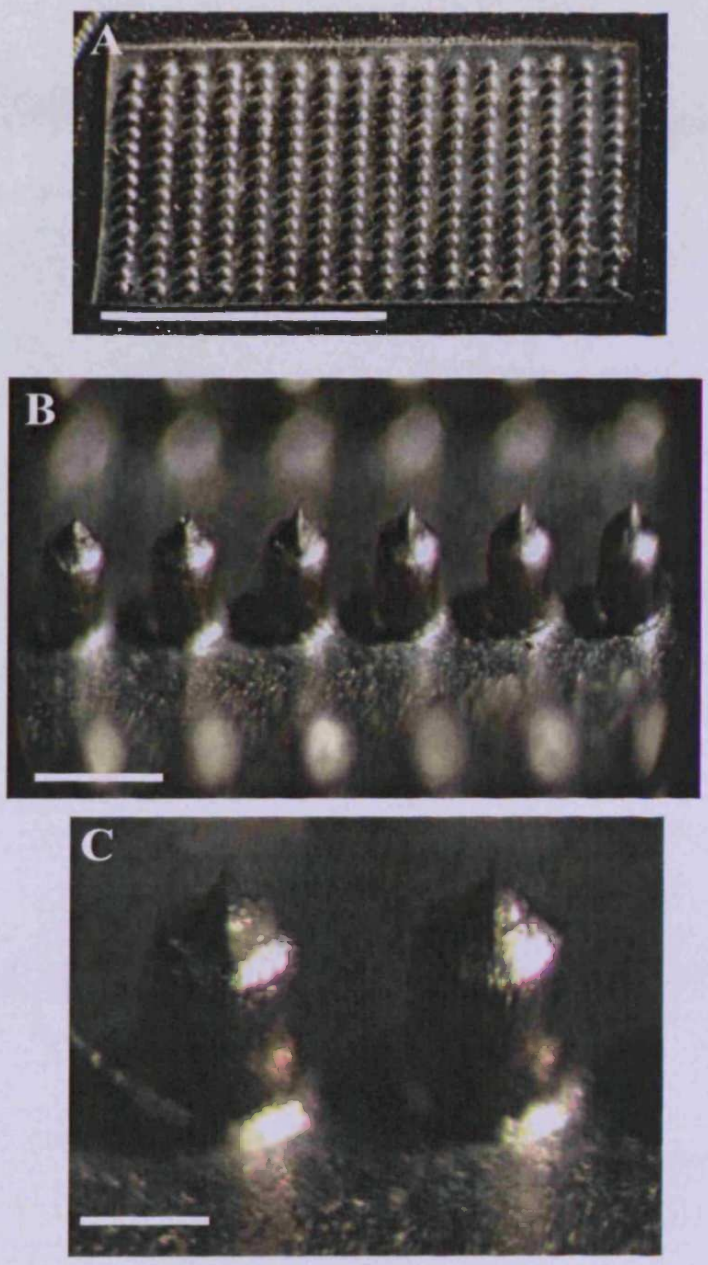

Figure 2.9 Characterisation of dry-etched microneedles by light microscopy. Manufacture results in arrays of microneedles in a 15 X 16 arrangement with a total of 240 individual needles (A; bar = 1cm). Higher magnification shows that all the microneedles are relatively uniform in shape (B; bar = 150μm), with sharp tips (C; bar = 150μm).

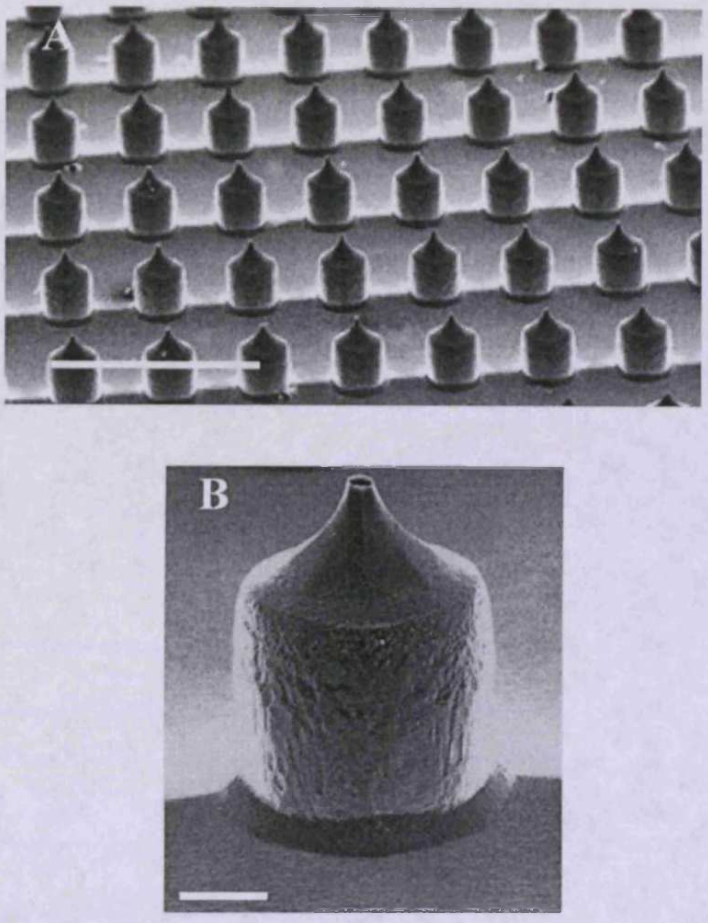

Figure 2.10 Characterisation of dry-etched microneedles by SEM. Manufacture results in arrays of microneedles in a 15 X 16 arrangement with a total of 240 individual needles, higher magnification shows that all the microneedles are relatively uniform in shape (A; bar = 500μm). Higher magnification shows that individual microneedles have a cylindrical body that give rise to a conical tip (B; bar = 50μm).

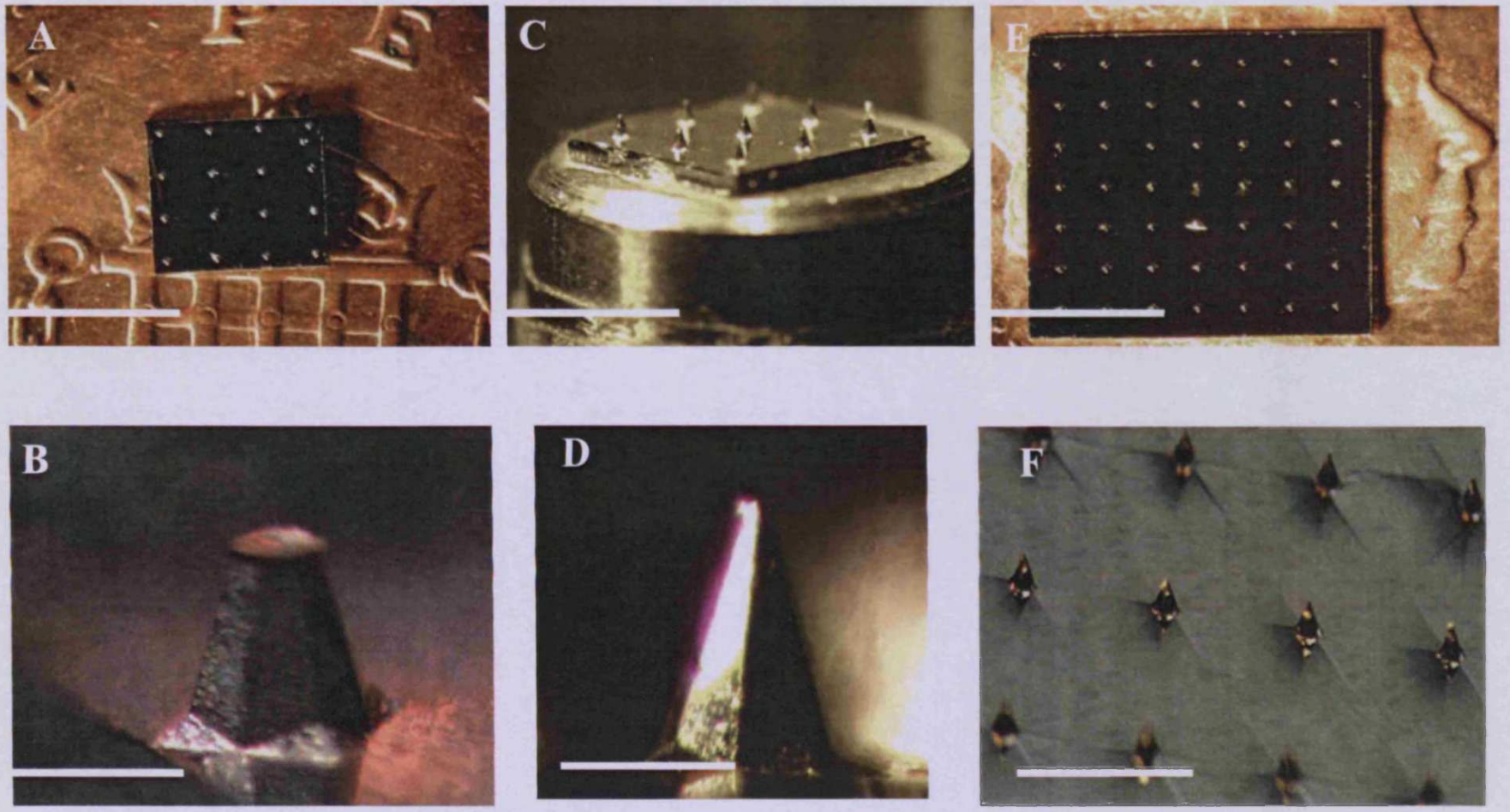

Figure 2.11 Characterisation of wet-etch microneedles by light microscopy. The wet-etch microneedle can be categorised into three arbitrary groups, frustum tip microneedles (A &B) have a relatively large flat tip; intermediate microneedles also have a flat tip but is considerable smaller than the frustum tip (C & D); and sharp tipped microneedles (E & F). A, C, and E Bar = 0.5cm; B, and D bar = 200μm; F bar = 300μm.

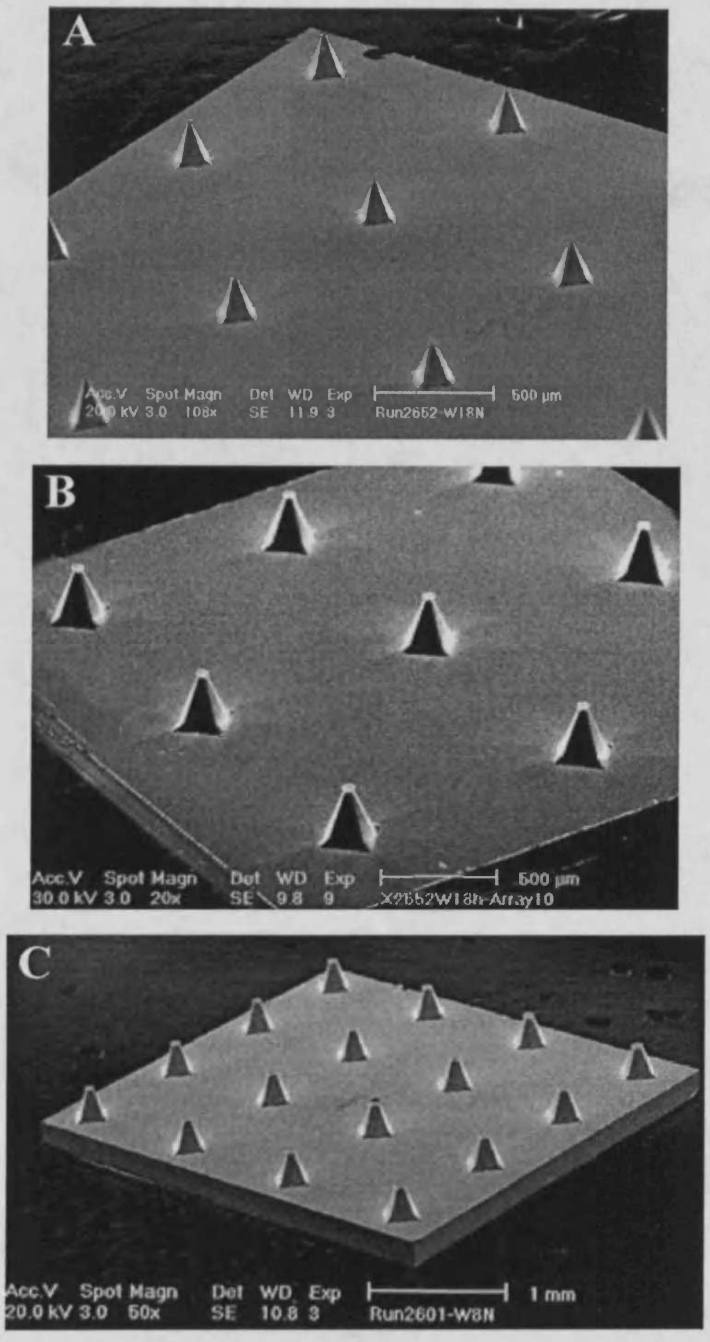

Figure 2.12 Characterisation of wet-etch microneedles by SEM. The different microneedle morphologies, sharp (A; bar = 500µm), intermediate (B; bar = 500µm), and blunt (C; bar = 1mm) are clearly apparent.

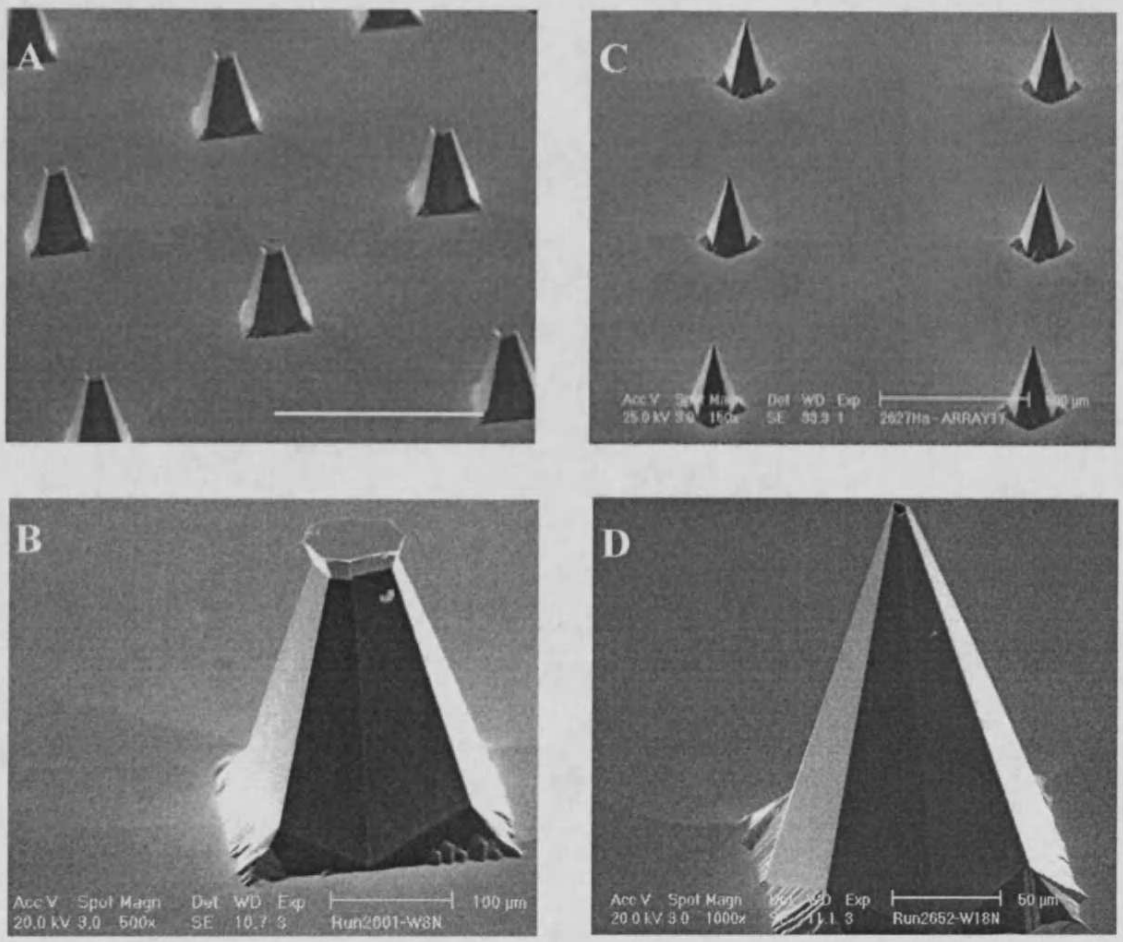

Figure 2.13 Characterisation of frustum and sharp tip microneedles by SEM at low magnification (A & B) and at higher magnification (C & D). A and B bar = 500µm; C bar = 100µm; and D = 50µm.

2.4.3 Polymer microneedle manufacture

Polymer microneedles were formed from two different kinds of polymer, Biresin® and Alparesin 12. The Biresin® polymer microneedle appeared grey in colour and typically ~1cm^2 had a fairly thick base, often 2-5mm thick (Figure 2.14 A). Light microscopy revealed that the microneedle were arranged exactly the same as the silicon master array, tip to tip distance of 1mm (Figure 2.14 B & C). At higher magnification the pyramidal structure becomes apparent and the sharp tips, characteristic of the sharp silicon microneedles, is clear (Figure 2.14 D). The Alparesin 12 polymer microneedles were yellowish in colour and were of similar dimensions to the Biresin® polymer needle but had a much thinner base.

However, SEM revealed that microneedles based on Biresin® polymers were extremely porous particularly in the base regions (Figure 2.15 A) but also the microneedles themselves were extremely porous (Figure 2.15 B). This is likely to reduce the mechanical strength the microneedle. In contrast the microneedle formed from the Alparesin 12 polymers did not appear to have any pores in either the base region (Figure 2.15 C) or in the microneedles (Figure 2.15 D). The polymer microneedle heights were 260μm in both cases, which is too be expected as they were formed in moulds created using 260μm silicon microneedle.

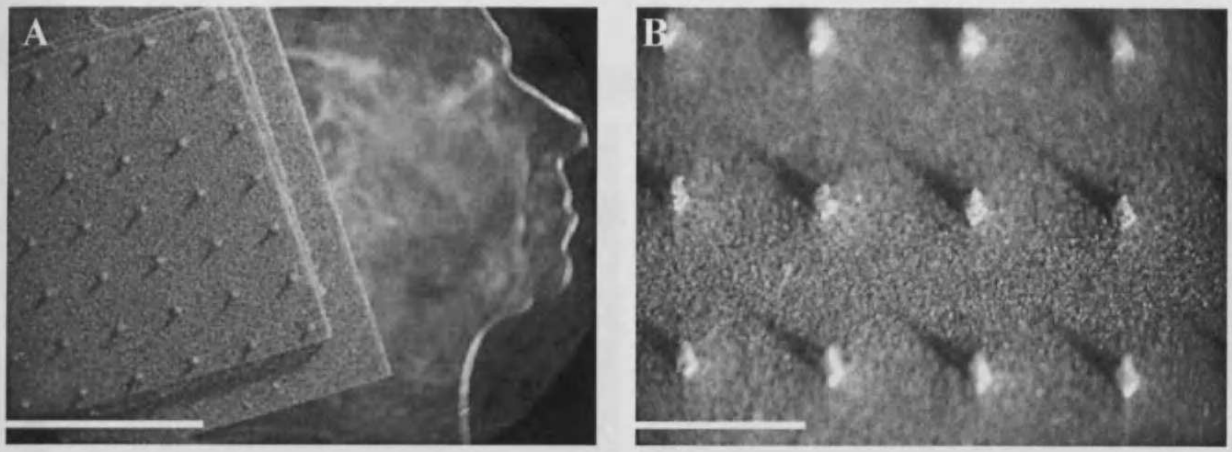

Figure 2.14 Microneedles manufactured from Biresin® polymer as observed by light microscopy. A bar = 0.4mm; B bar = 1mm.

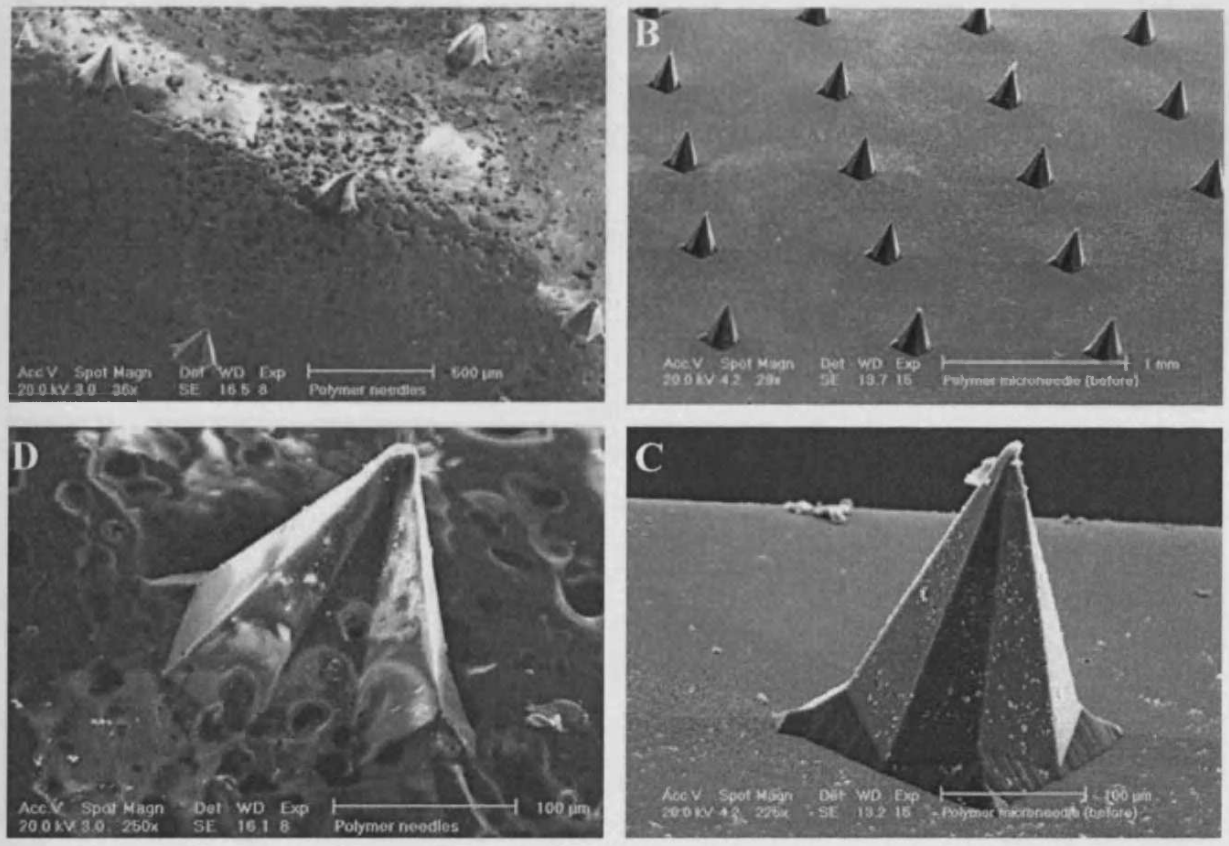

Figure 2.15 SEM images of microneedles manufactured from Biresin® (A & D) and Alparesin 12 (B & C). A bar = 500µm; B bar = 1mm; C & D bar = 100µm.

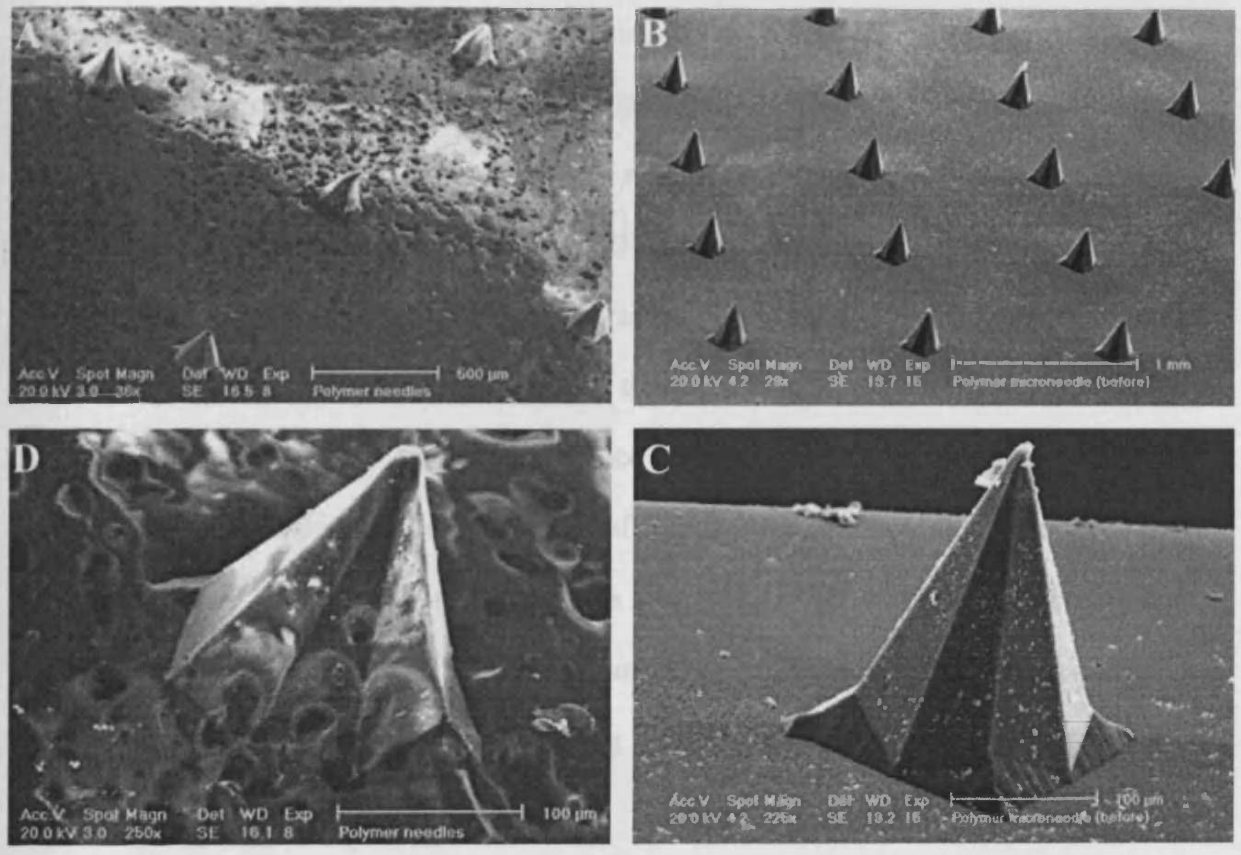

Figure 2.15 SEM images of microneedles manufactured from Biresin® (A & C) and Alparesin 12 (B & D). A bar = 500µm; B bar = 1mm; C & D bar = 100µm.

2.4.4 Hollow Microneedles

A single hollow microneedle array was manufactured, which had dimensions of ~1 by 0.5cm, it also possessed two capillary tubes that fed into the hollow chamber under the microneedles and could be attached to a syringe (Figure 2.16 A). Because they were manufactured by dry-etching they had a similar appearance to the dry-etch microneedle array described previously. Light microscopy revealed that the channels open on the side of the microneedle, retaining much of the tip (Figure 2.16 B). The channels were formed uniformly in each of the microneedle in the array (Figure 2.16 C). Using SEM it was possible to show that the microneedles had a tip to tip distance of ~250μm (Figure 2.16 D) and a height of 200μm. The channel orifice had a diameter of 50μm and passed the entire length of the microneedle though just off centre which ensured that part of the tip remained (Figure 2.16 E). The ability to pass solutions through the hollow microneedle device was confirmed using a blue dye solution, with little effort being required and minimal resistance observed, when injecting dye through the microneedles (data not shown).

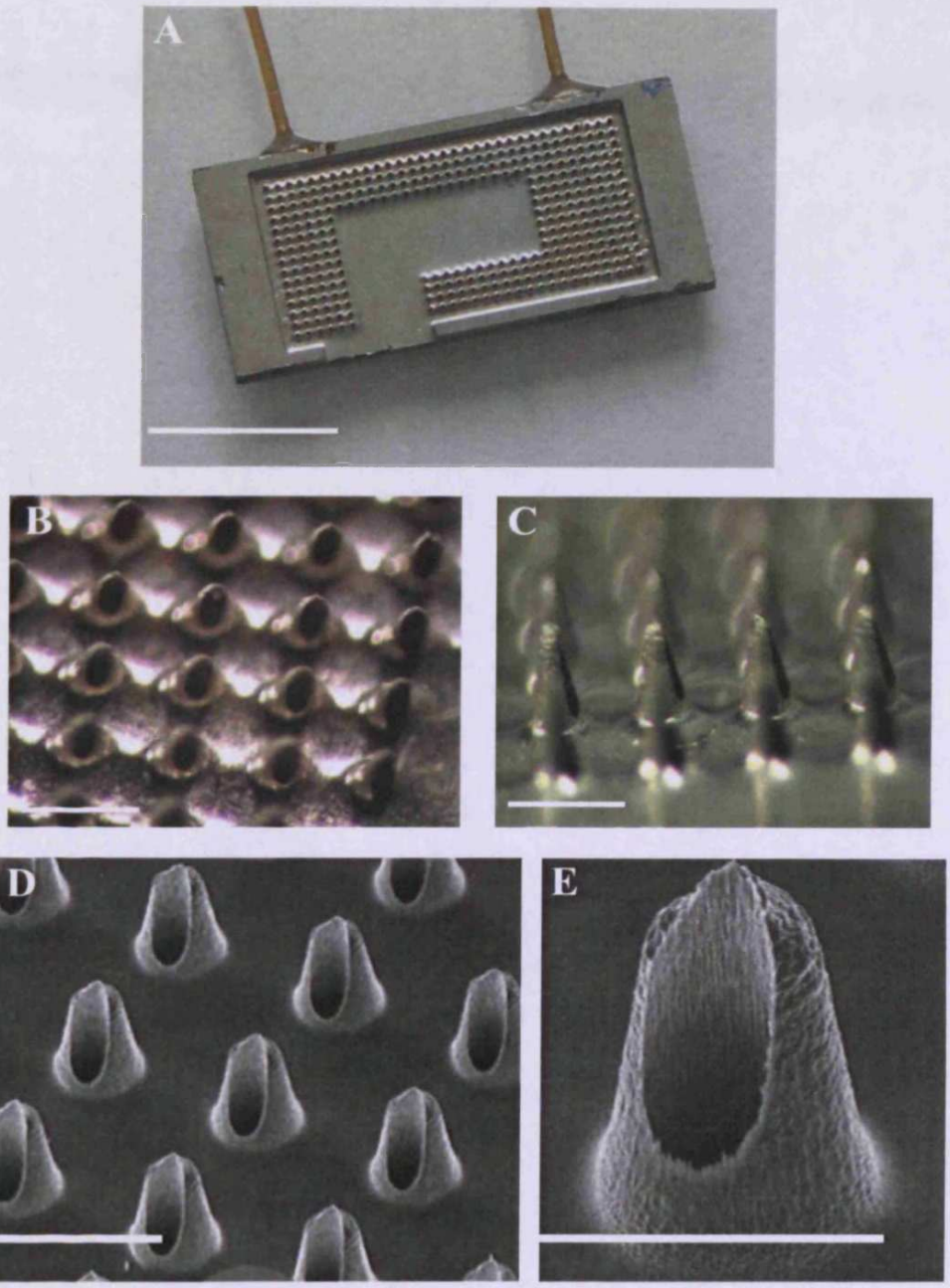

Figure 2.16 Hollow microneedle as they appear by light microscopy (A, B & C) and by SEM (D & E); Bar ~ 0.5cm for A; ~200μm for all other images.

2.4.5 Comparison of mounted and unmounted microneedles in disrupting the SC determined by transepidermal water loss (TEWL) measurements.

Excised human skin treated with microneedles alone, unmounted onto any applicator, showed no significant difference in TEWL compared to intact skin. Surprisingly, application of a 26G hypodermic needle also showed no significant difference compared to intact skin. However, this is probably due to the needle track closing up or collapsing as the hypodermic needle is removed. However, when mounted microneedles are applied to *ex vivo* skin there was a significant increase in TEWL compared to intact skin ($P = < 0.05$). Indicating that mounting the microneedle does have an effect on their ability to disrupt the SC (Figure 2.17).

2.4.6 TEWL measurement of mounted microneedles, applied flat or in a single rolling motion, to *ex vivo* human skin pinned out flat on a cork dissecting board

TEWL measurements showed that there was no significant difference between applying the microneedles either flat or in a rolling motion when *ex vivo* skin was pinned flat. Also there was no difference in skin treated with a 26G hypodermic needle. This indicates that pinning the skin on a flat cork dissecting board is not suitable for applying microneedles (Figure 2.18 A).

2.4.7 TEWL measurement of mounted microneedles, applied flat or in a single rolling motion, to *ex vivo* skin pinned over a curved cork support

Once again, when microneedles are applied flat to *ex vivo* skin pinned on a curved support there is no significant difference compared to intact skin. Similarly, there was also no significant difference between intact skin and the application of a 26G hypodermic needle. However, there was a significant difference ($P = < 0.05$) when the microneedles are applied in a single rolling motion to *ex vivo* skin pinned over a cork support (Figure 2.18 B).

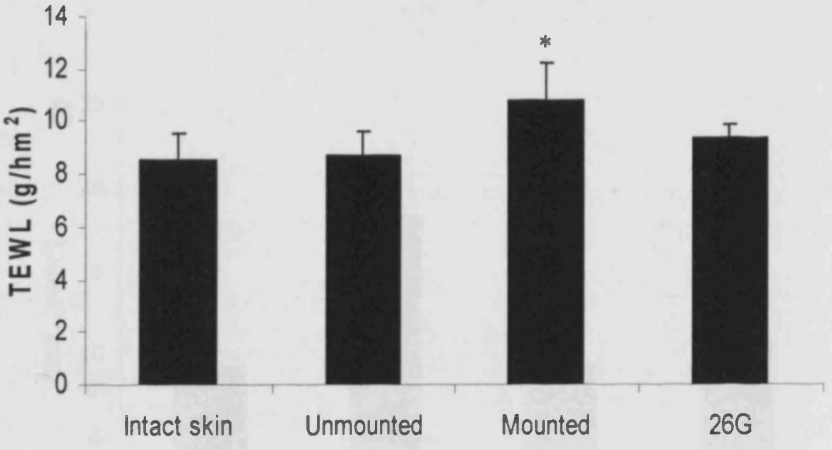

Figure 2.17 The effect of applying microneedle to skin either mounted or unmounted. Significant difference between intact skin versus mounted microneedles, $P = < 0.05$ (*). Indicating that applying microneedles mounted on a metal cylinder is a more effective means of disrupting the SC (n = 4 for each sample ±SD).

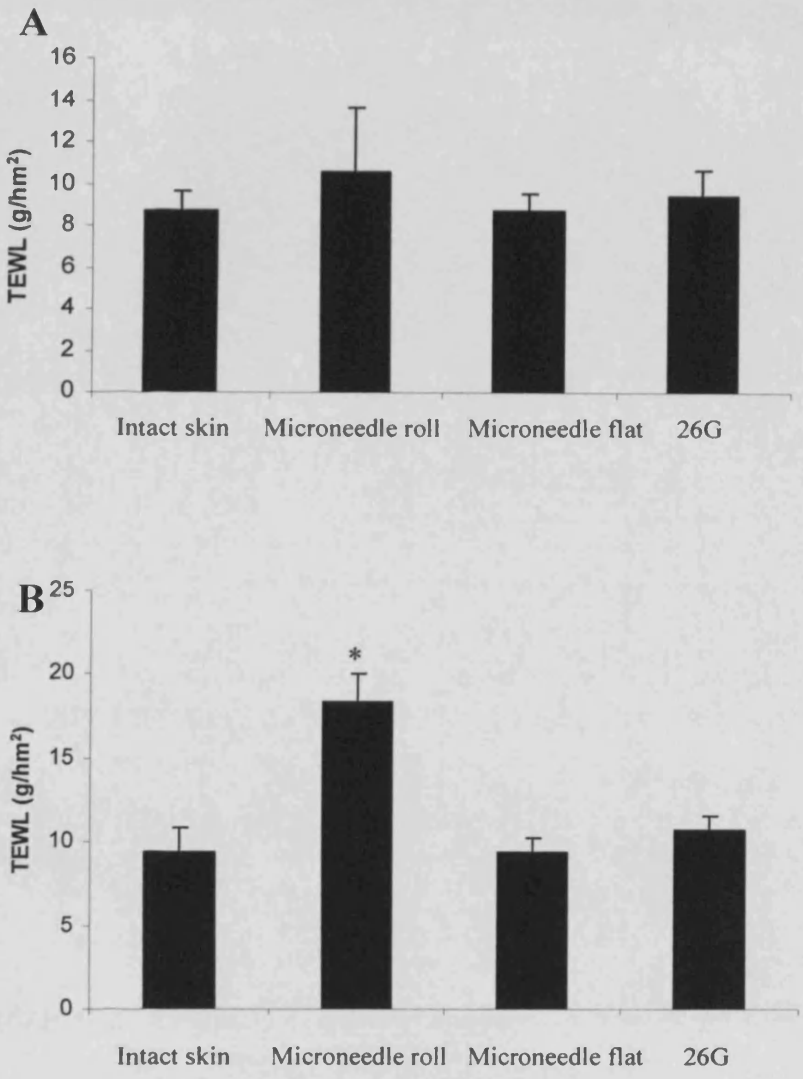

Figure 2.18 The effect of different methods of pinning ex vivo human skin for microneedle application, (A) are the results when the skin is pinned on a flat cork support and (B) when it is pinned over a curved cork support. A significant difference is observed ($p = < 0.05$) when the array is applied in a single rolling motion on the curved cork support ($n = 4$ ±SD for each sample).

When *ex vivo* skin was pinned over a cork support it mimics more the *in vivo* state compared to when the skin was pinned on a flat cork support. It is proposed that pinning *ex vivo* skin over a curved cork support generates significant tension in the skin that is lost when it is excised from the patient. Consequently, when microneedle are applied to skin pinned out flat the energy is dispersed through the tissue, and this "cushioning" effect limits the penetrative capabilities of the microneedles. In contrast, when the skin is pinned over the curved cork support the increased tension generated within the *ex vivo* skin ensures energy is more effectively transferred into the tips of the microneedles resulting in increased penetrative capabilities.

2.4.8 Comparison of the effect of different microneedle heights on the disruption of the SC as determined by TEWL

TEWL measurement showed that there was a significant difference between intact skin and skin treated with microneedles that have heights of 80μm ($P = < 0.05$). Microneedles that have heights of 180μm showed no significant difference in TEWL compared to intact skin. While, 280μm microneedles did show significant increase in TEWL compared to intact skin ($P = < 0.05$). Additionally, there was also a significant increase in TEWL ($P = < 0.05$) between 80μm and 280μm microneedles when applied to the skin (Figure 2.19). This demonstrates that microneedles with greater heights are more efficient at disrupting the SC compared to those with smaller needle heights. It is likely that microneedle with greater heights reach further into the epidermis creating more cellular disruption and accordingly creates bigger channels because a greater proportion of each individual microneedle penetrates the skin.

2.4.9 Comparison of polymer and silicon microneedles ability to disrupt the SC

Application of silicon and polymer microneedles resulted in a significant increase in TEWL compared to intact skin ($P = < 0.01$). There was no significant difference of TEWL between polymer and silicon microneedles, indicating that polymer microneedle and silicon microneedle are equally efficient at disrupting the SC (Figure 2.20).

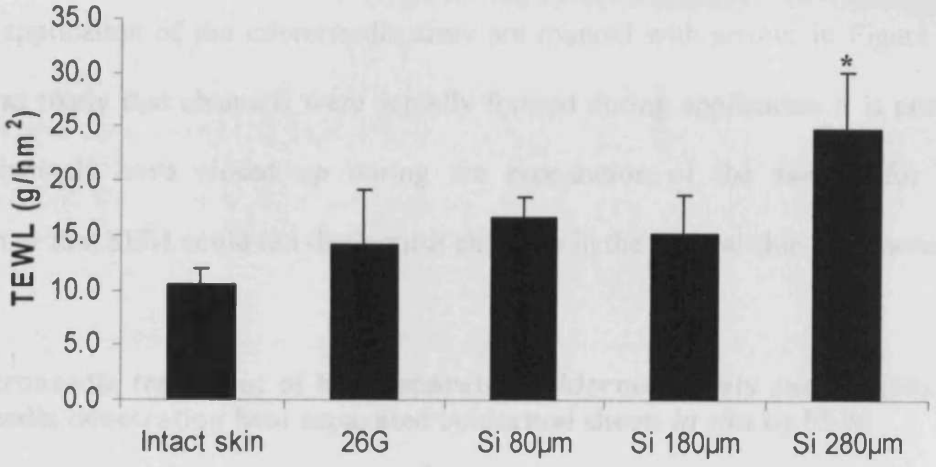

Figure 2.19 The effect of different height of silicon microneedles and their ability to disrupt the SC compared to that treated with a 26G hypodermic needle and intact skin (n = 4 ± SD for each sample).

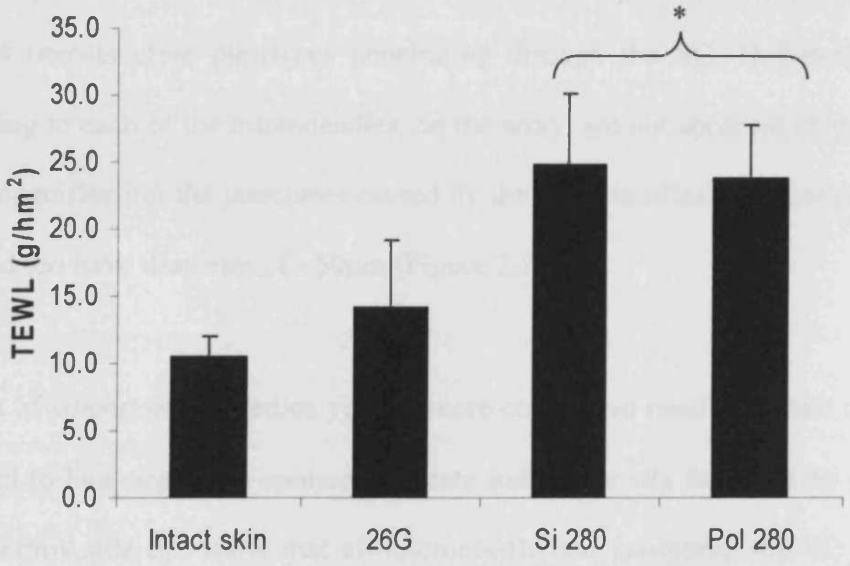

Figure 2.20 The effects of applying 280µm Biresin® polymer microneedles compared to 280µm silicon microneedles with identical array dimensions, both microneedles types significantly disrupt the SC (n = 4 ± SD for each sample).

2.4.10 Microneedle treatment of full thickness human skin viewed by SEM

SEM of full thickness human skin, treated with a 4 X 4 silicon array with microneedle heights of 280μm revealed no conclusive evidence of SC disruption. Potential channels caused by application of the microneedle array are marked with arrows in Figure 2.21. While it was likely that channels were actually formed during application it is probable that the channels have closed up during the preparation of the sample for SEM observation or that SEM could not distinguish channels in the general skin morphology.

2.4.11 Microneedle treatment of heat separated epidermal sheets and visualization of microneedle penetrating heat separated epidermal sheets *in situ* by SEM

Intact human heat separated epidermal sheets viewed *en face* by SEM reveals the natural crevices and ridges that constitute the fine structure of the skin surface (Figure 2.22 A). Following application of mounted polymer microneedles to heat separated epidermal sheet, SEM reveals clear punctures penetrating through the SC. However, punctures corresponding to each of the microneedles, on the array, are not apparent (Figure 2.22 B). At higher magnification the punctures caused by the microneedles are clearly visible and are observed too have diameter of ~50μm (Figure 2.22 C).

Application of silicon microneedles yielded more conclusive results. When microneedle were applied to heat separated epidermal sheets and left *in situ* followed by observation by SEM, dermis side up, show that all microneedle had punctured the SC and passed through the epidermal sheet (Figure 2.23A). Higher magnification shows clearly the tips of microneedle within the formed punctures (Figure 2.23 B). When the microneedle array was applied and removed and the heat separated sheet viewed epidermis sides up,

then the punctures through the SC are clearly apparent, each corresponding to a microneedle on a 4 X 4 microneedle array (Figure 2.23 C). What is apparent from Figure 2.23 C is that some of the channels are relatively large, with diameters between 150-200μm while others, particularly in the central regions are smaller ~50μm.

2.4.12 Microneedle robustness

Both unused polymer and silicon microneedle arrays were characterized by SEM to ensure that all microneedles were intact. After repeated applications to the skin (total of 10), the SEM of the microneedle arrays showed that all the microneedle remained intact (data not shown).

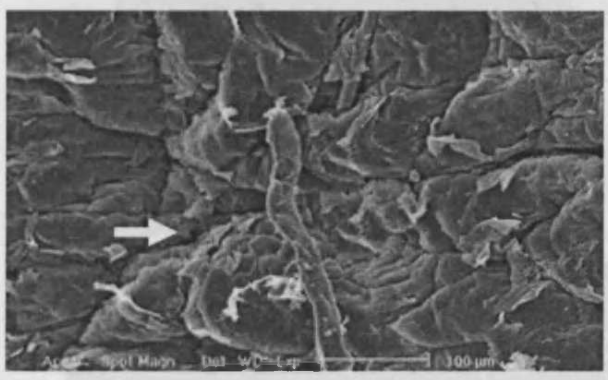

Figure 2.21 An SEM image taken of full thickness *ex vivo* human skin treated with a 4 X 4 silicon microneedle array with heights of 280μm. No conclusive punctures are visible, a possible channel is indicated with the arrow; bar = 100μm.

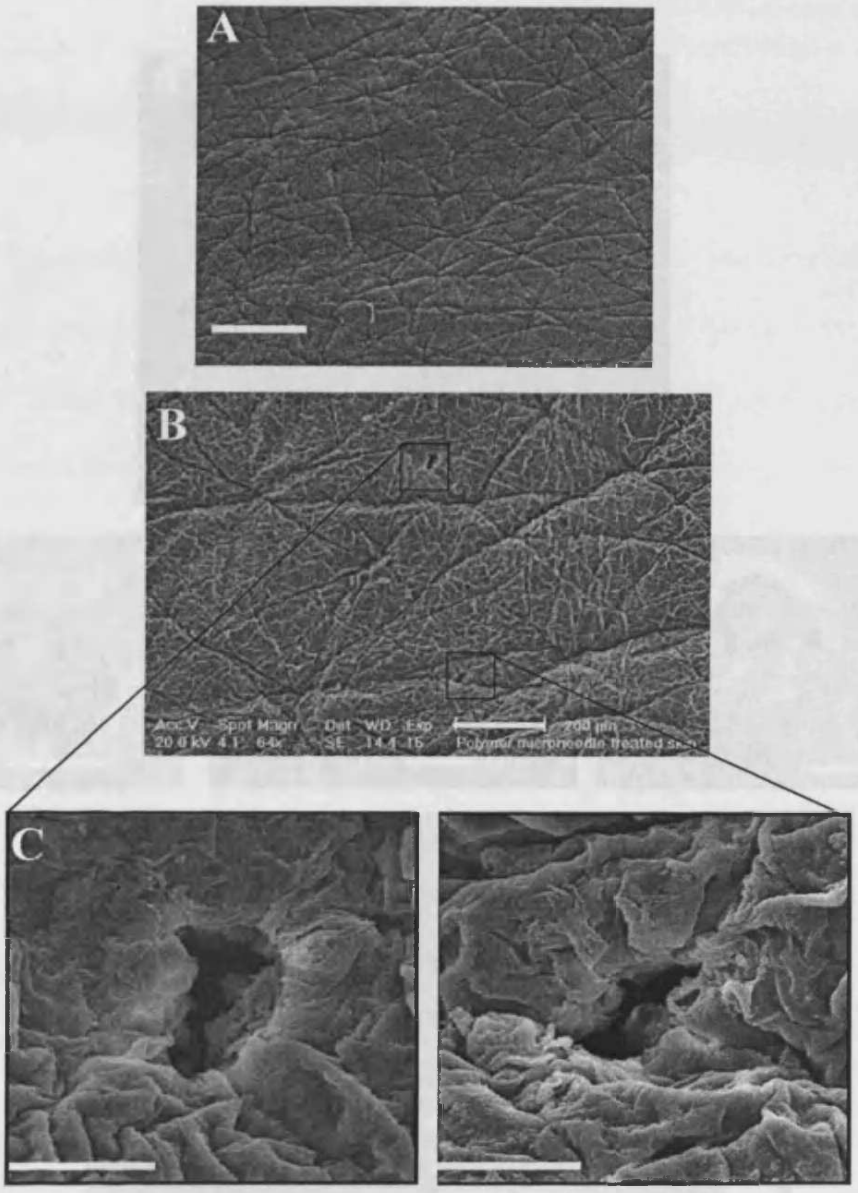

Figure 2.22 SEM images of human heat separated epidermal sheets. The skin surface of intact skin is shown in (A), following application of a polymer microneedle array 2 distinct punctures are clearly visible, highlighted in the black squares (B). At higher magnifications the 2 clear punctures are clearly apparent with diameters of ~50μm (C). A bar = 500μm, B bar = 200μm, and C bar = 50μm

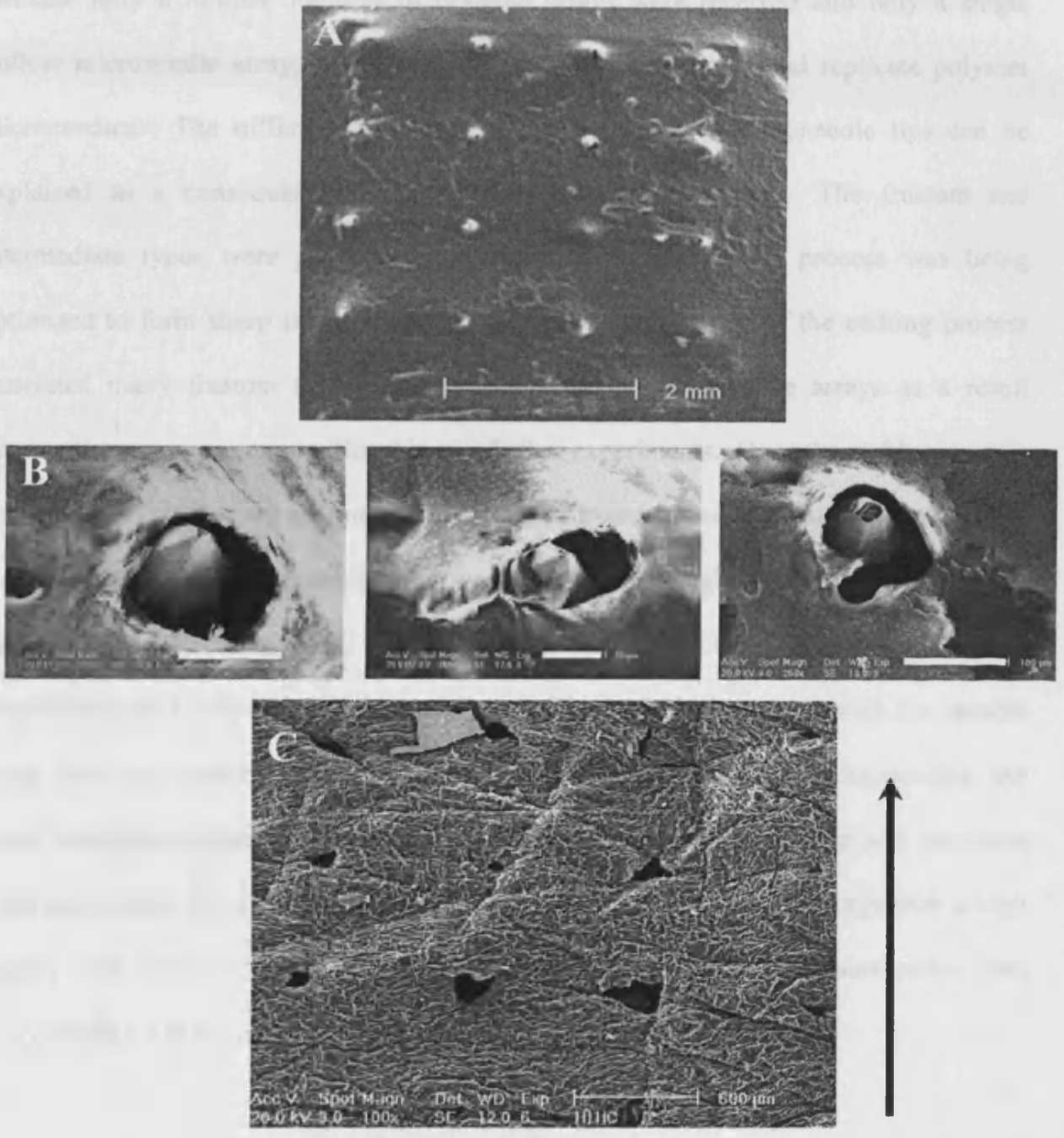

Figure 2.23 SEM images of silicon microneedles penetrating heat separated epidermal sheets, with the array remains *in situ* and observed dermal side up, tips of microneedles can be seen penetrating the basement membrane (A) and at higher magnifications (B). When the array is removed and the membrane is observed epidermis side up, clear punctures created by the array are evident (C). The arrow indicates the direction the microneedle array was rolled onto the skin. A bar = 2mm, B bar = 100μm, and C bar = 500μm.

2.5 Conclusions

Because only a limited numbers of dry-etch arrays were received and only a single hollow microneedle array, more focus was applied to wet-etch and replicate polymer microneedles. The different morphologies of the wet-etch microneedle tips can be explained as a consequence of sub-optimal etching conditions. The frustum and intermediate types were generated inadvertently; as the etching process was being optimized to form sharp tipped microneedles. The optimization of the etching process generated many frustum tipped arrays but not many intermediate arrays as a result intermediate types were not utilized in any further experiments. Once the etching process had been fully optimized all microneedle arrays formed contained sharp tipped needles. Furthermore, microneedles could be formed with various heights, ranging from 30μm to 300μm. Wet-etch microneedle also displayed a lower microneedle density per area of array compared to dry-etched microneedles (Wilke *et al* 2005). Along with the notable lower cost and technical involvement required to produce wet-etch microneedles, the lower microneedle density is likely to ensure that wet etch microneedle will penetrate more easily than dry-etch microneedles. This is because microneedle arrays with a high density will create a "bed of nails" effect, dispersing the applied pressure rather than concentrating it at the needle tips.

The polymer microneedle formed from Biresin® were very porous in appearance and because of this it is likely that the overall mechanical strength of the microneedles will be reduced, also many microneedle were bent or otherwise deformed (a close look at Figure 2.15 A demonstrates this). The reason for this was not clear but probably due to

errors during the manufacturing process rather than the polymer itself, possible failure to fully de-gas the polymer solution prior to pouring into the moulds. In contrast the Alparesin 12 polymer microneedles appeared virtually identical to silicon microneedle. There was virtually no deformation to the microneedle (Figure 2.15 C), and only the extreme tips of a small fraction appeared slightly bent (e.g. the tip in Figure 2.8 D is slightly bent).

The hollow microneedle array was able to conduct fluids (data not shown). However, from a design point of view there was a problem with the array that would inevitability influence application. During manufacture, etching was performed in the central region of a silicon wafer which resulted in the microneedles being formed in a depressed region of the wafer. This is usually not a problem because the raised regions of the wafer, if present, can be removed. However, in this case the raised part of the wafer was required to remain so that the wafer could be bonded with another to create the fluidic chamber under the microneedles. Consequently, much of the microneedle height was lost. Therefore application and subsequent disruption too the SC proved more difficult.

A clear factor that immerged from these studies was the need for the microneedles to be mounted onto an applicator rather than be used as received following manufacture. The reason for the increase SC disruption observed with mounted microneedles is due to more pressure exertion at the needle tips. Furthermore, presentation of the skin prior to microneedle application, i.e. weather it was pinned, pinned flat or pinned over a semi-circular curved cork support, affects SC disruption. *Ex vivo* skin loses a lot of its internal

tension and rigidity when it is excised from a patient. Therefore, when microneedles are applied, either mounted or unmounted, the skin deforms with the applied pressure, and consequently microneedle penetration is much reduced. In contrast, when the skin is pinned out tension is generated and rigidity returns to the skin. So when microneedles are applied, the pressure generated at the array surface is localized and the needles are able to penetrate the SC. Moreover, SC disruption is further increased when the mounted microneedles are applied in a single rolling motion. In this method of application only part of the array comes into contact with the skin surface initially, the needles that do are able to exert high pressure and therefore are highly penetrative. As the array passes through the rolling motion (Figure 2.8) the skin underneath is further stretched increasing the tension in the skin and also the entire applied pressure is concentrated on a single row of the microneedle array making it easier to penetrate. When the skin was observed after microneedle application this way punctures formed by the microneedles that first come into contact with the skin are much larger that those which come into contact later (Figure 2.23 C). These larger channels are likely to result from tears emanating from the punctures while the skin is being further stretched, however, it is also likely that processing the sample for SEM will also exaggerate the tears. Silicon and polymer microneedles arrays of the same dimensions were equally able to disrupt the SC (Figure 2.20) when applied in the same way, implying both types of needle were suitable for application in the skin. Both polymer and silicon microneedle arrays were demonstrated to show that they were sufficiently robust to be applied repeated to the skin with no observable damage being observed.

Therefore, we can conclude that microneedle arrays can be formed in a verity of ways resulting in needles with different morphologies. Because of the limited numbers of certain types of microneedle, e.g. hollow microneedle, only limited use could be made of them. Consequently, the majority of studies undertaken in this thesis will be conducted using solid silicon microneedle, both sharp and frustum tipped and also polymer microneedles but the emphasis will be with solid silicon microneedles. The best method for applying microneedles to *ex vivo* human skin requires that it be pinned over a semi-circular curved cork support and the microneedle mounted on a metal cylinder and applied in a single rolling motion. As a result, all applications of microneedle to *ex vivo* skin will be done this way, unless otherwise stated.

While these results show that microneedle are able to disrupt the SC it must be demonstrated that application can also facilitated the delivery of substance to the viable regions of the epidermis. This is the subject of the next chapter.

CHAPTER 3: The ability of microneedles to facilitate the passage of low molecular weight dyes, nanoparticles and macromolecules across the SC

3.1 Introduction

Microneedles are able to disrupt the SC, which results in the physical barrier properties of the skin being compromised (Birchall *et al* 2005). The subject of this chapter was to demonstrate that application of microneedles removes the barrier function of the SC facilitating the passage of substances into the epidermis, in particular macromolecules and nanoparticles. This is crucial because it is the epidermis that contains viable cells, e.g. keratinocyte and Langerhans cells, and these are the primary targets in cutaneous gene delivery strategies (Kendall 2006; Mullholland *et al* 2006). Since microneedle application to the skin results in the formation of microconduits of a depth equal to, or less than, the length of the microneedles, in principal, it should be possible to target the formulation to the epidermis by careful optimization of needle length. It is vital that the delivery formulation reach the deeper layers of the epidermis because these cells are metabolically active, genetically active and therefore capable of expressing exogenous DNA. This is in contrast to some of the other common methods, such as biolystics, where depth of penetration is often variable and is typically dependent on environmental factors such as temperature and relative humidity (Kendall *et al* 2004). Also, biolystic delivery often results in damage and death of the target cells, with the degrees of cell death being dependent on the number of micro-particles fired into the skin (Raju *et al* 2006). While it is likely that there will be a certain amount of cell damage and even death associated with microneedle application, it is likely to be considerable less compared to biolystic delivery, because of the lack of sonic shock waves and high velocity micro-particles (Kendall *et al* 2004).

3.1.1 Delivery formulation application and microneedle application

One important consideration when designing a microneedle delivery strategy is whether the formulation should be applied to the skin before or after microneedle application (Figure 3.1). Consider the application of microneedles prior to the introduction of a liquid formulation. It is reasonable to anticipate that air, trapped within the microconduit, would prevent migration of the formulation into the channel or alternatively that the microconduits closes up as the microneedles are removed. Additionally, even if the channel does not close to any degree, it is likely to fill with biological fluid through which the delivery formulation must travel to contact the target cells, therefore its imperative that the active ingredient of the formulation remains stable in the biological milieu. Biological fluid and the skin surface contain nucleases, which will degrade DNA formulations Barry *et al* estimate that 99% of naked DNA injected into skin and muscle is degraded most probably in the extracellular milieu within 90 minutes of injection (Barry *et al* 1999). Therefore, applying the delivery formulation and relying on passive movement, of the active ingredient to the viable cells, is introducing many factors that could ultimately reduce efficiency.

In contrast, if the delivery formulation is applied to the skin surface before the application of a microneedles array, then as each needle penetrate the SC a small quantity of the formulation will be taken with it (Figure 3.2). The process of microneedle insertion will result in some damage to epidermal cells adjacent to the microchannels. Although it is likely that major disruption of the cell membrane would bring about cell death it is also possible that minor disruption to the cell membrane may promote uptake of pDNA by

target cells (Budker *et al.* 2000). Therefore, by applying the formulation before microneedle application it might be expected to be a far more suitable and efficient method of applying the delivery formulation.

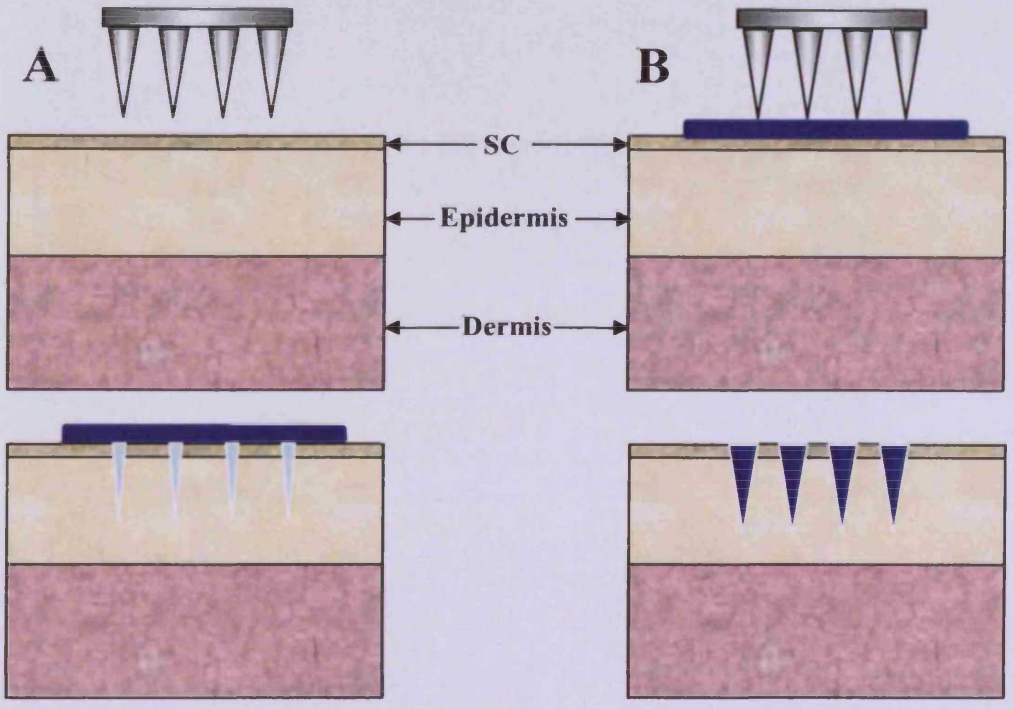

Figure 3.1 Delivery of a liquid formulation to the epidermis facilitated by microneedle. When the formulation is applied after the microneedles (A) it is proposed that resulting air pockets and microchannels constriction restrict the passage of the formulation to the target region. In contrast, when the array is applied after the formulation (B), the formulation is physically forced into the channels, therefore, delivering more of the formulation to the target region.

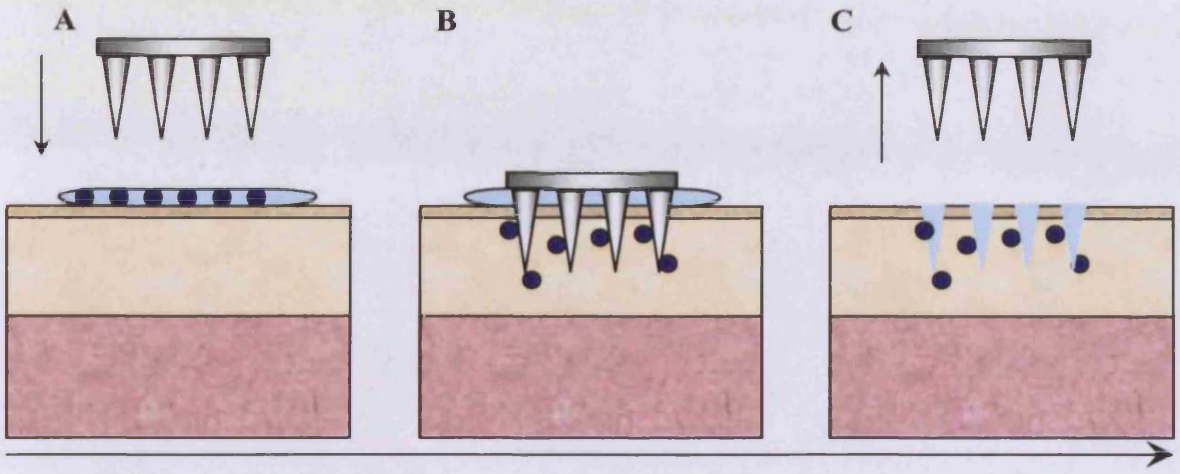

Figure 3.2 A schematic of the proposed mechanism for microneedle facilitated macromolecular delivery to the epidermis when the formulation is applied to the skin surface before microneedle application (A). Microneedle physically drive the macomolecules (blue circles) through the SC (B), depositing them in the viable epidermis (C).

3.1.2 Utilization of human *ex vivo* skin to demonstrate successful microneedle facilitated delivery of formulations through the SC

To demonstrate that microneedle are able to enhance passage of macromolecules and nanoparticles across the SC, *ex vivo* human skin was utilized. A regular supply of *ex vivo* skin was obtained through collaboration with surgeons at the Royal Gwent Hospital, Newport, UK. Initial studies attempted to further validate work performed by others (Chabri *et al.* 2004; Coulman *et al.* 2006; Henry *et al.* 1998; McAllister *et al.* 2000; McAllister *et al.* 2003; Prausnitz 2004), building on their work by delivering low molecular weight dyes, e.g. methylene blue, fluorescently labeled macromolecule, e.g. albumin, fluorescently labeled nanoparticles and pDNA.

3.1.3 Techniques

A number of methods were utilized and established in order to investigate the capabilities of microneedles for the delivery of substances across the SC.

3.1.3.1 Flourescent Microscopy

A flourophore is a molecule that is able to absorb light at a specific wavelength, i.e. imputing energy, this results in excitation of the flourophore. The excited state cannot be maintained and the ground state is regained. The extra energy is emitted as a longer wavelength photon, which is specific for the flourophore. Utilizing this phenomenon, in conjunction with microscopy, enables the specific location of the flouophore to be determined. In these series of experiments, fluorescent microscopy has been employed to detect fluorescent nanoparticles and macromolecules delivered by microneedle to human skin in both cryosections and tape strips.

3.1.3.2 Cryosectioning of treated samples for fluorescent microscopy

Delivery of fluorescently labeled substances, like FITC labeled albumin and fluorescent nanoparticles in human skin was detected by fluorescent microscopy following the generation of cryosection.

Cryosectioning permits a rapid means of generating sections for histological observation. It requires fixation of the tissue sample, in this case skin, so as to maintain the fine structure of the sample, followed by embedded in a suitable embedding medium, for

example optimal cutting temperature (OCT) media. The sample is sectioned using a cryostat, which is a microtome enclosed in a chamber maintained around -20°C. Cryosections can then be observed by light or fluorescent microscopy to providing information about depth and delivery facilitated by microneedles.

3.1.3.3 Tape stripping for fluorescent microscopy

A further method that can provide information regarding passage of delivery formulations across the SC, delivered by microneedles is to tape strip treated regions of skin and examine the strips by microscopy. This method is often used as a means of determining the depth of penetration of topically applied formulations (Rougier *et al* 1987). The easiest way is the application of adhesive tape designed specifically for the process. Application and removal of the adhesive tape results in sequential depletion of the skin surface, first the SC and then the deeper layers of the epidermis. Therefore, this provides a crude means of showing the depth a specific substance has penetrated. For example, if a fluorescent formulation was applied to the surface of intact skin and the region then subject to sequential tape strips followed by observation of the tape strips by fluorescent microscopy, the fluorescent signal should be lost after only a limited number of tape strip applications. The reason being the fluorescent formulation will be restricted by the SC, therefore cannot penetrate to any depth in the epidermis, thus requiring few tape strips to remove it. In contrast, if the fluorescent formulation was applied in conjunction with the microneedles it might be expected that the fluorescent formulation would be more effectively pushed deeper into the skin and therefore fluorescence would be observed on a greater number of tape strips.

3.1.3.4 Electrophoresis of pDNA through microneedle treated epidermal sheets

To demonstrate that microneedle create conduits through the SC for the passage of pDNA, essential for gene delivery strategies, can be achieved using heat separated epidermal sheets in conjunction with gel electrophoresis. If heat separated epidermal sheets are placed in front of electrically induced motive pDNA the SC should restrict the passage across the membrane. In contrast, application of microneedles should remove the SC barrier providing channels for the passage of the pDNA across the membrane.

3.1.3.5 Preparation of pDNA

Experiments in this chapter and in proceeding chapters require a source of pDNA; two plasmids were prepared each encoding a different reporter gene. The first, pEGFP-N1 is a plasmid composed of 4.7kb and encodes Enhanced Green Fluorescent Protein (EGFP). The second, pCMVβ is slightly larger at 7.2kb containing the reporter gene lacZ, which encodes the enzyme β-galactosidase; both reporter genes are under the control of the cytomegalovirus (CMV) promoter. Each plasmid contains a specific antibiotic marker gene that allows cells containing the plasmid to have a selective growth advantage over cells that do not, molecular maps of each plasmid are shown in Figure 3.3.

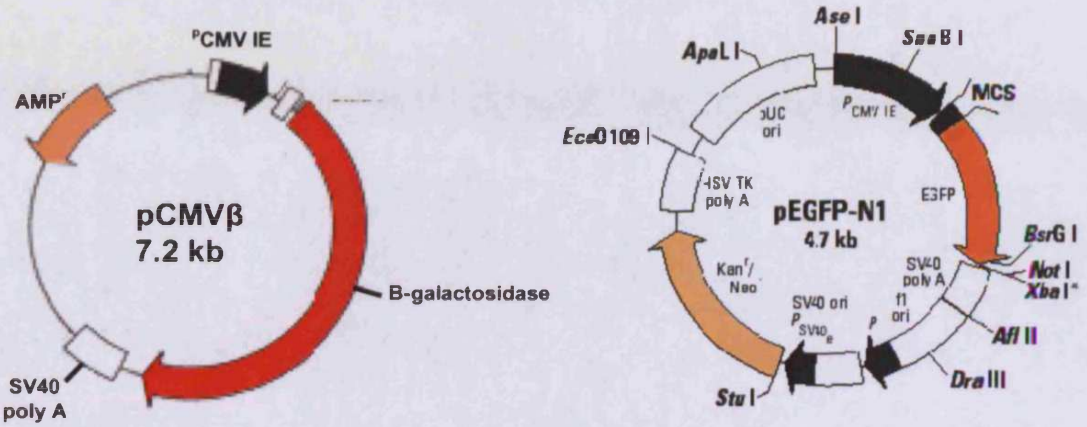

Figure 3.3 Molecular maps of the two reporter plasmids used in the proceeding studies. The maps show the various features and genes encoded by each plasmid.

3.1.3.6 Migration across heat separated epidermal sheets treated with microneedle

The ability of substances to migrate across surfaces can be assessed using Franz-type diffusion cells. A Franz-diffusion cell is composed of two individual components, a donor phase and a receptor phase. These two components can come together, allowing a diffusive surface to be mounted between them In this case the diffusive surface can be either an artificial membrane (Millipore polycarbonate track-etch membrane) or heat separated epidermal sheets treated with or without microneedles. Migration is assessed by measuring the passage of a formulation from the donor phase across the diffusive surface into the receptor phase by sampling from the receptor phase at predetermined time intervals.

3.2 Aims and objectives

3.2.1 Aims

The aim of this chapter is to demonstrate that microneedles cause sufficient disruption to the permit passage of macromoles and nonparticles across the SC. The dimensions and depth of penetration that the microneedle achieves will also be investigated.

3.2.2 Objectives

- To investigate the penetrative capabilities of microneedles in delivering formulations to the skin
- To observe if applying the formulation before or after microneedle treatment has any effect of delivery
- To further confirm the ability of microneedle arrays to compromise the SC
- To demonstrate that microneedles are able to deliver low molecular weight molecules, macromolecules and nanoparticles to *ex vivo* human skin.

3.3 Materials and methods

3.3.1 Materials

All reagents used during these studies, unless otherwise stated, were of analytical grade and purchased from Fisher Scientific (Loughborough, UK)

Ethidium bromide, fluorescent polystyrene nanospheres (both yellow/green and red), 50% glutaraldehyde solution, FITC conjugated albumin, Hoechst 33258, LB agar and broth were all obtained from Sigma Aldrich Limited (Poole, UK)

Agarose bought from Promega Corporation (Madison, USA). Loading dye obtained from Bioline Limited (London, UK)

Materials used for histological studies, such as adhesive microscope slides and OCT embedding media were purchased from RA Lamb Limited (Eastbourne, UK). Disposable microtombe blades (Leica Microsystems Limited UK, Milton Keynes, UK)

Plasmid preparation with a Qiagen-tip^{TM}2500 Mega kit (Qiagen Limited, Crawley, UK)

Adhesive film D-squame tape strips purchased from CuDerm Corporation (Dallas, USA).

Deionised water obtained from an Elga reservoir (High Wycombe, UK)

3.3.2 Methylene blue application to human skin *en face*

A sample of human skin (♀ 57 years of age) was removed from -20°C storage and allowed to defrost and equilibrate to local environmental conditions, ~2 hours. All subcutaneous fat was removed from the sample, by blunt dissection, which was then pinned over a semi-circular support, (Chapter 2; Section 2.3.12). A solution of methylene blue ($C_{16}H_{18}ClN_3S$), was prepared at a concentration of 1% w/v in deionized water to a region of the skin a mounted, sharpe tipped microneedle array (7 X 7 with needle heights of 280μm) is applied in a single rolling motion, (Chapter 2; Section 2.3.13) The treated region then received 20μl of the methylene blue solution and was incubated at room temperature for 10 minutes. Other regions of the skin sample were treated with methylene blue solution prior to microneedle application. The surface of each treated region of skin was then swabbed with a tissue dampened with 70% ethanol to remove excess methylene blue solution. The treated region was then carefully excised from the skin sample and rinsed in 2ml PBS for 10 minutes, fixed in 2ml 2% v/v glutraldehyde for 2 hours at 4°C and then rinsed twice in 2ml PBS each 15 minutes. Samples were viewed *en face* with a Stemi 2000-C Stereomicroscope (Zeiss, Welwyn Garden City, UK) with a Scott 1500 fibre optic external light source (Scott UK Ltd, Stafford, UK); images were captured using a Olympus DP-10 digital camera (Olympus Optical, London, UK). Select samples were processed for cryoscetioning, which involved placing each sample in a mould of liquid OCT followed by rapid chilling on dry ice until complete solidification and storage at -80°C.

3.3.3 Tape stripping human microneedles / fluorescent nanoparticles treated skin

3.3.3.1 Size determination of nanoparticles using photon correlation spectroscopy (PCS)

The size of nanoparticles was determined by PCS using a Coulter N_4 Plus machine (Coulter Electronics Ltd., Luton, UK). A working strength solution of nanoparticles (the purchased concentrate was diluted by adding 5µl to 1ml deionized water) was further diluted 1:10 with deionised water and placed in a clear sided cuvette. Measurements were made using a 4mW laser with a scattering angle of 90° at 25°C.

3.3.3.2 Application of the fluorescent bead formulation in conjunction with microneedles

A human skin sample (♀ 54 years of age) was removed from -20°C storage and allowed to defrost and equilibrate to local environmental conditions for ~2 hours. The subcutaneous fat was removed by blunt dissection and the skin pinned over a semi-circular support (Chapter 2; Section 2.3.12). A working solution of nanoparticles was prepared by diluting 5µl of the bead concentrate in 1ml of deionized water. A region of the skin was treated with a mounted, sharpe tipped microneedle array (7 X 7 with needle heights of 280µm), applied in a single rolling motion. The treated region then received 20µl of the working strengh nanoparticle solution and was incubated at room temperature for 10 minutes. To other regions of the skin sample 20µl of the nanoparticle solution was applied prior to microneedle treatment. Subsequently, D-squame adhesive strips with an area of 3.8cm^2 were consecutively applied to the treated regions (10 minute application

time), removed and attached to microscope slides, this was repeated to the same region with a fresh adhesive film a total of 25 times. All slides were protected from light before observation with an Olympus BX50 fluorescent microscopy (Olympus, Middlesex, UK).

3.3.4 Delivery of fluorescent beads and albumin formulations to human skin in conjunction with microneedles and generation of cryosections

3.3.4.1 Delivery of fluorescent beads

A human skin sample (♀ 56 years of age) was removed from storage and allowed to equilibrate before treatment with a red fluorescent bead solution and microneedle as described previously (Chapter 3; Section 3.3.3.2). Treated regions were excised from the skin and each rinsed in 2 ml PBS for 10 minutes, fixed in 2ml 2% v/v glutraldehyde for 2 hours at 4°C, followed by 2 rinses in 2ml PBS each 15 minutes. Samples were prepared for cryosectioning (Chapter 3; Section 3.2.2).

3.3.4.2 Delivery of fluorescent albumin.

A human skin sample (♀ 60 years of age) was removed from -20°C storage and allowed to defrost and equilibrate to local environmental conditions for ~2 hours. The subcutaneous fat was removed from the skin by blunt dissection and then pinned over a semi-circular support, described previously. A solution of fluorescein isothiocyanate (FITC) conjugated albumin was prepared at a concentration of 1mg/ml by dilution with deionized water and stored in an amber bottle. The skin was treated with 20µl of the FITC conjugated albumin solution followed by application of a mounted sharp tipped

microneedle array (7 X 7 with needle heights of 280μm) in a single rolling motion (Chapter 2; Section 2.3.13). The treated regions were shielded from light by covering with foil and incubated at room temperature for 10 minutes. The treated regions were carefully excised from the skin sample, rinsed in 2ml PBS for 10 minutes, fixed in 2ml 2% v/v glutraldyhyde for 2 hours at 4°C, and then twice rinsed in 2ml PBS (each 15 minutes). The samples were then prepared for cryosectioning (Chapter 3; Section 3.2.2).

3.3.4.3 Preparation of human skin for cryosection

Cylindrical moulds were prepared from aluminum foil approximately 2cm Diameter by 2 cm height; these were cooled in a polystyrene box containing soiled CO_2. The moulds were filled with OCT embedding media and further chilled on solid CO_2 until it visibly started to solidify. At this point the skin samples were carefully placed into the moulds and orientated so that the epidermal and dermal sides of the sample were known. Each sample was held in position with forceps until the OCT was firm enough to prevent movement of the immersed skin sample. Each mould was left to completely solidify on the solid CO_2 before being stored at -80°C.

3.3.4.4 Cyrosectioning human skin samples

Samples embedded in OCT moulds were sectioned using a Leica CM3050S Cryostat (Leica Microsystems, Milton Keynes, UK). Skin sections (either 10 or 12μm) were captured onto adhesive Superfrost Plus® microscope slides, dried overnight at room

temperature and observed with an Olympus BX50 microscope (Olympus, Middlesex, UK).

3.3.5 Electrophoresis of pDNA through microneedle treated human epidermal sheets

The use of an electromotive force to drive pDNA through microneedle treated human heat separated epidermal sheets is a simple demonstration that the created conduits are of sufficient dimensions to permit its passage.

3.3.5.1 Preparation of pDNA

The two plasmids used in this study are pCMVβ and pEGFP-N1. Glycerol stocks of the bacterium *Escherichia coli* DH5α containing either one of the plasmids was remove from storage (-80°C) and used to inoculate a plate of Luria-Bertani (LB) broth-agar containing the appropriate selective antibiotic (at a concentration 100μg/ml). LB agar plates were prepared by applying 20g of LB agar powder into 500ml of deionized water. This sterilized by autoclave, allowed to cool to before the correct antibiotic added and poured into plates. Inoculated plates were incubated at 37°C, 5% CO_2 overnight. Following incubation, a single colony was taken and used to inoculate 5ml of sterile LB broth containing 100μl correct selective agent at a concentration 100μg/ml (antibiotic was added after autoclaving when the broth had cooled to ~40°C). The inoculated broth was then incubated at 37°C for 8 hours with constant agitation. A sample of this culture (1ml) was subsequently used to inoculate a larger volume (4 x 125ml) of sterile antibiotic containing LB broth and this was incubated at 37°C for 18 hours under constant agitation.

The cultures were divided into two and poured into 500ml centrifuge tubes, centrifuged at 6000 rpm for 15 minutes at 4°C. Plasmid DNA was isolated using a commercially available kit in order to ensure a high yield of pure plasmid.

The isolated plasmid was then subjected to agarose gel electrophoresis in order to investigate plasmid molecular weight and purity. A 1% agarose gel was made by dissolving 1g of agarose in 100ml of tris-borate EDTA (TBE) buffer (performed in a 500ml conical flask and placed in microwave on full power for 1min). Once the dissolved agarose had cooled, ethidium bromide was added to a give a final concentration of 0.5μg/ml. A sample of isolated plasmid (1-2μl) was mixed with DNA loading dye and transferred to a well of the agarose gel. The gel was run for 1 hour at 100V and visualized and imaged under UV light with a Gel Doc 1000 and Molecular Analyst software (Biorad Laboratories, Hercules, CA, USA).

3.3.5.2 Generation of human heat separated epidermal sheets

Subcutaneous fat was removed from a sample of human skin (♀ 63 years of age). The skin sample was used immediately following surgery having been transported from hospital to laboratory in full culture media (94% DMEM, 5% FBS, 1% penicillin/streptomycin). The sample was then dissected into areas of ~2cm^2 and each piece of skin was incubated in a water bath at 60°C for 55 seconds. Subsequently the epidermal sheet (SC and viable epidermis) was removed by carefully peeling it away using forceps.

3.3.5.3 Passage of pDNA through human heat separated epidermal sheets

From a sheet of 1mm thick plastic, two identical 7cm by 2cm rectangles were cut. Within each of these rectangles a further section of $1cm^2$ was removed, (Figure 3.4). Heat separated epidermal sheets were prepared (Chapter 2; Section 2.3.16) and their integrity was confirmed by light microscopy (Stemi 2000-C Stereomicroscope, (Zeiss, Welwyn Garden City, UK) with a Scott 1500 fibre optic external light source (Scott UK Ltd, Stafford, UK)]. Heat separated epidermal sheets were then either left intact or placed back on top of the dermis, and treated with a single roll of a mounted sharp tipped microneedle array (7 X 7 with heights of 280μm) (Chapter 2; Section 2.3.13). One of the plastic rectangles was then covered in a layer of grease, to which the heat separated epidermal sheets is stuck so that the epidermal sheet covered the window. The other plastic rectangle was then fixed, again with grease, so that the epidermal sheet was "sandwiched" between the supporting plastic rectangles. Gaps between the plastic supports were sealed with more grease and held together with tape. The Heat separated epidermal sheet and supports were placed in a humidified chamber while an agarose gel was prepared as described previously (Chapter 3; Section 3.3.5.1). The plastic support containing the heat separated epidermal sheet were then placed into the gel tank and taped into position. The window exposing the heat separated epidermal sheet was carefully aligning with a well formed in the gel; the gel is then allowed to solidify. The experimental set-up is shown in Figure 3.3. Into a well 10μl of pCMVβ, 4μl loading buffer, and 6μl water was applied. The gel was run at 100V for 1 hour before being removed and visualized as described in (Chapter 3; Section 3.3.5.1).

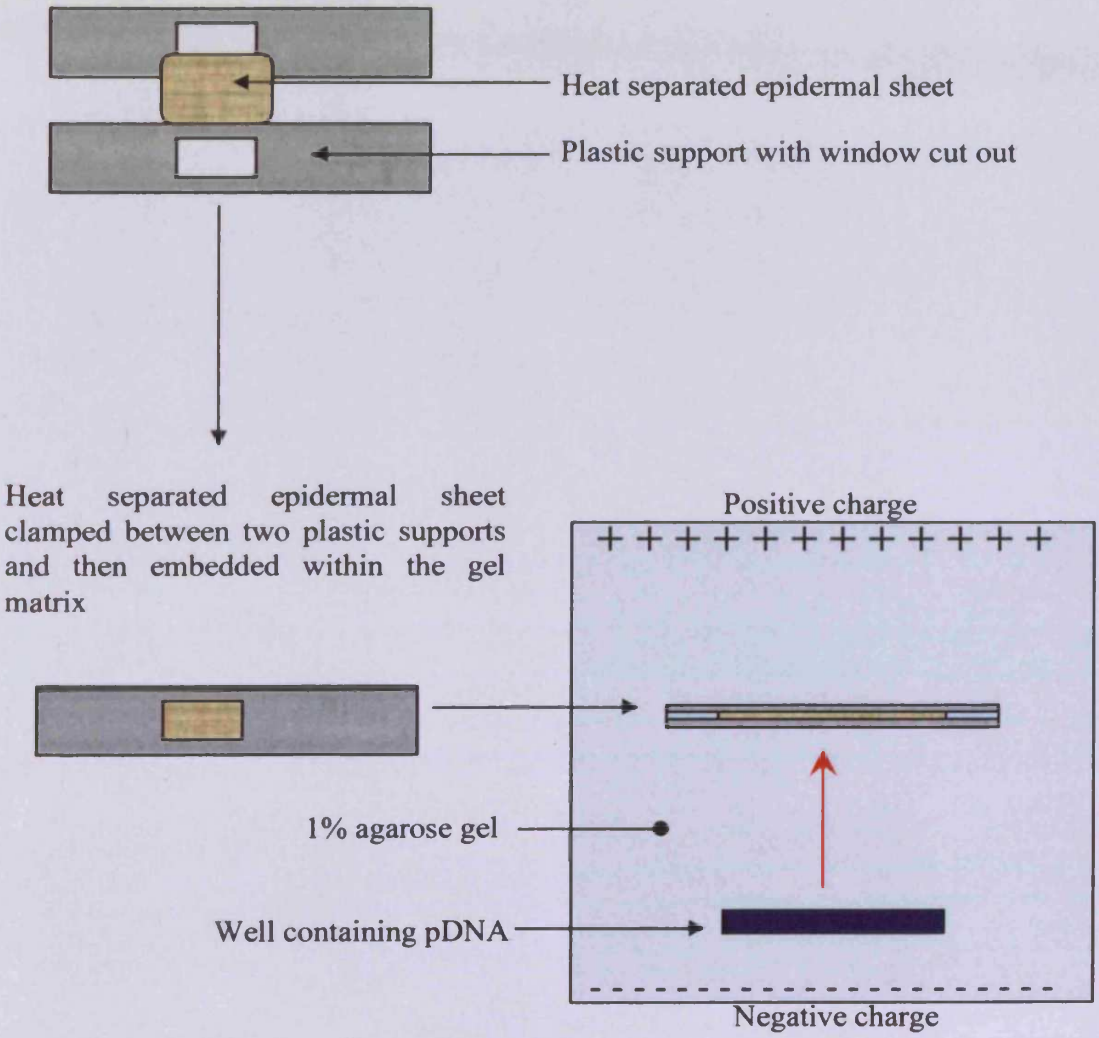

Figure 3.4 Schematic of the experimental set-up demonstrating that pDNA can move through microneedle treated epidermal sheets. After being clamped between two plastic supports the microneedle treated epidermal sheet is embedded in an agarose gel matrix and subject to electrophoresis. In an electric field the pDNA (red arrow) moves toward the positive region.

3.3.6 Franz-type diffusion cells and diffusion studies

Heat separated epidermal sheet consists of the SC and associated viable, nucleated epidermal layers. The viable cellular component does not constitute a barrier but does provide mechanical support for the SC. Therefore, heat separated epidermal sheets allow us to study the primary physical barrier of the skin, the SC.

Franz-type diffusion cells were prepared by clamping a diffusive surface between the donor and receptor phase and sealing with silicon grease (Figure 3.5). The receptor phase was filled with ~3 ml a suitable degassed buffer and loaded with a magnetic follower. Each diffusion cell was placed on a magnetic stirrer plate immersed in a water bath at 37°C. The donor phase of each diffusion cell was filled with 1ml of delivery formulation, the sampling arm and donor phase were sealed with Nasco film to limit evaporation. At pre-determined time intervals 200µl samples were removed from the receptor phase, which was replenished with an equal volume of suitable pre-warmed buffer. In all cases fluorescence was measured using a FLUOstar Optima fluorimeter (BMG Labtechnologies, Offenberg, Germany).

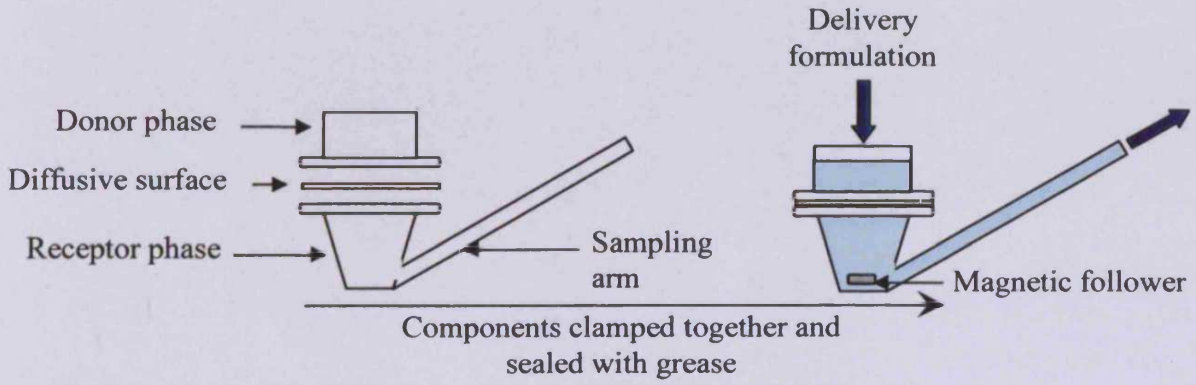

Figure 3.5 A diagram depicting the set-up of a Franz-type diffusion cell

3.3.6.1 Diffusion of fluorescent nanoparticles through microneedle treated human heat separated epidermal sheets

Epidermal sheets were prepared as described previously (Chapter 2; Section 2.3.16). Some of these were treated by a single rolling motion of a 7 x 7 sharp tipped microneedle array with needle heights of 280μm. Other epidermal sheets were treated once with a 26G hypodermic needle and still others were left intact (n = 4 for each). The treated epidermal sheets were clamped between the donor and receptor phase as described in Section 3.3.6. The receptor phase of each diffusion cell was filled with ~3ml of degassed PBS pH 7.4. Each donor phase received 1ml of working strength bead solution (Chapter 3; Section 3.3.3.1). The experiment was conducted over 24 hours with samples being taken at regular intervals.

3.3.6.2 Diffusion of FITC conjugated albumin through microneedle treated human heat separated epidermal sheets

Franz-type diffusion cells with treated epidermal sheets were prepared as in Section 3.3.6. Each receptor phase was filled with ~3ml of degassed PBS pH 7.4. Each donor phase received 1ml/mg FITC-albumin. Experimental duration was 24 hours with samples being taken at regular intervals.

3.3.6.3 Diffusion of pDNA through microneedle treated human heat separated epidermal sheets

Franz-type diffusion cells were prepared as described in Section 3.3.6. The receptor phase was filled with ~3ml of degassed TNE buffer (100mM Tris; 2.0M NaCl; 10mM EDTA; pH 7.4). Each donor phase received 1ml of pEGFP (1mg/ml). Samples were taken at regular intervals and the experiment preformed over 24 hours.

3.3.6.4 Hoechst assay

Plasmid permeation was monitored by measuring the total amount of DNA in each sample using Hoeschst DNA quantification assay (Rengaraian *et al.* 2002), fluorescence was measured with a FLUOstar Optima fluorimeter (BMG Labtechnologies, Offenberg, Germany).

3.4 Results and discussion

3.4.1 Methylene blue application to human skin *en face*

Following microneedle application to *ex vivo* human skin in conjunction with methylene blue, the dye was able to pass through conduits in the SC created by the microneedles and stain the epidermal cells in the vicinity (Figure 3.6). This was in contrast to control samples, not treated with microneedles, where no staining of epidermal cells occurred (data not shown). Staining of epidermal cells was observed in skin samples where the dye was applied before microneedle application and in samples where the stain was applied after (Figure 3.7). However, microneedle penetration was inconsistent, since the pattern of staining caused by the microneedle array often indicated that not all of the microneedles of the array actually penetrated the SC. For a 7 x 7 microneedle array applied in a single rolling motion a total of 49 points of stain should be expected if all microneedles successfully penetrate the SC. However, the *en face* images in Figure 3.6 show only ~70% of the channels exhibiting positive staining. A reason for this could be how the microneedle array is applied to the skin. It appears as though microneedles of the array that come into contact with the skin surface first (row 1) and last (row 7), the leading and trailing edge of the array, are more efficient at penetrating the SC than those in the middle of the array (Figure 3.8 A). This arises because the array, when applied in a rolling motion, initially contacts the skin at an angle of ~45° therefore not all of the needles come into contact. The rolling motion causes the skin to be stretched making it easier for the leading edge needles to penetrate. However, at the same time the region of skin directly in front of the microneedle array becomes slack so that when the array moves to a 90° the needles are being applied to slack skin that is easily deformable and

consequently difficult to penetrate. As the rolling action continues, the microneedle array pushes the skin surface back causing it to become tight resulting in more effective needle penetration (Figure 3.8 B). This is depicted schematically in Figure 3.9.

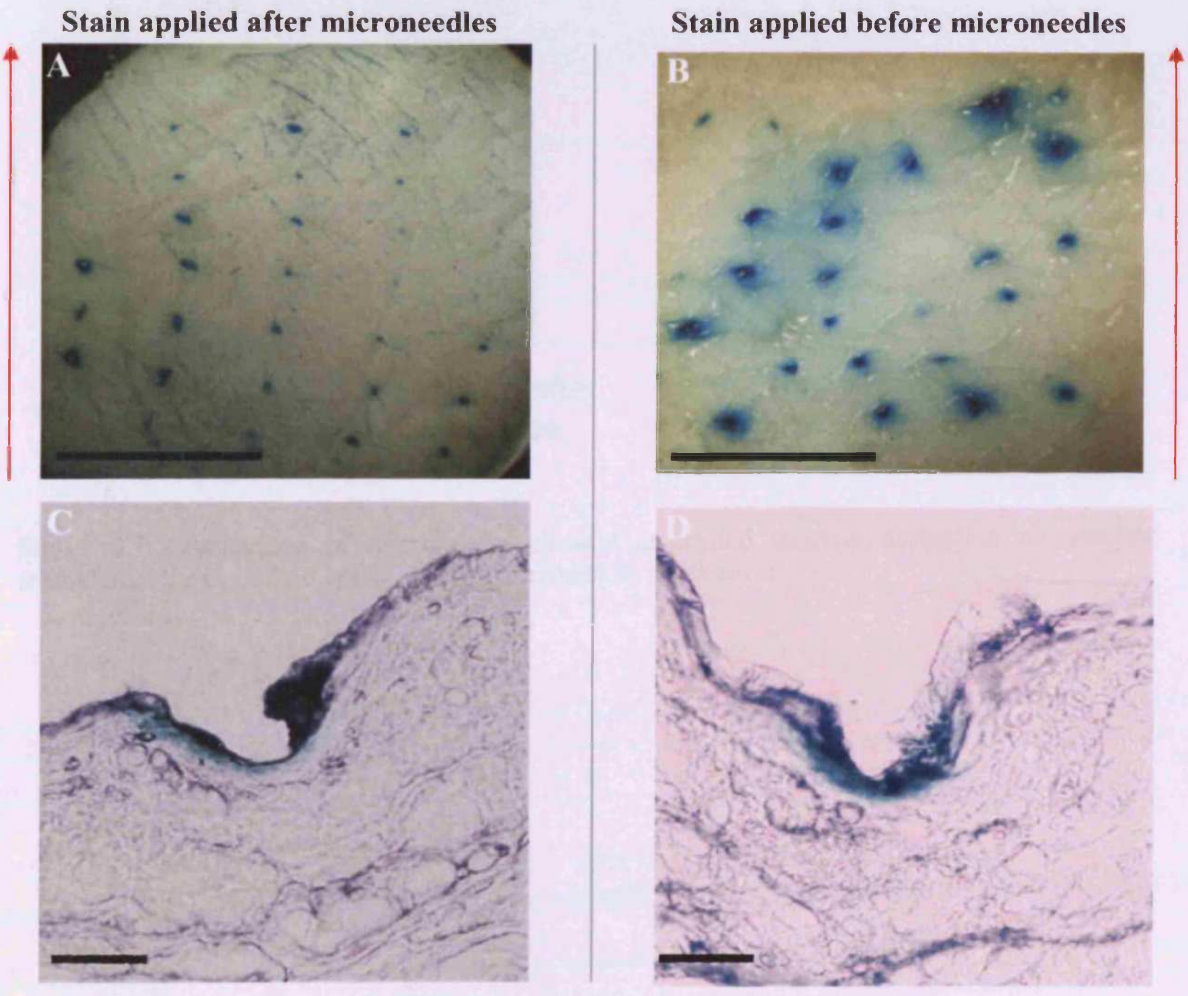

Figure 3.6 Delivery of methylene blue to *ex vivo* facilitated by microneedle. *En face* images show that there appears to be little difference in points of positive staining if the dye is applied before (A) or after microneedle application (B), red arrow indicates the direction of microneedle application. Cryosections reveal the dye in the vicinity of micro-channels with no obvious difference weather the dye was applied before (C) or after (D) microneedle application; bar = 2mm in A & B and 150μm in C & D.

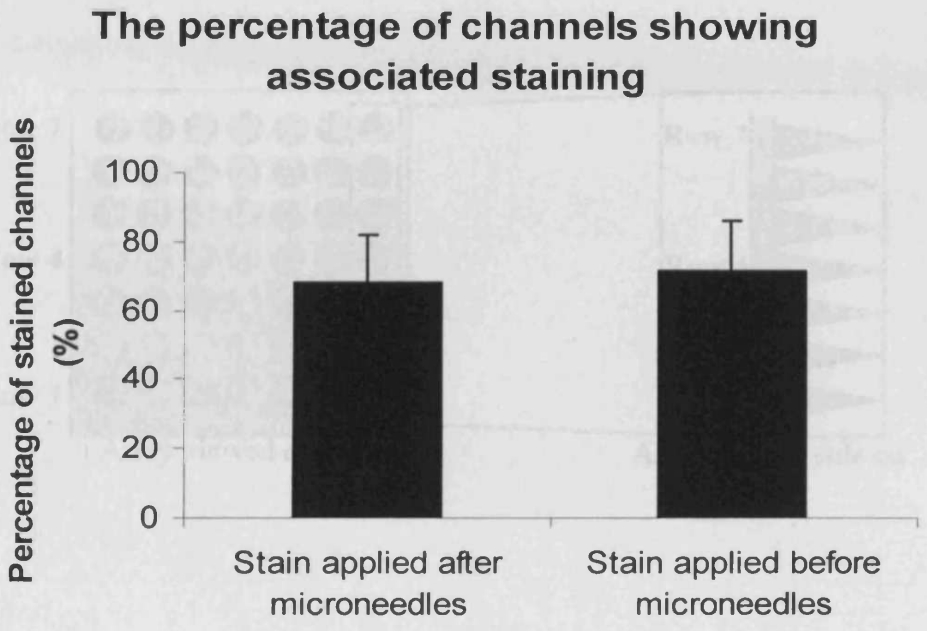

Figure 3.7 Comparison of microneedle channel associated staining depending on weather methylene blue is applied before or after microneedle application.

A

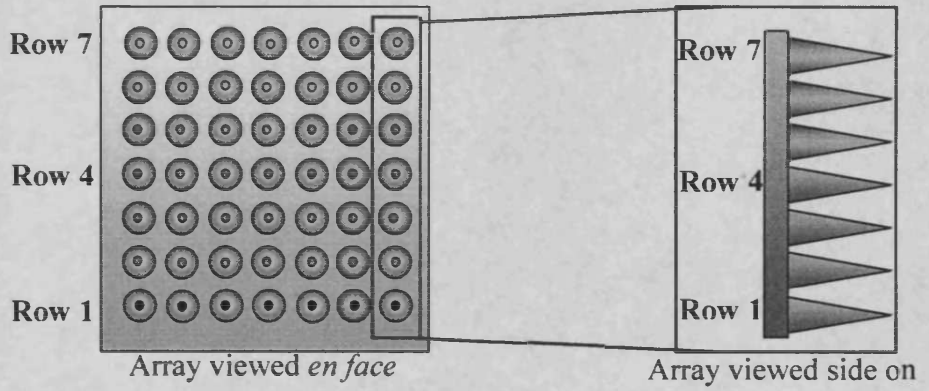

B

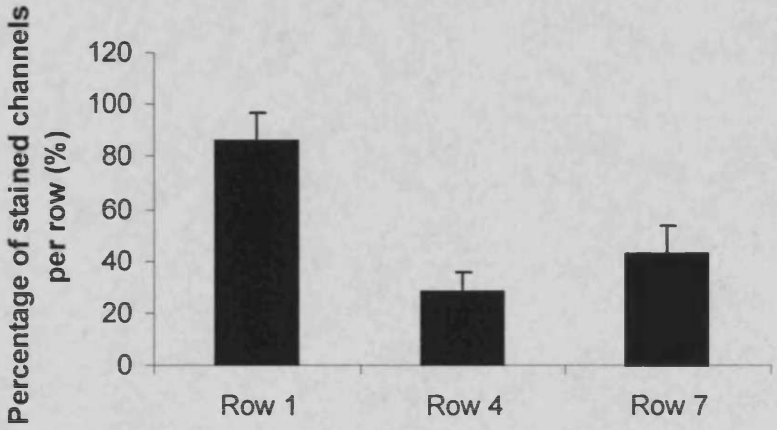

Figure 3.8 The microneedle array was divided into different rows (A). The row which contacts the skin first, row 1, are highly penetrative, with >80% of the channels positively stained (n = 4). Toward the centre of the array are rows (e.g. row 4) that contact the skin when the roll reaches ~90° and are least penetrative, ~30% showing positive staining (n = 4). The final row to contact the skin (row 7) does so at an angle not optimal for penetration (B), consequently ~40% of channels show positive staining (n = 4).

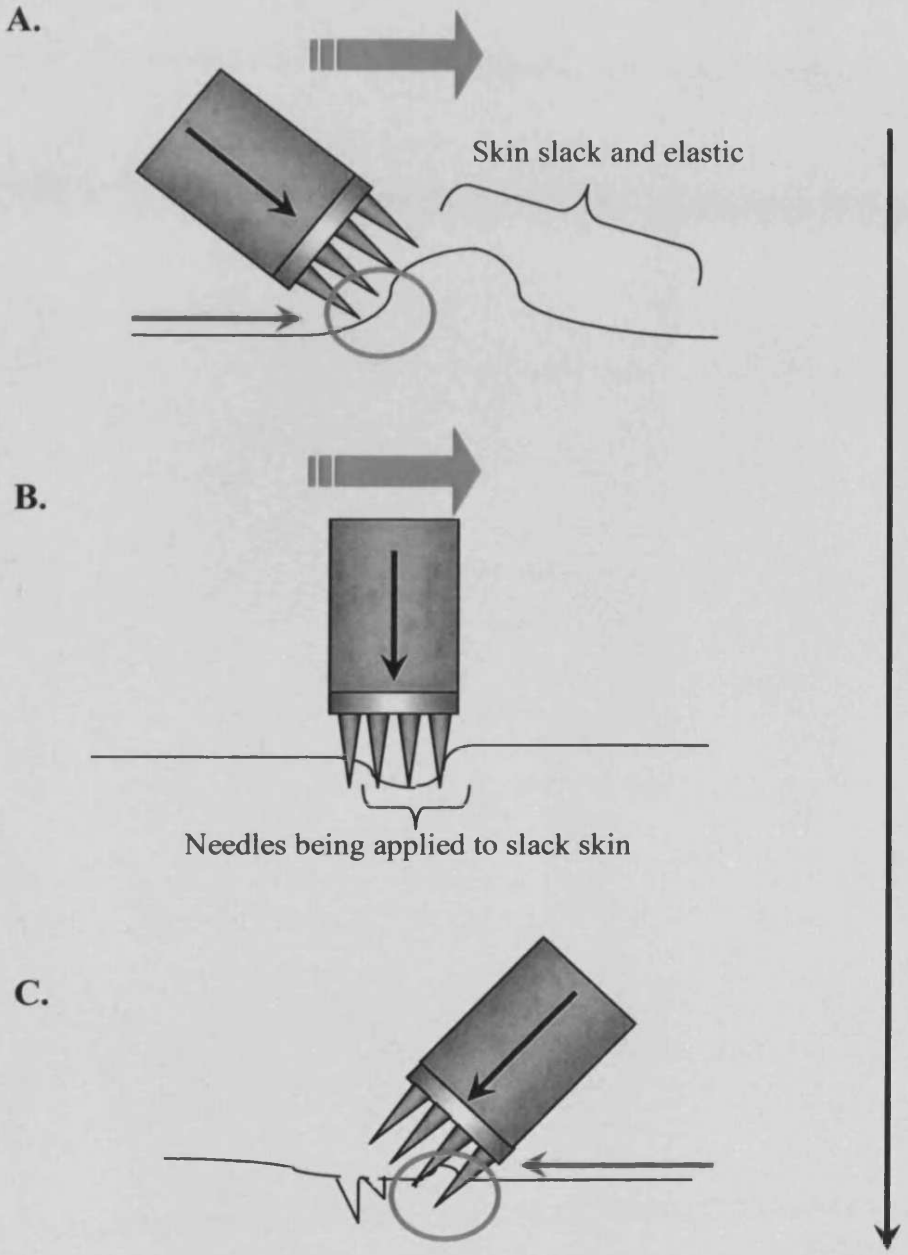

Fig 3.9 A schematic of the proposed model of microneedle application showing why penetration is more frequently observed at points where the array contacts the skin first and last. Application of a microneedle array at ~45° causes localized stretching of the skin, optimal for microneedle penetration (A). As the array approaches ~90° the microneedles are in contact with slack skin, which is more difficult to penetrate (B), finally, when the array reaches ~160° the skin is stretched again but the microneedles are not optimal for penetration but nevertheless still penetrate slightly (C).

Cryosections of *ex vivo* human skin treated with microneedles and methylene blue show that formed micro-conduits extended through the SC and into the epidermis to a depth of ~150μm (Figure 3.6). The cryosections show that the stain is visible in the immediate vicinity of the micro-channel and that only cells adjacent to the channel take up the stain. The dye appeared to have penetrated to a depth of ~10-20μm into the epidermis.

3.4.2 Tape stripping human microneedles / fluorescent nanoparticles treated skin

Although there does not seem to be a difference in *intra* microchannel staining if methylene blue stain is applied to the skin before or after microneedle treatment, there does seem to be a difference if fluorescently labelled nanoparticles are used (Figure 3.10) instead of methylene blue.

3.4.2.1 Size determination of nanoparticles using photon correlation spectroscopy (PCS)

The nanoparticles used were amine modified latex spheres and were determined by PCS to have a unimodal mean diameter of 131nm (+/- 22.3). These beads have previously been used as models for lipid-polycation-DNA (LPD) gene delivery vectors (Chabri *et al.* 2004).

3.4.2.2 Application of the fluorescent bead formulation in conjunction with microneedles

When a bead solution was applied to intact skin, without microneedle application, then subject to tape stripping, the fluorescent signal was rapidly lost (Figure 3.10 A). This was expected, since the relatively large nanoparticles were unable to cross the SC barrier. Consequently the entire fluorescent bead formulation remains on the skin surface. After 2 tape strips the fluorescent signal was still strong, but after 4 the signal rapidly diminished, with only beads residing in the natural folds and ridges of the skin still giving a signal. Nevertheless, the signal was completely lost after only 8 tape strips, indicating that the nanoparticles did not penetrate to any depth within the skin. Conversely, if a microneedle array is applied followed by a nanoparticles solution then a fluorescent signal is present to a much greater depth (Figure 3.10 B). After 8 tape strips a fairly strong fluorescent signal is still observed and appears strongest in an array pattern corresponding to where microneedles were applied. In fact, it is possible to see actual channels in the center of the stronger fluorescent signals (Figure 3.10 B). The signal is lost after 14 tape strips. If however, the nanoparticles solution is applied to the skin surface before the microneedle array is applied, then the signal is still apparent after further tape strips (Figure 3.10 C). The signal is still strong after 16 tape strips (Figure 3.10 C) and diminishes completely after 24 tape strips. This indicates that by applying the nanoparticles solution before the microneedle array, results in the nanoparticles being present at greater depth in the skin. This can only be explained by the actual physical delivery on the nanoparticles by the tips of the microneedles as they are applied. While tape stripping can be an extremely variable means of estimating depth, for example

Jacobi *et al* estimate that 66 ± 12% of the SC is removed with 20 tape strips and 95 ± 3% with 50 (Jacobi *et al* 2005). In contrast, Teichman *et al* suggest that the SC is removed completely with 40 tape strips (Teichman *et al* 2005). Therefore, in the present study a conservative estimate that 25 tape strips is still within the SC region, albeit approaching the viable epidermis.

While this study does not conclusively confirm that the fluorescent bead formulation was delivered to the viable epidermis it does demonstrate that applying the delivery formulation before the microneedle array results in a deeper penetration compared to if the formulation is applied after. Consequently, in all subsequent studies, the formulation will be applied to the surface of the skin prior to microneedle treatment.

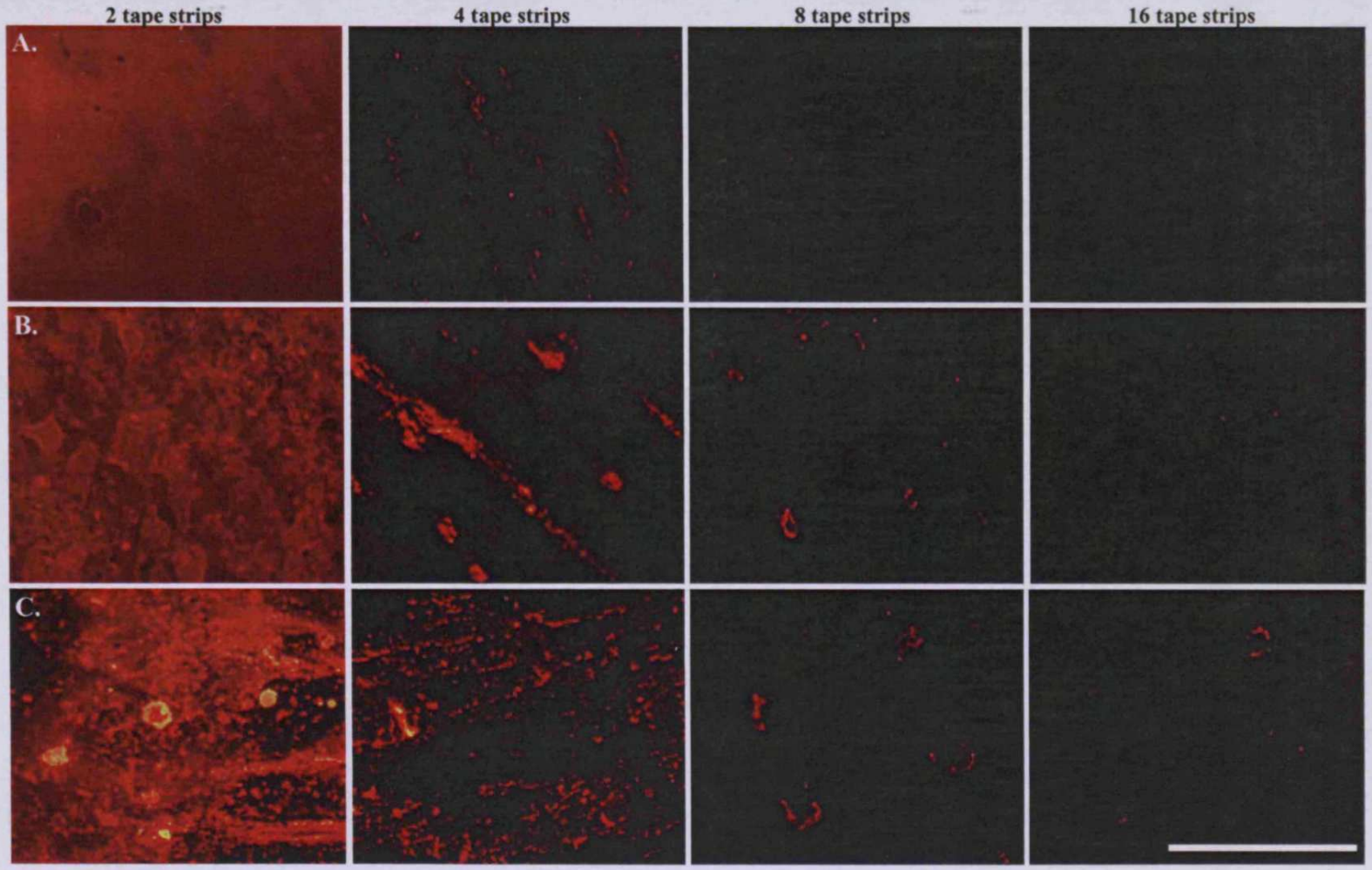

3.10 Tape strips of *ex vivo* human skin treated with fluorescently labelled nanoparticles. Untreated skin (A), nanoparticle solution applied after microneedle treatment (B) and nanoparticle solution applied before microneedle application (C); bar = 1mm

3.4.3 Delivery of fluorescent beads and albumin formulations to human skin in conjunction with microneedles and generation of cryosections

3.4.3.1 Delivery of fluorescent beads

An important point to note is that the skin sections autofluorescence green, when subject to fluorescent blue light (440–500nm). Figure 3.11 A shows a control skin sample treated only with microneedles, disruption of the SC was clearly apparent with a channel extending into the epidermis to a depth of ~150μm. Other control samples, where the nanoparticles solution was applied to skin and not treated with microneedles are shown in Figure 3.11B. Here the relatively large size and charge present on the surface of the nanoparticles prevent permeation across the intact SC. The nanoparticles were restricted to the external surface of the skin appearing as a bright red – yellow band and not observed within the epidermis. Samples that were treated with a nanoparticles and microneedles, Figure 3.11 C, show the formation of channels through the SC. A red fluorescent layer was once again observed on the external surface of the skin but at discreet loci channels of ~150μm depth were observed with an associated strong fluorescent signal localized to the sides of the channel. This suggests that the application of the microneedles to the surface of the skin had penetrated the skin surface and physically pushed nanoparticles into the resulting channel.

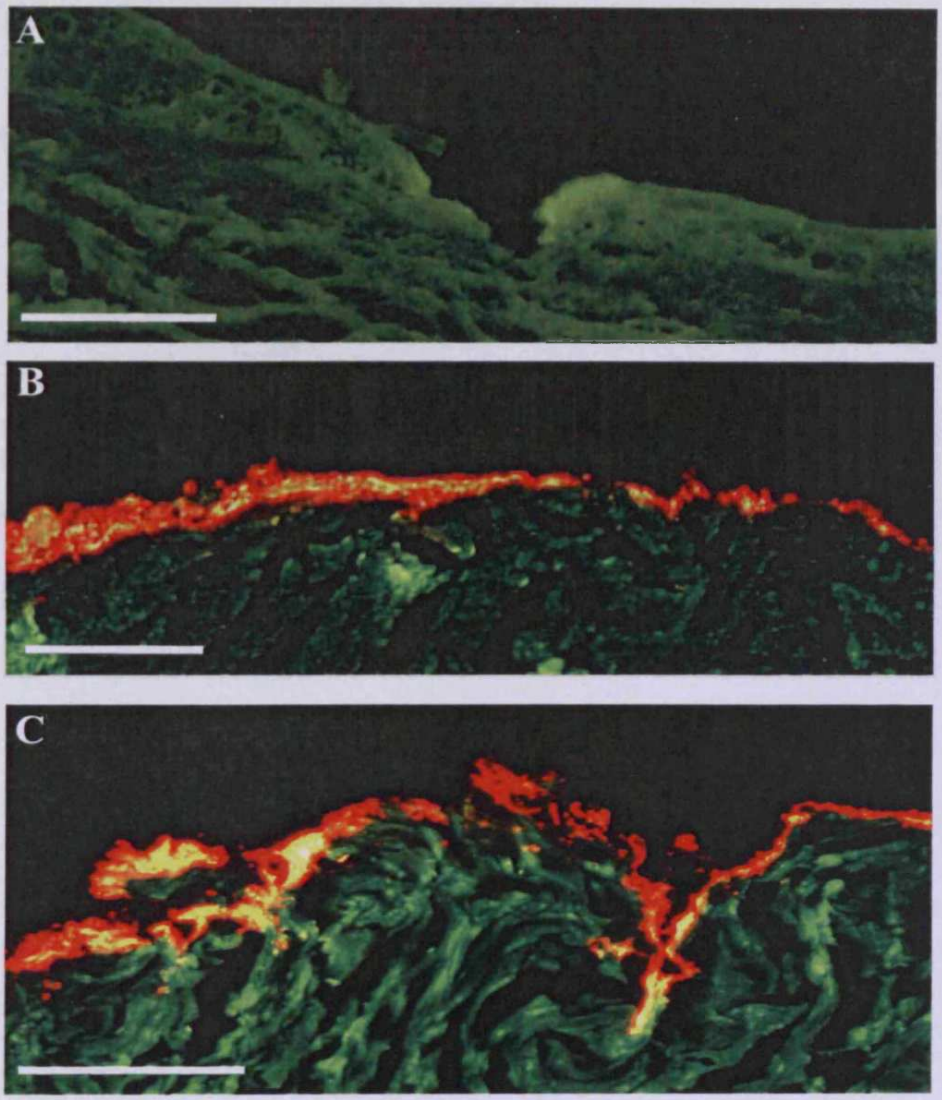

Figure 3.11 Solution of fluorescent nanoparticles applied to *ex vivo* human skin in conjunction with microneedles. Samples treated only with microneedles (A), only with bead formulation (B) and with bead formulation and microneedles (C); bar = 150μm in all cases.

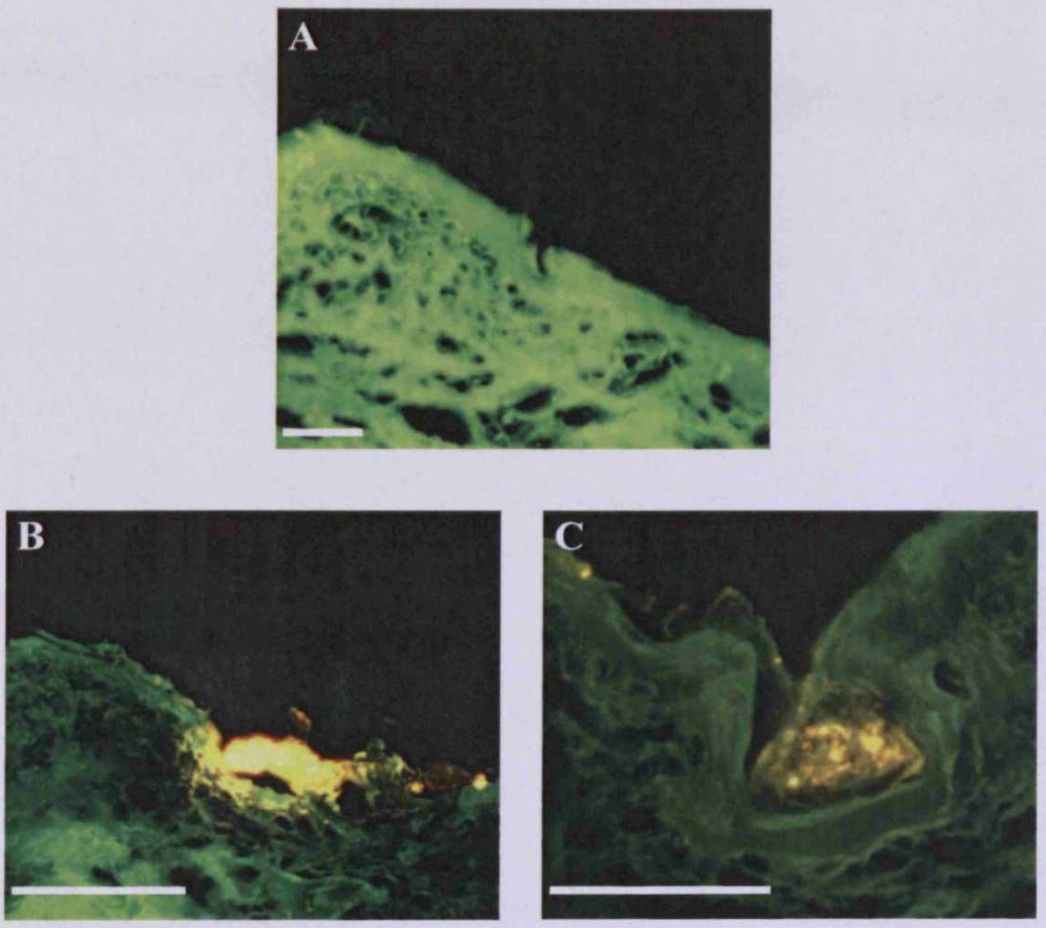

Figure 3.12 Application of FITC conjugated albumin to *ex vivo* human skin. Samples treated only with microneedles (A) are contrasted with those treated with FITC albumin and microneedle (B & C); bar = 150μm in all cases.

3.4.3.2 Delivery of fluorescent albumin

This effect is also observed when FITC conjugated albumin is applied in conjunction with microneedle. Control samples, where microneedles are applied without FITC conjugated albumin, show the formation of channels through the SC extending 150μm into the epidermis (Figure. 3.12 A). When FITC conjugated albumin is applied to microneedle treated *ex vivo* skin channels are observed again through the SC and with similar dimensions to those already described. Associated with the channels are strong yellow – orange fluorescent signals (Figures 3.12 B & C). This demonstrates that microneedles facilitate delivery of macromolecules to the viable epidermis.

3.4.4 Electrophoresis of pDNA through microneedle treated human epidermal sheets

3.4.4.1 Preparation of pDNA

Using a plasmid purification kit it was possible to obtain a high yield of supercoiled plasmid DNA, typically 3.3mg/ml and 3.6mg/ml for pCMVβ and pEGFP-N1 respectively. The purity was confirmed by absorbance at 260/280 and also electrophoresis (Figure 3.13). Electrophoresis also showed that the molecular weight of the pCMVβ (7.2kb) and the pEGFP-N1 (4.7kb) to be slightly less than, however this is a consequence of the supercoiled nature of the plasmid (Figure 3.14). In order for the true size to be determined by electrophoresis the plasmid should be linerised by a single restriction digest.

3.4.4.2 Passage of pDNA through human heat separated epidermal sheets

DNA subject to an electric field results in its movement from regions of negative charge to regions of positive charge. If a barrier is positioned in the way of the moving DNA it will be prevented from proceeding beyond the barrier (Figure 3.15A). Similarly, Untreated heat separated epidermal sheets prevent the passage of pDNA across the SC when subject to an electrical field (Figure 3.15 B). In contrast when the epidermal sheet is treated with microneedles the pDNA is able to pass through the channels (Figure 3.15 C).

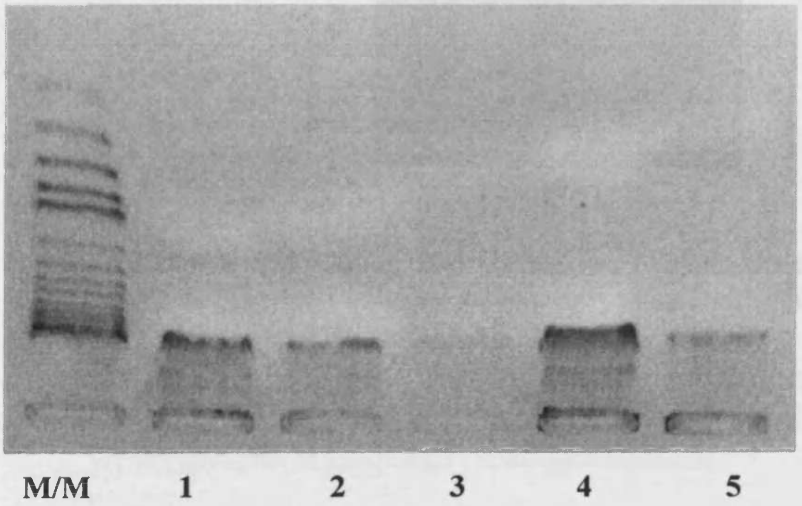

M/M = Molecular marker

Lane 1 = Cleared lysate, containing plasmid DNA as well as degraded RNA

Lane 2 = Flow through fraction, RNA removed

Lane 3 = First wash fraction, remaining traces of RNA are removed

Lane 4 = Elute which contains pure pDNA

Lane 5 = Purified pDNA

Figure 3.13 Electrophoresis of samples obtained at various points during the purification of pCMVβ, as directed in the manufacturer's protocol

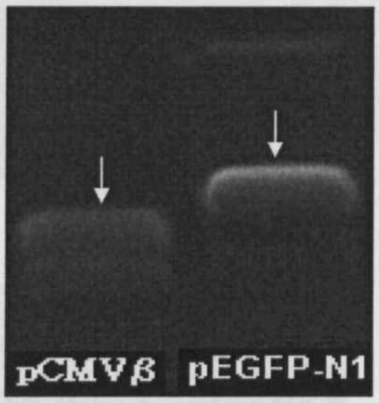

Figure 3.14. Purified plasmid DNA of the two plasmids used in this investigation run on an agarose gel at 100V for 1 hour and subsequently stained with ethidium bromide. Arrows indicate super coiled plasmid DNA.

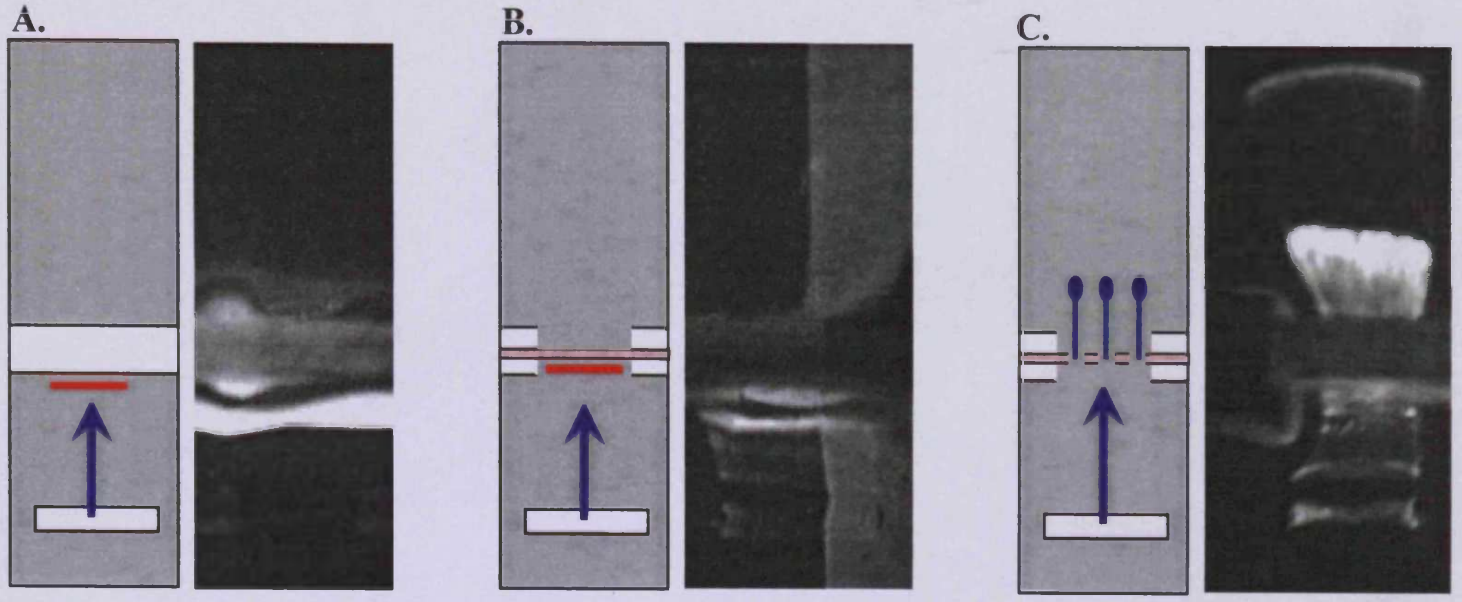

Figure 3.15 Electrophoresis of pDNA through heat separated epidermal sheets. The pDNA is mobilized in an electric field with motion toward positive regions. A plastic strip inserted in the path of movement prevents the passage of pDNA (A) as does an intact human epidermal sheets (B). Treatment of an epidermal sheet with microneedles permits passage of pDNA (C).

3.4.5 Franz-type diffusion cells and diffusion studies

Three independent experiments were conducted examining the migration of three substances across microneedle treated human heat separated epidermal sheets. The substances under investigation were polystyrene nanoparticles, FITC conjugated albumin and pDNA.

3.4.5.1 Diffusion of fluorescent nanoparticles through microneedle treated human heat separated epidermal sheets

Fluorescent latex nanoparticles have been used by other groups to investigate penetration across intact porcine skin (Kohli and Alper, 2004, Alvarez-Roman *et al* 2004). In both these studies the size and charge of the nanoparticles prevented penetration across the SC. However, this study demonstrates the ability of nanoparticles to pass the SC barrier once the SC has been compromised with microneedles (Figure 3.16). Treatment of epidermal sheets with microneedles resulted in the barrier property of the SC being reduced and this was noted as an increase in fluorescence sampled from the receptor phase over time. The signal from samples treated with microneedle did not reach the same levels as those treated with a hypodermic needle, 25% and 60% respectively, with intact samples reaching only 8% after 24 hours (Figure 3.16).

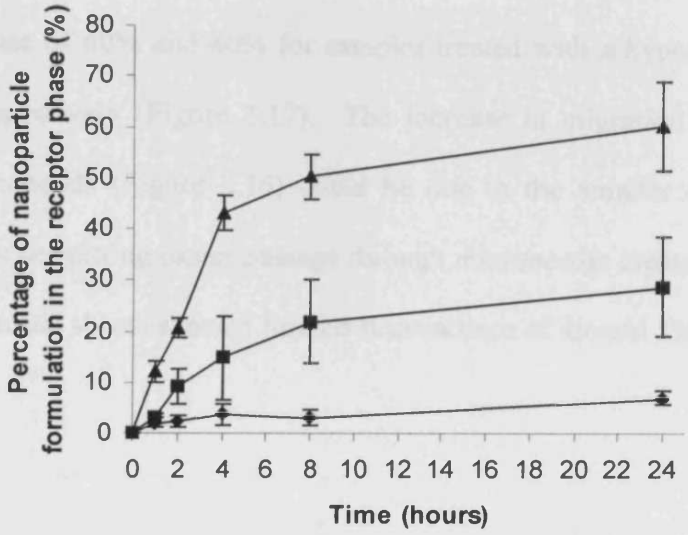

Figure 3.16 The migration of nanoparticles through microneedle treated human heat separated epidermal sheets, (♦) corresponds to intact epidermal sheet (n = 4), (▲) epidermal sheet treated with a 26G hypodermic needle (n = 4), (■) epidermal sheet treated with a single roll of a 7 X 7 mounted, sharp tip microneedle array with heights of 280μm (n = 4 ±SD for each sample).

3.4.5.2 Diffusion of FITC conjugated albumin through microneedle treated human heat separated epidermal sheets

The delivery of FITC albumin through heat separated epidermal sheets provided similar results to those obtained for nanobeads. There was an accumulation of the protein within the receptors phase of 60% and 40% for samples treated with a hypodermic needle and microneedles respectively (Figure 3.17). The increase in migration of FITC albumin compared to nanobeads (Figure 3.16) could be due to the smaller dimensions of the protein molecules permitting easier passage through microneedle created channels. Once again intact epidermal sheets showed limited fluorescence of around 5% after 24 hours.

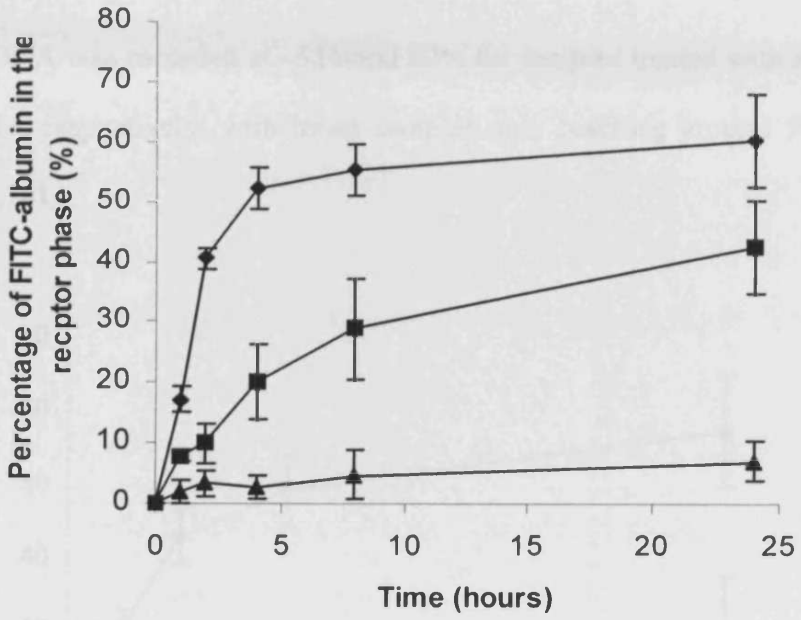

Figure 3.17 The migration of FITC conjugated albumin through microneedle treated human heat separated epidermal sheets, (▲) corresponds to intact epidermal sheet (n = 4), (♦) epidermal sheet treated with a 26G hypodermic needle (n = 4), (■) epidermal sheet treated with a single roll of a 7 X 7 mounted, sharp tip microneedle array with heights of 280μm (n = 4 ±SD for each sample).

3.4.5.3 Diffusion of pDNA through microneedle treated human heat separated epidermal sheets

Migration of pDNA was recorded at ~55%and 20% for samples treated with hypodermic and microneedles respectively, with intact samples only reaching around 5% after 24 hours (Figure 3.18).

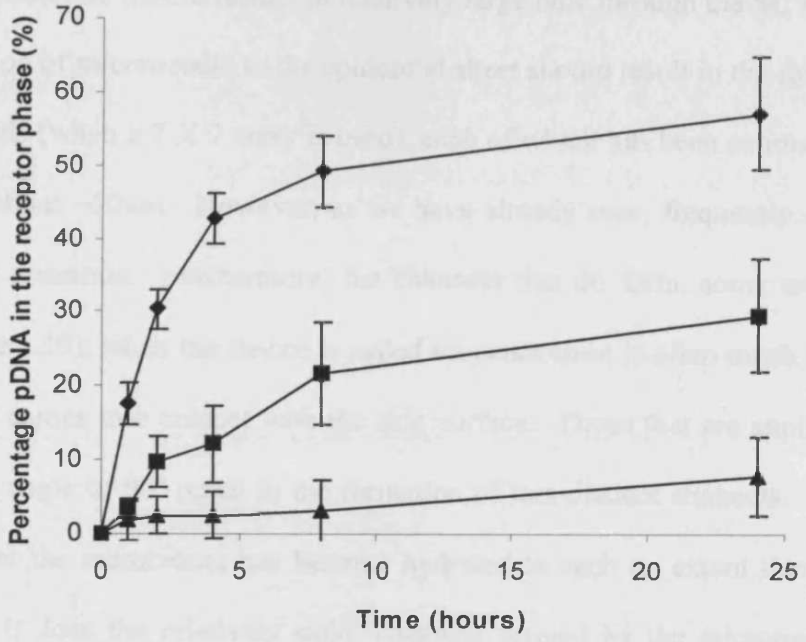

Figure 3.18 The migration of pDNA through microneedle treated human heat separated epidermal sheets as determined by Hoechst 33258 assay quantification, (▲) corresponds to intact epidermal sheet (n = 4), (♦) epidermal sheet treated with a 26G hypodermic needle (n = 4), (■) epidermal sheet treated with a single roll of a 7 X 7 mounted, sharp tip microneedle array with heights of 280μm (n = 4 ±SD for each sample).

3.4.5.4 Common features of the diffusion studies

The experimental results shown that indeed the passage of the nanoparticles into the receptor phase is enhanced when microneedles are applied compared to intact skin but not to the same degree as samples treated with the hypodermic needle (Figures 3.16, 3.17 & 3.18). But there are a number of factors why this is the case. Firstly, application of a 26 gauge hypodermic needle results in relatively large hole through the SC being created. The application of microneedle to the epidermal sheet should result in the formation of 49 micro-channels (when a 7 X 7 array is used), each of which has been estimated to have a diameter of about ~50μm. However, as we have already seen, frequently not all of the microneedles penetrate. Furthermore, the channels that do form, some are larger than others (Figure 3.19), when the device is rolled on penetration is often much better for the row that first comes into contact with the skin surface. Those that are applied when the array is at an angle of 90° result in the formation of less distinct channels. Also, during the experiment the membrane, can become hydrated to such an extent that it begins to swell and as it does the relatively small channels formed by the microneedle become more restricted, further preventing the passage as the experiment proceeds. Another effect is that the magnetic follower in the receptor phase creates a sink effect which has the effect of disrupting, and therefore mixing the contents of the receptor phase as well as the donor phase, when channels are present. While mixing will be reduced in both microneedle and hypodermic needle treated epidermal sheets, it will be considerably less in those treated with microneedles. As a result there will be much less mixing the donor phase of the microneedle treated systems, therefore the components will have more time

to interact and associate with the diffusive surface the lack of mixing could be such that this fraction is then, essentially removed from the experiment so that the ideal equilibrium will never be reached. Also, to note is that skin surface contains many nucleases, therefore, during experiments involving pDNA there is a chance that these play a role in actively degrading some of the pDNA, also removing it from the formulation.

In ideal conditions, it would be expected that intact epidermal sheet would prevent the passage of the nanoparticles and macromolecules completely and to a large degree that is what was observed in the experimental results (Figures 3.16, 3.17 & 3.18). The small amount of fluorescence that can be observed below the SC in the control samples arises due to either small breaks in the barrier formed during preparation and handling (not picked up during examination) or fluorescent compounds leaching out of the epidermal sheet into the sampling buffer. In addition the assay used to determine permeated pDNA is non specific and it is likely that endogenous DNA, leaching from the tissue, would give rise to degree of overestimation.

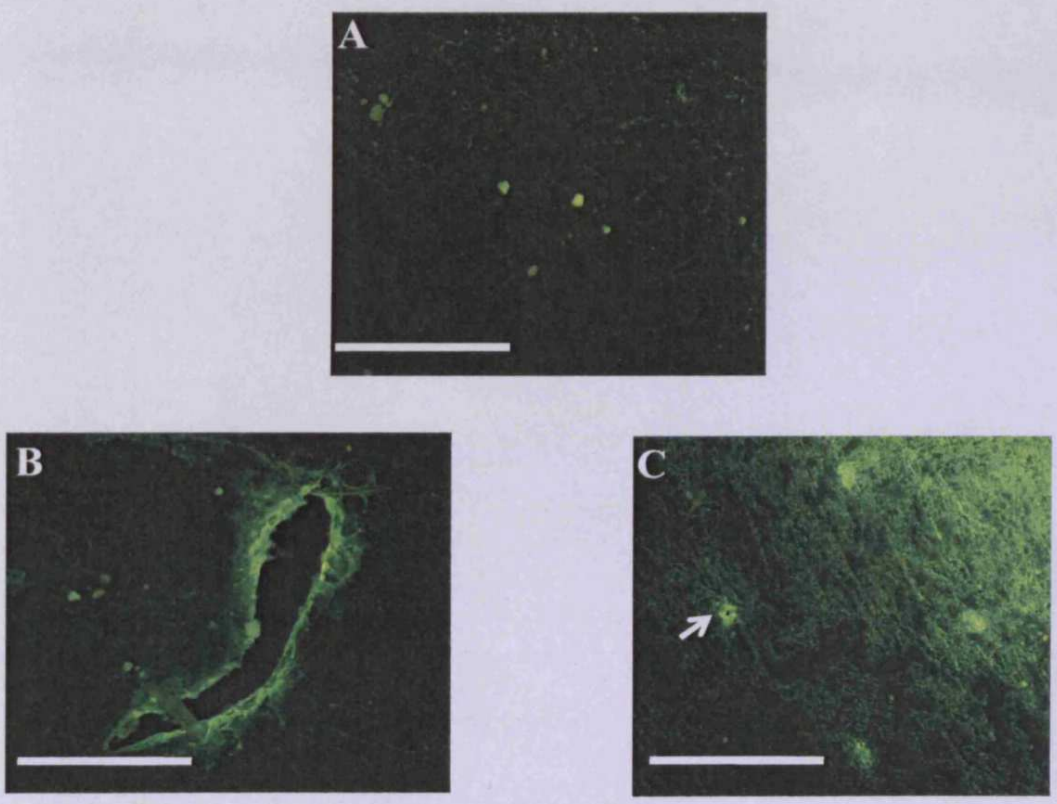

Figure 3.19 Examination of human epidermal sheets removed following FITC conjugated albumin diffusion experiment as seen by fluorescent microscopy. No notable disruption is seen in intact samples (A). In contrast, application of a 26G hypodermic needle (B) and microneedle (C) result in the formation of channels, White arrow indicates the presence of a microneedle channel; bar = 1mm.

3.5 Conclusion

Microneedle application to *ex vivo* skin enhances the delivery of low molecular weight dyes, e.g. methylene blue, macromolecules, e.g. FITC albumen and nanoparticles of around 120nm diameter to the viable regions of the epidermis. Applying the formulation before application of a mounted microneedle array seems to result in delivery of nanoparticles to greater depths than applying the formulation before. As a result all subsequent microneedle facilitated delivery will be conducted by applying the formulation before microneedle application.

Applying microneedle in a single rolling motion, as described in Chapter 1, results in more disruption to the SC compared to a flat application. However, it appears that applying the microneedle in this way does not consistently result in all the microneedle of the array penetrating the SC. It appears as though penetration is greatest in the region where the array is initially applied to the skin. The region of the skin that comes into contact with the microneedle as the array passes 90° are the regions where the skin is not penetrated all the time, consequently this will be the region where most variability in penetration is observed. Finally, the region where the needles are in final contact with the skin will contain channels but not as well formed as those of initial contact. Nevertheless, application of microneedle in this manor does result in sufficient disruption to the SC to facilitate the passage of nanoparticles and macromolecules, including pDNA. Therefore, this method of application, the single rolling motion, will still be employed as the principal means of microneedle application to *ex vivo* human skin.

This chapter and the preceding one demonstrate that microneedle arrays are effective at disrupting the SC and facilitate the passage of macromolecules and nanoparticles into the viable epidermis. The next objective was to demonstrate that microneedle can deliver functional pDNA to the viable epidermis, where it is taken up and expressed. This is a crucial factor and essential if microneedle facilitated cutaneous DNA vaccination is to occur, expression of functional pDNA in the epidermis is the subject of the next chapter.

CHAPTER 4: Optimised delivery of reporter pDNA to the viable epidermis with microneedles

4.1 Introduction

Since the first demonstrations that expression from pDNA can occur in mammalian tissue (Wolff *et al.* 1990) it has received considerable interest as a vector for the delivery of exogenous, therapeutic genes (Meykaden *et al.* 2005). This work has been progressed by Hengge and colleagues who have confirmed exogenous gene expression in murine models as well as porcine, canine mucosa and most importantly, *ex vivo* human skin (Hengge *et al.* 1996; Hengge *et al.* 1998). For reasons outlined in chapter 1 the skin has received considerable attention as a potential target for therapeutic gene delivery applications, most notably for DNA vaccination (Tang *et al.* 1997). Consequently, it is the potential to stimulate an immune response from pDNA delivered to the viable epidermis that is at the core of this thesis.

4.1.1 Microneedle facilitated delivery of pDNA to the epidermis of *ex vivo* skin

Currently, direct intra-dermal injection (Raz *et al.* 1994; Hengge *et al.* 1996; Sawamura *et al.* 2002) and biolistic (Kendall *et al.* 2004) approaches appear to be the most successful methods of delivering exogenous genes to the skin. The previous chapters have demonstrated that microneedles can disrupt the SC to facilitate the delivery of low molecular weight dyes, nanoparticles and macromolecules to the viable epidermis. It has been shown that pDNA can pass through channels created in the SC by microneedles. It has also been proposed that potentially microneedles offer a number of distinct advantaged over intra-dermal injection and biolistic delivery (Chapter 2). Therefore, in order to demonstrate that microneedles should be considered an effective and practical alternative to the aforementioned conventional methods it is essential to prove that microneedles can deliver functional pDNA to the viable epidermis. This will be explored in the current chapter.

4.1.2 Plasmids

Plasmids occur ubiquitously in bacterial species, existing principally as episomal entities. By definition plasmids are autonomously replicating molecules of DNA that can exist in a linear form but are more commonly found as a covalently closed circle (CCC). Consequently, plasmids contain genes that regulate replication and segregation between daughter cells following bacterial cell division. In nature, plasmids vary in size from around 1 kbp to 1000 kbp; these extremely large plasmids are called megaplasmids. Naturally occurring plasmids contain additional genes that are not essential for cell propagation under normal conditions, i.e. do not encode "house keeping" genes. However, they do have genes that encode proteins that could promote survival in certain situations, e.g. antibiotic resistance, genes for utilization of rare carbon sources or genes that encode toxins against other bacterial species.

There exists a whole plethora of techniques permitting the modification of naturally occurring plasmids, so that artificial plasmids can be created for certain functions, e.g. cloning vectors. Many artificial plasmids are engineered to contain reporter genes. When expressed, reporter genes provide either a direct or indirect means of confirming gene expression from the plasmid. Because all plasmids have a common structure, reporter plasmids can be used as models for plasmids which express a therapeutic protein.

4.1.3 Reporter plasmids

In the current project two different reporter plasmids will be used, pCMVβ and pEGFP-N1, which contain *LacZ* (encoding β-galactosidase) and enhanced green florescent protein (EGFP) respectively, both of which were introduced in the previous chapter. Expression of *LacZ* results in the creation of β-galactosidase, an enzyme that can be detected by histochemical staining. A substrate for β-galactosidase, such as 4-bromo-5-chloro-3-indoyl-β-D-galactopyrosanide (X-gal), is cleaved by the enzyme producing a product that is readily oxidised to form 5, 5'-dibromo-4, 4'-dichloro-indigo, a deep blue dye. The steps in the reaction are shown in Figure 4.1. Cells which have taken up pCMVβ and are expressing *LacZ* will consequently appear blue when incubated with X-gal. In contrast, expression from pEGFP-N1 can be detected directly by fluorescent microscopy. The protein product, EGFP is excited with blue light, optimally at 488nm, and as ground state is regained photons of green light are emitted. However, as mentioned in the previous chapter, upon excitation with blue light skin sections autofluoresce green. This will inevitably restrict visualization of EGFP protein in skin. The principal cause of the autofluorescence is the various connective tissues that constitute the skin. Therefore, if the dermis is removed, which is mainly connective tissue, the majority of the autofluorescence should consequently also be removed. Dermis/epidermis separation can be achieved by incubation of skin samples with EDTA, which results in desmosome destabilization; the result is the epidermis can be peeled away from the dermis.

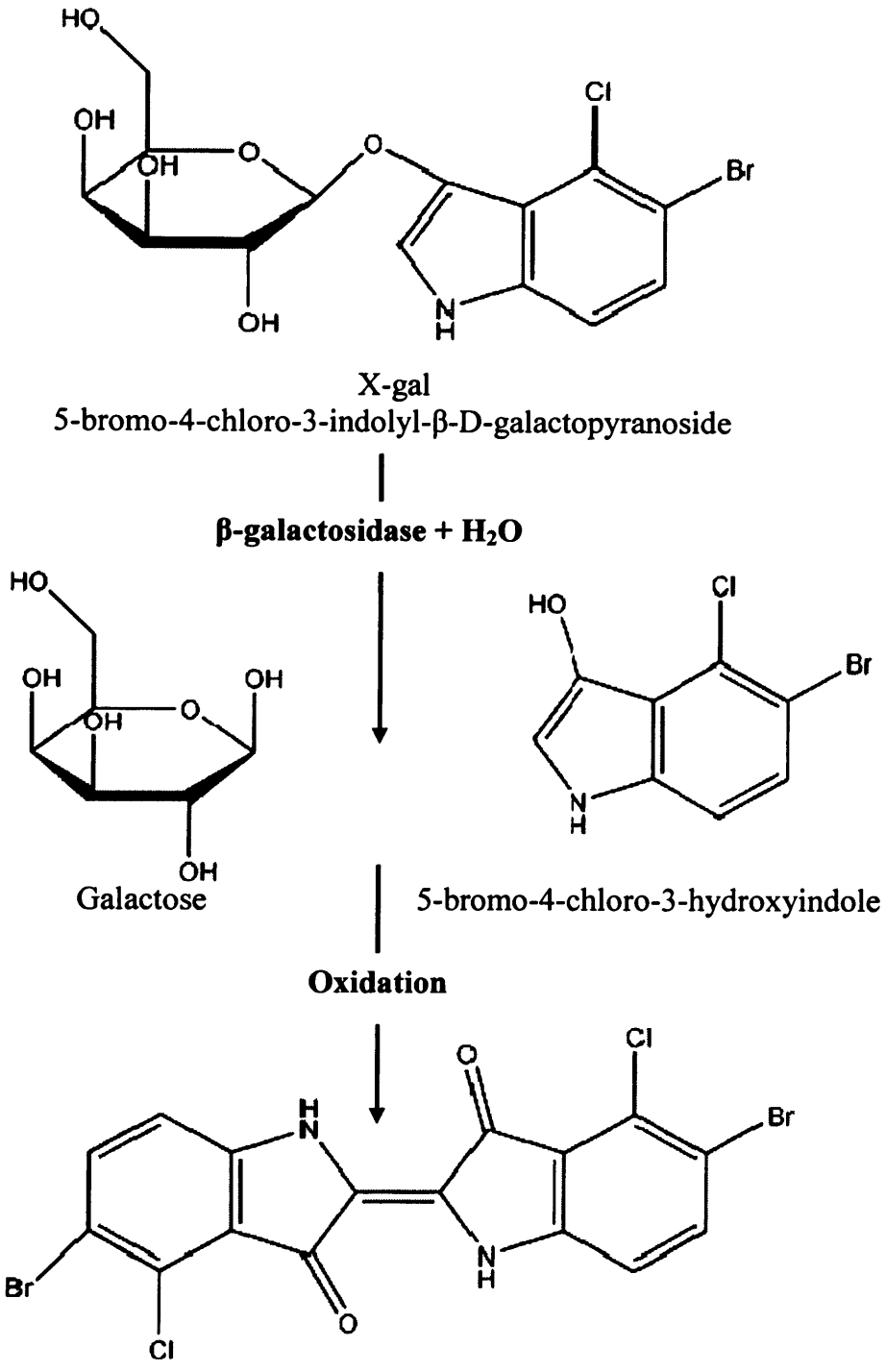

Figure 4.1 Cleavage of X-gal by β-galactosidase and formation of the blue pigment (5, 5'-dibromo-4, 4'-dichloro-indigo) that is observed to identify expression from the plasmid.

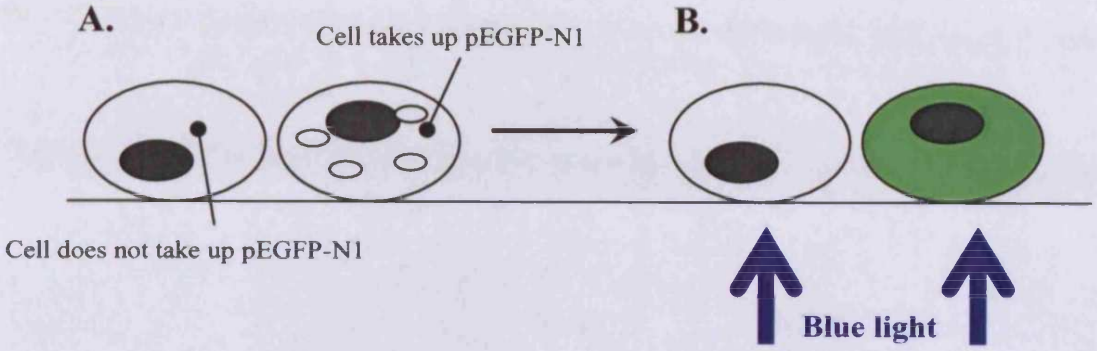

Figure 4.2. A diagram depicting positive expression from pEGFP-N1. Some cells take the plasmid up (A) and following a period of time EGFP is expressed. If these cells are subsequently exposed to blue light, transfected cells fluoresce green (B).

4.1.4 *Ex vivo* skin model

For pDNA to be expressed it must reside in an environment that promotes gene expression, e.g. the nucleus of a viable cell. Furthermore, the various cytoplasmic components that are required to translate the genetic information into a peptide must also be present and fully functioning. Frequently mouse and pig skin have been used as models for human skin, often adequately. However, there are well characterised biological and morphological differences between animal and human skin (Panchagnula *et al.* 1997). Ultimately, this thesis advocates that microneedles can be used in human patients; therefore, it is only by conducting test in human skin that true evaluation will be possible. While it is not possible to conduct tests in human volunteers at present, the development of a model system will offer a close approximation of the human *in vivo* state. Skin samples that are obtained immediately following surgery are maintained viable by culturing in an optimized organ culture system. As a result, it is also possible to mimic, as accurately as possible, microneedle facilitated gene delivery to human skin. Similar techniques have been employed by others investigating gene delivery to human skin (Hengge *et al.* 1996).

For this technique to be valid it is essential that the *ex vivo* skin remains viable prior to and during the experimental procedure, in this regard much can be learnt from skin graft techniques used in reconstructive surgery, where success depends on viable skin allografts (Bravo *et al.* 2000). Once the skin is removed from the patient it is transported to the laboratory. However, it has been noted that immediately following excision the tissue begins to deteriorate (Tomita *et al.* 2004). Consequently, successful organ culture is dependent on limiting the rate degradation occurs. Sterne *et al* have proposed that the principle cause of necrosis observed in *ex vivo* skin is a lack of nutrients and amassing of toxic waste products (Strene *et al.* 2000). Therefore, during transportation of the skin from the theatre to the laboratory necrosis is restricted by immersing the skin in nutrient supplemented culture media and reducing the temperature.

4.1.5 Organ culture set-up

The organ culture method that employed was based on a system developed by Trowell in the 1950's (Trowell 1954). This method requires that the skin is incubated at the air-liquid interface; to do this the skin samples are placed on top of metal grids, which have folded lens paper rested on top of them. The metal grid and lens paper are placed in a suitable culture dish which is filled with a suitable culture media until the ends of the lens paper touch the liquid. The lens paper then acts as a wick drawing up the media to the skin samples, nourishing the skin from the dermis side; this is shown schematically in Figure 4.3.

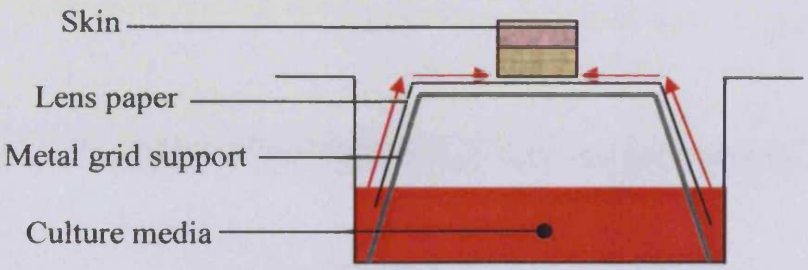

Figure 4.3 A schematic of the organ culture system based on that developed by Trowell in the 1950s that will be employed in these studies.

Split-thickness skin refers to skin that has been carefully dissected, longitudinally, to remove the majoritory of the dermis while leaving the epidermis intact (Strene *et al.* 2000; Bravo *et al.* 2000, Backvall *et al.* 2002). Split-thickness skin is commonly used as skin grafts in human patients requiring replacement skin. Frequently, in surgical applications, a device called a dermatome is used to create split-thickness skin (Ben-Bassat *et al.* 2001; Bravo *et al.* 2000, Strene *et al* 2000), but it can also be produced by careful dissection with a scalpel blade. The rational for using split-thickness skin, as opposed to full-thickness skin in organ culture, is the culture media does not have too travel as far in order to nurish and deliver oxygen to viable epidermal cells. A further considertion is the actual size of the sample cultured. The larger the size of the sample the more difficult it is to deliver oxygen and nutrient to the center, which will ultimately lead to necrosis. To address this, it has been proposed that cultured skin samples should be in the range of 2-3mm^2 (Varani 1998; Moll 2003, Backvell *et al.* 2002).

4.1.6 *Ex vivo* skin viability

Before any judgment can be made regarding exogenous gene expression, in *ex vivo* skin maintained in organ culture, a demonstration of skin viability must be made. Viability can be determined in a number of ways, for example by histological examination of cryosections of cultured skin, and by demonstrating that genes are sill being expressed in *ex vivo* skin during the culturing period, this is important because it demonstrates that the skin is still genetically viable. A suitable method for detecting expression from genes is by amplifying specific sequences of mRNA using a variation of the polymerase chain reaction (PCR). The technique of PCR allows a rapid and sensitive means of amplifying specific regions of a DNA molecule. The technique was first described in the 1980 (Mullis & Faloora 1987) and has rapidly become one of the most powerful of modern molecular biological techniques. Simply, a PCR reaction requires a DNA molecule (containing the region of interest), called template DNA, two oligonucleotide primers, typically composed of 17-30 nucleotides, which complentery bind the flanks of the region of the template DNA that is too be amplified, DNA polymerase, nucleoside-5'-triphosphates (dNTPs), and $MgCl_2$. The reaction mixture is heated until the DNA template molecule denatures, forming single stranded DNA molecules. The reaction is then cooled allowing the primers to anneal, followed by a polymerase reaction where dNTPs are complementary incorporated along the length of the single strand template DNA molecule catalysed by the polymerase enzyme (Figure 4.4). The reaction is then stopped by heating so the newly synthesized double stranded molecules denatures. The reaction is then cooled again so that primers are able to anneal and the polymerase reaction is repeated. This process is repeated a number of time resulting in vast amounts of the target sequence being generated.

The basic PCR reaction outlined above has since been modified and there now exist many variations of this currently employed, each achieving specific end goals. One such variation is reverse transcription-polymerase chain reaction (RT-PCR). This technique provides possibly the most sensitive methods currently available for the detection of specific messenger RNA (mRNA) molecules. The main advantage of this technique is its sensitively, because of the PCR component the starting material can be extremely small it has even been suggested from a single cell. This technique provides us with the ability too first ensure viability in the organ culture and also comfirm expression from the plasmid.

When a gene is expressed a complementary strand of mRNA is formed. The mRNA molecule moves out of the nucleus and into the cytoplasm where it is translated into an amino acid chain. However, in the cytoplasm mRNA is persistently being degraded, consequently, it is synthesized at a higher rate than would be expected for maintenance of a steady amount. Therefore, if the cell losses genetic viability, i.e. no longer expresses mRNA, we can assume that that cell is dead. Conversely, if the tissue is still expressing mRNA after a period of time in organ culture we can be confident that the tissue is still genetically viable. By performing RT-PCR to amplify a specific mRNA transcript after a period of time in organ culture will demonstrate that the *ex vivo* skin maintained in culture is viable.

The region of the DNA template molecule that is going to be amplified

Temperature of the reaction is raised so that the two anti-parallel strands denature, or melt. The reaction is the cooled to allow the binding of the primers, which flank the region that is going to be amplified.

The reaction temperature is then altered to that a new complementary strand is polymerised on each of the original strands.

The result is two new strands of DNA, each containing an original strand and each containing a new strand.

The temperature of the reaction is once again raised so that the double stranded DNA melts and then allowed to cool so that the primers can anneal.

The result of this cycle is four strands of DNA, two containing an original strand and a new strand and two that are completely made up of new strands, the first cycle products.

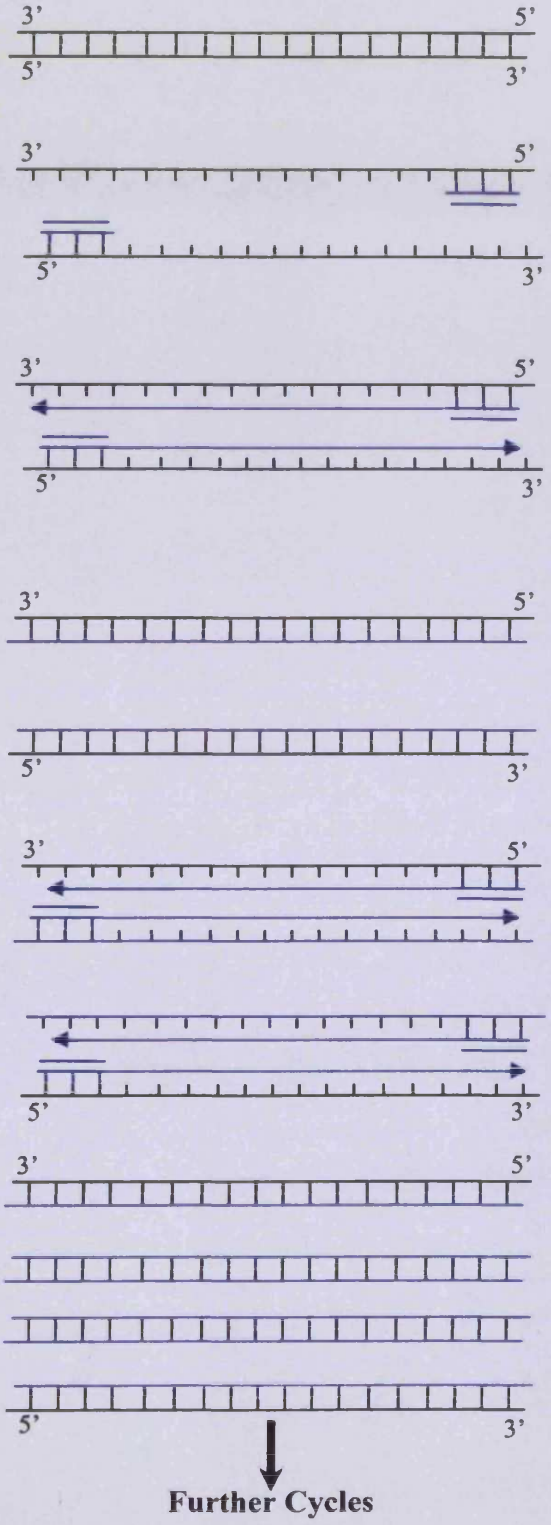

Figure 4.4 The principal steps involved in a basic PCR reaction

4.1.7 Attempt to increase transgene expression from pDNA

Viral vectors, as discussed in Chapter 1, have been used as vectors for the delivery of exogenous genes to the skin (Hengge & Mirmohammadsadegh 2000). Generally viral vectors are much more efficient at delivering exogenous nucleic acids to cells compared to non-viral vectors; however, there are a number of notable drawbacks associated with viral vectors (Chapter 1). Consequently, non-viral vectors are seen as an attractive alternative, but are notably less efficient with respect to exogenous DNA expression and microneedle facilitated delivery of pDNA is no exception.

However, there are a number of factors that can be investigated in order to try and improve the levels of gene expression with respect to microneedle delivery. For example, the effect of microneedle height will be investigated. The logic for this is that larger microneedle will penetrate further into the epidermis; they will stand more chance of penetration if applied to the natural folds and ridges of the skin, therefore exposing more epidermal cells to the pDNA formulation. Also, microneedle arrays with different tip morphologies will be investigated; sharp tipped microneedle versus frustum tipped microneedles. It is proposed that frustum tipped microneedles will cause disruption to the SC because of their morphology and in doing so expose more epidermal cells to the delivery formulation, thus increasing expression levels. Also, the number of times that an array is applied to the same region of skin might also enhance gene expression. Typically the array is applied in a single rolling motion but if the "number of rolls" is increased the effect could be to force more of the formulation into the formed channels and consequently to the epidermal cells. Furthermore, the concentration of applied pDNA will also be investigated. It is likely that increasing the amount of pDNA would make more DNA available for uptake and

limit the effect of nuclease degradation. Finally, the effect of occluding the treated surface can be investigated to determine weather this has any effect on transgene expression. Occlusion has been shown the hydrate the SC resulting in a 100 fold increase in penetration of a steroid compared to unoccluded treatments (McKenzie & Stoughton 1962).

4.2 Aims and objectives

4.2.1 Aims

The aims of this chapter are to investigate delivery of reporter pDNA facilitated by microneedles to human *ex vivo* skin and factors that might effect expression.

4.2.2 Objectives

- Demonstrate that recently excised human skin can be transported and cultured so as to maintain a genetically viable state.
- Show that microneedles can facilitate the delivery of functional pDNA to the viable epidermis and detect expression.
- Investigate weather levels of gene expression can be increased by simple modifications to the delivery protocol.

4.3 Materials and Methods

4.3.1 Materials

Qiagen® Plasmid 2500 Mega Kit was purchased from Qiagen® (Crawkey, UK)

Components of the X-gal staining solution were obtained from Sigma-Aldrich Chemical Company (Poole, UK).

Cell culture plastics utilised were bought from Corning-Costar (High Wycombe, UK)

Dulbecco's Modified Eagles's Medium (DMEM 25mM HEPES), foetal bovine serum (FBS) and penicillin-streptomycin were obtained from Invitrogen Corporation (Paisley, UK)

All histological materials were purchased from R.A. Lamb Ltd (Eastbourne, UK)

Harris' Haematoxylin, 1% Gurrs' eosin, Histomount®, and xylene were obtained from Lab 3 (Bristol, UK).

All other reagents were of anylitical grade an purchased from Fisher (Loughborough, UK)

4.3.2 Transport of *ex vivo* skin

All skin samples were obtained from the Royal Gwent Hospital and were transported in the same way. Immediately following surgery, theatre staff placed the excised skin sample into a plastic container containing 150ml of full culture media (94% DMEM, 5% FBS, and 1% penicillin/streptomycin). This container was then placed into a cool bag pre-chilled with ice packs to 4°C.

4.3.3 Preparation of *ex vivo* skin for organ culture

Once in the laboratory (designated containment 2 facility), the skin sample was removed from the transport media and blotted dry. The subcutaneous fat was removed and the skin cut into a rectangular shape, the size of which dependent on the size of the skin sample obtained. The skin was pinned, dermis side down, onto a cork dissection board. A shallow incision was made cross the narrower region of the skin (Figure 4.5 A & B). Then by careful under cutting, the epidermis/upper dermis was removed from the main body of the dermis, producing split-thickness skin (Figure 4.5 C). Split-thickness skin was used in all subsequent experiments, unless otherwise stated.

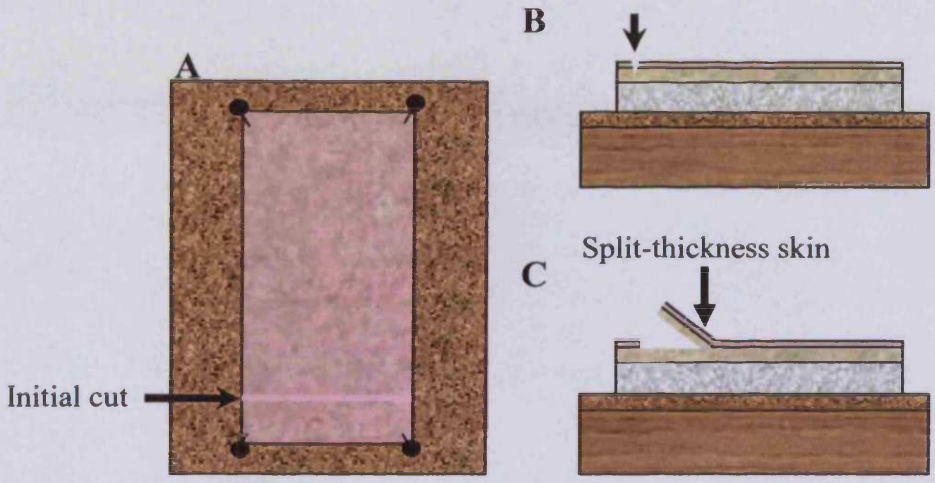

Figure 4.5 The formation of split-thickness skin. *Ex vivo* skin was pinned out on a flat cork dissection board as depicted in (A). The initial cut was made across the surface of the skin with care taken so as not to completely cut through (B). Careful under cutting with a scalpel blade yields split-thickness skin (C).

4.3.4 Organ culture system

Stainless steel grids were cut into rectangles approximately 5cm by 2cm. The ends of the metal grids were folded into a "table" shape (Figure 4.3). The grids were trimmed to fit into a 6-well culture plate. A grid was placed in each of the 6 wells along with a single piece of lens cleaning paper, folded so that it covered the surface of each grid and extending to contact the floor of the culture plate well. Into each well ~2ml of culture media was applied (94% DMEM, 5% FBS, 1% penicillin/streptomycin), so the base of the well was covered and the lens paper started to draw up the culture media (Figure 4.3). A fresh culture plate was made up prior to each experiment and incubated at 37°C for ~2 hours before each experiment commences. The organ culture system described was common to all subsequent experiments performed.

4.3.5 RNA isolation

Because RNA is prone to degradation by environmental Rnase contamination, all plastics were brought in especially and certified free from nucleases, other equipment e.g. pipettes, surfaces etc... were cleaned with RNase*Zap*®, a commercially available reagent that reduces environmental RNase contamination.

Each skin sample was snap frozen by immersion in liquid nitrogen and ground into a fine powder in a pestle and mortar under liquid nitrogen. To this 2ml of TRI reagent™ was added. TRI reagent™ is a mix of guanidine thiocyanate and phenol in a mono-phase solution, which has the ability to dissolve DNA, RNA and protein from lysed cells (Puissant and Houdebine 1990). TRI reagent™ and powdered skin sample were mixed, in the pestle and mortar, until a paste formed, which was divided and transferred equally into two 1.5ml centrifuge tubes. Each tube was vortexed and allowed to stand at room temperature for 5 minutes. All tubes were centrifuged at 14000 rpm, 4°C for 10 minutes. Supernatants were transferred to fresh 1.5ml centrifuge tubes and 200 µl of chloroform added to each, then vortexed for 15 seconds and allowed to stand at room temperature for 5 minutes. All tubes were centrifuged at 14000 rpm, 4°C for 15 minutes. This resulted in separation of the TRI reagent™ mixture into a dissolved chloroform phase which contained dissolved protein, a phenolic phase which contained DNA, and an aqueous phase in which was dissolved RNA. The aqueous phase was isolated and transferred into fresh 1.5 ml tubes and the RNA was precipitated by the addition of 0.5ml isopropanol, followed by incubation at room temperature for 10 minutes. The tubes were then centrifuged at 14000rpm, 4°C for 10 minutes. The supernatant was removed and the

RNA pellet washed in 1ml of 75% ethanol, vortexed for 15 seconds and centrifuged at 14000 rpm, 4°C for 10 minutes, the supernatant was removed and the pellets allowed too dry in air. The pellets were then dissolved in 50µl of DNase/RNase free water by pipetting and the two tubes combined.

To obtain RNA from cultured cells the culture media was removed and 2ml of TRI™ reagent was added directly into the flask containing the cells (cell culture methods will be discussed in chapter 6), the isolation procedure was followed as described above.

4.3.6 Removal of contaminating genomic DNA from RNA

RNA samples were subjected to DNA-*free*™ treatment to remove any contaminating genomic DNA. This commercially available kit uses recombinant DNase 1 (rDNase 1) to digest DNA so that levels cannot be detected by routine downstream PCR.

To each RNA sample 0.1 volume of 10X DNase 1 buffer was added and then 1ml of the rDNase1 solution. This was incubated at 37°C for 30 minutes. The reaction is stopped by the addition of 0.1 volume of DNase inactivation reagent, the sample was vortexed for 15 seconds and incubated at room temperature for 2 minutes. Each tube was centrifuged at 10 000 X g for 2 minutes; the supernatant was transferred to a fresh tube.

4.3.7 Agarose gel electrophoresis (RNA)

Agarose (1g) and TBE buffer (100ml) were added to a 500ml conical flask which was heated in a microwave until the solution boils and the agarose has completely dissolved. The flask was cooled to ~40°C before eithidium bromide was added to a final

concentration of 0.5μg/ml; the mix was poured into a gel tray and allowed to solidify. Wells were formed in the gel by the addition of a suitable comb into the molten gel. Each well was loaded with isolated RNA (2μg), loading buffer (4μl) and made up to a total of 20μl with nuclease-free water. The gel was subject to electrophoresis at 100V for 1hour before the gel was removed and visualized with a UV Gel Doc 1000 and Molecular Analyst™ software (Biorad Laboratories, Hercules, CA, USA).

4.3.8 One-step RT-PCR investigating skin viability

Split-thickness skin (♀ 60 years of age) was pinned on a flat cork dissecting board. To a section of the pinned skin, 20μl of pCMVβ (1 mg/ml) was applied. Repeated shallow slashes were then made to the region where the plasmid solution was applied, disrupting the SC facilitating delivery to the epidermis (n = 4). Other regions were treated with 20μl of PBS and repeatedly slashed (n = 4), while others regions were left intact (n = 2). The different regions of treated skin were excised (samples of ~0.8mm^2) and placed in organ culture for 24 hours. After incubation, each sample was placed in a 1.5ml centrifuged tube and snap-frozen by immersion in liquid nitrogen and stored at -80°C.

Total RNA was isolated and cleaned as described above (Section 4.3.5); 2μg was entered into a one-step RT-PCR reaction, according to the manufacturer's protocol. The primers used to amplify a region of the *lacZ* mRNA transcript were TTC ACT GGC CGT CGT TTT ACA ACG TCG TGA (5'-3') and ATG TGA GCG AGT AAC CCG TCG GAT TCT (5'-3') the reaction conditions were as follows:

30mins at 50°C (reverse transcription)
15mins at 95°C (PCR activation)

30s at 94°C
30s at 55°C } 3 step amplification X 40
2mins at 72°C

10mins at 72°C (final extension)
Hold at 4°C

The samples were then analyses by electrophoresis.

4.3.9 Agarose gel electrophoresis (RT-PCR products)

Agarose gels were prepared as described above. The RT-PCR products (2μl) along with loading buffer and nuclease free water to a volume of 20μl were added to each well and subject to electrophoresis at 100V for 1 hour, the gel was removed and visualized by a UV Gel Doc 1000 and Molecular Analyst software (Biorad Laboratories, Hercules, CA, USA).

4.3.10 Histological examination of cultured skin and viability

Split-thickness skin (♀ 60 years of age) was pinned on a flat cork dissecting board. Samples of ~0.8 cm^2 (n = 4) were cut directly out of the pinned skin, and each rinsed in 2ml of PBS for 10 minutes before being fixed in 2% v/v glutaraldeyde for 2 hours at 4°C. Each sample was further rinsed in 2ml of PBS at total of two times over 1 hour. The samples were embedded in OCT on dry ice and stored at -80°C. Other samples, again ~0.8 cm^2, were generated (n = 4) and cultured for 24 hours before fixation and embedded

as just described. Sections of 12μm were generated using a cryostat (described in chapter 3) and subsequently stained with Harris' haematoxylin and Gurrs'eosin (H & E). This process involves the slides being washed in tap water, followed by complete immersion in haematoxylin for 2 minutes. Slides were rinsed in tap water then immersed in acid alcohol (1% HCl (1M) in 70% ethanol) for ~10 secsonds. Slides were rinsed in tap water for ~30 seconds, followed by immersion in Gurrs' eosin for ~5 seconds. Slides were rinsed in tap water for 2-3 minutes and allowed to dry. Slides were observed by light microscopy to identify any gross morphological changes with an Olympus BX50 microscope (Olympus, Middlesex, UK).

4.3.11 Microneedle facilitated delivery of pCMVβ to *ex vivo* human skin

Split-thickness skin was pinned over a semi-circular cork support (described in Chapter 2). Specific regions of the pinned skin receive a volume of pCMVβ (1mg/ml), followed by the application of a mounted microneedle array applied in a single rolling motion. Controls involved applications of the same volume of pEGFP (1mg/ml) followed by the microneedle array in a single rolling motion, other regions received 20μl of PBS also followed by microneedles, untreated intact skin and skin only treated with microneedles. Each region of treated skin was excised (generating samples ~0.8 cm^2) and placed into organ culture for 24 hours.

Samples required for RT-PCR were removed from culture and placed into a 1.5ml centrifuge tube with 1ml of RNA*later*® and stored at -20°C. RNA*later*® is a commercially available reagent that allows the storage of tissue samples in such a way to

ensure cellular RNA remains intact. Skin samples were removed from RNA*later*® and snap frozen in liquid nitrogen. RNA extraction and RT-PCR conditions were described previously. Primers were TTC ACT GGC CGT CGT TTT ACA ACG TCG TGA (5'-3') and ATG TGA GCG AGT AAC CCG TCG GAT TCT (5'-3'), specific for a portion of the *lacZ* mRNA transcript.

Samples required for histochemical analysis were each rinsed in 2ml of PBS/$MgCl_2$ for 30 minutes before being fixed in 2% v/v glutaraldeyde for 2 hours at 4°C. Each sample was further rinsed in 2ml of PBS at total of three times over 6 hour. Each skin sample was then immersed in 2ml of X-gal staining solution for ~24 hours; the components of the X-gal solution are shown in Table 4.1.

Table 4.1 Components of X-gal staining solution

Component	**Volume**
X-gal (40mg/ml)	2.5ml
K^+ ferrocynide (0.6M)	420µl
K^+ ferricynide (0.6M)	420µl
$MgCl_2$ [1M]	100µl
H_2O	21.76ml
Tris-HCl [200mM]	25ml
Total	**50ml**

Samples were briefly rinsed in PBS/$MgCl_2$ before being viewed by light microscopy with a Stemi 2000-C Stereomicroscope (Zeiss, Welwyn Garden City, UK) and a Scott 1500

fibre optic external light source (Scott UK Ltd, Stafford, UK); images were captured using a Olympus DP-10 digital camera (Olympus Optical, London, UK) samples were viewed either directly or mounted between two microscope slides, to aid visualisation. Each sample was embedded in OCT and frozen on dry ice before storage at -80°C. Samples were removed from storage, mounted within the cryostat and allowed to equilibrate to ~-20°C; cryosections of 12μm were generated and captured on coated microscope slides. Captured sections were fixed by immersion in acetone and viewed both unstained and following differential staining with H & E. Observation of sections was by light microscopy with an Olympus BX50 microscope (Olympus, Middlesex, UK).

4.3.12 Microneedle facilitated delivery of pEGFP-N1 to *ex vivo* human skin

Split thickness skin (♀ 57 years of age) was pinned over a semi-circular cork support. To specific regions of the skin 20μl of pEGFP (1mg/ml) was applied followed by the application of a 7 X 7 mounted, sharp tipped microneedle array with heights of 280μm in a single rolling motion (n = 4). To other regions control samples were generated, consisting of 20μl of PBS applied in conjunction with microneedles (n = 4). Skin samples were cultured for 24 hours.

Each sample was placed in a vial containing a magnetic follower and a metal grid, thereby separating the vial. Each vial was filled with 10ml of 20mM EDTA and then placed on a magnetic stirrer plate immersed in a water bath heated to 37°C (Figure 4.6). Skin samples were placed in the vials and incubated for 2 hours. After incubation the epidermis was separated from the dermis by carefully pulling it away with forceps while

being viewed under a dissection microscope. The separated epidermis was rinsed in PBS for 10 minutes and fixed in 2% v/v glutaraldehyde, at 4°C for 30 minutes. The separated epidermis was further rinsed in PBS for 10 minutes before being mounted on a microscope slide, epidermis side up and viewed with an Olympus BX50 fluorescent microscope (Olympus, Middlesex, UK).

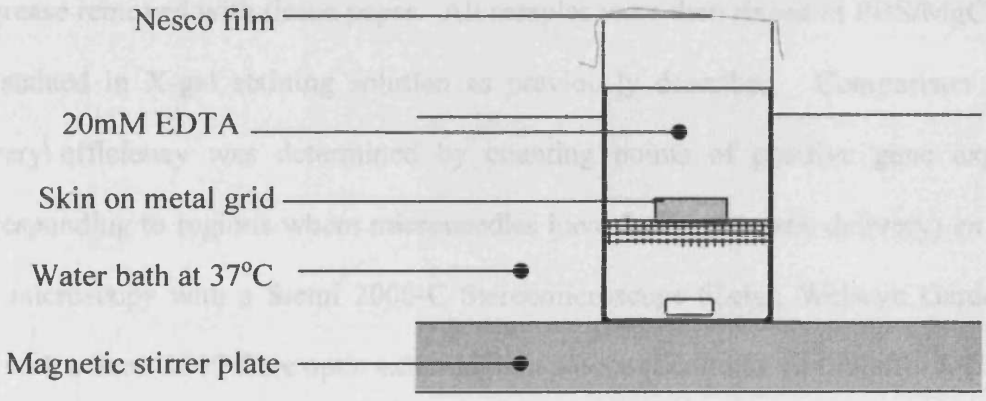

Figure 4.6 Experimental set-up for EDTA epidermal/dermal separation.

4.3.13 Attempts to improve gene expression efficiency

4.3.13.1 Occlusion of treated area

Split thickness skin (♀ 72 years of age) was pinned over a semi-circular cork support. To regions 20µl (1mg/ml) of pCMVβ was applied followed by 4 X 4 mounted microneedle array, with frustum tips of 260 µm in a single rolling motion (n = 4), these were excised and placed in organ culture. Other regions of skin received the same treatment (n = 4). However, after excision vacuum grease was applied all the way around the edge of each sample, with care being taken to ensure that no grease came into contact with the

pDNA/microneedle treated region. Each sample was covered with a piece of cling-film, fixed in place by the grease, samples then placed in organ culture. This experiment was repeated with another patient's skin tissue (♀ 63 years of age) and the results from the two experiments were combined.

After 24 hours each samples was removed from culture. Occluded samples carefully had the grease removed with tissue paper. All samples were then rinsed in PBS/$MgCl_2$, fixed and stained in X-gal staining solution as previously described. Comparison of gene delivery efficiency was determined by counting points of positive gene expression (corresponding to regions where microneedles have facilitated gene delivery) *en face* by light microscopy with a Stemi 2000-C Stereomicroscope (Zeiss, Welwyn Garden City, UK) with a Scott 1500 fibre optic external light source (Scott UK Ltd, Stafford, UK).

4.3.13.2 Multiple microneedle applications

Split-thickness skin (♀ 68 years of age) was pinned over a semi-circular cork support. Five distinct regions of skin were marked out, each received 4 individual applications 20μl (1mg/ml) of pCMVβ (n = 4) followed by a 4 X 4 mounted sharp tipped microneedles array. To the first region the array was applied in a single rolling motion as previously described. To the second region the array was rolled on as previous but instead of removing the array it was brought back to its original starting position, creating a double roll (n = 4). The number of rolls was increased by 2 in each region till a total of 16, Figure 4.7 (n = 4 in all cases).

Each treated sample, ~0.8cm^2 was excised, rinsed, fixed and stained in X-gal solution (described in Section 4.3.11). Each sample was prepared for microscopy as described in Section 4.3.13.1

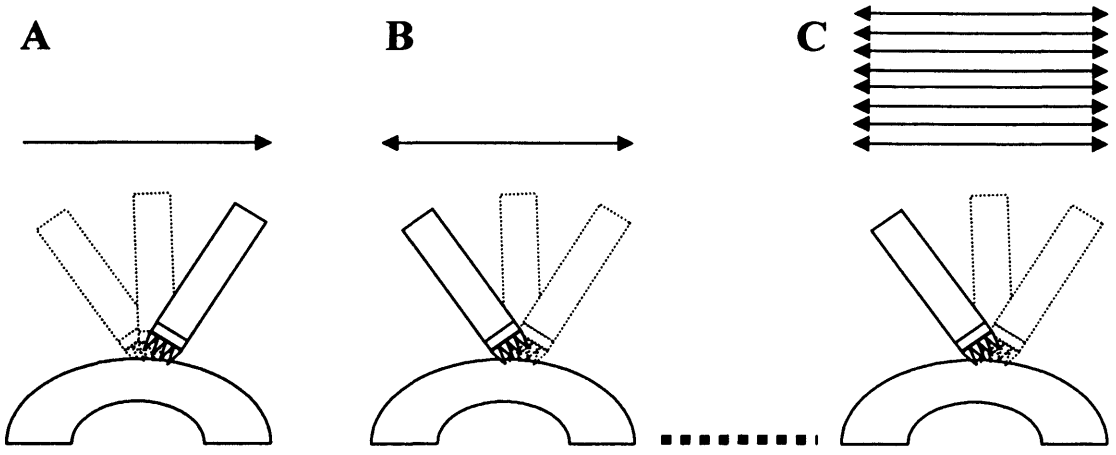

Figure 4.7 Increasing the number of rolls, in an attempt to increase levels of gene expression. A single roll is depicted in (A) however, if this process is continued, by bringing the array back to its original starting position (B) is called a double roll. The number of rolls can therefore be defined; a 16 roll is shown in (C).

4.3.13.3 Microneedle height

Split-thickness skin (♀ 63 years of age) was pinned over a semi-circular cork support. Distinct regions of skin receive 20µl (1mg/ml) of pCMVβ (n = 4) followed by a 7 X 7 mounted microneedle array with needle heights of 80µm. Other regions received 20µl (1mg/ml) pCMVβ followed by a 7 X 7 array with needle heights of 180µm (n = 4). Finally, a region received 20µl (1mg/ml) pCMVβ followed by a 7 X 7 array with needle

heights of 280μl (n = 4). All microneedle arrays were applied too the skin a single rolling motion.

All samples were excised and cultured for 24 hours and rinsed, fixed and stained in X-gal staining solution as previously described (Section 4.3.11). Gene delivery efficiency was first assessed *en face* by light microscopy Each sample was prepared for microscopy and viewed as described in Section 4.3.13 with the points of positive gene expression associated with a microneedle channel recorded.

4.3.13.4 Effect of pDNA concentration

Split thickness skin (♀ 68 years of age) was pinned over a semi-circular cork support. Three distinct regions of skin were marked out, to the first region 20μl (0.5 mg/ml) of pCMVβ was applied (n = 4), to the second 20μl (1mg/ml) of pCMVβ was applied (n = 4), and to the third 20μl (2mg/ml) of pCMVβ was applied (n = 4).

Each sample was treated with a 7 X 7 sharp tipped mounted microneedle array in a single rolling motion.

All samples were excised and cultured for 24 hours then rinsed, fixed and stained in X-gal staining solution, as previously described. Gene delivery efficiency was assessed *en face* by light microscopy as described in Section 4.3.13.

4.3.14 Delivery of pDNA with dry-etch microneedles

Split-thickness skin (♀ 65 years of age) was pinned over a semi-circular cork support. To distinct regions of 20μl of pCMVβ (1mg/ml) was applied followed by a 15 X 16 X dry-etch microneedle array with heights of 250μm (n = 2). The dry etch array was mounted onto an SEM stub by double sided carbon tape. The mounted array is applied to the skin in a downward or flat manor (described in chapter 2). Control samples involved the application of 20μl of PBS followed by the dry etch array (n = 2).

All samples were excised and cultured for 24 hours and then rinsed, fixed and stained in X-gal staining solution as previously described. Gene delivery efficiency was first assessed *en face* by light microscopy with a Stemi 2000-C Stereomicroscope (Zeiss, Welwyn Garden City, UK) and a Scott 1500 fibre optic external light source (Scott UK Ltd, Stafford, UK); images were captured using a Olympus DP-10 digital camera (Olympus Optical, London, UK), by counting points of positive gene expression. Samples were embedded in OCT on dry ice and 10μm cryosections generated and observed by light microscopy with an Olympus BX50 microscope (Olympus, Middlesex, UK).

4.3.15 Delivery of pDNA with polymer microneedles

Split thickness skin (female patient, 65 years of age) was pinned over a semi-circular cork support. To distinct regions of skin 20μl of pCMVβ (1mg/ml) was applied followed by a 7 X 7 Biresin® polymer microneedle array with heights of 280μm (n = 4). The Biresin®

polymer array was mounted and applied to the skin in a single rolling motion as previously described. Control samples involved the application of 20μl of PBS followed by the polymer array (n = 2).

Samples were excised and cultured for 24 hours, then rinsed, fixed and stained in X-gal staining solution as previously described (Section 4.3.11). Gene delivery efficiency was first assessed by light microscopy, *en face*, by counting the points of positive gene as described in Section 4.3.13. Samples were then embedded in OCT on dry ice and 10μm cryosections generated and observed by light microscopy with an Olympus BX50 microscope (Olympus, Middlesex, UK).

4.3.16 Delivery of pDNA with hollow microneedles

The hollow microneedle array was attached to a 1ml syringe through capillary tubes. Using the syringe approximately 100μl of (1mg/ml) pCMVβ was drawn up into the capillary system. The array was then applied to split thickness skin, pinned over a semi-circular cork support, in a downward or flat manor (Described in Chapter 2; Section 2.3.13). The fluid was then expelled through the microneedle array to infuse with the skin (n = 1). The treated skin sample was excised and cultured.

The sample was rinsed, fixed and stained in X-gal staining solution as described in Section 4.3.11. Gene delivery efficiency was determined by light microscopy as described in Section 4.3.13. Cryosection were prepared and observed as described in Section 4.3.10.

4.4 Results and discussion

Ex vivo skin samples proved to be variable. Typically the age of the patients that provided the tissue were in the range of 55-75 years of age. The amount of sub-cutaneous fat, thickness of dermis and/or epidermis, as well as the sample size all varied with each patient. Although this was to be expected it should also be considered when assessing results obtained from experiments involving *ex vivo* skin.

4.4.1 RNA isolation

Total RNA was successfully isolated from both *ex vivo* human skin which was snap frozen immediately following surgical procedure and from skin that was snap frozen after being cultured for 24 hours. However, isolating total RNA from skin proved to be extremely difficult, principally because the skin is extremely tough and robust in nature and because such small samples of skin were involved (consequence of culture conditions). Processing the frozen tissue in a pestle and mortar was extremely difficult. Better yields of RNA would probably be obtained if a mechanical homogenizer was utilized. Nevertheless, RNA of sufficient quantity and quality was obtained from *ex vivo* skin; 280/260 absorbance was above >1.8 and typical yields were in the range of 23.5 to 83μg/ml. Quality of the isolated RNA was also confirmed visually by running samples on a 1% agarose gel containing ethidium bromide, observed by UV light. A typical result is shown in Figure 4.8. RNA isolated from *ex vivo* human skin is compared with RNA isolated from cultured A549 lung epithelial cells (See chapter 6 for information regarding cell culture).

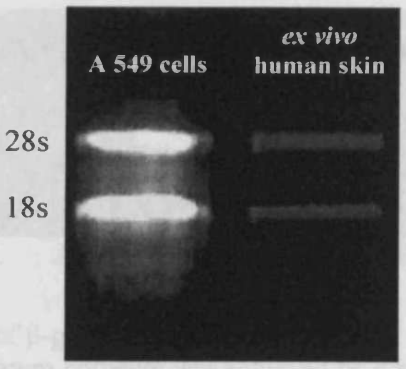

Figure 4.8 Appearance of isolated RNA samples run on 1% agarose gel.

Both samples have two distinct bands corresponding to the 28s and 18s ribosomal RNA (rRNA) molecules. The RNA isolated from *ex vivo* skin was not as bright as that obtained from the cell culture because less RNA was present, due to the lower yields obtained from *ex vivo* skin.

4.4.2 Production of β-galactosidase mRNA as an indicator of tissue viability

Following culturing of *ex vivo* skin treated with pCMVβ and with the integrity of the SC diminished by repeated slashes with a scalpel blade, RNA was successfully isolated and of sufficient quantity and quality for RT-PCR. Viability of the tissue would be confirmed if the PCR reaction successfully amplified a region of the β-galactosidase mRNA transcript in a sample that had been cultured for 24 hours. Because of the rapid turn over of mRNA by cells this would serve to demonstrate that the exogenous transcript was produced during the culturing period. The results are shown in Figure 4.9.

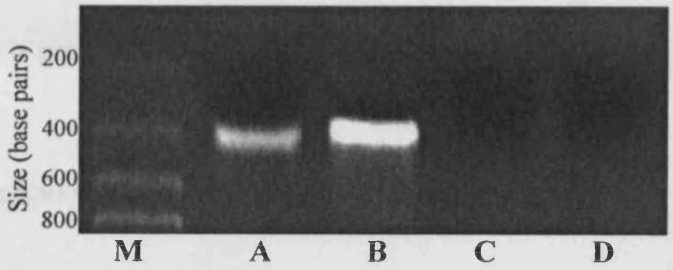

Figure 4.9 RT-PCR analysis of β-galactosidase expression in *ex vivo* human skin (A) and *E. coli* (B), disruption of the stratum corneum was achieved by repeated slashes with a sterile scalpel. The size of the fragment generated, in both cases, is consistent with predictions of 400bp when compared to a molecular marker (M). Lane (C) and (D) are negative controls for Lanes (A) and (B) respectively. Samples were run on a 1% agarose gel, stained with ethidium bromide before visualisation by UV.

To confirm that gene expression was occurring specifically during the incubation period the experiment was repeated but samples of RNA were obtained from skin that had just been treated with repeated scalpel slashes and pCMVβ, as well as from samples treated and cultured for 24 hours. The results are shown in Figure 4.10.

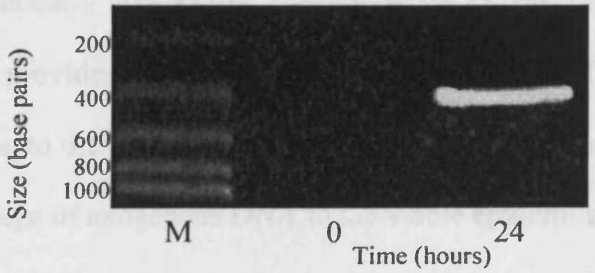

Figure 4.10 RT-PCR analysis of β-galactosidase expression in *ex vivo* human skin, disruption of the stratum corneum was achieved by repeated slashes with a sterile scalpel. If RNA is isolated from samples immediately after the plasmid is applied (time 0) then no expression is observed. Following 24 hours culturing, a clear signal is present corresponding to expression from the plasmid. This indicates that the skin remains genetically viable during the culturing period.

Figure 4.10 demonstrates that samples incubated for 24 hours in organ culture internalise the reporter plasmid and allow expression, indicating that the skin tissue maintained in organ culture is genetically viable during the culturing period.

4.4.3 Histological examination of cultured skin

Cryosections from skin, fixed ~2 hours post-surgery were compared with samples that had been cultured for 24 hours. Microscopic examination did not indicate any noticeable change in morphology of the skin following culture (Figure 4.11). The only possible difference was that the SC in the cultured samples may appear slightly thicker; this can be explained by the SC becoming hydrated and as a consequence swelling during the culturing period. However, this effect appears to be slight and is unlikely to have any significant effects.

Taken together these results demonstrate that the methods developed for transporting, processing, and culturing *ex vivo* human skin ensures that the *ex vivo* skin remains in a structurally and genetically viable state. Therefore, the *ex vivo* organ culture system that has been developed provides an extremely close approximation of *in vivo* human skin. It is possible, therefore, to draw satisfactory conclusion regarding the ability of microneedle to facilitate the passage of exogenous DNA to the viable epidermis.

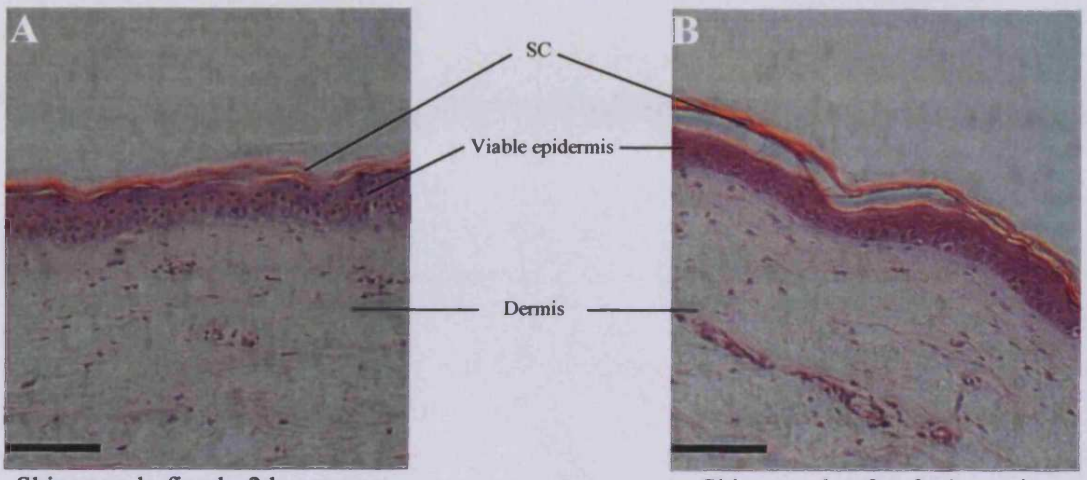

Skin sample fixed ~2 hours post surgery

Skin sample after 24 hours in organ culture

Figure 4.11. Histological examination of spit-thickness skin ~2 post surgery (A) and after 24 hours in organ culture (B); bar = 200μm in both cases.

4.4.4 Microneedle facilitated delivery of pCMVβ to *ex vivo* human skin

Total RNA isolated from skin samples treated with 20μl of pCMVβ (1mg/ml) in conjunction with microneedles and subjected to RT-PCR indicates the presence of *LacZ* mRNA (Figure 4.12 A). Total RNA isolated from regions of the same skin sample but treated with pEGFP-N1, as a negative control for the primers, in conjunction with microneedles yielded no signal (Figure 4.12 A). This indicates that the *LacZ* mRNA detected in the pCMVβ treated sample was indeed a consequence of expression from the plasmid and not amplification from some internal source. This was further confirmed in intact and PBS/microneedle treated skin (Figure 4.12 A). This demonstrates that pDNA delivered to the epidermis using microneedles results in expression of the exogenous DNA at least to the level of mRNA transcription.

Skin samples that were treated with pCMVβ and microneedles and subsequently immersed in X-gal staining solution and viewed *en face* contained blue regions corresponding to areas were the β-galactosidase enzyme is present. Typically, the blue regions are associated with microneedle created conduits. The blue regions are circular in appearance but vary in size, this is clear in Figure 4.12 B. The reason for this is probably due to variable numbers of cells in the different regions taking up and expressing the plasmid. Control samples, treated with PBS and microneedles and subject to X-gal staining showed no evidence of blue regions (Figure 4.12 C), therefore eliminating the possible that blue regions seen in the pCMVβ/microneedle treated samples were due to endogenous enzyme or artefact.

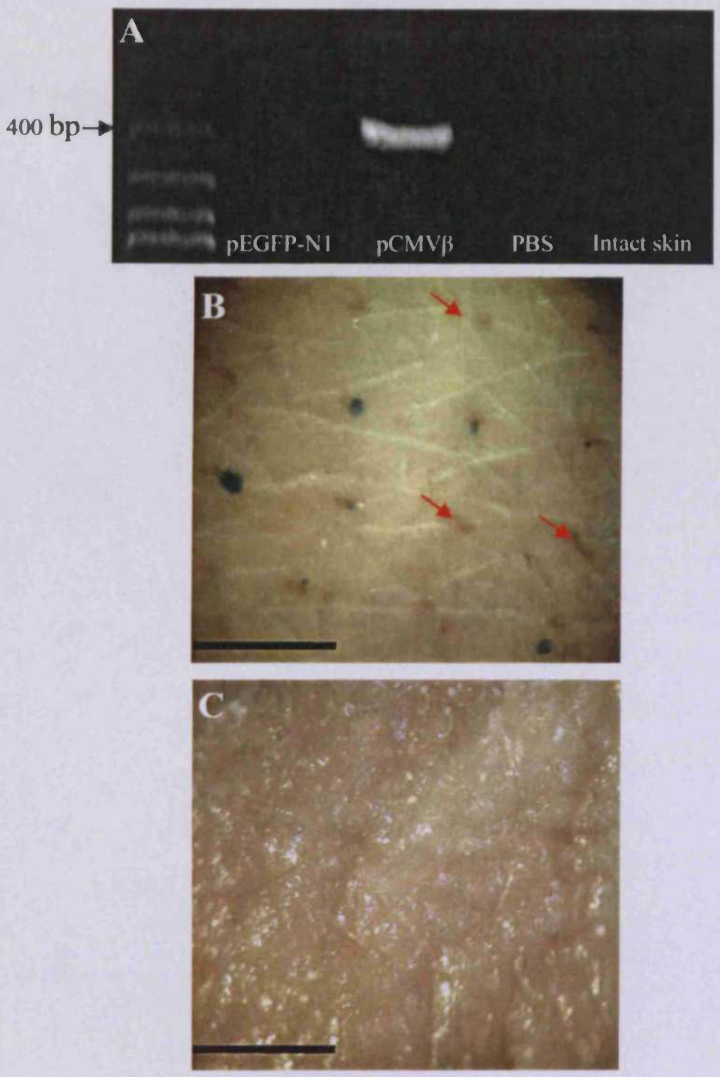

Figure 4.12 Positive expression from 20µl of 1mg/ml pCMVβ delivered to *ex vivo* skin with a mounted 4 X 4 frustum tipped microneedle array with heights of 260µm. Transcription from *LacZ* is confirmed by RT-PCR (A) and translation confirmed by histochemical staining with X-gal solution (B). This image also highlights that not all formed channels display positive expression (red arrows). Control samples, skin treated with pEGFP-N1 and microneedle show no evidence of expression when subject to X-gal solution (C); bar = 1mm

These results were replicated numerous times and expression was observed when pCMVβ was delivered using 260μm mounted frustum tipped microneedle in a 4 X 4 arrangement (Figure 4.12), 280μm mounted sharp tipped microneedles in a 7 X 7 arrangement (Figure 4.13) and mounted sharp tipped microneedles in a 4 X 4 arrangement, with heights of 260μm (Figure 4.14). However, expression was typically variable and not reproducible. It is clear however that for every experiment conducted over a three year period involving the delivery of pCMVβ with a single roll of the microneedle array, expression was never seen associated with every point of microneedle penetration. Indeed, Figure 4.12 shows the best result obtained during this period where 8 out of a possible 16 (50%) show associated expression. Frequently, only one or two points of expression were observed and it was not uncommon for expression not to be observed at all.

No doubt a major reason for this phenomenon are the associated low levels of expression of exogenous DNA delivered by in the absence of viral vectors. Nevertheless, there are also other reasons that contribute to the unpredictability and relatively poor efficiency of exogenous gene expression; these include inefficient delivery of pDNA into the formed microconduit, limited uptake of the pDNA into the cells located in the vicinity of the microconduit, excess cell damage or even cell death caused by microneedles (Birchall *et al.* 2005). In addition Couffinhal *et al* suggest that X-gal staining only detects approximately 80% of cells expressing β-galactosidase in the skin (Couffinhal *et al.* 1997). Also, it is possible that the X-gal stain is restricted or completely excluded from

the formed microneedle channels, therefore preventing it from coming into contact with enzyme arising from cells expressing pCMVβ.

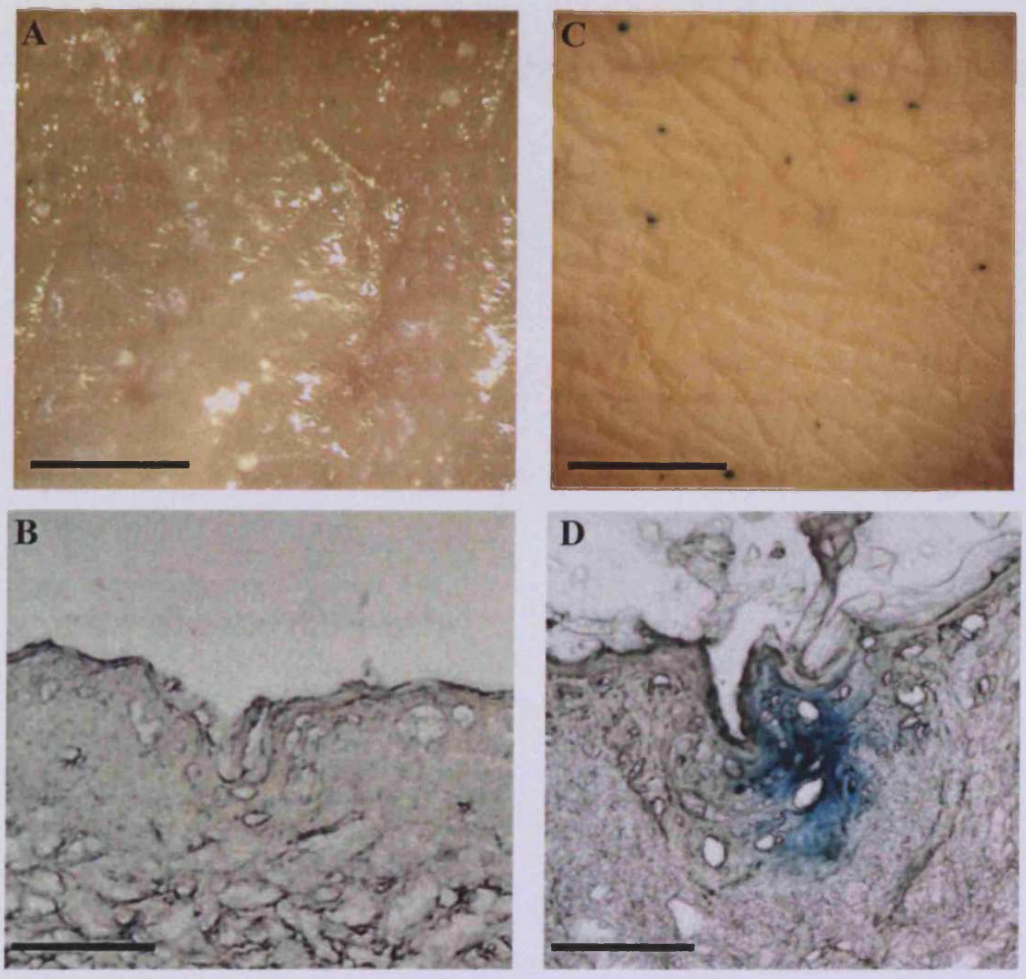

Figure 4.13 Positive expression from 20µl of 1mg/ml pCMVβ delivered to *ex vivo* skin by 280µm mounted sharp tipped microneedles in a 7 X 7 arrangement. Control samples comprising delivery of PBS with microneedle show no expression either *en face* (A) or 12µm cryosection (B). Plasmid delivered by microneedles however shows expression when viewed *en face* (C), which is shown in the vicinity of a microchannels as determined by observing 12µm cryosections (D). A & C bar = 1mm; B & D bar = 150µm.

Finally, the skin samples should be considered, which inevitably vary from patient to patient. It is likely that varying biological factors between patients, e.g. epidermal thickness, will significantly affect efficiency of exogenous gene delivery and subsequent expression, it is likely that some tissue will perform better in organ culture following treatment.

Cryosections generated from skin treated with pCMVβ in conjunction with microneedles, and control samples, showed formation of microconduits extending through the SC and viable epidermis to a depth of ~150μm (Figure 4.13 & 4.14). In control samples, there was no indication of expression associated with microconduits, as would be expected (Figure 4.14 A). However, samples treated with pCMVβ contained blue regions corresponding to expression of β-galactosidase (Figure 4.14 B) and frequently in close proximity to formed microconduits (Figure 4.14 C). Further staining of the sections with H & E confirmed that expression of exogenous DNA was confined to cells of the viable epidermis (Figure 4.14 D). Continuous sections through regions of positive expression reveal the diameter of the blue regions was typically between 70-100μm (Figure 4.15).

To date it is still not understood how exogenous DNA is taken up into cells. The cryosection images presented here clearly show that application of microneedles causes significant disruption to epidermal cells. It has been suggested by Budker *et al* that transient mechanical disruption to cell membranes, caused by microneedles, facilitate the intracellular uptake of exogenous DNA (Budker *et al.* 2000). However, this is not

conclusive and others have suggested that an active, receptor mediated uptake exists Basner-Tschakarjan *et al.* 2004).

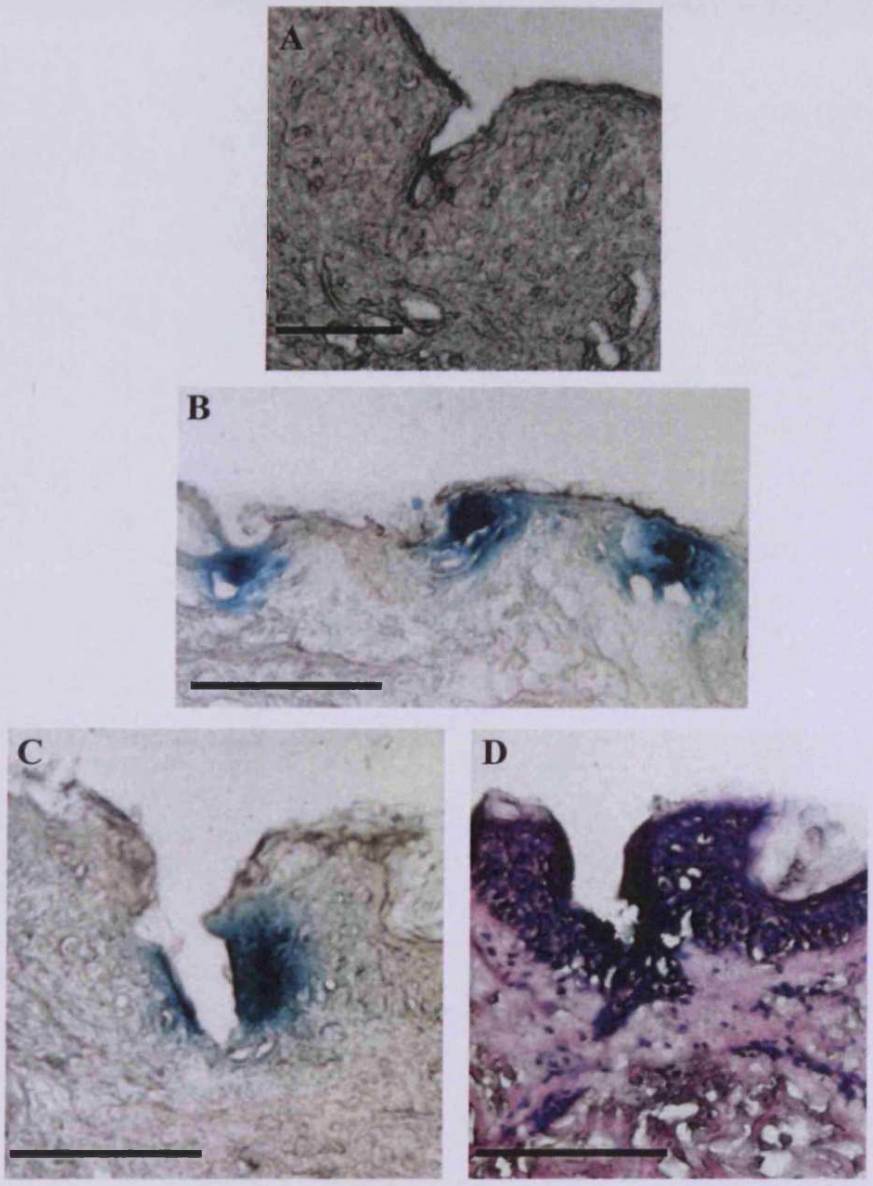

Figure 4.14 Cryosections positive expression from 10μl of 1mg/ml pCMVβ delivered by 260μm mounted microneedles. Control samples were PBS was delivered by with the microneedles shown no evidence of expression (A). Positive expression is observed when pCMVβ is delivered (B) shows three adjacent channels exhibiting expression. Expression is observed in the proximity of a microchannel (C) and confined to the epidermis, confirmed following H & E staining (D); bar = 150μm in all cases.

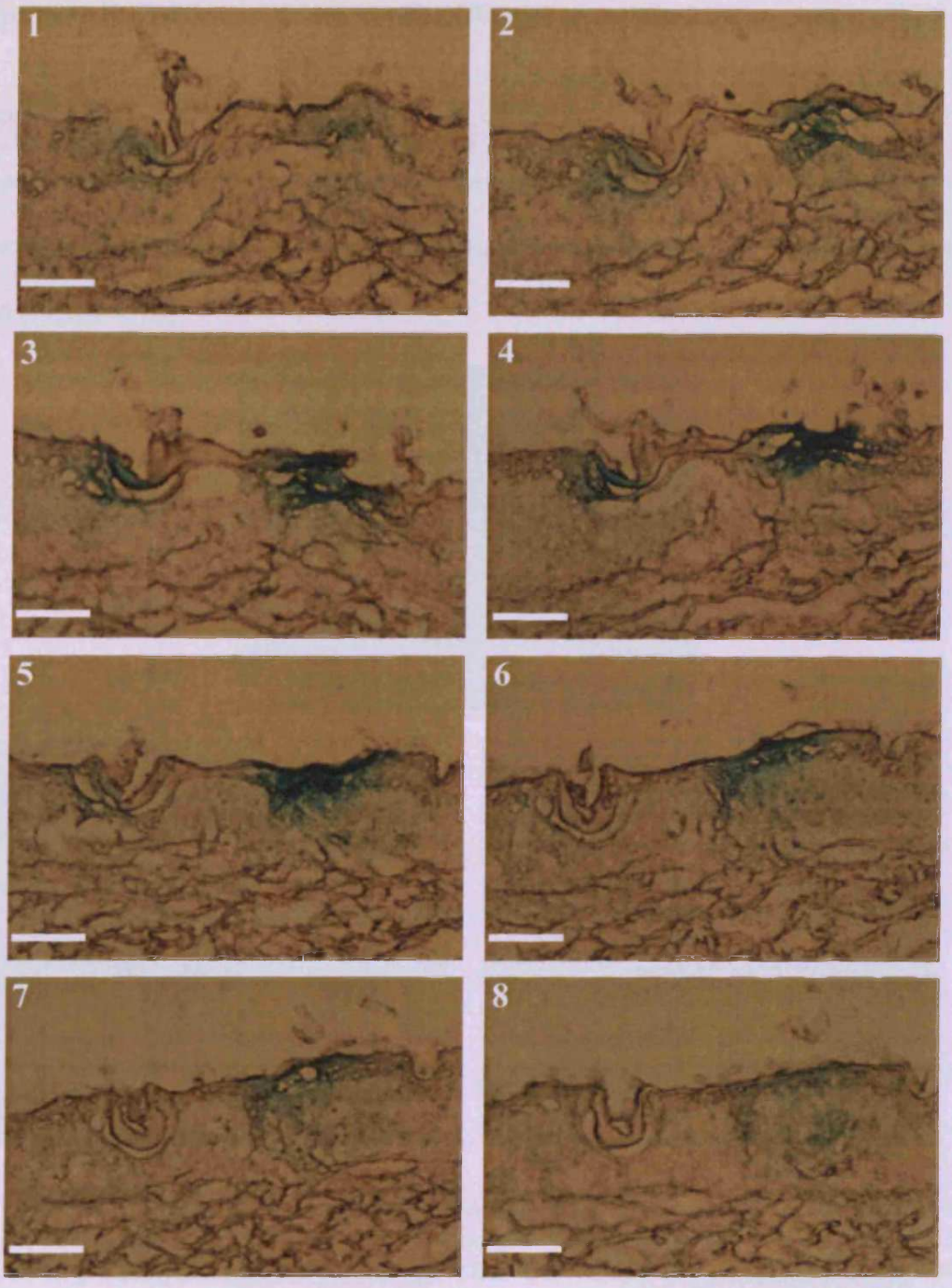

Figure 4.15 Consecutive 10μm cryosections through a region of pCMVβ/microneedle treated skin; bar = 100μm in all cases.

4.4.5 Microneedle facilitated delivery of pEGFP-N1 to *ex vivo* human skin

Expression of GFP from pEGFP-N1 plasmid delivered to *ex vivo* skin, facilitated by microneedles, was also observed. Following separation of the epidermis from the dermis and observation by fluorescent microscopy distinctive regions of green fluorescence was observed (Figure 4.16).

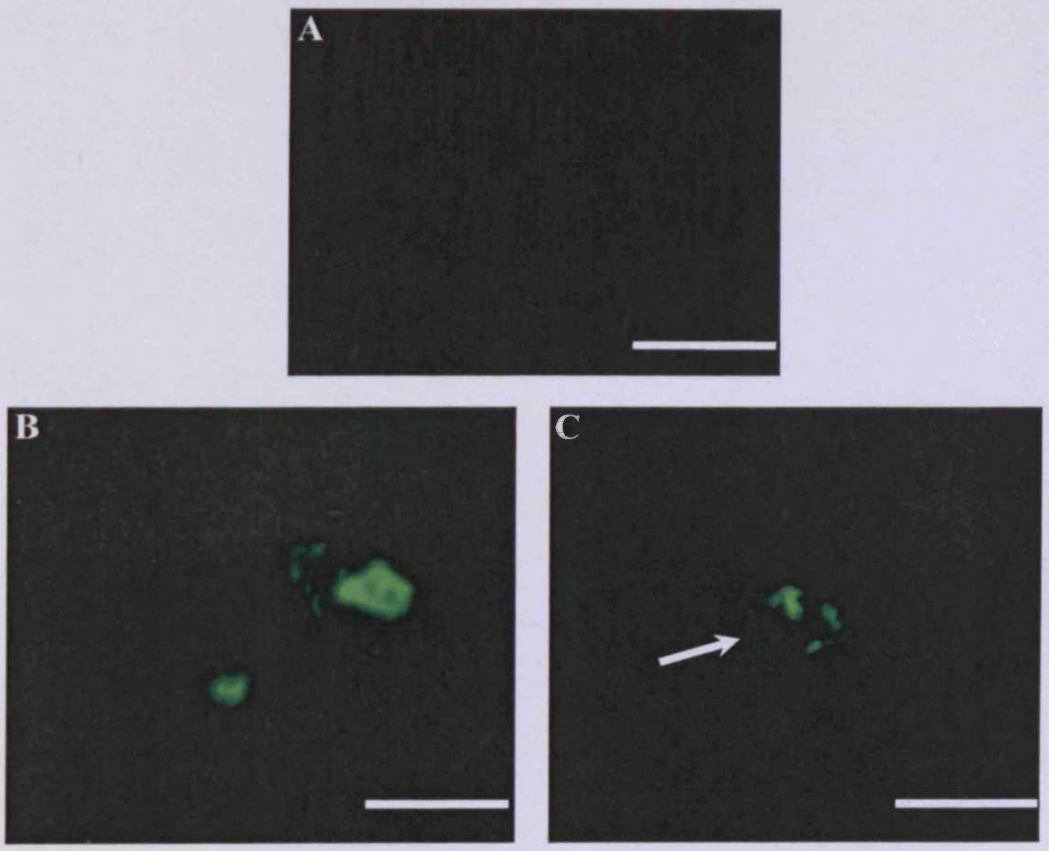

Figure 4.16 Positive expression from pEGFP-N1 delivered to *ex vivo* skin by mounted 280μm sharp tipped microneedles. Control samples show no indication of expression (A). Expression is observed in samples that received the plasmid (B & C). Careful observation of image (C) reveals the presence of a puncture (white arrow), created by a microneedle with associated expression. Bar = 150μm in all cases.

Control samples (Figure 4.16 A), PBS delivered by microneedles, show no fluorescence, while samples treated with pEGFP-N1 showed positive expression of similar numbers of channels created by microneedle show positive expression as observed in skin treated with pCMVβ. Once again expression was observed in the vicinity of punctures created by microneedle application, as apparent in Figure 4.16 C.

4.4.6 Attempts to improve exogenous gene expression

4.4.6.1 Effects of occlusion of the treated area

Occluding the surface of the skin following treatment with pCMVβ/microneedles did not improve gene expression. On the contrary, the results obtained suggest that occluding the surface reduces gene delivery efficiency (Figure 4.17). In a total of eight samples (from two individual donors) that were occluded not a single point of expression was observed. In contrast, samples that were not occluded but taken from the same skin donors did show expression (4 points of expression from a possible 64 in the first experiment and 5 from a possible 64 in the second). It is possible that occluding the sample creates a microclimate that elevates endogenous nuclease action. Also, occluding the surface may reduce the viability of the *ex vivo* skin, by introducing yet another factor to an already stressed tissue.

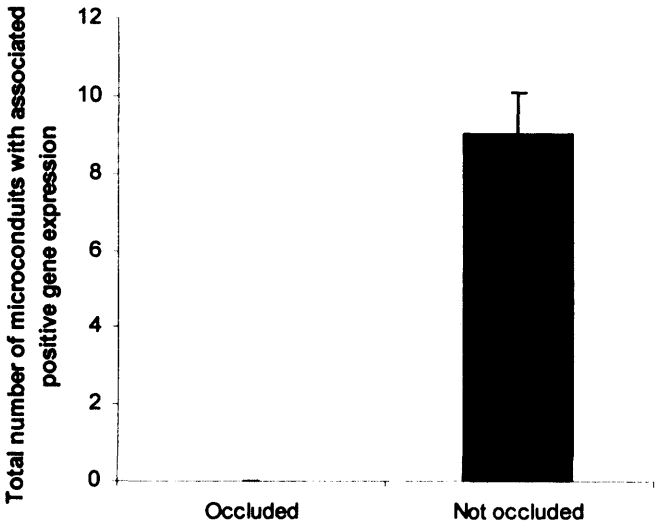

Figure 4.17. The pooled results from two independent experiments investigating the effects of occlude in the skin samples following treatment in *ex vivo* human skin. Samples that were occluded (n = 8) showed no indication expression, in contrast non-occluded samples that were from the same donor tissues did show expression.

4.3.4.2 Effects of increasing the number of rolls with the microneedle array

The vast majority of experiments conducted in this thesis involve the application of a microneedle device in a single rolling motion. However, it was found that increasing the number of rolls made by the microneedle device increased the number of points of expression (Figure 4.18). However, although the number of points of expression increased with the number of rolls, the points of expression became increasingly random and often appeared in regions where individual microneedles did not penetrate the skin (Figure 4.18 inserts). The reason for the general increase in positive points of expression with increasing rolls of the microneedle device could be that more of the pDNA solution is forced into the created channels. Also, as already mentioned it has been suggested that mechanical disruption caused by the application of the microneedle device facilitates the

uptake of exogenous DNA therefore, by increasing the number of rolls, we also increase the likelihood of mechanical damage caused by the microneedle array. However, it is also likely that increasing the number of roll will also increase the probability of damage to cells caused by the application of the array.

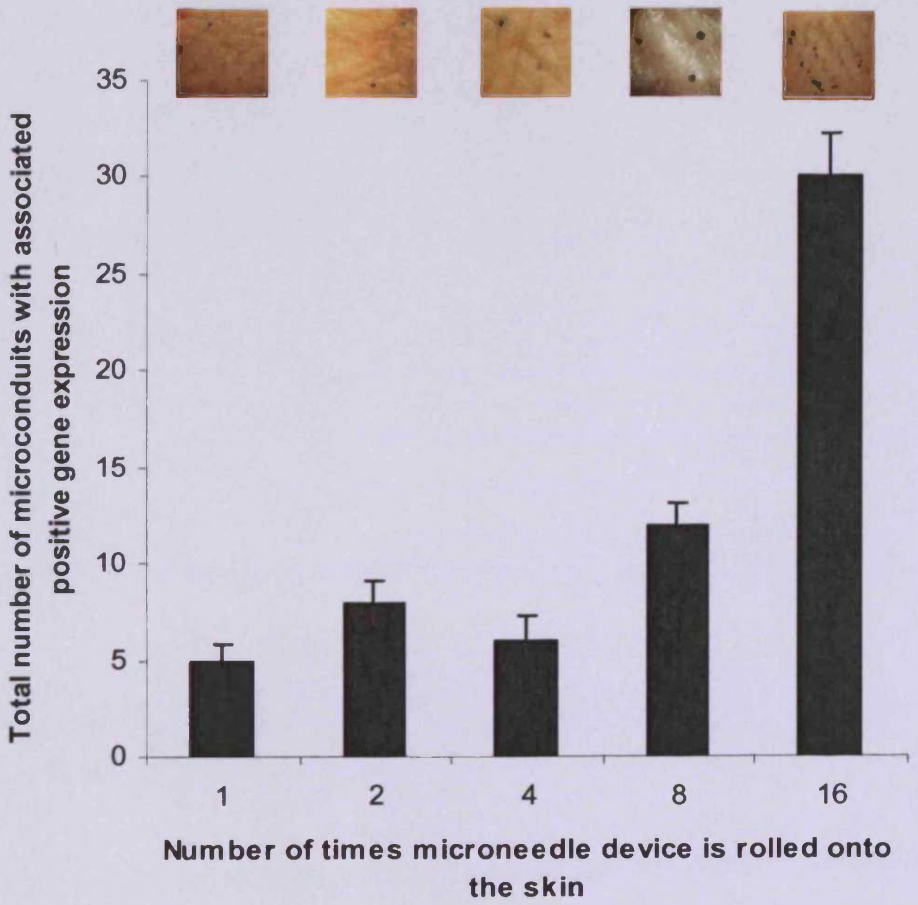

Figure 4.18 The effect of increasing the number of rolls of the microneedles array and points of gene expression.

Microscopic examination of samples that were subjected to repeated applications of the microneedle array reveal that the points of penetration were elongated resulting from the individual microneedles "slicing" into the skin as it was rolled (Figure 4.18 insert for 16 roll). Therefore, each roll results in the needles penetrating slightly different points on the skin. However, an explanation is required to explain the regions of expression that are not associated with microneedle penetration. It is likely that this is due to damage caused to the SC by parts of the array base and metal stub onto which the array is mounted as it is being repeatedly rolled onto the skin surface.

4.4.6.3 Effects of needle height

Microneedle arrays of identical dimensions, differing only in their needle heights (80, 180, and 280μm) were compared to asses their ability to facilitate exogenous DNA to human skin. Results show that microneedle array with needle heights of 80μm do not facilitate delivery to human skin (Figure 4.19). Similarly, microneedles with heights of 180μm proved only marginally better. Only the array with microneedle of 280μm resulted in low, but expression levels typical with microneedle facilitated delivery. It is likely that microneedle of 80μm did not efficiently disrupt the SC, the dermatoglyphs and innate elasticity of the skin probably prevented penetration through the SC. Similarly, microneedles of 180μm had the same problem. In contrast, microneedles with heights of 280μm transfer sufficient pressure to the tips of the needle to reproducibly puncture the SC and penetrate the viable epidermis.

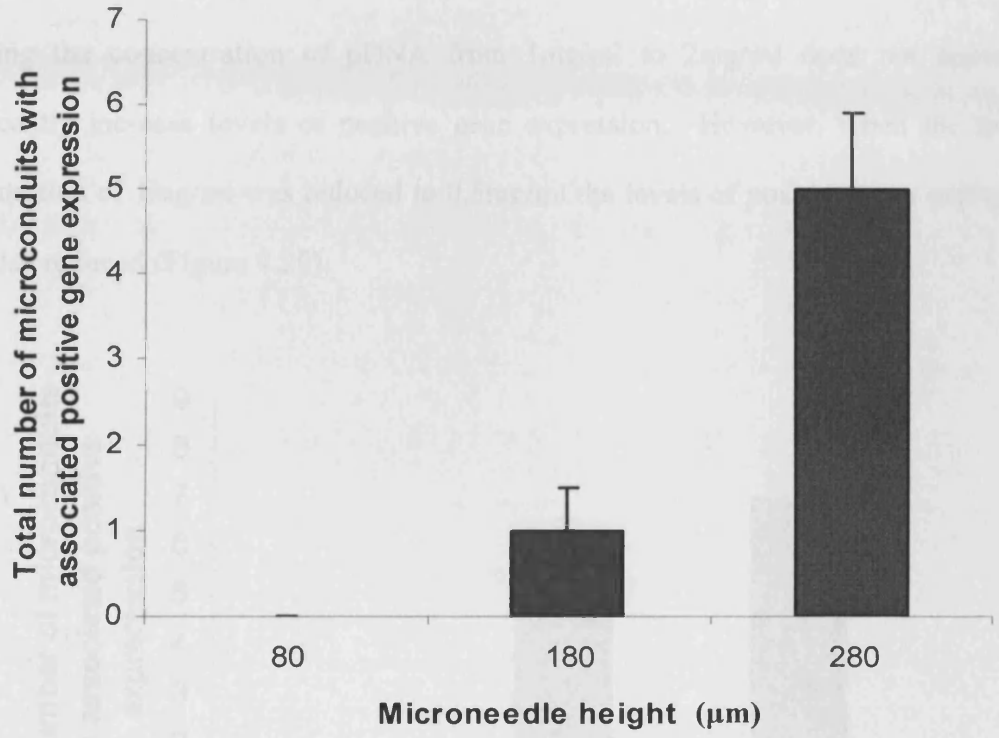

Figure 4.19. The effect of microneedle height on the ability to deliver pCMVβ to *ex vivo* human skin (n = 4 ±SD).

The logic of using smaller microneedles is that their application would result in less pain and reduced damage to the epidermis in the vicinity of application. However, it seems likely that microneedles have to be a certain height before they are capable of penetrating the SC, at least with current methods of application.

4.4.6.4 Effects of pDNA concentration

Doubling the concentration of pDNA from 1mg/ml to 2mg/ml does not appear to significantly increase levels of positive gene expression. However, when the typical concentration of 1mg/ml was reduced to 0.5mg/ml the levels of positive gene expression were also reduced (Figure 4.20).

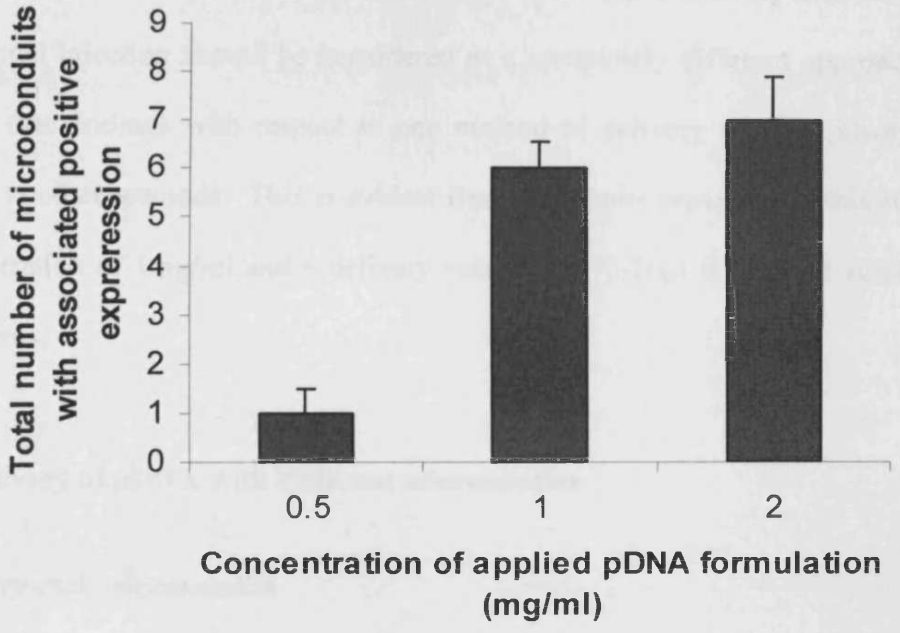

Figure 4.20. The effects of altering the concentration of pCMVβ in the delivery applied in conjunction with microneedles *ex vivo* skin (n = 4 ±SD).

Low concentrations of pDNA appear to result in reduced levels of positive gene expression. The reasons for this include insufficient amounts of pDNA being delivered to the cells (see discussion below), lower levels are more prone to complete degradation by endogenous nucleases and expression did occur but at levels that could not be detected by the staining process. In contrast, when the concentration of pDNA was doubled there

appears little effect and therefore our observations of low gene expression *per se* are not attributable to sub-optimal pDNA concentration. The literature suggests that levels in the range of 200 - 400μg/ml (Hengge *et al.* 1995; Sawamura *et al.* 2002) are optimal, with delivery volumes of 50-100μl as suggested by Hengge *et al* and 30μl by Sawamura *et al.* Delivery volumes are a vital factor in the case of microneedle facilitated delivery, as will become apparent. Regarding the present discussion it is important to note that the volumes suggested as optimal in the literature do not relate to delivery with microneedles. Intra-dermal injection should be considered as a completely different approach and it is possible that findings with respect to one method of delivery will not always directly translate to other methods. This is evident from the results presented in this study where a concentration of 1mg/ml and a delivery volume of 10-20μl is deemed suitable for all experiments.

4.4.7 Delivery of pDNA with different microneedles

4.4.7.1 Dry-etch microneedles

Successful expression of exogenous pDNA was observed when dry-etch microneedles were used to facilitate delivery (Figure 4.21 A & B). However, delivery proved practically more difficult compared to the wet-etch microneedles. Because the array were significantly larger that the wet-etch arrays (1cm X 2cm compared to 0.8cm^2) it is more difficult to penetrate the SC. The pressure is not transferred efficiently to the tips and a 'bed of nails' effect arises. Also, the array is applied flat and not in a roll, a consequence of how it is mounted. This has been shown in Chapter 2 to reduce the ability of

microneedle to puncture the SC of *ex vivo* skin. This suggests, along with experience gained in handling the devices that dry-etch microneedles are not as effective as wet-etch microneedles for delivering exogenous pDNA to *ex vivo* skin.

4.4.7.2 Polymer microneedles

Delivery of pDNA facilitated by polymer microneedles was indistinguishable from that achieved with wet-etch silicon arrays of the same dimensions (Figure 4.21 C & D). This is not surprising given the identical structural dimensions yet important as there are a number of disadvantages associated with silicon as the material to form microneedles (see chapter 2) and it is likely that in the future polymer microneedles will become more prevalent.

4.4.7.3 Hollow microneedles

Positive gene expression was observed when pDNA was delivered by a hollow microneedle array (Figure 4.21 E & F). However, it was not possible to draw any conclusions regarding efficiency because the array could only be used once, being a prototype it had a number of features that inevitably will be improved. For example, the capillaries run the length of the microneedle and when they are applied to the skin they become blocked (Figure 2.16). The blockages were particularly apparent in the regions where fluid flow in the reservoir chamber was low. Therefore, this suggests that a certain amount of fluid flow pressure is required in order to keep the capillaries open. To address this, microneedle designs where the capillaries emerge at the side, rather that at the tip region would be less likely to block up with skin debris.

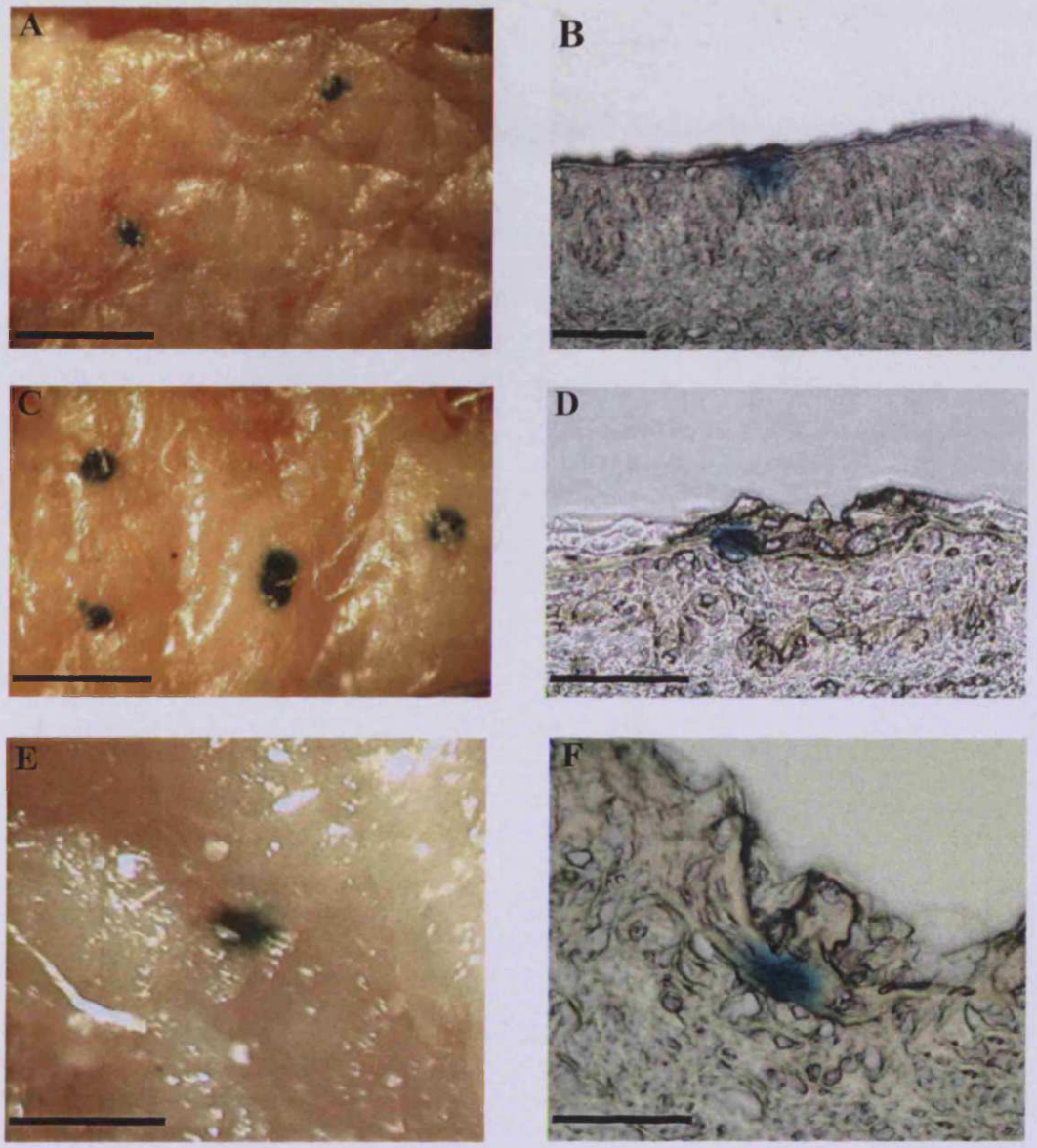

Figure.4.21 Positive expression from microneedle other than those formed by wet-etch techniques. Positive expression observed *en face* (A) and section (B). Expression observed *en face* (C) and section (D) facilitated by polymer microneedles. The results observed by delivery through hollow microneedles *en face* (E) and section (F). A, C, and E bar = 1mm; B, D, and F bar = 200μm.

4.4.8 Final comments on microneedle application

There are a number of factors that should be noted at this point in the discussion regarding the delivery of pDNA with microneedles to *ex vivo* skin. Firstly, using solutions of pDNA are not particularly suitable, they are uneconomical and inefficient. Consider a volume of pDNA applied to the skin surface. The microneedle array is applied in a rolling motion which results in the vast majority of the solution, perhaps as much as 95%, being forced out as the array approaches the vertical position (Figure 4.22).

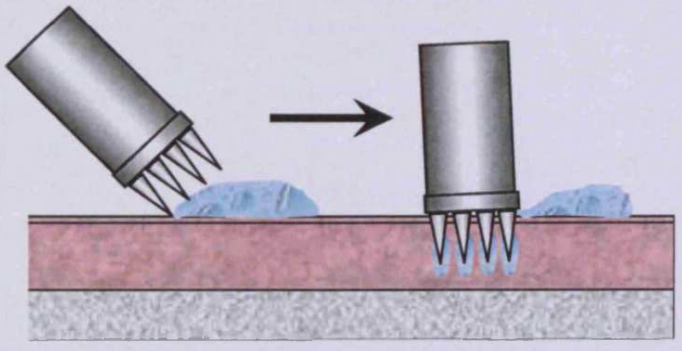

Figure 4.22 Inefficiency of current methods of microneedle application with liquid formulations. A significant proportion of the original applied formulation is lost as the array is rolled on.

Therefore, if 20µl of a pDNA solution is delivered it is apparent that only a small volume of this actually reaches the epidermis. Methods to address this issue include coating the microneedle with pDNA, however to date this has not been successfully achieved.

4.5 Conclusions

The method of transporting, processing and culturing *ex vivo* human skin, as described in this chapter, ensures viability of that skin for at least 24 hours (period of a typical experiment). Exogenous pDNA delivered to *ex vivo* skin facilitated by microneedles results in positive gene expression. When expression is observed it is predominately associated with a microconduit created by the microneedle device, unless the microneedle array is applied in a repeated rolling manor. However, delivery is inefficient and irreproducible. Wet-etch silicon and replicate polymer microneedles proved to be more effective at delivering pDNA to the epidermis compared with the more commonly exploited dry-etch designs, though typically only around 3% of the channels created with microneedles had associated positive expression from the exogenous pDNA.

Levels of expression associated with microconduits were not improved by occluding the skin surface or by increasing the concentration of the applied pDNA solution. However, reducing the concentration did reduce the levels of expression. Similarly, microneedle arrays with heights of less than 260μm, proved to have reduced levels of expression. Notable increases in levels of expression were only observed when the number of applications of the microneedle device was increased.

These results demonstrate that microneedle facilitated delivery of pDNA to *ex vivo* human skin is highly inefficient. Consequently, there is a need to address a number of factors that could improve this situation. The two areas main areas that need this attention are firstly, the need for a novel, effective applicator device for microneedle use

and secondly, a need to improve the delivery formulation. It is this second problem that will be investigated in the next chapter.

CHAPTER 5: Delivery of pDNA loaded hydrogels to the viable epidermis facilitated by microneedles

5.1 Introduction

Chapter 4 describes how microneedle facilitated delivery of pDNA to *ex vivo* human skin results in low, irreproducible expression of the exogenous DNA. The aim of this section of work was to investigate whether microneedles could be used in conjunction with a sustained release hydrogel formulation to address the low gene expression levels typically observed. It was hypothesized that pDNA loaded hydrogel formulation could be forced through the SC using a microneedle array. The resulting channels would become filled with the hydrogel providing a reservoir of pDNA, from which prolonged pDNA release would give rise in prolonged pDNA delivery (Figure 5.1).

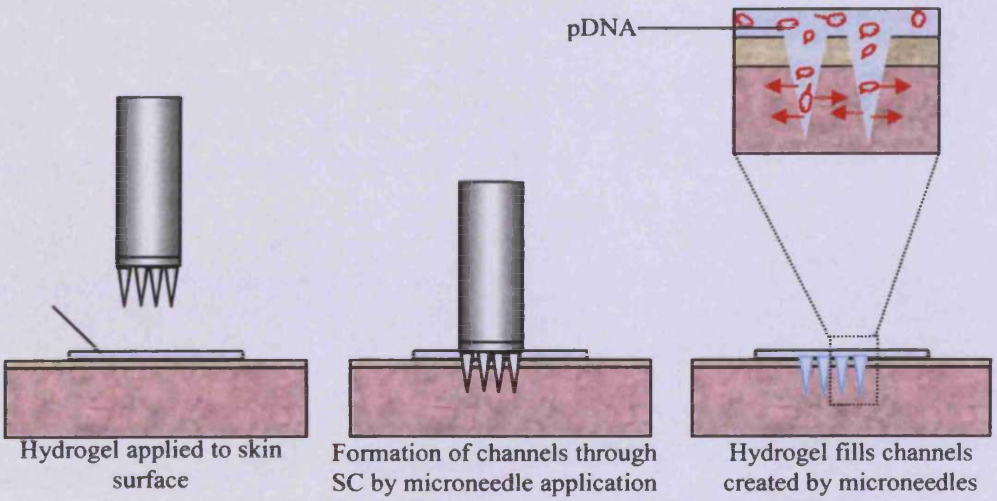

Figure 5.1 Delivery of a pDNA loaded hydrogel to the epidermis facilitated by microneedles.

5.1.1 Hydrogels as gene delivery systems

This study investigated two dissimilar hydrogels, Carbopol-940 polymers and a triblock copolymer of poly(lactide-co-glycolide) (PLGA) and poly(ethylene glycol) (PEG), i.e. poly(ethylene glycol-b-[DL-lactic acid-co-glycolic acid]-b-ethylene glycol) (PLGA-PEG-PLGA).

Commercially available Carbopol is typically supplied as a dehydrated flocculated powder, with diameters of ~0.2-6μm. In this form the polymer consist of intertwined collections of linear though coiled acrylic acid homopolymers chains (Figure 5.2), it is not possible to resolve these into individual polymer chains. When the flocculated polymer particles begin to uncoil and swell, it has been estimated up to 1000 times there original size (Hosmani 2006). However, in order for the polymers to completely uncoil, which is necessary for maximum viscosity, required in gel formation, the acidic residues must be converted to salts. This is achieved by neutralizing the Carbopol polymer with a base, such as sodium hydroxide (NaOH) or triethanolamine (TEA); this causes repulsion between the negative charges adding to the swelling, this is shown schematically in Figure 5.3.

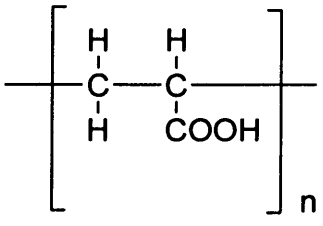

Figure 5.2 The general structure of a Carbopol polymer.

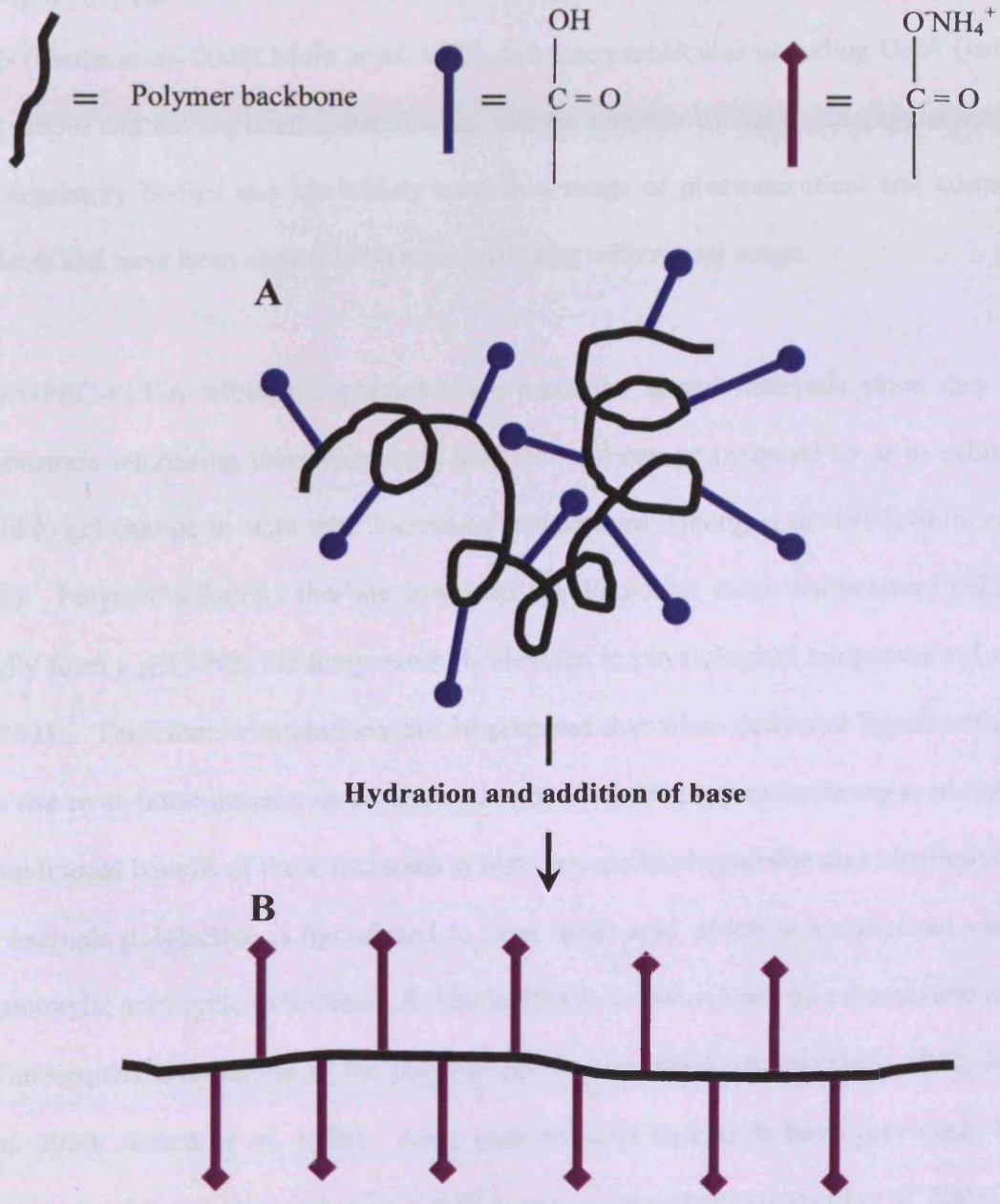

Figure 5.3 When dehydrated, Carbopol exists as coiled, intertwined linear polymers (A). However, when hydrated and neutralized with a base, the polymers form extended structures (B).

Carbopol hydrogels have been shown to harbor and release both low molecular weight drugs (Csoka *et al.* 2005; Mura *et al.* 1992) and macromolecules including DNA (Ismail *et al.* 2000) and having been established as safe for purpose by numerous regulatory and non-regulatory bodies and are widely used in a range of pharmaceutical and cosmetic products and have been shown to be non-sensitizing with repeat usage.

PLGA-PEG-PLGA triblock copolymers are particular useful materials since they can demonstrate interesting thermosensitive behavior and can be prepared so as to exhibit a liquid to gel change in state with increasing temperature (Jeong *et al.* 1997; Shim *et al.* 2002). Polymer solutions that are low viscosity liquids at room temperature (~25°C) rapidly form a gel when the temperature is elevated to physiological temperature (Lee *et al.* 2003). Therefore, formulations can be prepared that when delivered hypodermically give rise to an intramuscular or intradermal semi-solid drug reservoir (Jeong *et al.* 1997), An additional benefit of these materials is that they are biodegradable and bioeliminable. For example polylactide is hydrolysed to form lactic acid which is metabolized via the tricarboxylic acid cycle (Middleton & Tipton 2000), so that release of a therapeutic agent and subsequent elimination of the polymer can be controlled (Nieuwenhuis 1992; Jeong *et al.* 2000; Amass *et al.* 1998). Also, such polymer hydrogels have previously been shown to be able to house and release pDNA over an extended period (Li *et al.* 2003).

MacroMed Inc, now part of Protheics PLC, holds numerous U.S. and foreign patents associated with the temperature responsive PLGA-PEG-PLGA triblock copolymer which is commercially available under the name ReGel®. There primary use of the polymer

system is an injectable sustained release system for the drug paclitaxel, called OncoGel™. The OncoGel™ system has been designed for the treatment of solid tumors, where upon injection the hydrogel depot will release paclitaxel continuously for over four to six weeks ensuring a higher concentration of the drug at the tumor than can be obtained by intravenous injection (http://www.protherics.com/Products.oncogel.aspx). Furthermore, Protherics PLC are currently involved in phase II clinical trails in both the U.S. and EU with OncoGel™ aimed specifically at oesophageal and brain cancers.

The manufacturers also claim that upon intradermal injection of a ReGel® solution, gelation is extremely rapid, consequently little if any of the polymer solution is lost by traveling back up through the needle track (Fowers *et al.* 2003). This is important from the point of view of the current study because it is anticipated that a solution of a PLGA-PEG-PLGA polymer could fill the microneedle generated channels where the body will warm it, resulting in sol-gel- transition occurring subsequently forming the pDNA/hydrogel depot.

Both types of hydrogel will be investigated in order to assess their ability to both store and release pDNA.

5.1.2 Chemical synthesis of PLGA-PEG-PLGA polymers

The PLGA-PEG-PLGA tri-block copolymer was synthesized by ring opening polymerization of poly L-Lactide and glycolide monomers onto both ends of a central PEG block, a reaction catalysed with stannous octoate (Tin (II) 2-Ethylhexanoate; Figure

5.4). A number of other catalysts have been reported for this type of reaction, e.g. aluminium isopropoxide and calcium acetylacetonate, but in this case stannous octoate was used since it carries FDA approval for use as a food preservative and therefore has an established safety profile (http://en.wikipedia.org/wiki/Polyglycolic_acid). The polymer product was characterised by ^{1}H-NMR and GPC. The sol-gel transition temperature will be estimated by performing tube inversion tests of the polymer where the formation of a gel in the range of physiological temperature will be sought.

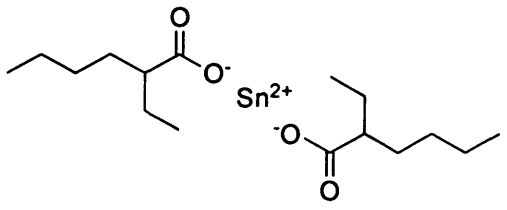

Figure 5.4 Stannous octoate

5.1.3 Techniques

The ability of microneedles to facilitate the delivery of hydrogels to skin was demonstrated using *ex vivo* human skin. Initially hydrogels loaded with a fluorescent marker were used to demonstrate the presence of the hydrogel in the formed microchannel. The migration of nanoparticles and pDNA out of both types of hydrogel was also investigated using Franz-type diffusion cells using a model diffusive barrier (polycarbonate track-etch membrane with a representative pore size) and human heat separated epidermal sheets treated with microneedle arrays.

Gene expression, resulting form the successful delivery of pDNA from a microneeedle/hydrogel, into human *ex vivo* tissue was also investigated using the organ culture system described in Chapter 4.

5.2 Aims and objectives

5.2.1 Aims

The aims of this chapter are to investigate weather hydrogel formulations can be used in conjunction with microneedle arrays to delivery pDNA to the viable epidermis with a view towards improving gene delivery efficiency.

5.2.2 Objectives

- The formation and characterization of Carbopol hydrogel formulations
- The synthesis and characterization of PLGA-PEG-PLGA triblock copolymer and the resultant hydrogel
- To shown that microneedle are capable of delivering hydrogels to the viable epidermis
- To demonstrate that hydrogels can house and release pDNA over time
- To exhibit that pDNA loaded hydrogels can be delivered with microneedle to the epidermis and result in expression from the plasmid

5.3 Materials and Methods

5.3.1 Materials

Amplification and purification of the pCMVβ reporter plasmid were as described previously (Chapter 4).

DL-Lactide (3, 6-dimethyl-1, 4-dioxane-2, 5-dione), stannous 2-ethylhexanoate, poly (ethylene glycol) (PEG) 1000, amine modified fluorescent nanoparticle suspension (L-1280), Hoechst 33258 (Bisbenzimide), deuterated chloroform ($CDCl_3$) and constituents of the X-gal staining solution were from Sigma-Aldrich Chemical Company (Poole, UK).

Triethanolamine (TEA) and Carbopol-940 were from Acros Organics (Geel, Belgium).

Glycolide (1,4-dioxane-2,5-dione) was a gift from Purac (Gorinchem The Netherlands).

All culture plastics were from Corning-Costar (High Wycombe, UK). Dulbecco's Modified Eagle's Medium (DMEM), foetal bovine serum (FBS), penicillin-streptomycin solution were from Invitrogen Corporation (Paisley, UK).

Histological materials were from RA Lamb Ltd (Eastbourne, UK).

Other materials were of analytical grade and from Fisher Scientific UK (Loughborough, UK).

5.3.2 Synthesis of carbopol-940 hydrogel

Stock solutions of pDNA were diluted to an appropriate concentration in a specified volume, typically 1ml. This solution was added to a pre-weighed quantity of Carbopol-940 polymer and mixed for 2 minutes and allowed to fully swell for ~1 hour. Typically 1ml of a 1% w/v carbopol-940 hydrogel was prepared containing 1mg of pCMVβ. Fluorescent nanoparticle loaded carbopol-940 hydrogels were also prepared in the absence of pDNA using the same procedure. All Carbopol-940 hydrogels were neutralised (pH 6.5-7) with triethylamine (TEA).

5.3.3 Synthesis of PLGA-PEG-PLGA tri-block co-polymers and hydrogels

Synthesis of the PLGA-PEG-PLGA tri-block co-polymer was performed by ring opening polymerisation of lactide and glycolide using a stannous 2-ethylhexanoate catalyst using a method described by Zentner *et al;* Figure 5.5 (Zentner *et al.* 2001). Polyethylene glycol 1000 was dried in a three-neck flask under vacuum at 150°C for 3 hours. DL-lactide (14.1g) and glycolide (3.8g) were added (3:1 molar ratio), and the flask heated at 150°C for a further 30 minutes. To the reaction 50μg of stannous 2-ethylhexanoate was then added and the temperature increased to 155°C where it was maintained for 5 hours. The resulting crude polymer mix was dissolved in 500ml of ice cold water and precipitated by heating to 80°C. This was repeated three times in order to removed unreacted monomers and low molecular weight polymers. Subsequently, the polymer was dehydrated by freeze drying and stored in a dried state at 4°C.

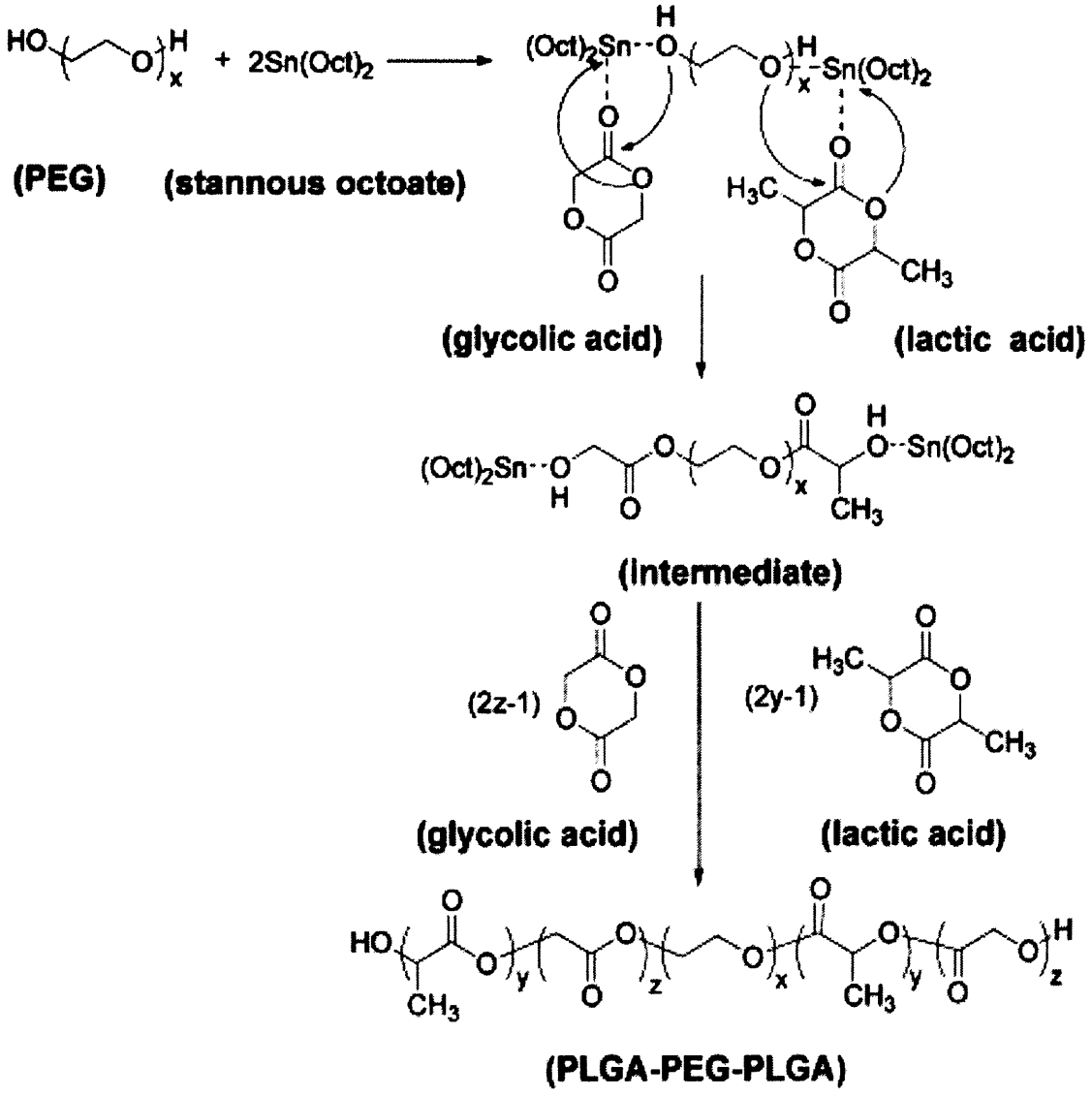

Figure 5.5 The formation of the triblock copolymer PLGA-PEG-PLGA by ring opening polymerization (adapted from Zentner *et al.* 2001).

5.3.4 SEM of hydrogel formulations

Small samples (~100mg) of both a carbopol-940 and the PLGA-PEG-PLGA triblock copolymer were placed in 1.5ml centrifuge tubes. These were immersed in liquid nitrogen and freeze dried over night. The samples were mounted onto an SEM stub with double sided carbon tape and sputter coated in gold, samples viewed by a Philips XL-200 scanning electron microscope (SEM) (FEI Company, Eindhoven, The Netherlands).

5.3.5 TEM of PLGA-PEG-PLGA

Approximately 20µl of PLGA-PEG-PLGA solution is pipetted onto a copper TEM grid and incubated at room temperature for 3 minutes. Excess sample is the carefully removed and the grid is stained with 30µl of UA for 30 seconds. The grid is then subject to two rinses with 30µl of filtered H_2O, excess liquid being wicked off with filter paper. Samples were observed using a Philips EM 208, (FEI Company, Eindhoven, The Netherlands).

5.3.6 ^{1}H nuclear magnetic resonance (NMR) analysis

Approximately 10mg of PLGA-PEG-PLGA tri-block co-polymer was dissolved in $CDCl_3$. NMR spectra were obtained using a Bruker 300MHz NMR spectrometer (Bruker, Coventry, UK).

5.3.7 Gel permeation chromatography (GPC) analysis

Approximately 10mg of PLGA-PEG-PLGA tri-block co-polymer was dissolved in 1ml of tetrahydrofuran (THF) containing 20µl of toluene by stirring at room temperature for ~30

minutes. Samples were analyzed at ambient temperature using an integrated PL-GPC 20 GPC system (Polymer Laboratories Ltd, Shropshire, UK) with two ResiPore columns (particle size 3μm, both 7.5mm x 300mm) in series (Polymer Laboratories Ltd, Shropshire, UK) detection was made using a deflection refractive index detector. THF was employed as a mobile phase with a flow rate of 1ml/min and molecular weight of the polymer was determined relative to polystyrene standards.

5.3.8 Sol-gel transition at a physiological temperature demonstrated by tube inversion test

A PLGA-PEG-PLGA triblock copolymer solution was prepared at a concentration of 23% w/v in distilled water to a volume of 2ml in 15ml falcon tubes. The tubes were immersed in a water bath set at 37°C for 20 minutes. Each tube was then inverted to determine weather a sol-gel transition had occurred, inversion test based on a method described by Jeong *et al* (1999).

5.3.9 Microneedle facilitated delivery of fluorescent nanoparticle loaded hydrogels to skin

A human skin sample (♀ 62 years of age) was removed from -20°C storage and allowed to defrost and equilibrate to room temperature for ~2 hours. Approximately 20µl of each nanoparticle loaded hydrogel (prepared as described in Section 5.3.2) was applied to the surface of the excised human skin. A mounted frustum-tipped microneedle array (4 X 4 containing 16 microneedles with heights of 260µm) was applied to the hydrogel treated area using a single rolling motion. Downward force was maintained throughout the application. Following treatment the skin surface was washed in PBS, for 30 minutes, before fixation in 2% v/v glutaraldehyde for 2 hours at 4°C. Residual fixative was removed by washing in 2ml of PBS. Samples were subsequently embedded in OCT medium and stored at -80°C, before cryosection were generated with a Leica CM3050S Cryostat (Leica Microsystems, Milton Keynes, UK), as described in Chapter 3.

5.3.10 Diffusion of nanobeads from hydrogel systems

Carbopol-940 (1% w/v) and PLGA-PEG-PLGA (23 % w/v) hydrogels were prepared with the aqueous phase composed of a fluorescent nanobead solution (5µl nanobead concentrate in every 1ml of deionized water). The Franz diffusion cell was set up as described in Chapter 3. The donor compartment was loaded with 1ml of hydrogel and subsequently occluded with foil. The diffusive surface was a polycarbonate track-etched membrane (pore size 10µm), clamped between the donor and receptor phase and sealed with silicon grease. The receptor phase of each diffusion cell was filled with ~3ml of PBS buffer (pH 7.4) and was stirred at 37°C, for 120 hours. At pre-determined time intervals, 200µl samples were removed from the receptor phase, via the sampling arm,

which was replenished with an equal volume of PBS buffer. Fluorescence was measured using a FLUOstar Optima fluorimeter (BMG Labtechnologies, Offenberg, Germany).

5.3.11 Diffusion of pDNA from hydrogel systems

Carbopol-940 (1% w/v) and PLGA-PEG-PLGA (23% w/v) hydrogels were prepared, each contained 1mg/ml pCMVβ. The donor compartment of a static Franz type diffusion cell was loaded with 1ml of hydrogel and subsequently occluded with foil. The diffusive surface was heat separated epidermal sheets treated with a 4 X 4 frustum tipped mounted microneedle array, clamped between the donor and receptor phase and sealed with silicon grease. The receptor compartment of each diffusion cell was filled with ~3ml of TNE buffer (100mM Tris; 2.0M NaCl; 10mM EDTA; pH 7.4) and was stirred at 37°C, for 72 hours. At pre-determined time intervals 200µl samples were removed from the receptor compartment which was replenished with an equal volume of TNE buffer. Plasmid permeation was monitored by measuring the total amount of DNA in each sample using Hoeschst DNA quantification (Rengaraian *et al.* 2002). Fluorescence was measured using a FLUOstar Optima fluorimeter (BMG Labtechnologies, Offenberg, Germany).

5.3.12 Skin organ culture, pDNA delivery and detection of expression

All gene delivery studies were performed on recently excised human breast skin transported, processed and pinned as described in chapter 4. Hydrogel formulations (1% w/v Carbopol-940 and 23% w/v PLGA-PEG-PLGA containing pCMVβ in a concentration of 1mg/ml, (n = 4 for both hydrogels) were applied and spread over a surface of the skin, coating a region ~2cm^2. A mounted frustum-tipped microneedle array (4 X 4 containing 16 microneedles with heights of 260μm) was applied to the region of hydrogel treated skin, in a single rolling motion. Control samples involved the application of the hydrogel containing no pDNA (n = 4 for both hydrogels) The regions of the skin that have been treated with the microneedle array and hydrogel formulation (~0.8cm^2) are subsequently excised and placed in organ culture for 24 hours, as described in Chapter 4.

All samples were then rinsed in PBS/$MgCl_2$ for 30minutes, and fixed in 2% v/v glutaraldehyde/PBS/$MgCl_2$ at 4°C for 2 hours. Subsequently, each sample was rinsed three times in PBS/$MgCl_2$ for 2 hours. Samples were then immersed in X-gal staining solution (0.2% X-Gal, 2mM $MgCl_2$, 5mM $K_4Fe(CN)_6$, 5mM $K_3Fe(CN)_6$ prepared in PBS) for 24 hours at 37°C. Samples were observed *en face* by light microscopy with a Stemi 2000-C Stereomicroscope (Zeiss, Welwyn Garden City, UK) and a Scott 1500 fibre optic external light source (Scott UK Ltd, Stafford, UK); images were captured using a Olympus DP-10 digital camera (Olympus Optical, London, UK), prior to each sample being embedded in OCT medium and stored at -80°C.

5.3.13 Preparation of skin cryosections and H&E staining

Samples embedded in OCT blocks were sectioned using a Leica CM3050S Cryostat (Leica Microsystems, Milton Keynes, UK). Skin sections (12μm) were captured onto Superfrost Plus® microscope slides, dried overnight and observed with an Olympus BX50 microscope (Olympus, Middlesex, UK). Selected slides were further stained with Haematoxylin and Eosin (H&E) staining (described in Chapter 4) to assist visualisation of skin architecture.

5.3.14 Lateral application of microneedle device and loaded hydrogel formulation

Excised human breast skin (♀ aged 57 years of age) was transported, processed and pinned as previously described. Hydrogel formulations (1% w/v carbopol-940 and a 23% w/v PLGA-PEG-PLGA containing pCMVβ in at a concentration of 1mg/ml, n = 4 for both hydrogels) were applied and spread over a surface of the skin, approximately 2 X 3cm. A mounted frustum-tipped microneedle array (4 X 4 containing 16 microneedles with heights of 260μm) was applied to the hydrogel treated skin at an angle of 90° so that the array is applied flat (see Chapter 2). The array was then dragged across the surface of the skin, for approximately 2cm (Figure 5.6). The region of the skin that has been treated with the microneedle array was dissected and placed in organ culture, as described in Chapter 4.

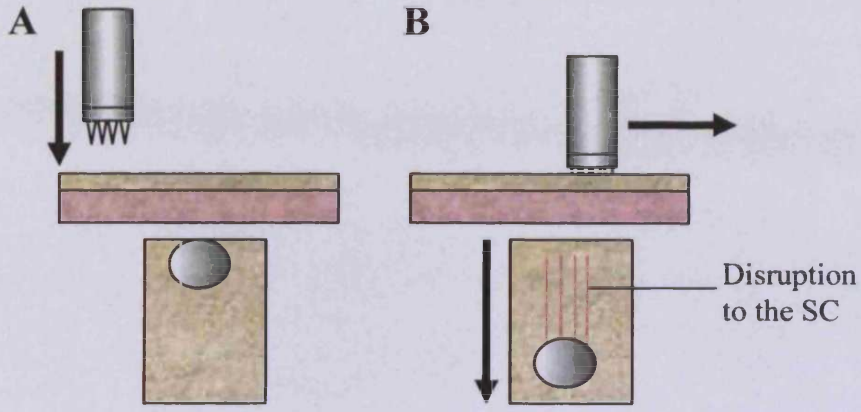

Figure 5.6 Application of a microneedle array in a lateral motion. The array was first applied at a 90° angle to the skin surface (A). The array was then dragged in a single motion across the skin surface (B).

After 24 hours all samples were rinsed in PBS/$MgCl_2$ for 30 minutes, and fixed in 2% v/v glutaraldehyde/PBS/$MgCl_2$ incubated at 4°C for 2 hours. Following this each sample was rinsed three times in PBS/$MgCl_2$ each for 2 hours. Samples were then immersed in X-Gal staining solution (0.2% X-Gal, 2mM $MgCl_2$, 5mM $K_4Fe(CN)_6$, 5mM $K_3Fe(CN)_6$ prepared in PBS) for 24 hours at 37°C. Samples were observed *en face* using Stemi 2000-C Stereomicroscope (Zeiss, Welwyn Garden City, UK) and a Scott 1500 fibre optic external light source (Scott UK Ltd, Stafford, UK); images were captured using a Olympus DP-10 digital camera (Olympus Optical, London, UK), prior to each sample being embedded in OCT medium and stored at -80°C.

5.4 Results and discussion

5.4.1 Carbopol-940 hydrogel characterisation

Commercially available Carbopol-490 polymers were obtained in the form of a dehydrated, fluffy, white powder. Once fully hydrated, it appeared as a transparent, stiff gel (Figure 5.7 A). Observation of Carbopol-940 hydrogels under SEM (following dehydration) shows numerous extended clusters of poly acrylic acid polymers (Figure 5.8). The mesh-like appearance forms a three dimension structure, which was clearly apparent at high magnification by SEM (Figure 5.8). There are no methods available to measure the precise molecular weight of cross-linked polymers of this kind, however, they are generally estimated too be in the range of 740 000 – 4-5 million (Hosmani 2006).

5.4.2 PLGA-PEG-PLGA characterisation

The PLGA-PEG-PLGA polymer appeared as a white-yellow resinous mass (Figure 5.7 B), the fine structure were not apparent by SEM (up to X 2500 magnification). Other groups have successfully obtained detailed SEM images of similar polymers revealing a similar structure to that of Carbopol (Li *et al.* 2003).

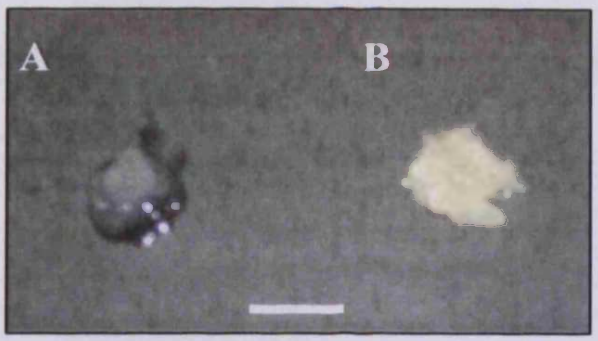

Figure 5.7 The appearance of a 1% Carbopol-940 hydrogel (A) and purified PLGA-PEG-PLGA polymer (B). Bar = 1cm

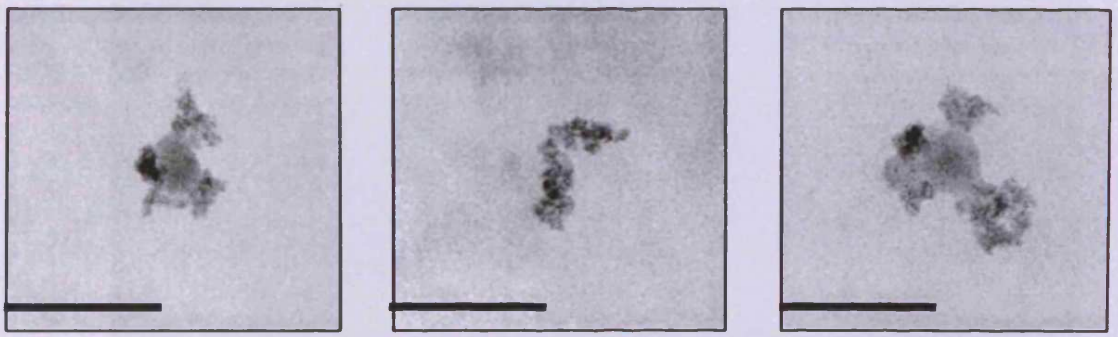

Figure 5.8 The appearance of PLGA-PEG-PLGA triblock copolymers as revealed by TEM; bar ~ 100nm in all cases.

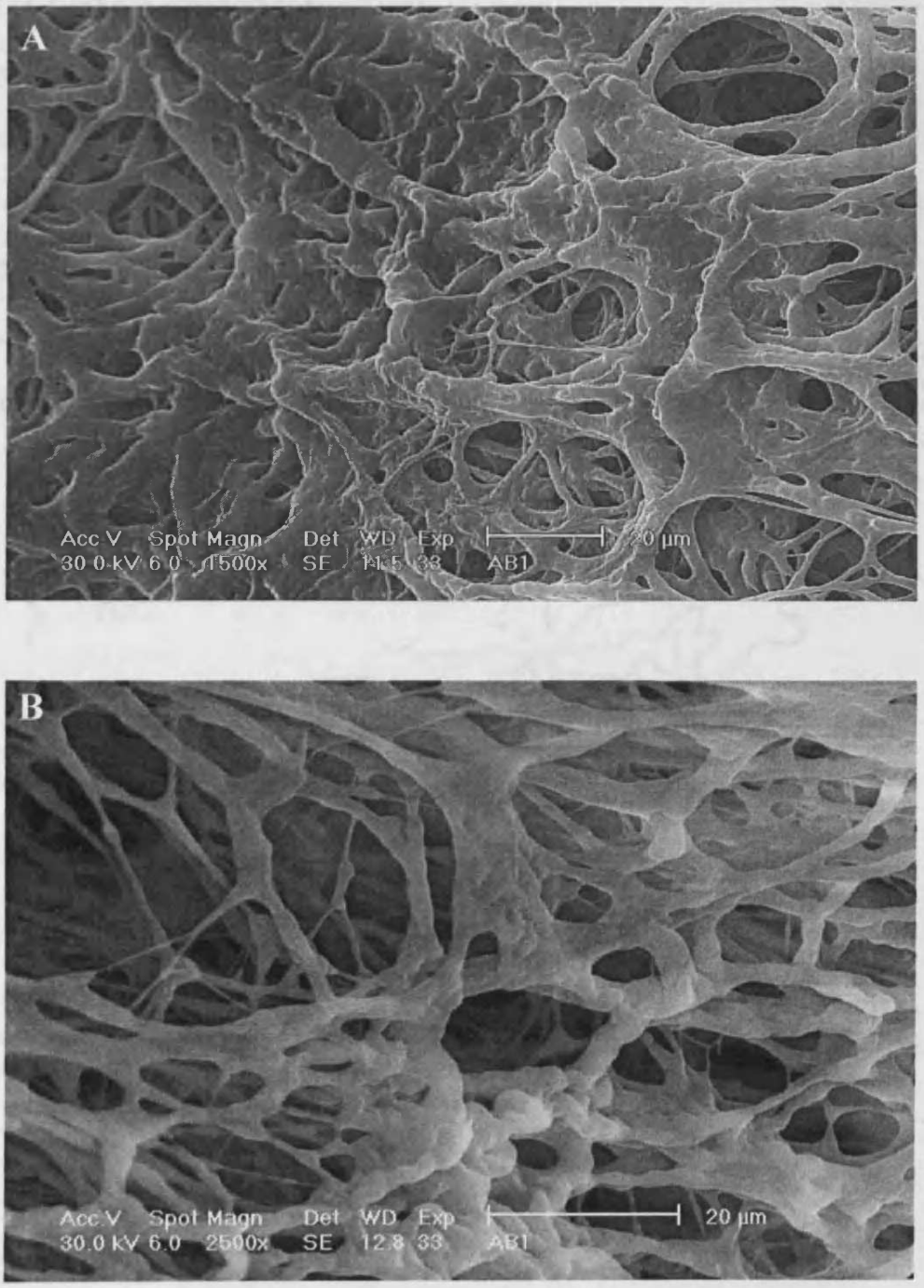

Figure 5.9 SEM images of 1% Carbopol hydrogels

5.4.3 TEM of PLGA-PEG-PLGA

TEM revealed that the polymer formed a suspension of conglomerates all with a similar structure. There appeared to be a relatively large central region, which appeared as dense mass in close proximity were filaments that did not appear as dense (Figure 5.8). It is proposed here that the dense regions are hydrophobic PLGA domains while the filamentous structures correspond to the hydrophilic PEG domains. A schematic representation is shown in Figure 5.10.

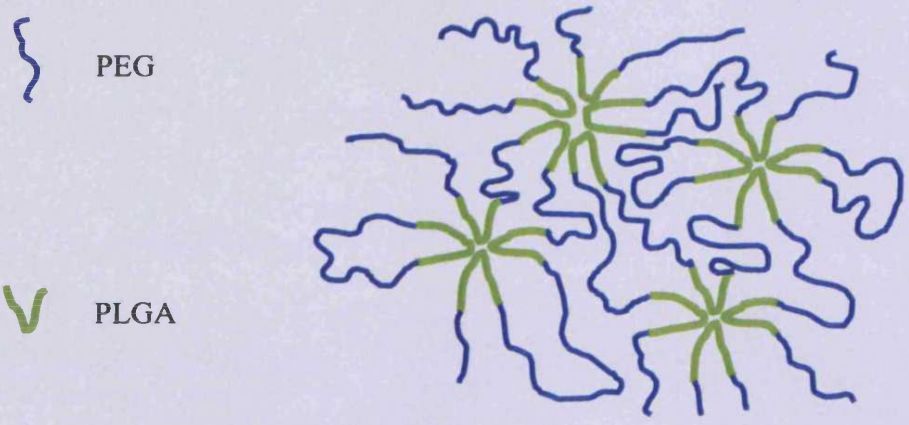

Figure 5.10 A diagrammatic representation of the TEM findings. The hydrophobic PLGA domains are internalized while the hydrophilic PEG domains coated their surface (adapted from Qiao *et al.* 2005).

5.4.5 PLGA-PEG-PLGA ^{1}H NMR

The structure of PLGA-PEG-PLGA tri-block copolymer (Figure 5.11 A) was confirmed by ^{1}H-NMR spectroscopy (Figure 5.11 B). Signals corresponding to the methine and methyl proton of the DL-lactide constituent (5.2 and 1.5 ppm, respectively), the methylene hydrogen of the glycolide component (4.8 ppm), and the methylene hydrogen of the PEG (3.6 ppm) were observed, which are consistent with the finding of Chen *et al.* and Qiao *et al* (Chen *et al.* 2005; Qiao *et al.* 2005. Each signal exists as a complex multiplet due to the highly variable nature of the polymer network due to the random incorporation of the monomers during synthesis and variability in conformation arising due to folding, branching and relative proximity of the central PEG. Such 'untidy' spectra are a common feature in NMR analysis of polymers.

The ratio of polylactide to polyglycolide in the polymer was determined directly from ^{1}H NMR spectra to be 1.74, this value is lower than that reported by others, for example 2.08-3.18 reported by Chen *et al* (Chen *et al.* 2005). The low ratio indicates that there is a relatively high polyglycolide component. This is likely to result in the in relatively rapid degradation of the polymer when in an aqueous environment since the glycolide component possesses a higher amount of bound reactive water which results hydrolysis (Zweers *et al.* 2004).

A

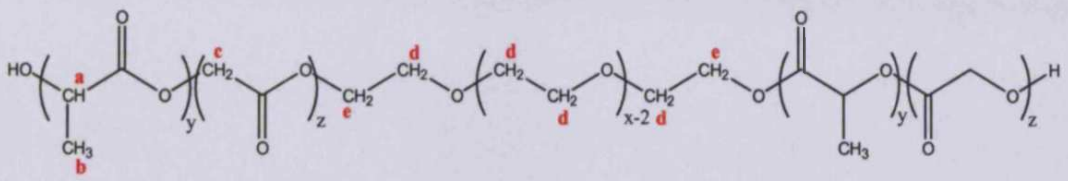

B

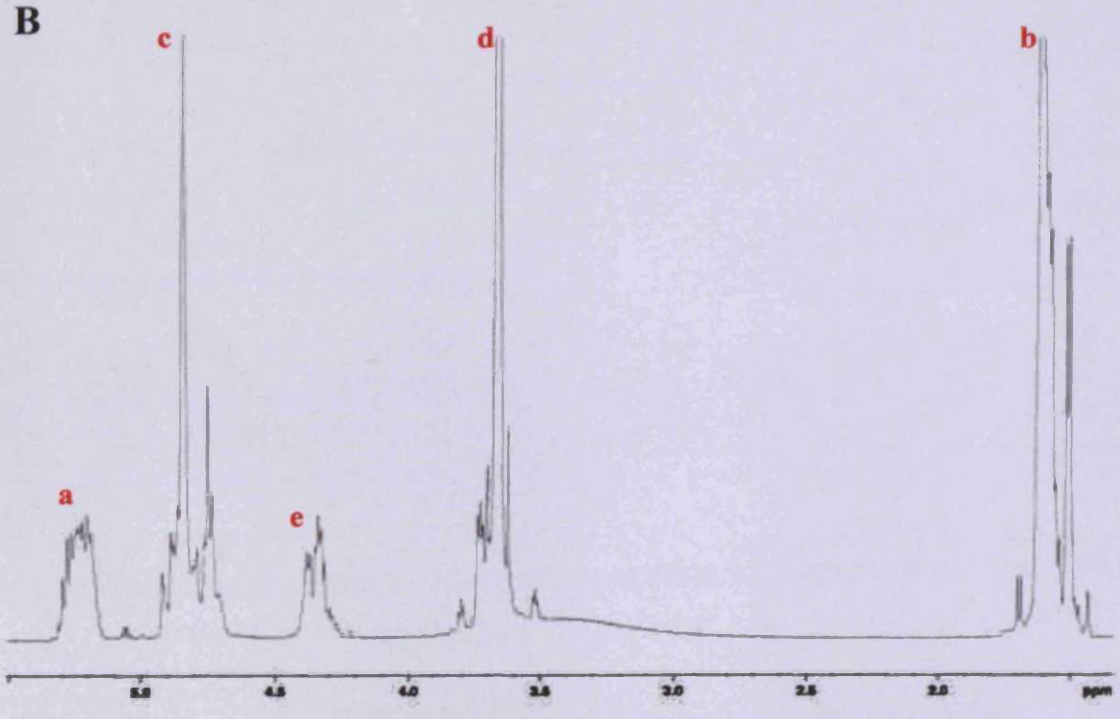

Figure 5.11 The molecular structure of a PLGA-PEG-PLGA polymer (A) and a typical ^{1}H NMR spectra (B).

5.4.6 GPC analysis of PLGA-PEG-PLGA

The molecular weight and polydispersity index of the PLGA-PEG-PLGA tri-block copolymer was determined by GPC (Table 5.1). Polymers of this size have been shown to display thermoreversible sol-gel transitions when present in specific concentrations in aqueous solutions (Chen *et al.* 2005).

Table .5.1 Molecular weight of the synthesized PLGA-PEG-PLGA as determined by GPC

Molecular weight of PLGA-PEG-PLGA		
M_w	M_n	Polydispersity index
3882	2986	1.14

5.4.7 PLGA-PEG-PLGA sol-gel transition

Below the lower critical solution temperature (LCST) the polymer solution remains in a liquid state and behaves as a Newtonian fluid (Chen *et al* 2005). Above this temperature the polymer solution forms into a gel. For a 23% w/v solution of the synthesized PLGA-PEG-PLGA (synthesized as decribed in Section 5.3.3), gelation was determined by test tube inversion and found to occur at 32°C. At temperatures above 40°C the polymer precipitated out of solution, but when cooled below the LCST reverted back to a solution (Figure 5.12). Gelation is thought to occur when polymeric micelles aggregate. Therefore by increasing the concentration of the polymer the sol-gel temperature can be reduced, thus, these polymers can be modified to suite different purposes (Chen *et al.* 2005).

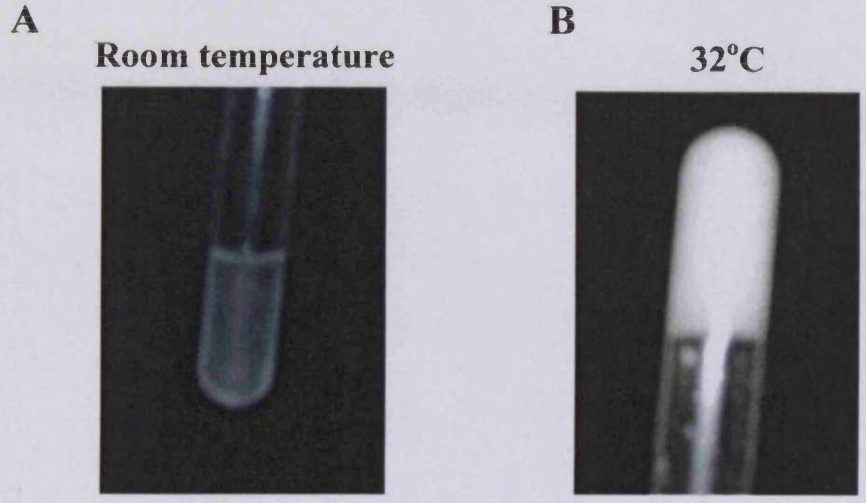

Figure 5.12 Demonstration of the temperature dependent sol-gel transition of a 23% PLGA-PEG-PLGA formulation. At room temperature it behaves as a typical fluid (A), however, when subject to an elevated temperature of 32°C rapidly forms a gel (B)

5.4.8 Microneedle facilitated delivery of fluorescent nanoparticle loaded hydrogels to skin

Previous studies have utilized 100nm fluorescent latex nanoparticles as a readily identifiable models for non-viral gene delivery vectors, for example LPD (Chabri *et al.* 2004). In this study fluorescent latex nanoparticles were utilized as an intra-hydrogel marker in order to reveal hydrogel skin deposition following microneedle facilitated delivery. Figure 5 shows 10μm cryosections of *ex vivo* human skin treated with hydrogels loaded with fluorescent nanoparticles (red) observed by fluorescent microscopy. The green fluorescence observed in all sections is a consequence of the autofluorescent properties of skin components and not the result of staining. In areas of the skin untreated with microneedles neither hydrogel was observed to penetrate the SC. In these areas the red fluorescent signal emitted from the nanoparticles loaded hydrogel remaining

on the external surface (Figure 5.13 A, B). In some cases the gel could be observed residing in skin ridges and other natural folds however the SC was still seen to be intact and no underlying red fluorescence was observed (Figure 5.13 B). However, when the hydrogel/nanoparticle formulations were applied to microneedle treated skin, Red fluorescence was observed localised to microneedle created channels. This suggests that the application of the microneedles to the surface of the skin had penetrated the skin surface and pushed the nanoparticle containing hydrogel formulations into the resulting microchannels. (Figure 5.13 C, D). Significant disruption to the SC is clearly evident in these images, leading to the formation of conduits with typical depths of 150-200μm and nanoparticles can clearly be observed as red or yellow (combination of red nanoparticle and green autofluorescence) against the green autofluorescent background within the viable epidermis.

These images confirm the hypothesis (Figure 5.1) that microneedle-hydrogel formulations are capable of delivering hydrogel material to the viable epidermis.

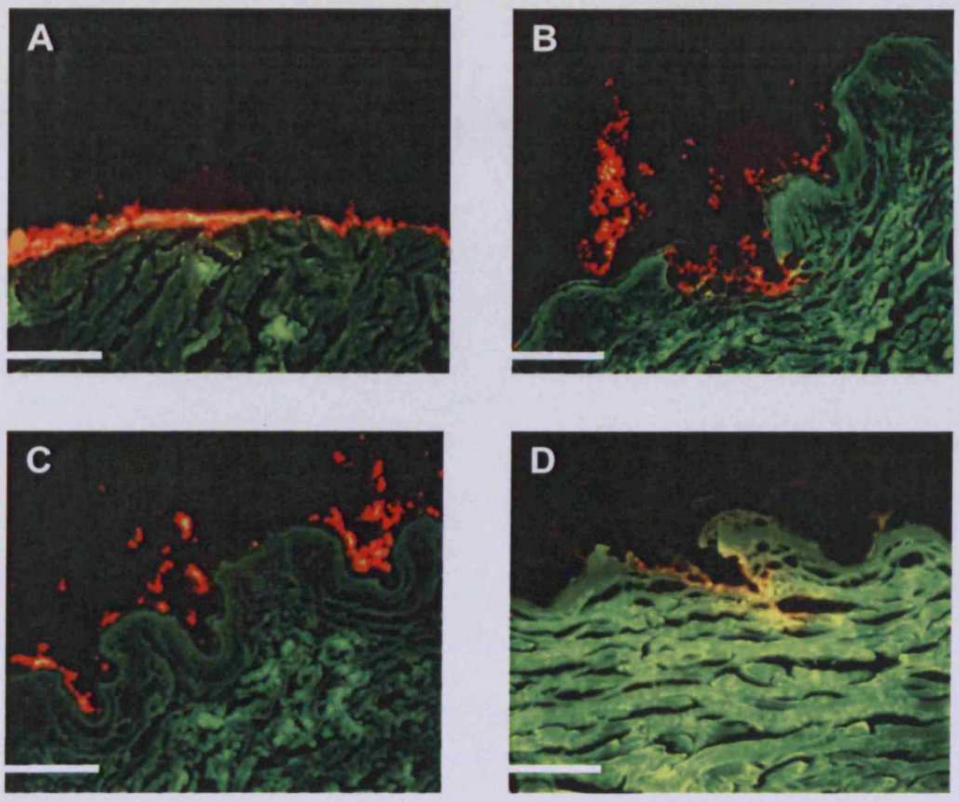

Figure 5.13 The appearance of 10μm cryosections of *ex vivo* human skin observed by fluorescent microscopy, note the green autofluorescence of the skin. Figure 5 A and B shows the application of a 1% w/v carbopol hydrogel containing red fluorescent nanobeads to intact skin. The SC restricts the passage of hydrogel into the viable epidermis. Figure 5 (C) and (D). In contrast to (A and B), microneedle application removes the SC integrity and the hydrogel formulations are able to reach the epidermis, (C) a 1% w/v Carbopol-940 and (D) a 23% w/v PLGA-PEG-PLGA hydrogel respectively; bar = 100μm in all cases.

5.4.9 Diffusion of nanobeads from hydrogel systems

Release of nanoparticles from hydrogel formulations and the resulting diffusion into the receptor phase was determined over 24 hours at 37°C (Figure 5.14). The migration of a control formulation of aqueous nanoparticles resulted in a release profile characteristic of that resulting from a finite single applied dose.

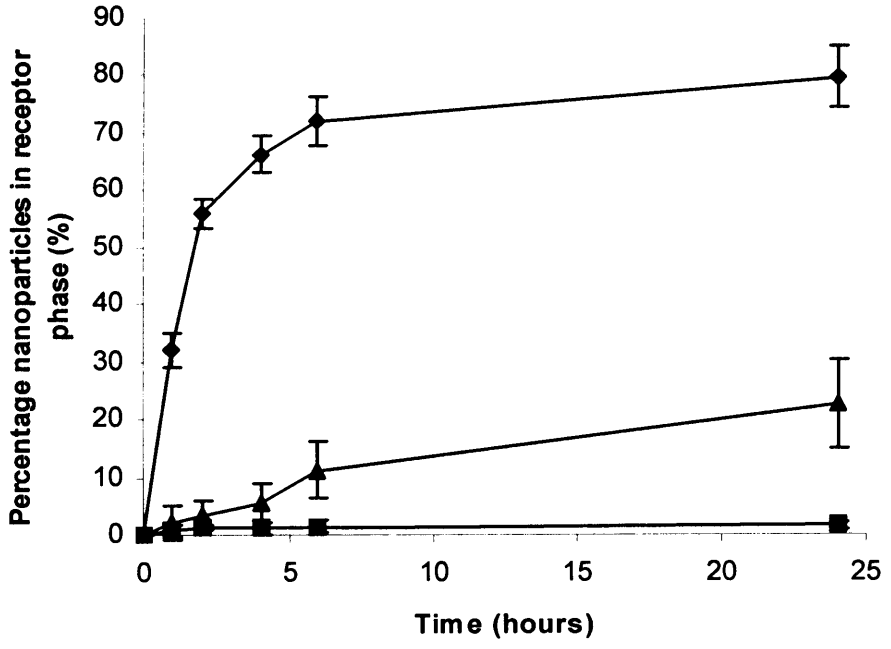

Fig 5.14 The migration of nanoparticles through a polycarbonate track-etch membrane with pore sizes of 10μm from different formulations, a solution of nanoparticles (♦), 1% w/v Carbopol hydrogel (■), and 23% w/v PLGA-PEG-PLGA triblock copolymer hydrogel (▲).

The release of nanoparticles from the Carbopol-940 hydrogel was extremely low, typically only 1.3% of the applied nanoparticles were found in the receptor phase after 24 hours. In contrast, release from the triblock copolymer was significantly greater, with approximately 20% of the nanoparticles migrating into the receptor phase after 24 hours. These results will be discussed in Section 5.4.10.

5.4.10 Diffusion of pDNA from hydrogel systems

Release of pDNA from the hydrogel and the resulting diffusion into the receptor phase was determined over 5 days at 37°C (Figure 5.15). In general, the migration of a control formulation of aqueous pDNA across the microneedle treated epidermal sheet was lower than predicted. This suggests that the microchannels, formed by the microneedle array, were either becoming obstructed by debris release from the epidermal sheet or possibly that the channels were closing due to hydration of the epidermal sheet, causing swelling and subsequent constriction of the channels. Release from the hydrogel formulations was distinct. Release of pDNA was retarded in both types of hydrogel; however, release was significantly greater from the PLGA-PEG-PLGA hydrogel. In fact, the amount of pDNA released from the Carbopol hydrogel was negligible. The mechanism of pDNA release might be expected to differ for the two types of hydrogel. In both systems migration of pDNA through the gel matrix will determine the release rate, however in the thermosensitive hydrogel the PLGA-PEG-PLGA polymers are prone to ester hydrolysis in aqueous environments and as a result the integrity of the polymer matrix is easily lost (compared to Carbopol) at physiological temperatures, particularly when the glycolide:lactide ratio is high (Zweers *et al.* 2004) this was previously found to be the

case with the synthesized PLGA-PEG-PLGA (Section 5.3.3). Therefore, for the PLGA-PEG-PLGA hydrogel matrix erosion effects will significantly influence pDNA release (Chen *et al.* 2005). Furthermore, it is important to note that release from hydrogels in the static Franz diffusion cell is not representative of how hydrogels might typically be applied to skin. In the Franz diffusion cell experiments the formulation was applied to a relatively small surface area of skin (area of 2-3cm^2), in a real in use situation it would be expected that a similar mass of formulation would be applied more thinly over a much larger skin area. Consequently, it is likely that the experimental system is an underestimation of *in vivo* application.

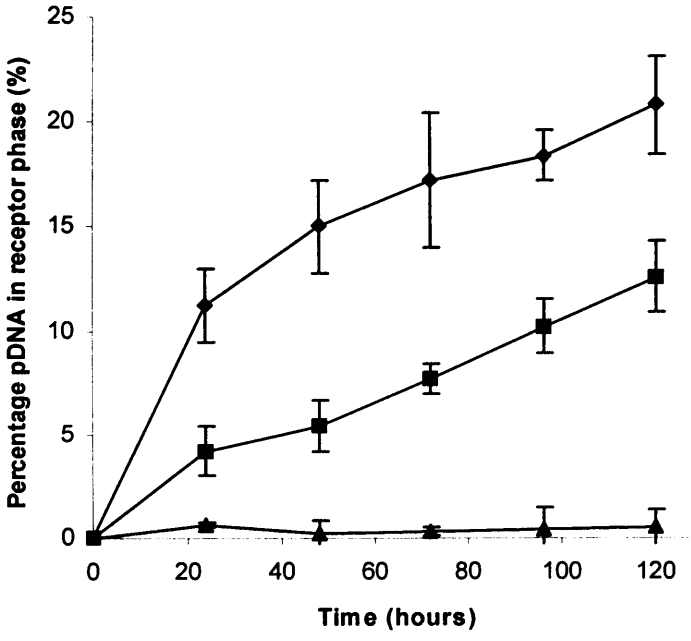

Figure 5.15. The migration of pDNA through a microneedle treated human heat separated epidermal sheet from different formulations, a solution of pDNA (♦), 1% w/v Carbopol hydrogel (▲), and 23% w/v PLGA-PEG-PLGA triblock copolymer hydrogel (■).

5.4.11 Delivery of hydrogels containing pCMVβ to skin facilitated by microneedles

5.4.11.1 Application of microneedles in a single rolling motion

An *ex vivo* organ culture system was used (as described in Chapter 4; Section 4.2.11) to demonstrate that a combination of microneedle application and hydrogel formulation can be used to deliver genes to the viable epidermis. Figure 5.16 shows *en face* images of *ex vivo* human skin treated with pCMVβ loaded hydrogel formulations and microneedle following immersion in X-Gal staining solution.

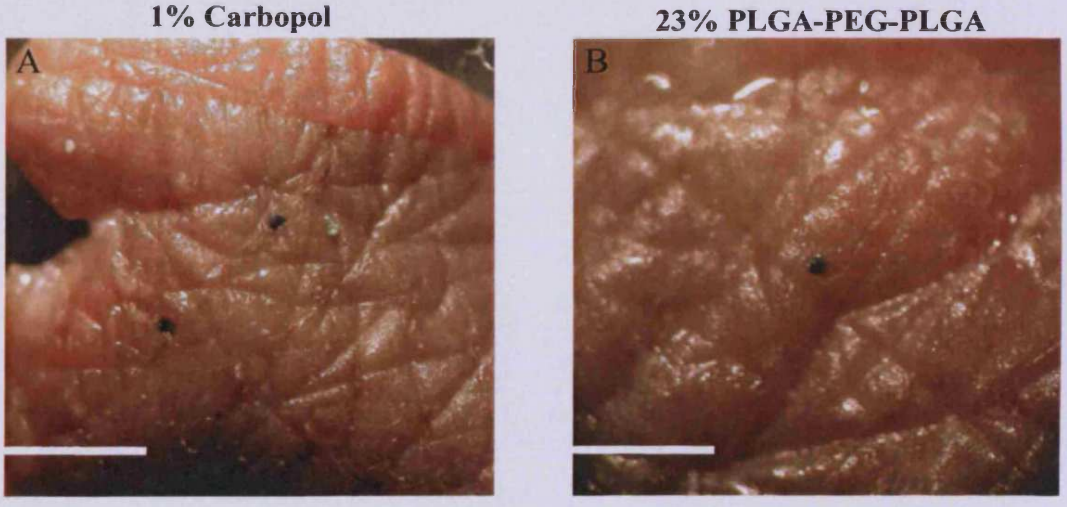

Figure 5.16. Positive expression from pCMVβ delivered to *ex vivo* human skin (female patient age 62) following X-gal staining; (A) 1% Carbopol-940 hydrogel and (B) 23% w/v PLGA-PEG-PLGA triblock copolymer hydrogel, facilitated by microneedles and both observed *en face*; bar = 1mm in both cases.

Both the 1% w/v Carbopol-940 and 23% w/v PLGA-PEG-PLGA tri-block copolymer hydrogels were shown to release functional pDNA which was able to transfect skin cells and express the gene product β-galactosidase. The blue coloration results from β-galactosidase mediated conversion of substrate (5-bromo-4-chloro-3-indolyl-β-D-galactopyranoside) to a blue coloured product (5, 5'-dibromo-4, 4'-dichloro-indigo) as

shown in Figure 4.1. In control experiments, where pDNA hydrogels were applied to un-microneedle treated skin gene expression was not observed. To determine the location of β-galactosidase expression in skin layers 12μm cryosections were taken from the same samples and observed using light microscopy. Figure 5.17 A & C reveals that reporter gene expression was proximal to a microconduit (typically between150-200μmin depth). H & E staining of the sections showed that areas of gene expression were limited to the cells of the epidermis (Figure 5.17 C & D).

Levels of gene expression were low, even by the standards established previously for application of solutions of pDNA (Figure 5.18). In these studies a total of three experiments were performed on three individual skin samples and the results combined. This gave a total of 12 separate microneedle applications for each formulation (the same amount of pDNA delivered in each experiment), which corresponds to a potential total of 192 points of positive gene expression for each formulation. For pDNA applied in the conventional way, with the solution applied to the skin surface followed by the application of the microneedle array in a single rolling motion, ~4.7% of the channels showed positive gene expression. This is in contrast to the two hydrogel formulations, ~1.6% for 1% Carbopol-940 and ~1% for 23% PLGA-PEG-PLGA. The reason for the reduction in observable gene expression is the physical retardation of the pDNA in the hydrogel matrix, resulting in less pDNA coming into contact the epidermal cells over the relatively short incubation period. Therefore, it was difficult to conclude whether gene expression would, if the delivery period was extended, result in more gene expression. This is ultimately, a limitation of organ culture systems. In order to address this issue it

would require the experiments be repeated but in an animal model. Thermosensitive hydrogels based on similar polymers to those presented here have been delivered, by intradermal injection, to rats. The gel formation was observed to be rapid, evident because the formed gel was compact and localized to the region of injection, where it persisted for more than a month (Lee *et al.* 2003; Jeong *et al.* 2000). Release studies of pDNA from a similar polymer hydrogel, using a detection method more sensitive to the one described in this thesis determined release was approximately constant for 15 days (Li *et al.* 2003). Whilst it is unlikely that release would be protracted over such a period when delivered with microneedle due to the small amount delivered, the turn over rate of the skin and the potential for hydrogel removal during contact with the environment.

The results presented in this thesis suggest that microneedles,-hydrogel-pDNA formulations may result in prolonged delivery of pDNA to cells of the viable epidermis.

What is apparent from these experiments is that pDNA can residue within the hydrogel formulations in a functional form. It is unlikely that the hydrogel formulations effect or otherwise modify the pDNA in any way that prevents expression from the plasmid because expression has been observed from pDNA released by both hydrogels. Therefore, the hydrogel formulation will ultimately protect the pDNA from the hostile biological environment, in which pDNA is prone to rapid degradation.

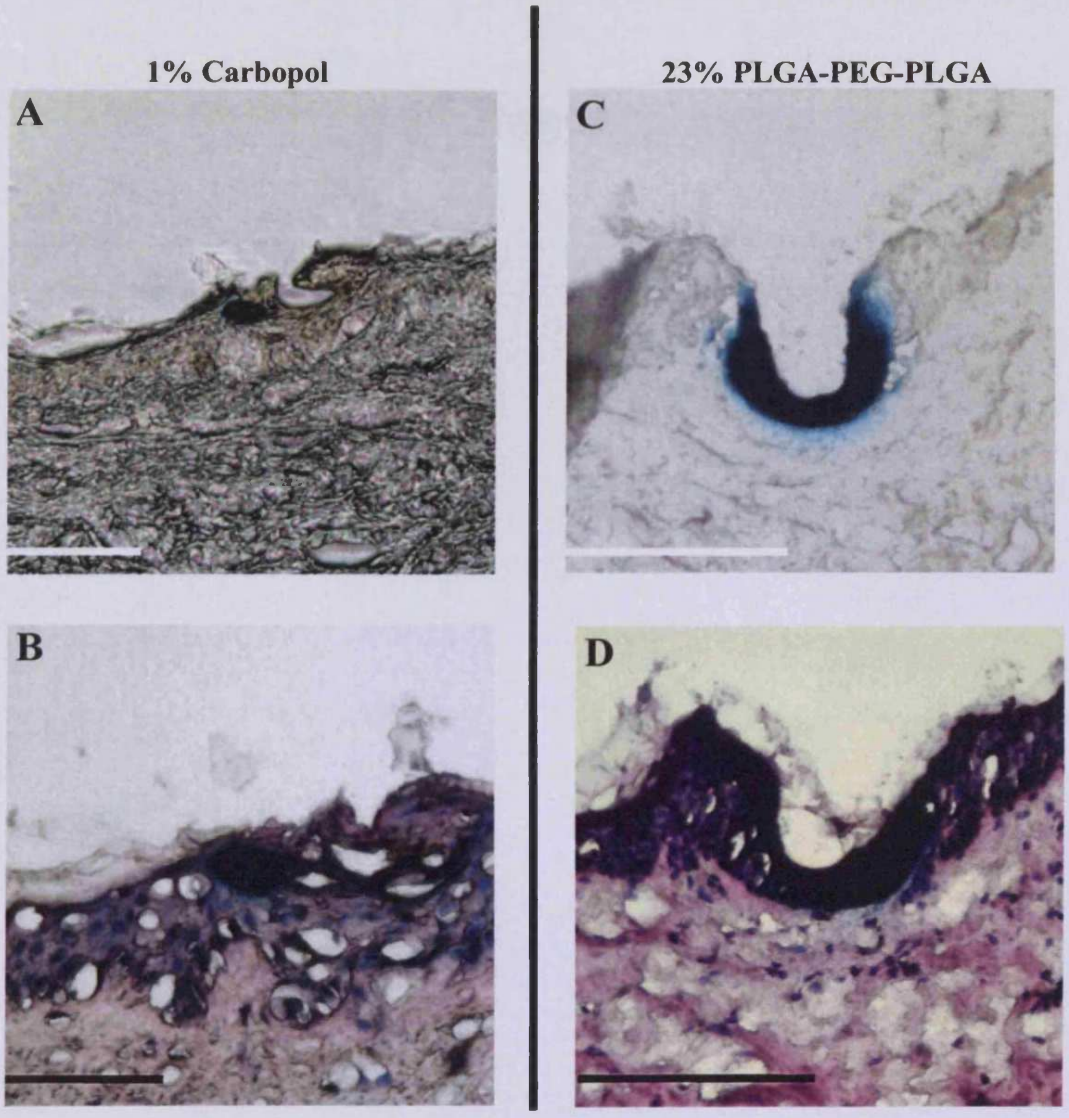

Figure 5.17 Cryosection of *ex vivo* human skin (♀ 62 years of age) treated with pCMVβ loaded hydrogels in conjunction with microneedles. (A) and (C) shows positive expression in the vicinity of a clear microneedle channels (bar = 150μm in both cases), while (B) and (D) shows a section from the same sample after H & E stain confirming expression is localised to the viable epidermis; bar = 100μm in both cases.

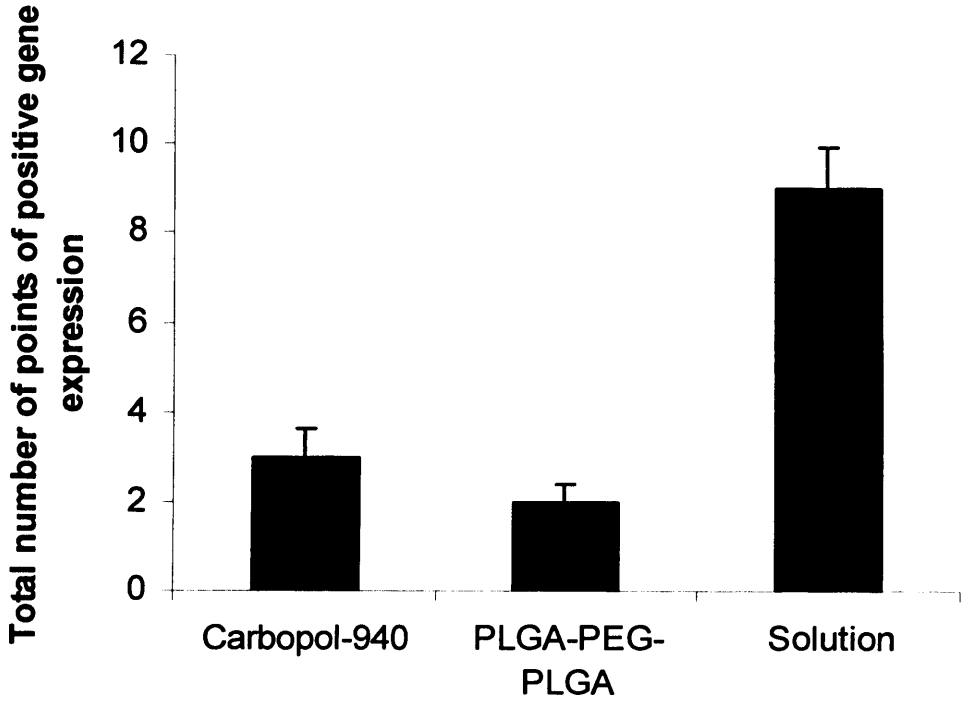

Figure 5.18 The total number of positive points of gene expression associated with a formed microchannel from different delivery formulations (n = 4 in all cases).

5.4.11.2 Application of microneedle in a single lateral scrape

Microneedle applied in a single lateral motion resulted in comprehensive disruption to the SC (Figure 5.20). Applying the microneedle in this way results in four clearly visible parallel channels, which correspond to the four microneedles on the leading edge of the as it is applied. The benefit of applying microneedles in this way is that it exposes far more epidermal cells to the exogenous pDNA, and therefore more cells are able to take up and express the pDNA.

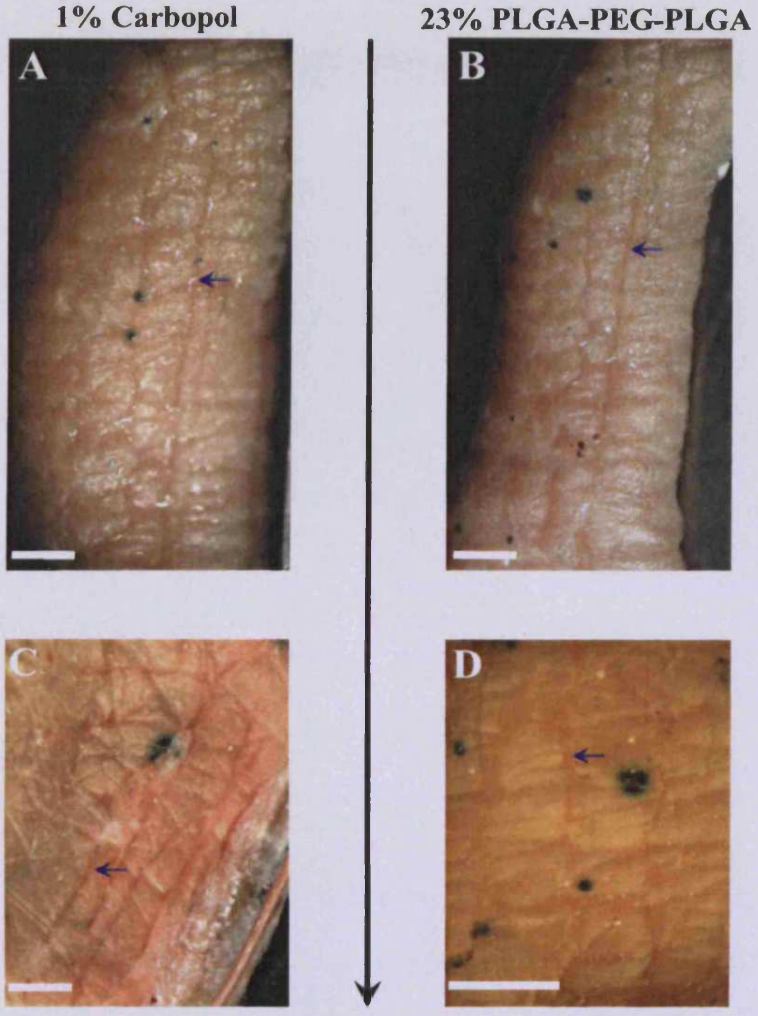

Figure 5.20 Delivery of pDNA loaded hydrogels with microneedles applied in a single lateral scrape. The disruption caused by the microneedles is indicated by the blue arrows. Expression from pDNA loaded in carbopol polymers A & C and PLGA-PEG-PLGA hydrogel B & D. The large black arrow indicates the direction the microneedle array was applied; bar = 1mm in all cases.

It was noted that most of the points of positive expression, generated from a lateral scrape, from both types of hydrogel, were in the region where the array was first applied and initially scraped. As the scrapping motion continues the points of positive expression become fewer. It is likely that scrapping the array results in far more cellular damage than applying the microneedle in a rolling motion, so that as the scrap proceeds it insults the cells to such an extent that they are killed. Another reason could be that as the scrap proceeds it becomes less efficient at delivering the formulation to the epidermis and the lower levels of expression are a consequence of little or no formulation reaching them.

5.5 Conclusions

Commercially available Carbopol was reconstituted to form hydrogels which contained fluorescent nanobeads and pDNA. Successful chemical synthesis was undertaken in order to form polymers of PLGA-PEG-PLGA, which subsequently can be used to form hydrogels that display thermoresponsive behaviours. The synthesised PLGA-PEG-PLGA polymers were reconstituted at a concentration of 23% w/v and were determined to undergo a sol-gel transition at around 32°C. At this temperature such a system would undergo gelation at physiological temperatures. When 23% w/v PLGA-PEG-PLGA and a 1% Carbopol hydrogels loaded with fluorescent nanoparticles were applied to *ex vivo* human skin in conjunction with microneedles the result was effect delivery of each formulation into the epidermis. This demonstrates that the concept of microneedle/hydrogel delivery valid. However, experiments using the same formulations conducted in Franz diffusion cells demonstrated that migration of the nanoparticle occurs, though release for Carbopol is extremely low. A similar release profile was observed when pDNA was investigated rather than fluorescent nanoparticles. This suggests that in the case of pDNA Carbopol polymers might not be suitable for gene delivery purposes. However, it appeared as though pDNA release was much greater over the time period from PLGA-PEG-PLGA and consequently a far more promising system for gene delivery.

Gene delivery studies demonstrated that channels through the SC, created by microfabricated microneedles can "house" hydrogel formulations based on Carbopol and PLGA-PEG-PLGA polymers. The hydrogel delivery systems are able to harbor pDNA in

the microneedle-facilitated microchannel and release the plasmid in a functional form for gene expression in the viable epidermis. The combination of the microneedle physical delivery strategy and sustained release formulation could potentially be employed for clinical applications where it is an advantage for large molecules to enter the viable epidermis over prolonged periods; this could be required for DNA vaccination strategies.

CHAPTER 6: Delivery of pCMV.M to viable *ex vivo* human skin by microneedles

6.1 Introduction

Somatic transgene vaccination (STV), more commonly know as DNA vaccination, involves the delivery of exogenous DNA containing a sequence that upon expression, within the body, elicits an immune response (Kumar & Sercharz 1996). During 1990 Wolff *et al* demonstrated that pDNA introduced to mammalian cells *in vivo*, is taken up and expressed (Wolff *et al.* 1990). Specifically, Wolff *et al*'s study involved an intramuscular injection of an aqueous solution of pDNA to the leg muscle of a mouse, expression was observed, locally in the leg and persisted for a least 2 months following administration (Wolff *et al.* 1990). Since then many DNA vaccination approaches and strategies have been proposed, with many centred on plasmid or naked DNA.

As well as the advantages non-viral vectors, in particular naked pDNA, have over viral-vectors (Chapter 1), there are a number of distinct advantages of using pDNA to achieve vaccination compared to conventional vaccination methods. For example, the native structure of expressed antigenic protein from plasmids is preserved; this is in contrast to subunit or attenuated vaccines where it is often lost (Hartle *et al.* 2004). DNA vaccines have been shown to induce long lasting, strong humoral and cellular immunity; efficiently generating $CD8^+$ cytotoxic T cells and $CD4^+$ T helper 1 (Th1) cells - vital for antibody production (Pardoll & Beckerleg 1995). Therefore, this approach may possibly prove useful in clearing viral and intracellular bacterial infections (Kumar & Sercharz 1996). Importantly, as delivery formulations contain nothing more than purified pDNA there is little chance of virulence or toxicity, as pDNA has been shown to be well tolerated (Parker *et al* 2001). Furthermore, such approaches have scope for increasing

immunogenic reactivity through modifications made to the vector and/or by incorporation of adjuvant sequences (Klinman *et al* 2004; Greenland & Letvin 2007) and also there exist the potential for the delivery of multiple antigens.

Recent studies have investigated the potential of DNA vaccination in anti-tumor strategies (Lowe *et al* 2007), to tackle re-emerging health concerns like Tuberculosis (Zhang *et al* 2007), and endemic diseases of the third world, but becoming prevalent in the west, like HIV (Kent *et al.* 2007). Thus DNA vaccination is regarded as a diverse and wide ranging application.

Potential routes of administration for DNA vaccines include intramuscular, intradermal, intravenous, intranasal and intraperitoneal (Fynan *et al.* 1993), though the most common approaches are intradermal and intramuscular injections (O'Hagan *et al.* 2004). Following intramuscular delivery to the mouse, pDNA becomes located in the majority of tissues, because it is transported through the circulation, but only for a short period of time. A small percentage remains at the site of injection for a much longer period of time, internalized by myocytes (Parker *et al* 1999). However, the muscle may not a good site to elicit an immune response due to low levels of MHC I and a lack of MHC II and co-stimulatory factors (Hohlfeld & Engel 1994). Though immune responses have been observed following intra-muscular injections, it is likely that these are the result of resident antigen presenting cells (APC) capturing and processing antigen released from myocytes subsequently priming both $CD8^+$ and $CD4^+$ T cells once migrated to draining lymph nodes (Kumar & Sercharz 1996).

The skin, in contrast, is a far more attractive location, for reasons highlighted in Chapter 1. Briefly, because the skin is the interface between our bodies and the physical environment there is a considerable likelihood of encountering foreign antigens. Consequently, the skin has evolved a sophisticated immune surveillance system - the skin associated lymphoid tissue (SALT). A component of the SALT and a primary APC in the skin is the Langerhans cells (LC), which reside within the epidermis. Earlier chapters' of this thesis have shown that microneedles are readily capable of delivering pDNA to this region (Chapters 1 and 2). This chapter will place that work in a therapeutic context by attempting to deliver a plasmid encoding an antigenic protein, specifically to the epidermis. It is proposed that the dimensions of the microneedles will specifically target the antigen encoding plasmid to the epidermis and therefore in the vicinity of both keratinocytes and LC.

Theoretically, the LCs that take up and express the antigenic transgene could subsequently process the peptide and present it to naïve T-cells, which could potentially generate an immune response, shown schematically in Figure 6.1 (Norbury & Sigal 2003). However, keratinocytes themselves could act as "mini-factories" producing the antigenic protein which is then released and subsequently taken up, processed and presented to the local LC population (Birchall *et al.* 2005). However, in order for keratinocytes to behave in this way it is likely further sequences would have to be spliced into the plasmid. For example, Hauser *et al* have constructed plasmids containing a sequences which targets newly translated antigen down the secretary pathway and then specifically to DC's (Hauser *et al.* 2004).

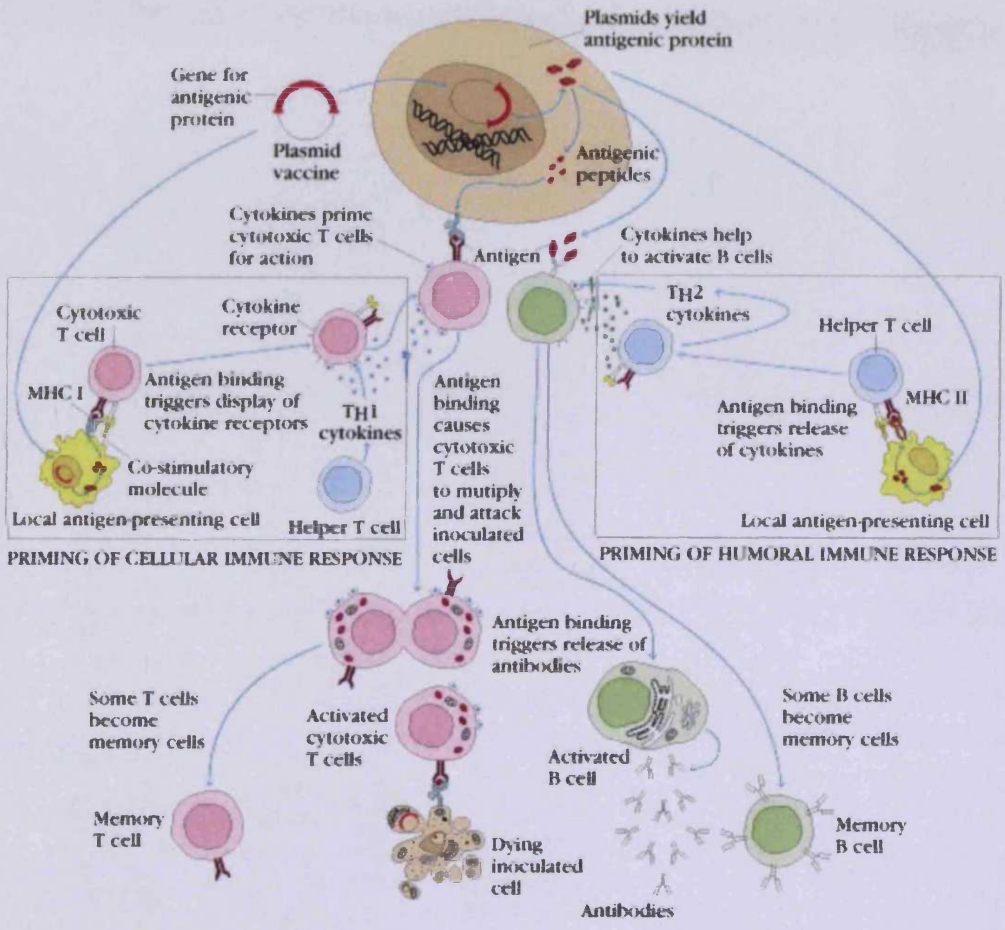

Figure 6.1 A schematic showing both cell mediated and humoral immune responses resulting from expression from a plasmid encoding a antigen. Imaged from http://home.inje.ac.kr/~lecture/immunobiotech/ch2/ch2microbimmunity.htm

The plasmid used in this study was obtained as a gift from Aldevron (Fargo, USA) and encodes the small and middle forms of the Hepatitis B virus (HBV) surface antigen (HBsAg). A simplified molecular map of the plasmid is shown in Figure 6.2. There is a plethora of information in the literature regarding HBV because it is such a relevant public health concern; the virus is endemic in much of the world where it is estimated that more than 2 billion people have come into contact with the virus and 350 million are chronic carriers (Zuckerman & Zuckerman 2000). Also, it has recently been anticipated that differences in the HBV genotypes can influence the course of an infection (Shaefer 2005). Therefore, for vaccination strategies to be most effective, vaccines may need to be targeted at particular stains in different locations. DNA vaccination is particularly well suited to this kind of scenario because sequence manipulation of pDNA is relatively easy; consequently DNA vaccines can be tailored rapidly to suit different locations and applications.

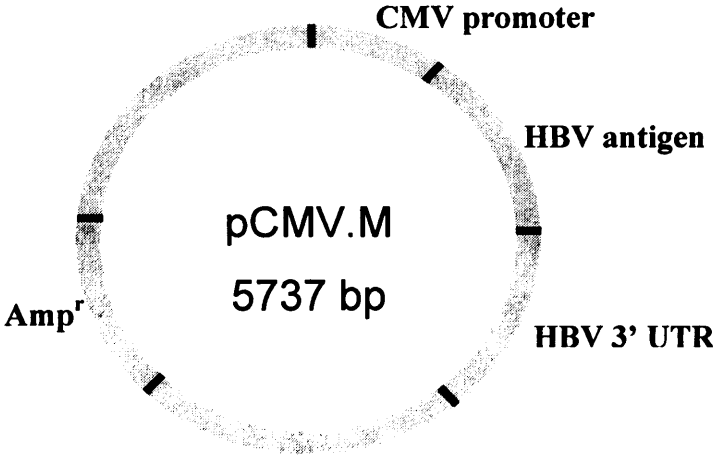

Figure 6.2 A molecular map of pCMV.M encoding the small and middle forms of HBsAg.

While delivery of pCMV.M to *ex vivo* skin will not result in an immune response being generated, because the tissue is isolated away from the body, it may demonstrate that expression occurs from pCMV.M, in regions of the skin where LC's are located, i.e. the epidermis. Therefore this is a crucial proof-of-concept step in progressing microneedle/DNA vaccination strategies.

Expression from pCMV M, both *in vitro* and in *ex vivo* human skin, will result in no direct visual indication of positive expression, like that observed from reporter plasmids. Expression will be confirmed by immunocytochemistry (ICC) and immmunohistochemistry (IHC) for cells *in vitro* and *ex vivo* tissues respectively. Both these techniques require a specific antibody, which preferentially binds to a protein of interest, in this case HBsAg. While the delivered antibody can have a conjugated marker attached (direct method), more typically a secondary antibody that recognises the first antibody is applied (indirect method) which has a conjugated marker. The method of ICC and IHC used here utilize a mouse monoclonal antibody (clone 3E7) specific for the "a" determinant on subtypes *ayw1*, *ayw2*, *ayw3*, *ayw4*, *ayr*, *adw2*, *adw4*, and *adr* determinants of HBsAg (DakoCytomation mouse monoclonal antibody data sheet). Detection of the anti-HBsAg mouse primary antibody is made with a secondary anti-mouse antibody that is conjugated to an enzyme or a fluorescent tag both of which enable direct visual conformation of the primary antibody and hence the location of the antigen. Because low levels of gene expression are expected a horse radish peroxidase (HRP) labelled polymer conjugated to secondary goat anti-mouse immunoglobulin was purchased. According to the manufactures protocol, the detection system is particularly

well suited for the detection of low concentrations of primary mouse antibodies, thus well suited to detect limited expression from pCMV.M in *ex vivo* skin.

Because of the innate variability of human skin samples, as previously alluded to, an attempt to deliver the antigen directly i.e. purified HBsAg, to *ex vivo* skin in conjunction with microneedles will also be made. There are two reasons for doing this. Firstly, it will act as a control for experiments performed with pCMV.M. If the detection system cannot detect the purified antigen in the skin it is highly unlikely that considerably lower levels of the antigen expressed from the plasmid will be found. Secondly, successful detection will confirm the successful delivery of an antigenic peptide to the target region of the skin, i.e. the epidermis, facilitated by microneedles.

While expression from the plasmid in *ex vivo* skin will not result in an immune response being generated, successful expression will be the first demonstration of a therapeutic gene being expressed in human tissue that has been delivered by microneedles.

6.2 Aims and objectives

6.2.1 Aims

The aims of this chapter are to prepare stock solutions of a therapeutic plasmid, pCMV.M, for delivery facilitated by microneedles into *ex vivo* human skin.

6.2.2 Objectives

- To reconstitute, amplify and produce stocks of pCMV.M.
- To demonstrate that expression of HBsAg occurs from pCMV.M *in vitro* and can be detected.
- To detect the presence and determine the location of purified HBsAg delivered by microneedles to *ex vivo* skin.
- To observe expression from pCMV.M in viable *ex vivo* human skin delivered by microneedles.

6.3 Materials and methods

6.3.1 Materials

The plasmid pCMV.M was received as a gift from Aldevron (Fargo, USA).

Purified HBsAg was obtained from AbCam (Cambridge, UK).

E.coli DH5α cells, Dulbecco's modified eagle medium (DMEM), Penicillin, Streptomycin, Foetal Bovine Serum and Trypsin-EDTA were purchased from Invitrogen (Paisley, UK).

Mouse monoclonal antibody and EnVision+ mouse monoclonal antibody detection kit were purchased from Dako (Glostrup, Denmark).

All other reagents were purchased from Fisher Scientific (Loughborough, UK).

6.3.2 Reconstitution, amplification, purification and characterisation of pCMV.M

6.3.2.1 Recovery of pCMV.M

Aldevron (Fargo, USA) supplied 2-4μg of pCMV.M dried onto filter paper. Reconstitution involved placing the paper into a sterile 1.5ml microcentrifuge tube followed by the addition of 100μl of Tris-EDTA, and incubation at room temperature for 30 minutes. The tube was vortexed for 2 minutes and the remains of the paper removed by centrifugation, with the supernatant being transferred to a fresh 1.5ml microcentrifuge tube.

6.3.2.2 Transformation of DH5α™ E.coli with pCMV.M

As only a small amount of plasmid was received from Aldevron, it was essential that the plasmid was amplified and stored to ensure sufficient amounts were obtained for further studies. Amplification of plasmid was achieved by transforming a suitable strain of bacteria and allowing the culture to grow. Transformation is not completely efficient; therefore it is essential that the plasmid has a selectable marker, typically an antibiotic resistance gene. This ensures that only cells that have taken up the plasmid can survive when grown in media containing the antibiotic (ampicillin in this case). Transformation ensures that stocks of bacteria, containing the plasmid of interest, can be made and stored indefinitely.

DH5α™ competent *E.coli* cells were allowed to thaw completely on ice, before 100μl was aliquoted into a chilled 17 X 100 mm polypropylene tube. To these cells 14ng of pCMV.M was added and the cell suspension carefully agitated with the pipette tip,

followed by incubation on ice for 30 minutes. The cells were heat shocked by immersion in a water bath at 42°C for 45 seconds, followed by immediate incubation on ice for 2 minutes. S.O.C. media (900µl) was added to the cells followed by incubation at 37°C, in an orbital shaker (225rpm) for 1 hour. During this time 2 LB agar plates containing ampicillin (100µg/ml) were prepared. Under sterile conditions, 100µl of the transformed cell culture was applied and spread over each of the selective agar plates and incubated at 37°C overnight.

6.3.2.3 Preparation of glycerol stocks

A single colony was picked from the plate prepared previously (Section 6.3.2.2) and used to inoculate 10ml of sterile LB medium containing ampicillin (100µg/ml) in a McCarthy bottle, which was grown at 37°C overnight. Into a sterile 1.5ml microcentrifuge tube 500µl of the overnight culture was added followed by 500µl of sterile 30% glycerol. The cell culture/glycerol solution was gently mixed and frozen in a dry ice/ethanol bath then stored at -80°C.

6.3.2.4 Plasmid preparation

Selective LB agar plates were prepared as described previously (Section 6.3.2.2) and streaked with *E.coli* transformed with pCMV.M then grown over night at 37°C. Concurrently two McCarthy bottles, each containing 5ml LB media, were prepared along with four 500ml conical flasks, each containing 125ml of LB media and sealed by double capping with foil, all were sterilized by autoclaving. Each of the McCarthy bottles had ampicillin added (100µg/ml) before inoculation with a single colony

obtained from the selective plate and then grown in a shaking water bath at 37°C for 8 hours.

A sample of this culture (1 ml) was subsequently used to inoculate each of the 4 conical flasks (which had been supplemented with ampicillin (100μg/ml) before inoculation) and incubated at 37°C, in an orbital shaker at 160rpm overnight. The plasmid was purified using a Qiagen Plasmid Mega kit, as described previously (Chapter 3).

6.3.3 Characterisation and functionality of pCMV.M

Confirmation that the plasmid purified from the prepared stocks (Section 6.3.2.4) was indeed pCMV.M was demonstrated by restriction digest of the plasmid. Restriction endonucleases recognise and digest specific restriction points within the plasmid. The result is fragments of the plasmid being generated, each of a specific size. These can be compared to the theoretical predictions of fragment numbers and size as determined by the plasmid map.

As previous chapters have shown, delivering genes into *ex vivo* human skin is not efficient or reproducible. Therefore, functionality of the plasmid plus the ability to detect expression must be confirmed before delivery to skin. In order to do this the plasmid is first assessed *in vitro,* because continuous cell lines provide reproducible and easily controllable conditions that simply are not available in *ex vivo* skin model systems. However, it has been noted that delivering naked DNA too mammalian cells *in vitro* is not effective; indeed it is important to note the lack in correlation between transfection *in vitro* and *ex vivo*. For cultured cells to take up exogenous DNA, it

must be complexed with other factors, for example cationic lipids. This is in stark contrast to the situation in *ex vivo* skin, where delivering DNA complexes is not an effective way of delivering DNA (Birchall *et al* 2005). Nevertheless, cell culture is essential to demonstrate that pCVM.M is viable and immuno-detection can be optimized and shown valid.

Suitable gene delivery vectors for *in vitro* transfection include lipid: peptide: DNA (LPD) complexes, a system that has been well characterized (Birchall *et al.* 2000). The formation of a LPD complex begin first the DNA component being condensed with a cationic peptide, e.g. protamine, which is then surface coated with a cationic lipid The lipid components of the LPD vectors used in this study were formed into liposomes, discussed in Chapter 1. Formation of liposomes is relatively simple, because lipid membranes spontaneously form a consequence of unfavourable interactions between hydrophobic lipids and water. Characterisation of formed LPD complexes was achieved by TEM, PSC and determination of zeta potential (ξ)

6.3.3.1 Restriction digest

Sterile 1.5 ml eppendorff tubes were set-up containing the restriction enzymes EcoR1 and Hind III as shown in Table 6.1.

Table 6.1 Constituent reagents for restriction digest of pCMV.M

Tube	Enzyme (µl)	Buffer (µl)	BSA (µl)	Sterile water (µl)	pCMV.M (µl)
1	**EcoR1 -1**	**2**	**0.2**	**15.3**	**2.5**
2	**Hind III - 1**	**2**	**0.2**	**15.3**	**2.5**
3	**EcoR1 - 1**	**4**	**0.4**	**9.1**	**2.5**
	Hind III - 1	**4**			
4	**None**	**17.5**	**None**	**2.5µl**	**None**

All tubes were pulse spun in a microcentrifuge to ensure all reagents were located in the bottom of each tube, which were then placed in a pre-warmed water bath at 37°C for 2 hours. Each tube received 5µl of loading buffer and loaded into a 1% agarose gel for electrophoresis (described in Chapter 3; Section 3.3.5.1).

6.3.3.2 Liposome preparation (Fluorescent and normal)

Liposomes were prepared from the cationic lipid 1,2,-Dioleoyl-3-Trimethylammonium-propane (DOTAP). DOTAP lipid (10mg) was added to a round bottomed flask and dissolved in 5ml of chloroform. For fluorescent lipid 9.5ml of DOTAP and 0.5mg of $NBDC_{12}$-HPC lipid are used. The solvent was removed, under vacuum, in a rotary evaporator immersed in a water bath set above the glass transition

temperature of the constituent lipid(s), forming a film of lipid on the inside of the round bottomed flask. Warmed sterile water (37°C) was added (10ml) to hydrate the film and the flask vortexed. The result was a heterogeneous suspension of multi-lamellar lipid vesicles (MLVs). A more uniform unilamellar population of liposomes was prepared by subjecting the MLV solution to high pressure extrusion. The extrusion apparatus (The Extruder, Lipex Biomembranes Inc., Vancouver, Canada) had its thermobarrel warmed above the T_c of the lipid(s) and was connected to a nitrogen cylinder. The MLV suspension was placed into the extruder and nitrogen was introduced at 100-150 psi, this forces the MLV solution through a 25mm diameter 100nm pore size polycarbonate Isopore® membrane (Millipore UK Ltd., Watford, UK), this was repeated a total of ten times.

6.3.3.3 LPD preparation

LPD formulations at a ratio of 3:2:1 lipid: Protamine: pDNA were formed by the sequential addition of protamine sulphate (1mg/ml in sterile water) to 1,2 Dioleoyl-3-trimethylammonium-tropane (DOTAP) liposomes (1mg/ml in sterile water) to pCMV.M (1mg/ml in Tris-EDTA) with a 10 minutes incubation time between each addition.

6.3.4 Physical characterisation of LPD complexes

6.3.4.1 Transmission electron microscopy (TEM)

Each sample was carefully pipetted (~20µl) onto a 100 mesh Nickel grid and allowed to stand for 3 minutes. Excess fluid was wicked off filter paper and the grid was stained with freshly centrifuged and filtered 2% uranyl acetate for 30 seconds. Each

grid was washed twice in distilled water before observation with a Philips EM 208 (FEI Company, Eindhoven, The Netherlands).

6.3.4.2 Particle size analysis by photon correlation spectroscopy

The size of particles was determined by photon correlation spectroscopy (PCS) using a Coulter N_4 Plus (Coulter Electronics Ltd., Luton, UK). A sample of the extruded liposomes was diluted in deionised water, placed in a clear sided cuvette and analysed using a 10 mW laser with a scattering angle of 90° at 25°C, particle size was expressed in unimodal and Size Distribution Processor (SDP) mode (n = 4).

6.3.4.2 Zeta potential

Microelectrophoresis was employed to determine the zeta potential of liposomes and LPD complexes using a Malvern Zetasizer 2000 (Malvern Instruments Ltd., Malvern, UK). The instrument was washed with degassed deionised water and calibrated using AZ55 polystyrene standards. Samples were diluted in degassed deionised water before injection into the instrument, measurements were made at 25°C.

6.3.5 *In vitro* delivery of LPD complexes

A-549 cells (human lung epithelial carcinoma) at passage 50 were removed from liquid nitrogen storage and allowed to defrost at 37°C. The cells were dispersed by gentle repeated pipetting up and down before being transferred into a sterile 50ml centrifuge tube. The cells were centrifuged at 4000 rpm for 10 minutes. The supernatant was removed and 7ml of fresh culture media (89% DMEM, 10% FBS, 1% penicillin/streptomycin) was added carefully, one drop at a time. Cells were

transferred to a T-25 cell culture flask and incubated at 37°C, 5% CO_2. Once the cells were established old culture media was removed and fresh, pre-warmed media added approximately every 2 days. Once cells approached confluency, culture media was removed and the flask rinsed twice with 5ml sterile PBS, followed by the addition of 3ml of trypsin-EDTA for 90 seconds. The trypsin-EDTA was removed and the flask incubated at 37°C for 5 minutes, cells were dislodged from the flask by gentle tapping. The flask received 5ml of fresh culture media followed by repeated gentle pipetting to disperse the trypsinised cells. Approximately 100µl of the cell suspension was removed and a cell count performed with a haemocytometer by light microscopy. A fresh T-25 cell culture flask was seeded with the appropriate volume of cell suspension containing 1 million cells, followed by the addition of 7ml fresh media. Transfection studies are subsequently performed in 24-well plates with each well being seeded at a density of 72, 000 cells.

6.3.5.1 Delivery of pCMV.β, pEGFP-N1 and pCMV.M to A-549 cells

A 24-well plate, seeded at a density of 72, 000 cells, was allowed to grow at 37°C for 48 hours in full culture media (DMEM 89%, FBS 10 %, and Pen/Strep 1%). The media was removed and the cells washed twice with 1ml phosphate buffered saline (PBS). LPD formulations, containing pCMV.M, pEGFP-N1, or pCMVβ were made prior to commencement of each experiment at a ratio of 3:2:1 lipid: Protamine: pDNA (described in Section 6.3.3.3) in DMEM. Enough LPD/DMEM formulation was made so that each well received 5µg of pDNA in 1ml of DMEM. The LPD/DMEM formulation was applied to each well and incubated for 6 hours at 37°C, 5% CO_2. After this period, the LPD/DMEM formulation was removed and fresh media added

followed by incubation at 37°C, 5 % CO_2 for 24 hours, the cells were then analysed for gene expression.

6.3.5.2 Histochemical X-gal staining of A-549 cells transfected with pCMVβ

Cells transfected with pCMVβ were removed from incubation and the culture media was removed. The wells were rinsed twice with 1ml of PBS (0.01 mol/L) and subsequently fixed in 1ml of 4% formalin (diluted in PBS) for 15 minutes, followed by a double rinse with 1ml of PBS. Each well received 0.5ml of X-gal staining solution (for 5ml, 50µl potassium ferricyanide 400mM, 50µl potassium ferrocyanide 400mM, 50µl magnesium chloride 200mM, 250µl X-gal (20mg/ml in DMF), 4.6ml PBS) and incubated at 37°C for 1 hour. Staining solution was removed and each well rinsed twice with 1ml PBS. Cells were viewed under 0.5ml PBS by light microscopy (Olympus IX-50585 Inverted Microscope System, Olympus Optical, London UK).

6.3.5.3 Fluorescent microscopy of A-549 cells transfected with pEGFP-N1 in a fluorescent LPD complex

A-549 cells transfected with pEGFP-N1 (Section *6.3.5.1*) were removed from incubation periodically (1, 2, 3, 4 and 5 hours) and viewed by fluorescent microscopy. After 6 hours the culture media was removed and each well rinsed twice with 1ml of PBS (0.01 mol/L) and fixed in 1ml 4% formalin (diluted with PBS) for 15 minutes, each well was rinsed twice with 1ml PBS. Each well received 0.5ml PBS, to prevent cells drying out during visualisation by fluorescent microscopy (Olympus IX-50585 Inverted Microscope System, Olympus Optical, London UK).

6.3.5.4 Immuno-cytochemistry (ICC) of A-549 cells transfected with pCMV.M

All ICC was performed using an EnVision™ + System-HRP (DAB) kit obtained from DakoCytomation, specifically designed to detect mouse monoclonal antibodies, and used according to the manufacturer's protocol. Cells cultured in a 24-well plate transfected with pCMV.M were removed from incubation and culture media removed and each well rinsed with 1ml PBS (0.01 mol/L). Fixation was achieved by adding 1ml of 4% formalin (diluted in PBS) to each well for 15 minutes at room temperature, followed by two rinses with 1ml PBS. Cells were made permeable by the addition of 1ml of 0.5% Trition X-100 (in PBS) for 10 minutes which was removed and replaced with 1ml of 0.1% Trition X -100 (in PBS) for 10 minutes both incubations at room temperature. The Triton X – 100 was removed and each well rinsed twice with 1ml PBS. The PBS was removed and the bottom of each well covered with 0.03% hydrogen peroxide containing sodium azide for 5 minutes, which quenches endogenous peroxidase activity. Each well was subsequently rinsed with wash buffer (0.02mol/l PBS). Each well then received 0.02ml of primary antibody (Mouse anti-HBsAg, 3E7) diluted 1:50 (dilution buffer 0.05mol/L Tris-HCL, pH 7.2, with 1% BSA) and incubated for 30 minutes at room temperature. The wells were rinsed with wash buffer (0.02mol/l PBS) before a peroxidase labelled polymer was added to each well ensuring a complete covering of the bottom of the well, followed by incubation at room temperature for 30 minutes. The peroxidise polymer was removed and each well rinsed with wash buffer (0.02 mol/l PBS). DAB+ substrate chromogen (prepared according to manufacturer's protocol) was added to each well and incubated for 10 minutes at room temperature; this provides the visual confirmation of antibody presence, results were observed by light microscopy (Olympus IX-50585 Inverted Microscope System, Olympus Optical, London, UK)

6.3.6 Microneedle facilitated delivery of HBsAg (Ayw) protein to *ex vivo* skin model system

Human skin (♀ 59 years of age) was obtained following surgery, transported and processed to form split-thickness skin as previously described (Chapter 4). Split-thickness skin was pinned over a semicircular cork support, the surface dried with a paper towel and then 5μl (500μg/ml) of purified Hepatitis B virus surface antigen (HBsAg) protein (Ayw) applied to the skin surface. A mounted sharp tipped microneedle array in a 7 X 7 arrangement with needle heights of 280μm was applied in a single rolling motion to the region treated with the antigen (n = 4); other regions of the same skin samples were treated only with microneedles (n = 4). All treated regions were carefully excised and immediately processed for immuno-histochemistry (see below).

6.3.7 Delivery of pCMV.M to *ex vivo* skin facilitated by microneedles

Human skin (♀ 62 years of age) was obtained following surgical procedure, transported and processed too form split-thickness skin as described previously (chapter 4). Spilt-thickness skin was pinned over a semi-circular cork support, dried with a paper towel and 20mg of pCMV.M applied to a precise region of the skin. To the same region of skin mounted sharp tipped microneedles, in a 7 X 7 arrangement with heights of 280μm, were applied in a single rolling motion (n = 4). Each treated region was carefully excised and processed for IHC.

6.3.8 Preparation of human skin samples for immuno-histochemistry (IHC)

Skin samples treated with both purified HBsAg/microneedles and pCMV.M/microneedles were rinsed in 2ml PBS for 1 minute. Each skin sample was fixed in 2ml 10% v/v formalin for 20 hours at room temperature. Residual fixative was removed by two sequential rinses in 2ml PBS each for 15 minutes. This was followed by dehydration using an ethanol gradient (30%, 30%, 50%, 50%, 70%, 70%, 90%, 90%, 100%, 100%, and 100%) for 15 minutes in each step. Next, each sample was immersed in 2ml ethanol and chloroform (50:50 v/v) for 30 minutes, followed by 2ml chloroform (100% v/v) for 30 minutes, this step was repeated. Samples were placed into a jar of molten paraffin and placed into an oven at ~60°C for 1 hour. Each sample was then placed into a fresh jar of paraffin and incubated for a further 1 hour. A plastic mould was filled with molten paraffin and the skin samples placed into the paraffin filled mould and left to solidify on a cold plate (~-12°C) for 1 hour. Embedded samples were stored at 4°C.

6.3.9 Generation of human skin sections, and rehydration for IHC

Paraffin block containing skin samples were mounted into a microtome (Leica RM2125, Leica Microsystems (UK) Ltd, Milton Keynes, UK) and 7 μm sections were generated. The resultant sections were first floated in a water bath at room temperature for ~5 minutes. These were subsequently transferred to a water bath at ~35°C for ~10 minutes before being captured on a Super Frost® coated microscope slide and placed on a warmplate, at ~40°C, for ~30 minutes. Slides were transferred to an oven, at 56°C over night.

Removal of paraffin from slides was achieved by two submersions in baths of 100% xylene, each for 2 minutes. Rehydration of each section was achieved by sequential immersion in an ethanol gradient (100%, 100%, 90%, 90%, 70%, 70%, 50%, 50%, 30%, 30%, and water) each for 2 minutes.

6.3.10 Immuno-histochemistry (IHC) in *ex vivo* human skin

All IHC was performed using an EnVision™ + System-HRP (DAB) kit obtained from DakoCytomation, specifically designed to detect mouse monoclonal antibodies, and used according to the manufacturer's protocol. First, each slide containing skin sections was covered in 0.03% hydrogen peroxide containing sodium azide for 5 minutes too quench endogenous peroxidase activity. Next, the sections were rinsed with a wash buffer (0.02 mol/l PBS), with excess fluid carefully tapped off and wicked away with lens tissue. Each slide was incubated with primary antibody (Mouse anti-HBsAg, 3E7) diluted 1:50 in buffer (0.05 mol/L Tris-HCL, pH 7.2, with 1% BSA) for 30 minutes. Each slide was washed with wash buffer (0.02 mol/L PBS) before excess fluid was carefully tapped off and wicked away with lens paper. Sections were incubated with peroxidase labelled polymer for 30 minutes, then rinsed in wash buffer (0.02 mol/L PBS) with excess fluid removed by careful tapping and wicking. The slides were then incubated for 10 minutes with DAB+ substrate chromogen (prepared according to manufacturer's protocol), which provides the visual indication. Slides were counter stained by immersion in haematoxylin for ~1 minute and rinsed under flowing tap water for ~2 minutes. Suitable specimens were permanently mounted by the addition of histamount® mounting media followed by a cover slip, these were then observed by light microscopy (Olympus BX-50, Olympus Optical, London UK).

6.4 Results and Discussion

6.4.1. Recovery, amplification and purification of pCMV.M

Dehydrated pCMV.M was reconstituted, according to the supplier's instructions, and used to transform competent DH5α™ *E.coli* cells, from which stocks were prepared. Following amplification, from the prepared stocks, as described in Chapter 3, pure pCMV.M was obtained though the yield of plasmid obtained was considerably less compared to both reporter plasmids. The quantity of prepared pCMV.M was 1.78 mg/ml in contrast to typical yields of 3.3 mg/ml and 3.6 mg/ml for pCMVβ and pEGFP-N1 respectively. A reason for the discrepancy in plasmid DNA yields has not been elucidated at present. It is possible that pCMV.M is a lower copy number plasmid, if this is the case each bacterial cell will contain less plasmid and therefore there will be less available for purification.

6.4.2 Characterisation and functionality of pCMV.M

6.4.2.1 Enzymatic restriction digest

A restriction digest was performed to confirm that the plasmid obtained was indeed pCMV.M and also confirm that the plasmid was present in a super-coiled form (Figure 6.1). Lanes 1 and 2 are the result of a single digest opening the once covalently closed circular molecule into a linear form. Although the plasmid contained in lanes 1, 2 and 4 are the same size there is a slight discrepancy in the distance they have moved, i.e. the super-coiled pDNA (lane 4) has moved slightly further because of its compact size. The linear molecules movements are restricted more and consequently have not travelled as

far. Lane 3 is the result of a double digest of pCMV.M with both EcoR1 and Hind III. As both these are unique restriction sites on the plasmid the result is the formation of two bands. The EcoR1 enzyme restriction site is at position 908 and Hind III recognises a sequence at position 889. As pCMV.M is a total of 5737 base pairs, restriction with these two enzymes will result in a very small fragment of 19 base pairs (yellow arrow) and a much larger fragment of 5718 (red arrow), clearly indicated in Figure 6.1.

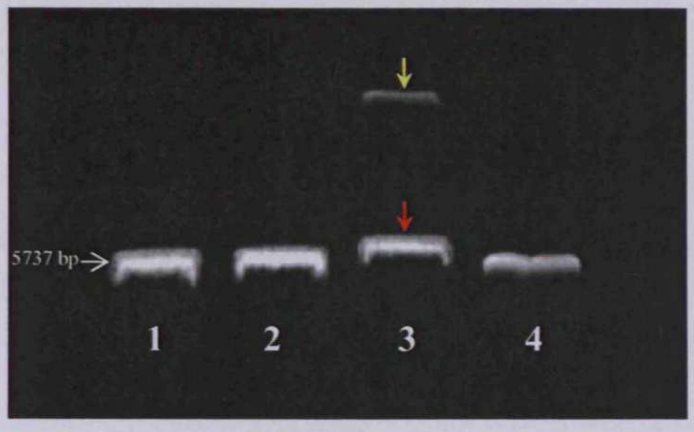

Figure 6.1 Restriction digests of pCMV.M, lanes 1 and 2 single digests with EcoR1 and Hind III respectively. Lane 3 is a double digest of pCMV.M with EcoR1 and Hind III, the yellow arrow indicates a 19 base sequence liberated from the digest. Lane 4 is intact super-coiled pCMV.M

In order to test functionality of pCMV.M and to confirm the specificity of the immuno-detection methods a number of studies were conducted *in vitro*. Naked plasmid is not readily taken up by cultured cells, therefore it is necessary to complex it with a "carrier", a well established method involving the use of a cationic peptide and cationic lipid to form an LPD, i.e. lipid, peptide, DNA, complex. Although cationic liposome complexed to DNA have been demonstrated to successfully transfer DNA to cells *in vitro* the addition of a peptide, e.g. protamine have been shown to further increase transfection

efficiencies (Birchall *et al.* 2000). Characterisation of resultant LPD complexes was made by TEM, PCS and microelctrophoresis (to determine zeta potential).

6.4.3 Physical characterisation of LPD complexes

6.4.3.1 Transmission electron microscopy (TEM)

With TEM electron transparent regions appear as bright regions against a dark background negative stain (New 1990). Plasmid DNA appears as long filamentous threads under TEM (Figure 6.2 A), the diameter of the threads ~5nm. When plasmid DNA is incubated with protamine the respective negative and positive charges causes an attraction, which results in the formation of aggregates (Figure 6.2 B). The unimodal mean diameter of the aggregates was 119.3 nm (± 34.5) but with no regular shape. LPD formation is complete by incubation of DNA and protamine with DOTAP cationic liposomes (6.2 C). The result was a fairly homogenous population of LPD particles, with some random clumping (Figure 6.3 A). Individual LPD particles were spherical structures with a size of ~100nm diameter, at higher magnifications the multilamaer structure of the LPD complexes became apparent (Figure 6.3 B).

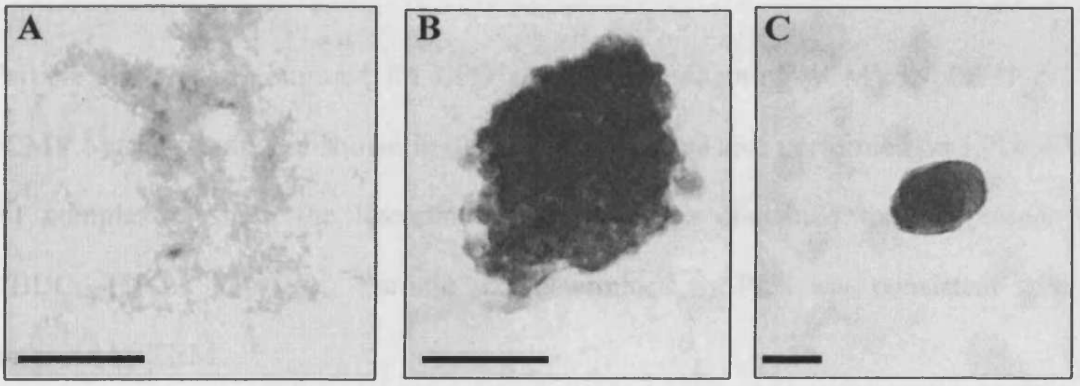

Figure 6.2 Formation of LPD complexes as revealed by TEM. Plasmid DNA (A) appears as long, diffuse filamentous threads. However, when incubated with protamine charge interactions cause the formation of irregular shaped aggregates (B). When the pDNA/protamine aggregates are incubated with the cationic lipid DOTAP, further charge interactions occur resulting in the formation of an LPD particle; bar ~ 50nm.

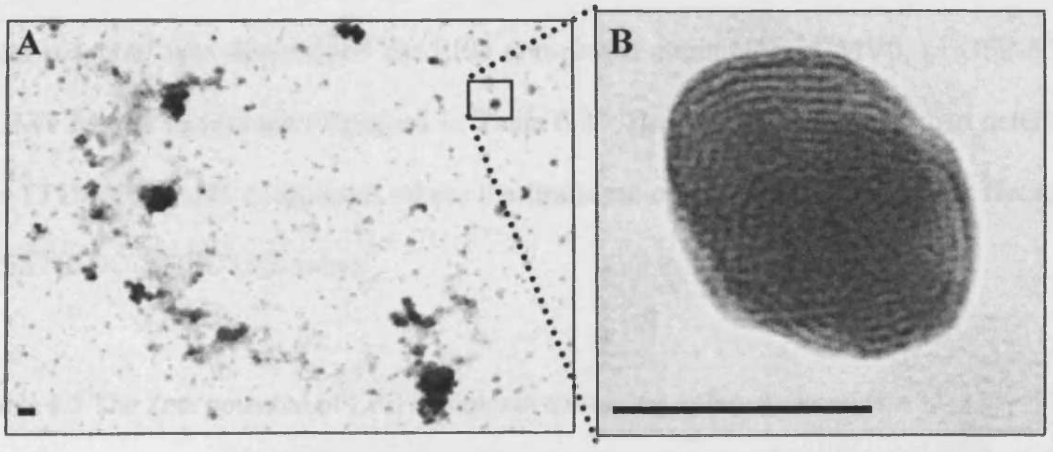

Figure 6.3 Formed LPD complexes consist of a fairly homogenous population of spherical particles but with some random clumping (A). The size of individual LPD particles was determined to be approximately 100 nm; bar ~ 100nm in both cases.

6.4.3.2 Particle size analysis by PCS

Particle size was determined for LPD complexes containing pCMVβ, pEGFP-N1 and pCMV.M, the results are shown in Table 6.2. PSC was also performed on LPD/pEGFP-N1 complexes where the liposome component also contained the fluorescent lipid $NBDC_{12}$-HPC (5% w/w). Particle size determined by PCS was consistent with that observed by TEM.

Table 6.2 The results of size analysis of LPD complexes containing different plasmids

	Mean diameter (nm)	
	Non-fluorescent	**Fluorescent**
pEGFP-N1	121.1 (± 32.2)	112.6
pCMVβ	94.1 (± 26.6)	-
pCMVM	131(± 22.3)	-

6.4.3.3 Zeta potential

Zeta potential was determined for LPD complexes containing pCMVβ, pEGFP-N1 and pCMV.M, the results are displayed in Table 6.3. The zeta potential was also determined for LPD/pEGFP-N1 complexes where the liposome component contained the fluorescent lipid $NBDC_{12}$-HPC (5% w/w).

Table 6.3 The Zeta potential of LPD complexes containing different plasmids

	ξ potential (pH ~7.4)	
	Non-fluorescent	**Fluorescent**
pEGFP-N1	22.9 (± 2.3)	22.4 (± 1.5)
pCMVβ	41.1 (± 3.4)	-
pCMVM	39.3 (± 2.3)	-

6.4.4 *In vitro* delivery of LPD complexes

LPD complexes containing pCMVβ, pEGFP-N1 and pCMV.M were prepared and delivered to A-549 lung epithelial cells *in vitro*. The A-549 cells used in these studies are well characterised mammalian cell type that has biochemical and morphological appearance of pulmonary type II cells.

6.4.4.1. Delivery of pCMV.β to A-549 cells

Positive expression from pCMV.β was observed when individual cells appeared blue once exposed to the X-gal staining solution (Figure 6.4 A). The blue pigmentation results from the action of β-galactosidiase on the X-gal substrate (Chapter 4). Furthermore, expression was only observed in cells that had received the plasmid as part of an LPD complex. When the plasmid was delivered uncomplexed, i.e. naked, no expression was observed (Figure 6.4 B). Transfection efficiency was determined to be ~10% (Figure 6.4 C), with cells expressing the plasmid spread uniformly throughout the cell monolayer (Figure 6.4 A).

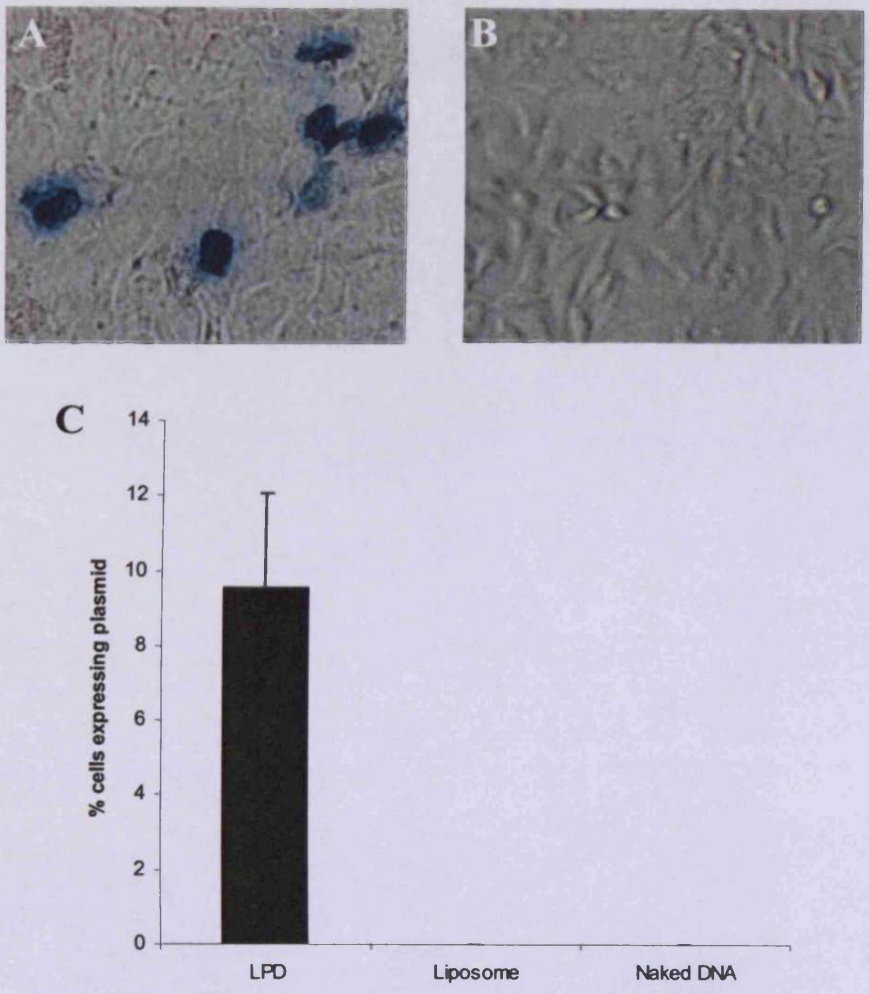

Figure 6.4 The delivery of LPD complexes containing the reporter plasmid pCMV.β to A-549 cells *in vitro*. Cell expressing the plasmid stained blue when exposed to the X-gal solution (A). Cells which received pCMV.β "naked", not in the form of an LPD complex, showed no evidence of expression (B). The transfection efficiency of cell treated with LPD complexes was determined to be approximately 10% (C). Magnifications (A) X 400 and (B) X 200.

6.4.4.2 Delivery of pEGFP-N1 contained in a fluorescent LPD complex to A-549 cells

Studies involving the delivery of pEGFP-N1 were performed using LPD containing a fluorescent component in the liposome, $NBDC_{12}$-HPC (5% w/w), which enabled the fate of the lipid component to be observed. At set points following the delivery of the LPD complex the culture vessel was removed from incubation and observed by fluorescent microscopy (Figure 6.5). The results reveal a proportion of LPD complexes associated with cellular membranes after 1 hour. The intensity of the fluorescent signal increases with time and after 5 hours all the cells of the monolayer are exhibiting fluorescence with much intracellular accumulation. The nuclear regions of the cells are apparent because of the lack of uptake of the LPD lipid component. It has been proposed that LPD complexes can by pass the lysosomal compartment and exist within the cytoplasm intact, however, they are excluded from the nucleus because of there size (Kostarelos and Miller 2005). This scenario could explain what is being observed in Figure 6.5. However, further work would be required to confirm this.

Results of expression from pEGFP-N1, delivered with the fluorescent LPD system are presented in Figure 6.6. Transfection efficiencies were approximately the same as those obtained for pCMVβ (data not shown). However, it was noted that although all the cells contained the signal from the lipid most were not expressing the plasmid. Reasons for this could be the inherent low transfection efficiencies associated with non-viral vectors and also, it is likely that during formation many LPD complexes were formed that contained no DNA.

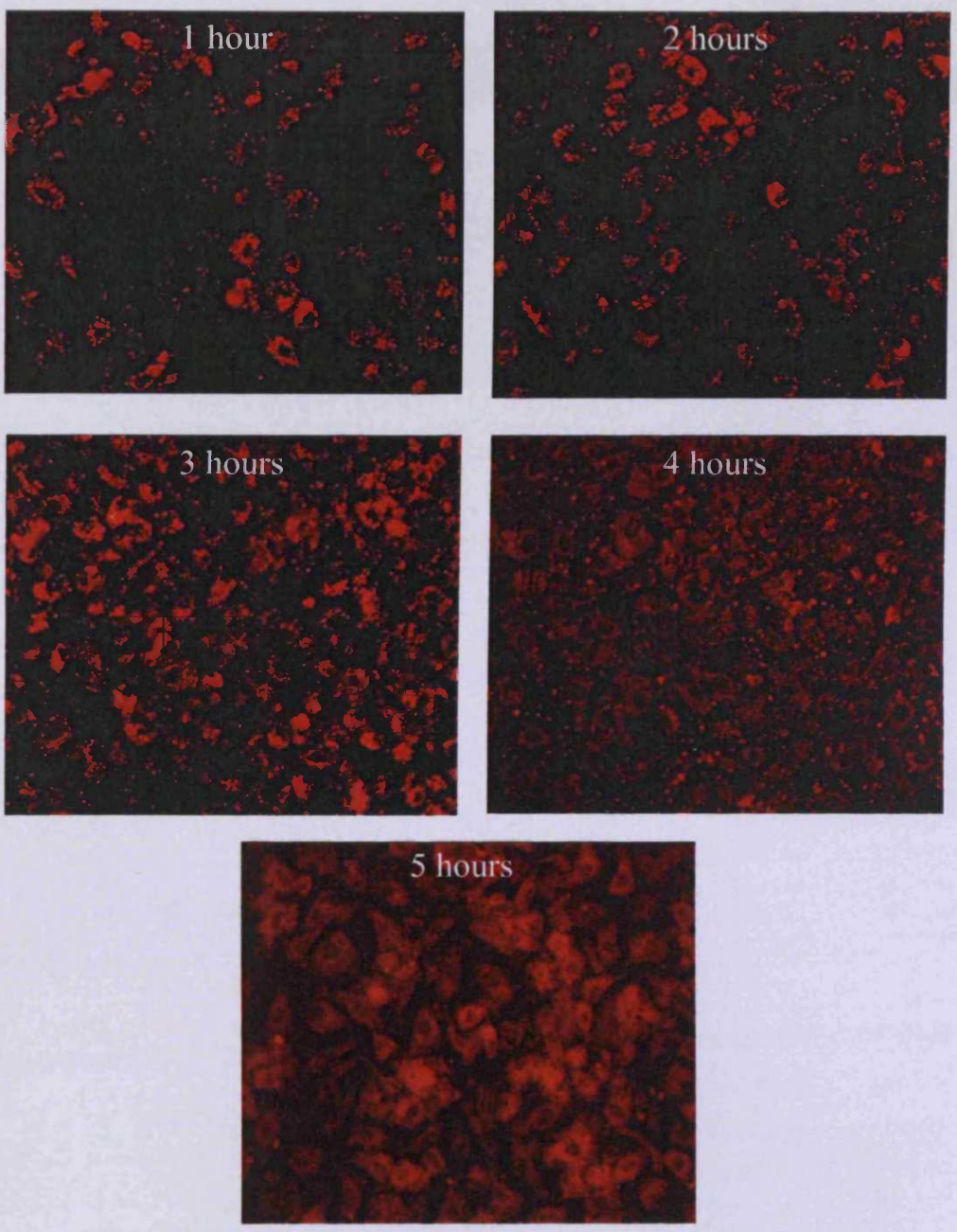

Figure 6.5. The fate of the lipid component of LPDs delivered to A-549 cells as revealed by fluorescent microscopy. DOTAP LPD complexes were made containing the fluorescent lipid $NBDC_{12}$-HPC and following delivery the culture was periodically examined; magnification X 200.

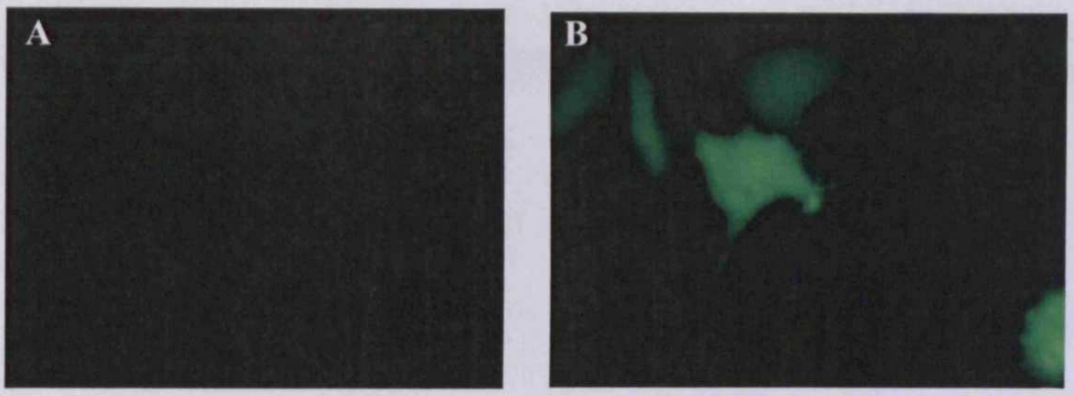

Figure 6.6 Delivery of pEGFP-N1 to A-549 cells. Naked DNA (A) is contrasted with DNA complexed forming LPDs (B), observed at X 400.

6.4.4.3 Delivery of pCMV.M to A-549 cells

Expression from pCMV.M in A-549 cells delivered with LPD vectors are shown in figures 6.7 & 6.8, detection was achieved by immunocytochemistry (ICC). Transfection efficiency was similar to those observed with pCMVβ (Figure 6.4), ~10%.

A-549 cells that expressed the HBsAg fragment were stained brown (Figure 6.7). Expression was typically observed in single isolated cells, occurring uniformly through the monolayer. Control samples, naked DNA (Figure 6.7 B & D) and liposome (Figure 6.8 A), showed no signs of expression. The expressed protein was detected uniformly throughout the cytoplasm of each transfected cells (Figure 6.8 B, C & D). Many of the observed cells appeared to show an increase in staining on the cytoplasmic side and in the immediate vicinity of the nuclear envelope (Figure 6.7 C). Though it is possible that this is an artefact of staining and further work would need to be performed to confirm this as a phenomenon.

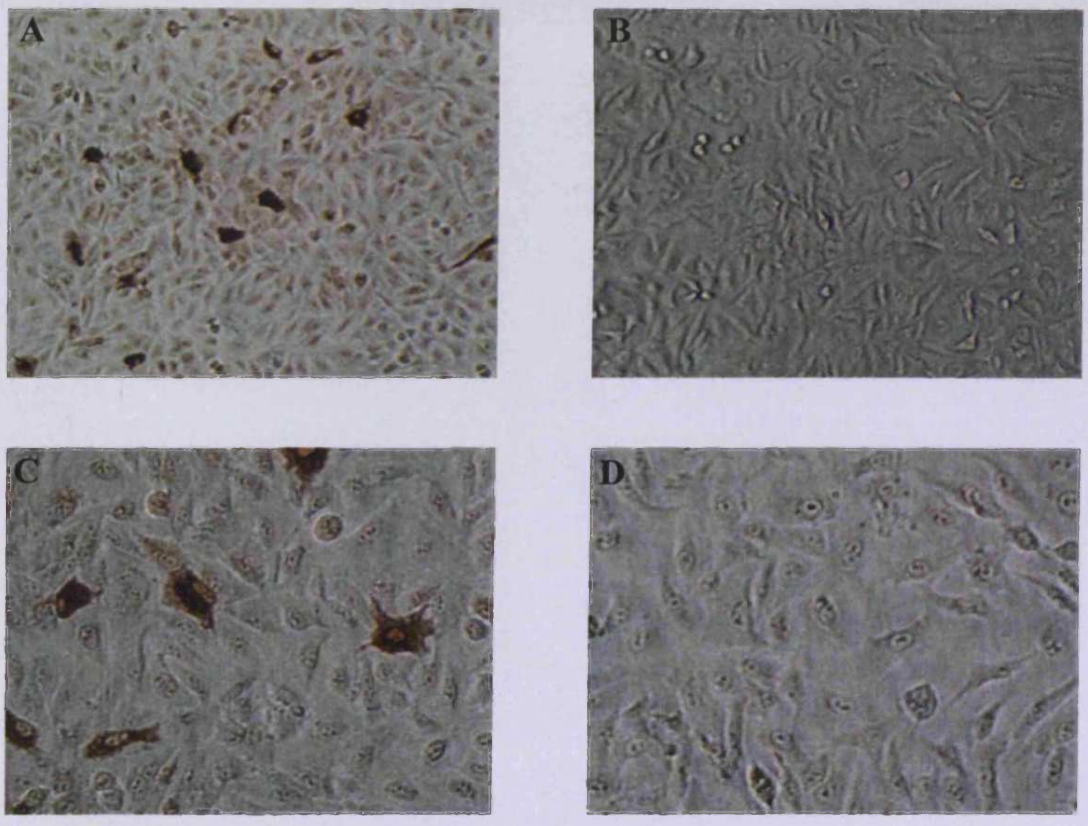

Figure 6.7 The result of A-549 cells treated with pCMV.M as part of an LPD complex (A) and (C) contrasted with uncomplexed, naked pCMV.M (B) and (D). Magnification of (A) and (B) X 200; (C) and (D) X 400.

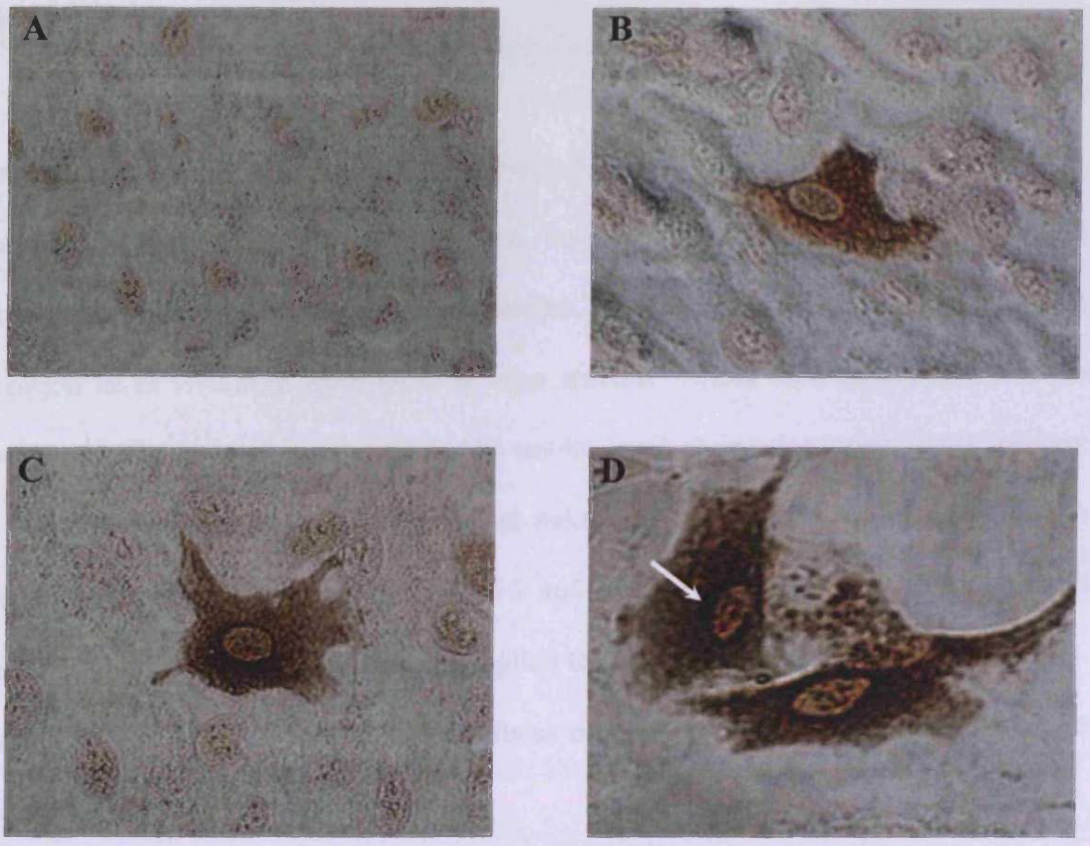

Figure 6.8 Further ICC studies of A-459 cells, (A) received liposome and no pCMV.M and consequently displayed no signs of expression. In contrast cells that have been treated with pCMV.M complexed to form LPD particles do express the antigen (B), (C) & (D). The nuclear region is clearly apparent in these images as less intensely stained compared to the cytoplasm. However, in the immediate vicinity of the cytoplasmic side of the nuclear envelope frequently are regions of intense staining (arrow in D). All images are at X 600

6.4.5 Microneedle facilitated delivery of HBsAg (Ayw) protein to *ex vivo* skin model system and IHC

The ICC results reveal two important facts. Firstly, the HBsAg fragment must have been expressed because it was successfully detected, therefore the plasmid is functional. Secondly, the method of detection employed, including the HBsAg specific monoclonal antibody, was suitable for confirming expression. However, little can be made regarding expression in *ex vivo* skin from these in vitro studies. It has been established that the delivery of LPD complexes to *ex vivo* skin results in no expression, why this is the case still has not been established. In contrast naked DNA is expressed in *ex vivo* skin (Chapter 4 & 5) but not *in vitro* (Figure 6.7 and 6.8). Therefore, conclusions obtained from *in vitro* studies cannot be directly applied to other model system, e.g. *ex vivo* skin. Consequently, it was imperative that the focus of the work was brought back to the *ex vivo* skin model system.

Before experiments were conducted with pCMV.M, purified HBsAg was delivered to *ex vivo* skin facilitated by microneedles. Once the antigen was delivered it was fixed in formalin, dehydrated and embedded in paraffin, this procedure limits the potential for physical relocation of the antigen. Additionally, specimen's prepared this way allow identical serial sections to be made, particularly useful for investigating microneedle created channels. The results of IHC performed on the specimens are presented in figure 6.9. Control samples where PBS was delivered, indicated the formation of a microneedle channel extending through the SC into the epidermis reaching a depth of ~150μm, with no evidence of false positive staining from the detection system (Figure 6.9 A). In

contrast, sample that received purified HBsAg again showed the formation of channels with a depth of ~150μm but with localized brown pigmentation, indicating the presence of the antigen (Figure 6.9 B & C).

These results are significant for two reasons. Firstly, the methods of tissue fixation, embedding, sectioning and IHC allow for the detection of HBsAg in *ex vivo* human skin and that our HBsAg is effective. Therefore, providing confidence that expression from pCMV.M delivered to *ex vivo* skin can successfully be detected. Secondly, the results demonstrate the delivery of a potentially therapeutic peptide (for vaccination) to the epidermis facilitated by microneedles, building directly on work presented in Chapter 3. While no conclusion regarding immunological effect can be made, as with the case of plasmids, it is possible to confirm that the antigen has been delivered to the region of the skin that is the site of powerful initiators of immune responses, the LC

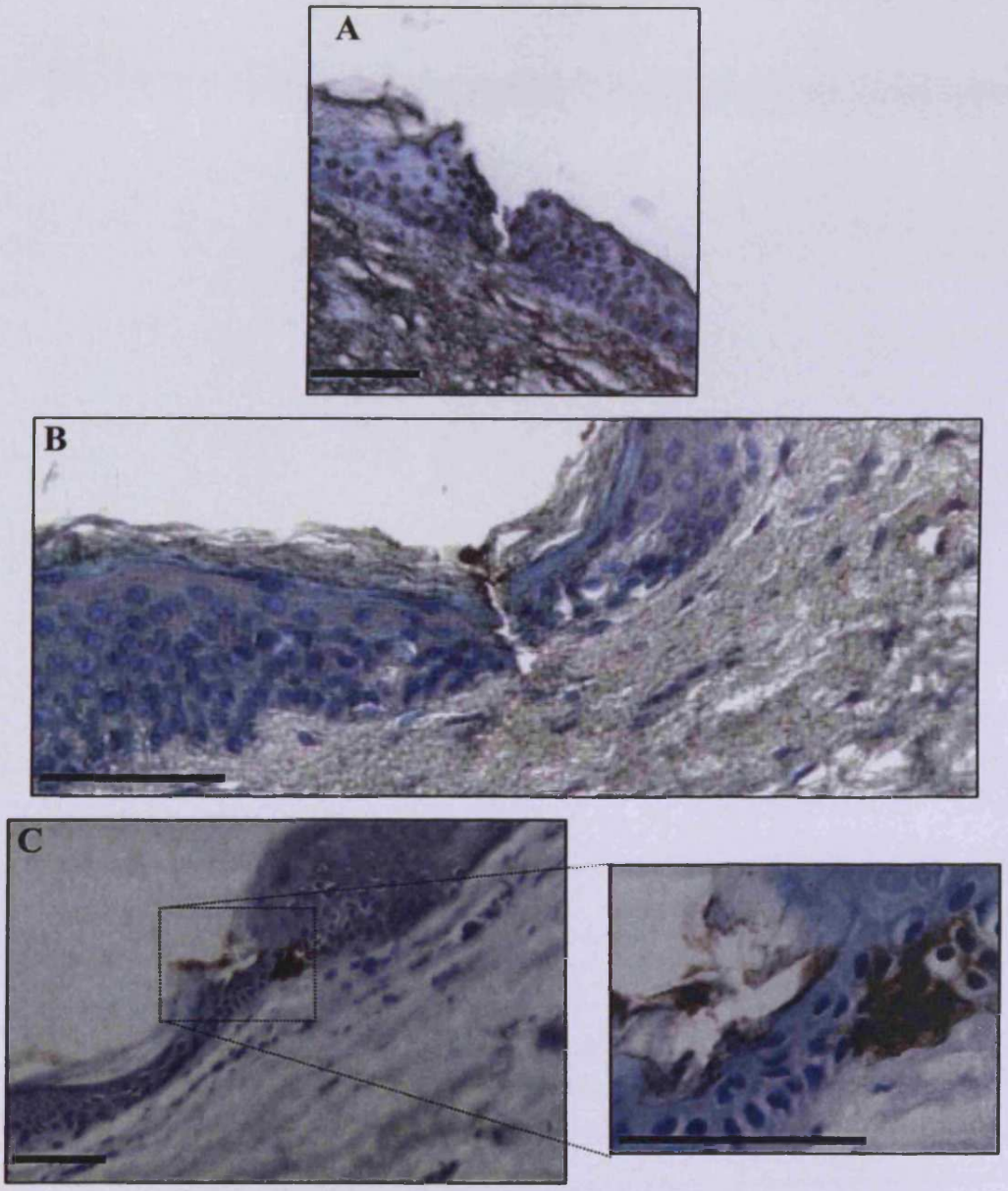

Figure 6.9 The delivery of HBsAg to *ex vivo* human skin by microneedles. Control samples, where the microneedle were applied with no antigen, produced channel extending into the epidermis to a depth of ~150 μm but no antigen was detected (A). In contrast, samples treated with HBsAg and microneedle displayed channels, again extending ~150 μm into the epidermis but this time the channels were displaying the presence of the antigen (B) and (C) as brown pigmentation deposits; bar = 150 μm in all cases.

6.4.6 Delivery of pCMV.M to *ex vivo* skin facilitated by microneedles and IHC

Since purified antigen was delivered and detected it was possible to proceed to the next step in these series of experiments, the delivery of pCMV.M to *ex vivo* skin. Delivery of pCMV.M was performed exactly as described previously for reporter plasmids (chapter 4); however, after culturing it was processed for IHC.

The results obtained from this study are shown in Figure 6.10. Control samples showed no evidence of brown pigmentation and therefore no false positive results caused by microneedle application. Channels created by application of the microneedle array were identified and were shown to extend ~150μm into the epidermis (Figure 6.10 A). Samples that were treated with pCMV.M and microneedles did shown evidence of positive expression (Figure 6.10 B & C). Brown pigmentation corresponding to regions were HBsAg was located were seen in two of the four *ex vivo* skin samples. The results obtained show that one of the samples had a single point of positive expression, while the other had two; these are consistent with levels of expression obtained in earlier experiments involving reporter genes (Chapter 4). Expression was localized to the microneedle disruption and confined to the epidermis and therefore in the vicinity of LCs.

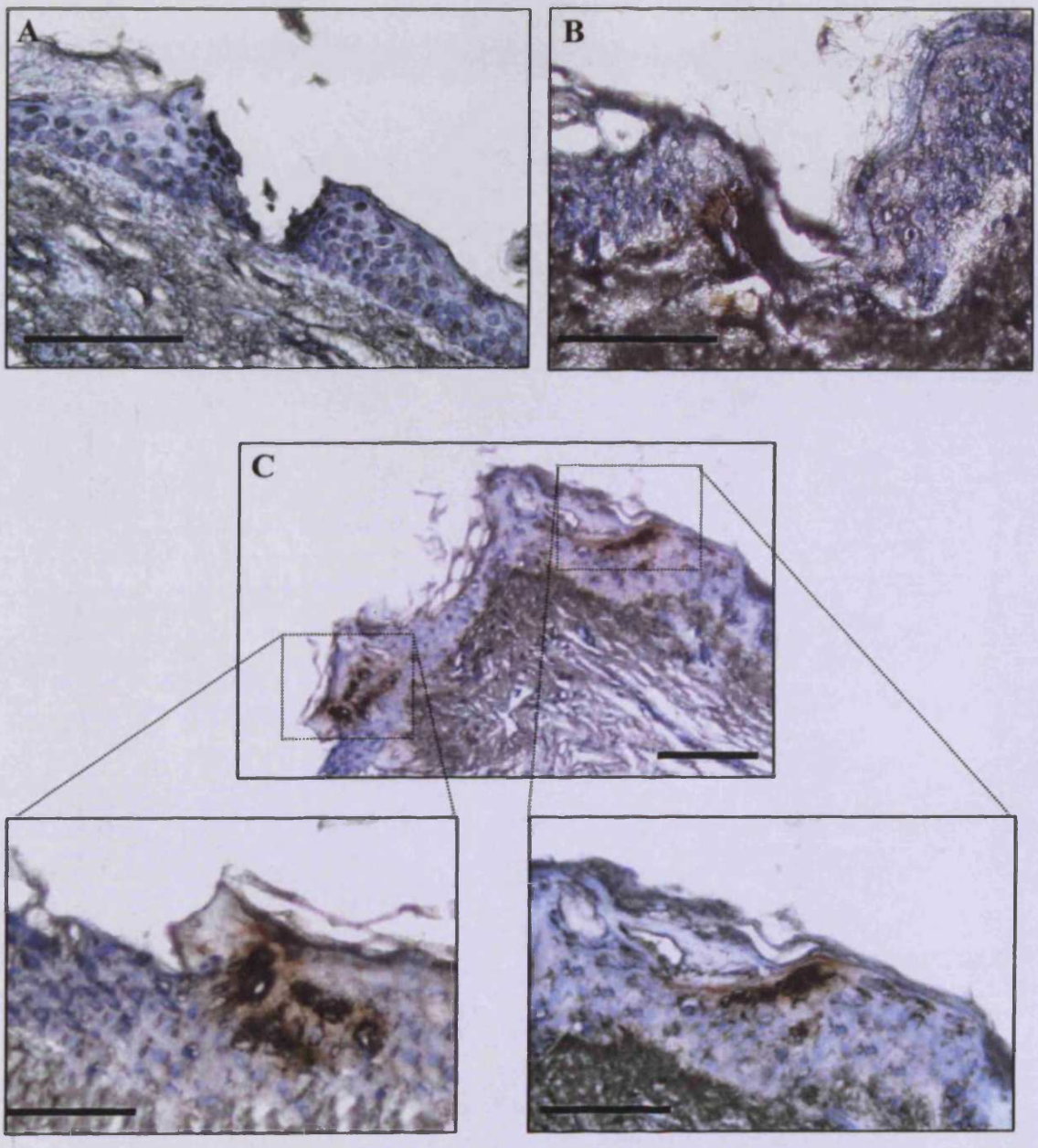

Figure 6.10 Delivery of pCMV.M to *ex vivo* human skin by microneedles, expression detected by IHC. No false positive results were detected in control samples (A). Expression was observed in skin treated with the plasmid in conjunction with microneedles (B) and (C). Expression was confined to the epidermis and in the vicinity of microneedle disruptions; bar = 150 μm in all cases.

6.5 Conclusions

These studies have demonstrated that microneedles are capable of delivering a plasmid to the viable epidermis and therefore into the vicinity of LCs. However, these results do not allow the confirmation of cells type(s) that are expressing the plasmid only that expression is occurring. In order for DNA vaccination to work the expressed antigen must find its way to LCs. There are two ways that this can be achieved firstly, the plasmid can be delivered directly to the LC, where it would be expressed and subsequently processed then presented via the MHC I pathway. Conversely, the plasmid could be expressed by keratinocytes and then somehow escape the cell and then be picked up by LCs, this would ultimately lead to presentation of the antigen by the MHC II pathway (Chapter 6 page 242). Presently it is not possible to indicate which of these processes are occurring in the skin. It is likely that the majority of the cells are expressing the plasmid are keratinocytes, simply because this is the most numerous cell type of the skin. However, LC's do constitute a significant proportion of the internal area of the epidermis because of their many cellular protrusions. Further studies would be required to show weather a bias exists regarding which cell types take up and expresses the plasmid. This is an important factor because if antigen is trapped within a keratinocyte, i.e. is not secreted and released in same way then it cannot come into contact with LCs and no immune response can be generated. This would mean that for this technology to work modifications would have to be made to the plasmid, similar to those described by Hauser *et al*, to ensure that the antigen is released from the keratinocytes and targeted toward the LCs (Hauser *et al* 2004).

CHAPTER 7: General discussion

7.1 Discussion

This thesis was an attempt to build on the work of others in establishing microneedle as a means of delivering therapeutic agents to the skin, in particular pDNA. Because of the proximity of the skin to the environment it has evolved a sophisticated immune surveillance system and it was proposed that this could be harnessed to stimulate immunity by the technique of DNA vaccination. However, because this field of research is still relatively new, considerable work needs to be performed before its realisation in a clinical setting. The results presented in this thesis are a small contribution toward this goal.

Microneedle arrays manufactured out of silicon were shown to be capable of disrupting the SC thereby reducing its barrier function. The two classes of solid microneedle prepared by wet- and dry-etch processes both proved capable of disrupting the SC. Wet-etch microneedles were most effective however, principally because dry-etch microneedle were more fragile and also contain a higher microneedle density consequently creating a "bed of nails effect", therefore not effectively transmitting applied pressure to microneedle tips for penetration. In contrast, wet-etch microneedles were significantly more robust and possessed a much reduced microneedle density. This limited the "bed of nails effect", transmitting pressure to the needle tips more effectively. Because of these favourable characteristics, wet-etch arrays were used in virtually all subsequent experiments. Wet-etch microneedle arrays were made containing as few as 9 microneedles in a 3 X 3 arrangement on a silicon wafer of $0.3mm^2$ or as many as 49 in a 7 X 7 arrangement on a silicon wafer of $0.8mm^2$. Different arrays contained

microneedles of different heights ranging from arrays with 80μm microneedles to 280μm. Interestingly, the tips of wet-etch microneedles could be either sharp of frustum tipped, with other arrays intermediate between the two extremes.

Polymer microneedles utilized were of similar dimensions to the wet-etch silicon arrays because these arrays were used to cast the moulds from which polymer arrays were created. The polymer arrays were comparable in robustness to silicon arrays for application to human skin. It is likely polymer arrays will supersede silicon arrays, particularly for clinical applications, because of the difficulties of working with silicon and because of safety issues associated with silicon already discussed (Chapter 2).

A single prototype hollow microneedle array capable of conducting fluids was also characterised and briefly investigated. The array was formed on a silicon wafer of ~1cm by 0.5cm, individual needle heights were ~200μm and each possessed a channel of 50μm diameter through the entire microneedle core. Due to design constraints of the hollow microneedle array (Chapter 2; Section 2.4.4) and the uniqueness of the array, the effectiveness for gene delivery to human skin could not be fully elucidated. However, it was shown that successful expression occurred with its application, although observed expression was not significantly different to that observed with solid arrays. It is to be expected that the use of hollow arrays will introduce further variables, for example, the use of small capillary tubes to feed the solution into the array will generate great shear forces which could affect the integrity of DNA. Consequently it is likely that many

engineering problems need to be addressed before the true efficiency of hollow microneedle arrays can be determined.

Wet-etch microneedle arrays were proficient at puncturing the SC creating distinct punctures in heat separated epidermal sheets. Additionally, wet-etch microneedles were capable of facilitating the delivery of low molecular weight dyes, macromolecules and nanoparticles to the viable epidermis.

It was found that the method of microneedle application was a fundamental concern. Application of microneedle arrays by single rolling motion facilitated the delivery of functional reporter pDNA to the viable epidermis and was determined to be the most efficient and reproducible method. Nevertheless, application by the single rolling method did result in variable, although frequent gene expression. Expression was primarily observed in cells in the immediate vicinity of the formed microchannel (Chapter 4). However, observations made *en face* of the treated skin showed that expression did not occur at every point where microneedle contacted the skin. This inevitably was due to low expression efficiencies associated with non-viral gene delivery vectors (discussed in Chapter 1) but also because of different penetrative properties that each microneedle has when applied in a rolling motion. In Chapter 2 it was proposed that the row of microneedles that contact the skin first and last have far more penetrative capabilities that the microneedles which contact the skin when the array reaches ~90°. Therefore, it is likely that low gene expression levels are also influenced by reduced intra-array penetrative capabilities; parts of the array do not sufficiently disrupt the SC for gene

delivery to occur. Nevertheless, the rolling application method was still more effective at disrupting the SC than the flat method of application because this method induces a greater "bed of nails" effect. The problem of application is a current limitation of the microneedle technology but one that is finally being addressed (Sivamani *et al.* 2007).

A further limitation of the rolling method was that application onto a pre-applied volume of plasmid solution was extremely wasteful. The act of rolling the array causes the vast majority of the formulation to be physically excluded from the treatment region. Therefore, it is only possible to state the accurately the amount of plasmid applied to the skin surface, while nothing can be said of the actual amount which was delivered to the viable epidermis. Using microneedles that incorporate a fix amount of drug during their formation would be a possibility to address this problem. Such arrays have recently been described, for example Park *et al* (2006).

Although expression occurs primarily in the vicinity of a microchannel there is an exception, when the array was applied in a rocking motion, i.e. increasing the number of rolls (Chapter 4; Section 4.3.6.2). Application with multiple rolls results in expression being observed in regions where microneedle had penetrated the SC but also in regions where the base of the microneedle array and the applicator rod had contacted the skin. It therefore appears that regions of the array and/or applicator that contacted the skin were sufficient to mechanically disrupt the SC and permit plasmid into the viable epidermis, though this was even more variable and unpredictable than observed with microneedles applied without multiple rolls.

Methods to improve the low levels of gene expression were evaluated using microneedle arrays in conjunction with a sustained release hydrogel formulation. It was proposed that the hydrogel provides a reservoir of pDNA, enabling it to migration out of the hydrogel over time, supplying fresh pDNA for cellular transfection. It was anticipated that the micro-channels created by the microneedle device could be loaded with the pDNA hydrogel, which would act as a sustained release depot. Two distinct hydrogels were investigated, Carbopol-940 polymers and triblock copolymer of PLGA-PEG-PLGA. PLGA-PEG-PLGA triblock copolymers can display thermosensitive behavior so that a liquid to gel change in state occurs with increasing temperature. Polymers based on PLGA-PEG-PLGA, which are also biodegradable, have also been shown to house and release pDNA over extended period (Li *et al* 2003). The approach discussed in this thesis was to produce an array of microreservoirs, from either hydrogel, located at an appropriate level in the skin from which pDNA could migrate out and enter keratinocytes in the immediate vicinity where upon it is expressed. The results obtained showed that hydrogel delivery systems were able to harbour pDNA in microchannels and release plasmid in a functional form for gene expression to occur in the viable epidermis. However, points of expression were not significantly different compared to microneedle/pDNA solution delivery. There are a number of reasons that hydrogel delivery may not effective: the pDNA cannot escape the hydrogel matrix in sufficient quantities for expression, the pDNA could be degraded or modified to reduce expression or the 24 hour period over which the experiment was run was to short to allow both plasmid release, from the hydrogel, and subsequent cellular gene expression.

Consequently, it is proposed that an animal model would be a better system in which to study sustained plasmid associated with microneedle/hydrogel delivery systems. However, the experiments presented in this thesis have demonstrated an important concept in that microneedles/hydrogels systems can deliver functional pDNA to human skin.

A plasmid, pCMV.M encoding a therapeutically relevant gene, the small and middle forms of the HBV surface antigen, was also investigated. Prior to microneedle facilitated delivery in *ex vivo* human skin the functionality of the plasmid stocks were confirmed by demonstrating transfection of cells *in vitro*. Additionally, *in vitro* work also permitted the initial development of an immuno-detection system for the expressed gene. The IHC detection system was further developed and optimized by delivering purified HBsAg to human skin facilitated by microneedles. The antigen was successfully located within the viable epidermis, in close proximity to formed microneedle channels. This provided confidence in the sensitivity of the IHC method and it was possible to move onto experiments involving the pCMV.M in viable *ex vivo* human skin. Furthermore, the optimization process was a further demonstration of microneedles ability to effectively deliver macromolecules to the viable epidermis, this time an antigenic protein, which was successfully delivered into the vicinity of the SALT.

Experiments involving the delivery of pCMV.M in conjunction with microneedles to viable *ex vivo* skin, followed by IHC, confirmed positive expression. The numbers of points of expression were consistent with that observed with reporter plasmids.

Expression was observed in the same regions of the skin as seen with reporter plasmids, i.e. at all levels in the viable epidermis, with expression always in close association with a microneedle channel. Expression was localized within the viable epidermis and therefore in the locality of the SALT. This was the first demonstration of the delivery and expression of a therapeutically relevant gene into human skin by using microneedles. Although experiments did not show that an immune response was generated they did show that the fundamental mechanics of pDNA microneedle delivery to the immuno-sensitive regions of the viable epidermis are in place and well characterised.

The various experiments conducted during the course of these studies demonstrate that microneedles should be considered as a means of disrupting the SC for the delivery of pDNA, primarily for DNA vaccination. However, these studies have also highlighted the need for more research in this field in order for this technology to be realized in a clinical setting.

7.2 Future studies

A key factor that was noted early on in these studies was the need for an effective applicator device for the microneedle arrays. While arrays mounted onto metal cylinder exhibited positive gene expression, this was not reproducible. Close handling of these arrays and direct use of them in human skin highlighted that application was fundamental and that arrays mounted onto metal rods probably would not be effective in a clinical setting. Therefore, development of a device that can consistently puncture all human skin types in a reproducible manor is essential for the clinical success of microneedles.

Application of solutions and hydrogels in conjunction with microneedles is extremely wasteful and the actual amount delivered cannot be determined with any degree of confidence. Therefore, it would be impossible to determine the amount of delivered plasmid required to produce a biological response, for example how much pDNA encoding an antigen is required to illicit an immune response in an animal model. Consequently, it is vital that a method is developed which can be utilized to determine the actual amount of pDNA delivered to the viable cells of the epidermis. A less wasteful method of delivery would be to incorporate pDNA into the matrix of a biodegradable polymer microneedle array. Such work is currently being undertaken, for example in the group of Mark Prausnitz (Park *et al.* 2006). However the emphasis of this work is the incorporation of small molecules and not pDNA. Therefore, future studies should investigate the feasibility of incorporating pDNA into such microneedles.

In addition, much has been described in the literature and in this thesis regarding the ability of microneedles to penetrate the SC, creating channels deep into the viable epidermis. However, the damage caused by microneedle application has not been widely investigated, similarly the time it takes for the formed channels to completely close and heal. Whilst it is likely that microneedle application will result in little damage and their size should ensure a rapid healing, these questions have not been addressed in a robust manor and warrant subsequent investigation.

Further investigations regarding the uptake and intracellular transportation of pDNA are required because little information is available at present. This could also help to explain why non-viral gene delivery is generally low. It is proposed that an in depth understanding of uptake and intracellular transportation would provide a means of improving stability and targeting of the vector which would inevitably result in increased expression.

Finally, there is a need to move these studies into animal models. The *ex vivo* human skin organ culture system described in this thesis has provided significant information regarding microneedle application and demonstrated that they are a suitable device for application in human skin. However, as this skin is removed from the body it is impossible to demonstrate certain biological responses, for example the generation of an immune response. Therefore, it is vital that future experiments be preformed in animal models and the results combined with those obtained from *ex vivo* human skin studies.

References

Amass, W., Amass, A., and Tighe, B.: A review of biodegradable polymers: uses, current developments in the synthesis and characterization of biodegradable polyesters, blends of biodegradable polymers and recent advances in biodegradation studies. Polymer International **47:** 89-144, 1998.

Azzoni, A. R., Ribeiro, S. C., Monteiro, G. A., and Prazeres: The impact of polyadenylation signals on plasmid nuclease-resistance and transgene expression. The Journal of Gene Medicine **9:** 392-402, 2007.

Babiuk, S., Baca-Estrada, M., Babiuk, L. A., Ewen, C., and Foldvari, M.: Cutaneous vaccination: the skin as an immunologically active tissue and the challenge of antigen delivery. Journal of Controlled Release **66:** 199-214, 2000.

Backvall, H., Wassberg, C., Berne, B., and Ponten, F.: Similar UV responses are seen in a skin organ culture as in human skin in vivo. Experimental Dermatology **11** (4): 349-56, 2002.

Banks, G. A., Roselli, R. J., Chen, R., and Giorgio, T. D.: A model for the analysis of nonviral gene therapy. Gene Therapy **10:** 1766-1775, 2003.

Barry, B. W.: Breaching the skin's barrier to drugs. Nature Biotechnology **22:** 165-167, 2004.

Basner-Tschakarjan, E., Mirmohammadsadegh, A., Baer, A., and Hengge, U. R.: Uptake and trafficking of DNA in keratinocytes: evidence for DNA-binding proteins. Gene Therapy **11** (9): 765-774, 2004.

Bauer, J., Bahmer, F. A., Wörl, J., Neuhuber, W., Schuler, G., and Fartasch, M.: A strikingly constant ratio exists between Langerhans cells and other epidermal cells in human skin. A stereological study using the optical dissector method and

confocal laser scanning microscope. Journal of investigative dermatology **116:** 313-318, 2001.

Behl, C. R., Flynn, G. L., Kurihara, T., Harper, N., Smith, W., Higuchi, W. I., Ho, N. F., and Pierson, C. L.: Hydration and percutaneous absorption: I. Influence of hydration on alkanol permeation through hairless mouse skin. Journal of Investigative Dermatology **75** (4): 346-352, 1980.

Ben-Bassat, H., Chaouat, M., Segal, N., Zumai, E., Wexler, M. R., and Eldad, A.: How long can cryopreserved skin be stored to maintain adequate graft performance? Burns **27** (5): 425-431, 2001.

Benson, H. A.: Transfersomes for transdermal drug delivery. Expert Opinions on Drug Delivery **3** (6): 727-737, 2006.

Birchall, J., Coulman, S. A., Anstey, A., Gateley, C., Sweetland, H., Gershonowitz, A., Neville, L., and Levin, G.: Cutaneous gene expression of plasmid DNA in excised human skin following delivery via microchannels created by radio frequency abalation. International Journal of Pharmaceutics **312** (1-2): 15-23, 2006.

Birchall, J. C., Coulman, S. A., Pearton, M., Allender, C., Brain, K., Anstey, A., Gateley, C., Wilke, N., and Morrissey, A.: Cutaneous DNA delivery and gene expression in *ex vivo* human skin explants via wet-etch microfabricated microneedles. Journal of Drug Targeting **13** (7): 415-421, 2005.

Birchall, J. C., Marichal, C., Campbell, L., Alwan, A., Hadgraft, J., and Gumbleton, M.: Gene expression in an intact ex-vivo skin tissue model following percutaneous delivery of cationic liposome-plasmid DNA complexes. International Journal of Pharmacy **197** (1-2): 233-238, 2000.

Blaese, R. M., Culver, K. W., Miller, A. D., Carter, C. S., Fleisher, T., Clerici, M., Shearer, G., Chang, L., Chiang, Y., Tolstoshev, P., Greenblatt, J. J., Rosenberg, S. A., Klein, H., Berger, M., Mullen, C. A., Ramsey, W. J., Muul, L., Morgan, R. A., and Anderson, F. A.: T Lymphocyte-directed gene therapy for ADA SCID: initial trail results after 4 years. Science **270** (5235): 475-480, 1995.

Bowen, I. D., and Farhana, A.: Tumour cell death. *In* Programmed cell death in animals and plants, ed. by J. A. Bryant, S. G. Hughes, and J. M. Garland, pp. 253-264, BIOS, Guilford, 2000.

Bravo, D., Rigley, T. H., Gibran, N., Strong, D. M., and Newman-Gage, H.: Effect of storage and preservation methods on viability in transplantable human skin allografts. Burns **26** (4): 367-378, 2000.

Budker, V., Budker, T., Zhang, G., Subbotin, V., Loomis, A., and Wolff, J. A.: Hypothesis: naked plasmid DNA is taken up by cells in vivo by a receptor-mediated process. J Gene Med **2** (2): 76-88, 2000.

Cevc, G.: Lipid vesicles and other colloids as drug carriers on the skin. Advanced Drug Delivery Reviews **56** (5): 675-711, 2004.

Chabri, F., Bouris, K., Jones, T., Barrow, D., Hann, A., Allender, C., Brain, K., and Birchall, J.: Microfabricated silicon microneedles for nonviral cutaneous gene delivery. British Journal of Dermatology **150** (5): 869-877, 2004.

Chargaff, E.: On the dangers of genetic meddling. Science **192** (4243): 938-940, 1976.

Chen, S., Pieper, R., Webster, D. C., and Singh, J.: Triblock copolymers: synthesis, characterization, and delivery of a model protein. International Journal of Pharmaceutics **288** (2): 207-218, 2005.

Clemo: R., Birchall, J.C., and John, D.N. Pilot studies on public perception of microneedle technology. Perspectives in Percutaneous Penetration **10A**: 124, 2006a.

Clemo, R., John, D.N., Anstey, A., and Birchall, J.C. Microfabricated microneedles in clinical practice: Healthcare professional perceptions on microneedle technology. Perspectives in Percutaneous Penetration **10A**: 125, 2006b.

Cormier, M., Johnson, B., Ameri, M., Nyam, K., Libiran, L., Zhang, D. D., and Daddona, P.: Transdermal delivery of desmopressin using a coated microneedle array patch system. Journal of Controlled Release **97** (3): 503-511, 2004.

Couffinhal, T., Kearney, M., Sullivan, A., Silver, M., Tsurumi, Y., and Isner. J.M.: Histochemical staining following *LacZ* gene transfer underestimates transfection efficiency. Human Gene Therapy **8:** 929-934, 1997.

Coulman, S. A., Barrow, D., Anstey, A., Gateley, C., Morrissey, A., Wilke, N., Allender, C., Brain, K., and Birchall, J. C.: Minimally invasive cutaneous delivery of macromolecules and plasmid DNA via microneedles. Current Drug Delivery **3** (1): 65-75, 2006.

Crofts, C., and Krimsky, S.: Emergence of a scientific and commercial research and development infrastructure for human gene therapy. Human Gene Therapy **16:** 169-177, 2005.

Csoka, I., Csanyi, E., Zapantis, G., Nagy, E., Feher-Kiss, A., Horvath, G., Blazso, G., and Eros, I.: *In vitro* and *in vivo* percutaneous absorption of topical dosage forms: case studies. International Journal of Pharmaceutics **291** (1-2): 11-19, 2005.

Cui, F. D., Asada, H., Jin, M. L., Kishida, T., Shin-Ya, M., Nakaya, T., Kita, M., Ishii, M., Iwai, M., Okanoue, T., Imanishi, J., and Mazda, O.: Cytokine genetic adjuvants facilitates prophylactic intravascular DNA vaccination against acute and latent herpes simplex virus infection in mice. Gene Therapy **12:** 160-168, 2005.

Cutroneo, K. R.: Gene therapy for tissue regeneration. Journal of Cellular Biochemistry **88** (2)**:** 418-425, 2002.

Danna, K., and Nathans, D.: Specific cleavage of simian virus 40 DNA by restriction endonuclease of Hemophilus influenzae. Proceeding of the National Academy of Sciences U S A **68:** 2913-2917, 1971.

Davis, S. P., Landis, B. J., Adams, Z. H., Allen, M. G., and Prausnitz, M. R.: Insertion of microneedles into skin: measurement and prediction of insertion force and needle fracture force. Journal of Biomechanics **37** (8)**:** 1155-1163, 2004.

Davis, S. P., Martanto, W., Allen, M. G., and Prausnitz, M. R.: Hollow metal microneedles for insulin delivery to diabetic rats. IEEE Transactions on Biomedical Engineering **52** (5)**:** 909-15, 2005.

Díaz-Flores, L., Madrid, J. F., Gutiérrez, R., Varela, H., Valladares, F., Alvarez-Argüelles, H., and Díaz-Flores, L.: Adult stem and transit-amplifying cell location. Histology and Histopathology **21** (9)**:** 995-1027, 2006.

Dujardin, N., and Preat, V.: Delivery of DNA to skin by electroporation. Methods in Molecular Biology **245:** 215-226, 2004.

Dujardin, N., Van Der Smissen, P., and Preat, V.: Topical gene transfer into rat skin using electroporation. Pharmaceutical Research **18** (1)**:** 61-66, 2001.

Editorial: Gene therapy - a loss of innocence. Nature Medicine **6** (1): 1, 2000.

Elias, P. M.: Epidermal lipids, membranes and keratinization. International Journal of Dermatology **20:** 1-9, 1981.

Fire, A., Xu, S., Montgomery, M. K., Kostas, S. A., and Driver, S. E.: Potent and specific genetic interference by double-stranded RNA in *Caenorhabditis elegans*. Nature **391:** 806-811, 1998.

Fluhr, J. W., Feingold, K. R., and Elias, P. M.: Transepidermal water loss reflects permeability barrier status: validation in human and rodent *in vitro* and *ex vivo* models. Journal of Experimantal Dermatology **15** (7): 483-492, 2006.

Fowers, K. D., Baudys, M., Rathi, R., and Shih, C.: Thermosensitive polymer delivery: http://www.drugdeliverytech.com/cgi-bin/articles.cgi?idArticle=154, accessed on 2/8/2007.

Freeman, S. M., Abboud, C. N., Whartenby, K. A., Packman, C. H., Koeplin, D. S., Moolten, F. L., and Abraham, G. M.: The "bystander effect": tumor regression when a fraction of the tumor mass is genetically modified. Cancer Research **53** (21): 5274-5283, 1993.

Freidmann, T.: Stanfield Rogers: insights into virus vectors and failure of an early gene therapy model. Molecular Therapy **4** (4): 285-258, 2001.

Friedl, K. E.: Analysis: optimizing microneedles for epidermal access. Diabetes Technology and Therapeutics **7** (3): 546-548, 2005.

Fynan, E. F., Webster, R. G., Fuller, D. H., Haynes, J. R., Santoro, J. C., and Robinson, H. L.: DNA vaccines: protective immunizations by parenteral, mucosal

and gene-gun innoculations. Proceedings of the National Academy of Science, USA **90:** 11478-11482, 1993.

Gary, D. J., Puri, N., and Won, Y. Y.: Polymer-based siRNA delivery: Persectives on the fundamental and phenomenological distinctions from polymer-based DNA delivery. Journal of Control Release **121** (1-2): 64-73, 2007.

Gerstel, M. S., and Place, V. A.: Drug Delivery Device, 3,964,482, USA, 1976.

Ghazizadeh, S., and Taichman, L. B.: Multiple classes of stem cells in cutaneous epithelium: A lineage analysis of adult mouse skin. The EMBO Journal **20** (6): 1251-1222, 2001.

Ghazizadeh, S., and Taichman, L. B.: Organization of stem cells and their progeny in human epidermis. Journal of Investigative Dermatology **124** (2): 367-372, 2005.

Greenland, J. R., and Letvin, N. L.: Chemical adjuvant for plasmid DNA vaccines. Vaccine **25** (19): 3731-3741, 2007.

Hamilton, J. G.: Needle phobia: a neglected diagnosis. The Journal of Family Practice **41** (2): 169-175, 1995.

Hammer, R. E., Palmiter, R. D., and Brinster, R. L.: Partial correction of murine hereditary growth disorder by germ-line incorporation of a new gene. Nature **311** (5981): 65-67, 1984.

Hartl, A., Weiss, R., Hochreiter, R., Scheiblhofer, S., and Thalhamer, J.: DNA Vaccines for allergy treatment. Methods **32** (3): 328-339, 2004.

Hauser, H., Shen, L., Gu, Q. L., Krueger, S., and Chen, S. Y.: Secretory heat-shock protein as a dendritic cell-targeting molecule: a new strategy to enhance the potency of genetic vaccines. Gene Therapy **11** (11): 924-932, 2004.

Hengge, U. R., Chan, E.F., Foster, R.A., Walker., P.S., and Vogel, J.C. (1995) Cytokine expression in epidermis with biological effects following injection of naked DNA. Nature Genetics 10, 161-166: Cytokine Expression in Epidermis with Biological Effects Following Injection of Naked DNA. Nature Genetics **10:** 161-166, 1995.

Hengge, U. R., and Mirmohammadsadegh, A.: Adeno-associated virus expresses transgenes in hair follicles and epidermis. Molecular Therapy **2** (3): 188-194, 2000.

Hengge, U. R., Pfutzner, W., Williams, M., Goos, M., and Vogel, J. C.: Efficient expression of naked plasmid DNA in mucosal epithelium: prospective for the treatment of skin lesions. Journal of Investigative Dermatology **111** (4): 605-608, 1998.

Hengge, U. R., Walker, P. S., and J.C., V.: Expression of naked DNA in Human Pig and Mouse Skin. The Journal of Clinical Investigation **97** (12): 2911-2916, 1996.

Henry, S., McAllister, D. V., Allen, M., and Prausnitz, M. R.: Microfabricated Microneedles: A Novel Approach to Transdermal Drug Delivery. Journal of Pharmaceutical Sciences **87** (8): 922-925, 1998.

Hohlfeld, R., and Engel, A. G.: The immunobiology of muscle. Immunology Today **15:** 269-274, 1994.

Hosmani, A. H.: Carbopol and its pharmaceutical significance: a review: http://pharmainfo.net/exclusive/reviews/carbopol_and_its_pharmaceutical_signifi cance:_a_review/, accessed 2/8/2007.

Hybbinette, S., Boström, K., and Lindberg, K.: Enzymatic dissociation of keratinocytes from human skin biopsies for *in vitro* cell propagation. Experimental Dermatology **8** (1): 30-38, 1999.

Ismail, F. A., Napaporn, J., Hughes, J. A., and Brazeau, G. A.: *In situ* gel formulations for gene delivery: release and myotoxicity studies. Pharaceutical Development and Technology **5** (3): 391-7, 2000.

Jackson, D. A., Symons, R. H., and Berg, P.: Biochemical method for inserting new genetic information into DNA of Simian virus 40: circular SV40 DNA molecules containing Lambda phage genes and galactose operon of *Escherichia coli*. Proceeding of the National Academy of Sciences, U.S.A **69** (10): 2904-2909, 1972.

Jacobi, U., Weigmann, H.-J., Ulrich, J., Sterry, W., and Lademann, J.: Estimation of the relative stratum corneum amount removed by tape stripping. Skin Research and Technology **11** (2): 91, 2005.

Jacques, S. L., McAuliffe, D. J., Blank, I. H., and Parrish, J. A.: Controlled removal of human stratum corneum by pulsed laser. Journal of Investigative Dermatology **88** (1): 88-93, 1987.

Jeong, B., Bae, Y. H., Lee, D. S., and Kim, S. W.: Biodegradable block copolymers as injectable drug-delivery systems. Nature **388** (6645): 860-862, 1997.

Jeong, B., Bae, Y.H., and Kim, S.W.: Biodegradable Thermosensitive Micelles of PEG-PLGA-PEG Triblock Copolymers. Colloids and Surfaces B: Biointerfaces **16:** 185-193, 1999.

Jeong, B., Bae, Y.H., and Kim, S.W.: *In situ* gelation of PEG-PLGA-PLG triblock copolymer aqueous solutions and degradation thereof. Journal of Biomedical Material Research **50:** 171-177, 2000.

Kaiser, J.: Gene therapy. Seeking the cause of induced leukemias in X-SCID trail. Science **299:** 495, 2003.

Kasid, A., Morecki, S., Aebersold, P., Cornetta, K., Culver, K., Freeman, S., Director, E., Lotze, M. T., Blaese, R. M., Anderson, W. F., and Rosenberg, S. A.: Human gene transfer: Characterization of human tumor-infiltrating lymphocytes as vehicles for retroviral-mediated gene transfer in man. Proceeding of the National Academy of Sciences USA **87:** 463-477, 1990.

Kendall, M.: Engineering of needle-free physical methods to target epidermal cells for DNA vaccination. Vaccine **24** (21): 4651-4556, 2006.

Kendall, M., Mitchell, T., and Wrighton-Smith, P.: Intradermal ballistic delivery of micro-particles into excised human skin for pharmaceutical applications. Journal of Biomechanics **37** (11): 1733-1741, 2004a.

Kendall, M., Rishworth, S., Carter, F., and Mitchal, T.: Effects of relative humidity and ambient temperature on the ballistic delivery of micro-particles to excised porcine skin. Journal of Investigative Dermatology **122** (3): 739-746, 2004b.

Kent, S., De Rose, R., and Rollman, E.: Drug evaluation: DNA/MVA prime-boost HIV vaccine. Current opinions in Investigational Drugs **8** (2): 159-167, 2007.

Kent, S. J., Cameron, P. U., Reece, J. C., Thompson, P. R., and Purcell, D. F.: Attenuated and wild-type HIV-1 infections and long terminal repeat-mediated gene expression from plasmids delivered by gene gun to human skin ex vivo and macaques in vivo. Virology **287** (1): 71-78, 2001.

Klinman, D. M.: Use of CpG oligodeoxynucleotides as immunoprotective agents. Expert Opinions in Biological Therapy **4** (6): 937-946, 2004.

Kostarelos, K., and Miller, A. D.: Synthetic, self-assembly ABCD nanoparticles; a structural paradigm for viable synthetic non-viral vectors. Chemical Society Reviews **34:** 970-994, 2005.

Kumar, V., and Sercarz, E.: Genetic vaccination: the advantages of going naked. Nature Medicine **2** (8): 857-859, 1996.

Lasch, J., Weissig, V., and Brandi, M. (2003) Preparation of Liopsomes. Liposomes: Preparation of Liopsomes. Liposomes, Oxford University Press, Oxford, 2003.

Lechardeur, D., Sohn, K. J., Haardt, M., Joshi, P. B., Monck, M., Graham, R. W., Beatty, B., Squire, J., O'Brodovich, H., and Lukacs, G. L.: Metabolic instability of plasmid DNA in the cytosol: a potential barrier to gene transfer. Gene Therapy **6** (4): 482-497, 1999.

Lederberg, J.: Experimental genetics and Human evolution. The American Naturalist **100** (915): 519-531, 1966.

Lee, P., Li, Z., and Huang, L.: Thermosensitive hydrogel as a Tgf-ß1 gene delivery vehicle enhances diabetic wound healing. Pharaceutical Research **20** (12): 1995-2000, 2003.

Lee, S., McAuliffe, D. J., Flotte, T. J., Kollias, N., and Doukas, A. G.: Photomechanical transcutaneous delivery of macromolecules. Journal of Investigative Dermatology **111** (6): 925-929, 1998.

Lei, H., Ju, D. W., Yu, Y., Tao, Q., Chen, G., Gu, S., Hamada, H., and Cao, X.: Induction of potent antitumor response by vaccination with tumor lysate-pulsed macrophage engineered to secrete macrophage colony-stimulating factor and interferon-gamma. Gene therapy **7** (8): 707-713, 2000.

Lin, W., Cormier, M., Samiee, A., Griffin, A., Johnson, B., Teng, C. L., Hardee, G. E., and Daddona, P. E.: Transdermal delivery of antisense oligonucleotides with microprojection patch (Macroflux) technology. Pharmaceutical Research **18** (12): 1789-1793, 2001.

Liu, Y., Truong, N. K., Kendall, M., and Bellhouse, B. J.: Characteristics of a micro-biolistic system for murine immunological studies. Biomedical Microdevices **9** (4): 465-474, 2007.

Lowe, D. B., Shearer, M. H., Jumper, C. A., and Kennedy, R. C.: Towards progress on DNA vaccines fro cancer. Cellular and Molecular Life Sciences **Epub ahead of print** (Accessed on 9/9/07): 1-13, 2007.

Ma, D. R., Yang, E. N., and Lee, S. T.: A review: The location, molecular characterisation and multipotency of hair follicle epidermal stem cells. Annals of the Academy of Medicine, Singapore **33**: 784-788, 2004.

Marechal, V., Naffakh, N., Danos, O., and Heard, J. M.: Disapperance of lysosomal storage in spleen and liver of mucopolsaccharidosis VII mice after transplantation of genetically modified bone marrow cells. Blood **82** (4): 1358-1365, 1993.

Martanto, W., Davis, S. P., Holiday, N. R., Wang, J., Gill, H. S., and Prausnitz, M. R.: Transdermal delivery of insulin using microneedles in vivo. Pharmaceutical Research **21** (6): 947-952, 2004.

Maruyama, K., Iwasaki, F., Takizawa, T., Yanagie, H., Niidome, T., Yamada, E., Ito, T., and Koyamma, Y.: Novel Receptor-Mediated Gene Delivery System Comprising Plasmid/Protamine/Sugar-Cotaining Polyanion Ternary Complex. Biomaterials **25:** 3267-3273, 2004.

Matriano, J. A., Cormier, M., Johnson, J., Young, W. A., Buttery, M., Nyam, K., and Daddona, P. E.: Macroflux® microprojection array patch technology: a new and efficient approach for intracutaneous immunization. Pharmaceutical Research **19** (1): 63-70, 2002.

McAllister, D. V., Allen, M. G., and Prausnitz, M. R.: Microfabricated microneedles for gene and drug delivery. Annual Review of Biomedical Engineering **2:** 289-313, 2000.

McAllister, D. V., Wang, P. M., Davis, S. P., Park, J. H., Canatella, P. J., Allen, M. G., and Prausnitz, M. R.: Microfabricated needles for transdermal delivery of macromolecules and nanoparticles: fabrication methods and transport studies. Proceeding of the National Academy of Sciences, USA **100** (24): 13755-13760, 2003.

McKeever, D. J., Awino, E., and Morrision, W. I.: Afferent lymph veiled cells prime $CD4^+$ T cell responses *in vivo*. European Journal of Immunology **22** (1): 3057-3061, 1992.

McKenzie, A. W., and Stoughton, R. B.: Methods for comparing percutaneous absorption of steroids. Archives of Dermatology **86:** 608-610, 1962.

Merino, G., Kalia, Y. N., and Guy, R. H.: Ultrasound-enhanced transdermal transport. Journal of Pharmaceutical Science **92** (6): 1125-1137, 2003.

Meykadeh, N., Mirmohammadsadegh, A., Wang, Z., Basner-Tschakarjan, E., and Hengge, U. R.: Topical application of plasmid DNA to mouse and human skin. Journal of Molecular Medicine **83** (11): 897-903, 2005.

Mezei, M., and Gulasekharam, V.: Liposomes - a selective drug delivery system for the topical route of administration. Life Sciences **26:** 1473-1477, 1980.

Middleton, J. C., and Tipton, A. J.: Synthetic biodegradable polymers as orthopedic devices. Biomaterials 21: 2335-2346, 2000.

Mikszta, J. A., Alarcon, J. B., Brittingham, J. M., Sutter, D. E., Pettis, R. J., and Harvey, N. G.: Improved genetic immunization via micromechanical disruption of skin-barrier function and targetted epidermal delivery. Nature Medicine **8** (4): 415-419, 2002.

Moll, I.: Human skin organ culture. Methods in Molecular Medicine **78:** 305-310, 2003.

Moolten, F. L.: Tumor chemosensitivity conferred by inseted herpes thymidine kinase gene: paradigm for a prospective cancer control strategy. Cancer Research **46:** 5276-5281, 1986.

Mukerjee, E. V., Collins, S. D., Isseroff, R. R., and Smith, R. L.: Microneedle array for transdermal biological fluid extraction and in situ analysis. Sensors and Actuators **114:** 267-275, 2004.

Mulholland, W. J., Arbuthnott, E. A. H., Bellhouse, B. J., Cornhill, J. F., Austyn, J. M., Kendall, M. A. F., Cui, Z., and Tirlapur, U. K.: Multiphoton high-resolution 3D imaging of Langerhans cells and keratinocytes in the mouse skin model adopted for epidermal powdered imminization. Journal of Investigative Dermatology **126** (7): 1541-1548, 2006.

Mullis, K. B., and Faloora, F.: Specific synthesis of DNA in vitro via a polymerase catalysed chain reaction. Methods in Enzymology **155:** 335-350, 1987.

Mura, P., Bettinetti, G. P., Liguori, A., and Bramanti, G.: Improvement of clonazepam release from a Carbopol hydrogel. Pharmaceutica Acta Helvetiae **67** (9-10): 282-288, 1992.

Murthy, S. N.: Magnetophoresis: an approch to enhance transdermal drug diffusion. Pharmazie **54** (5): 377-379, 1999.

Nabel, G. J., Chang, A. E., Nabel, E. G., Plautz, G. E., Fox, B. A., Huang, L., and Shu, S.: Immunotherapy of malignancy by *in vivo* gene transfer into tumors. Human Gene Therapy **3:** 399-410, 1992.

Nathans, D., and Smith, H. O.: Restriction endonucleases in the analysis and restructuring of DNA molecules. Annual Review of Biochemistry **44:** 273-293, 1975.

Nathwani, A. C., Benjamin, R., Nienhuis, A. W., and Davidoff, A. M.: Current status and prospects for gene therapy. *Vox Sanguinis* **87:** 73-81, 2004.

New, R. R. C.: Liposomes: A practical approach, Oxford University press, USA, Boston, 1990.

Nirenberg, M. W.: Will society be prepared. Science **157** (3789): 633, 1967.

Norbury, C. C., and Sigal, L. J.: Cross priming or direct priming is that really the question? Current Opinions in Immunology **15** (1): 82-88, 2003.

O'Hagan, D. T., and Rappuoli, R.: Novel approaches to vaccine delivery. Pharmaceceutical Research **21** (9): 1519-1530, 2004.

Pardoll, D. M., and Beckerleg, A. M.: Exposing the immunology of naked DNA vaccines. Immunity **3:** 165-169, 1995.

Park, J. H., Allen, M. G., and Prausnitz, M. R.: Biodegradable polymer microneedles: fabrication, mechanics and transdermal drug delivery. Journal of Control Release **104** (1): 51-66, 2005.

Park, J. H., Allen, M. G., and Prausnitz, M. R.: Polymer microneedles for controlled-release drug delivery. Pharaceutical Research **23** (5): 1008-1019, 2006.

Parker, S. E., Borellini, F., Wenk, M. L., Hobart, P., Hoffman, S. L., Hedstrom, R., Le, T., and Norman, J. A.: Plasmid DNA malaria vaccine: Tissue distribution and safety studies in mice and rabbits. Human Gene Therapy **10:** 741-758, 1999.

Parker, S. E., Monteith, D., Horton, H., Hof, R., Hernandez, P., Vilalta, A., Hartikka, J., Hobart, P., Bentley, C. E., Chang, A., Hedstrom, R., Rogers, W. O., Kumar, S., Hoffman, S. L., and Norman, J. A.: Safety of a GM-CSF adjuvant-plasmid DNA malaria vaccine. Gene Therapy **8** (13): 1011-1023, 2001.

Pasquini, S., Xiang, Z., Wang, Y., He, Z., Deng, H., Blaszczyk-Thurin, M., and Ertl, H. C. J.: Cytokines and costimulatory molecules as genetic adjuvenets. Immunology & Cell Biology **75** (4): 397-401, 1997.

Pinnagoda, J., Tupker, R. A., Agner, T., and Serup, J.: Guidelines for transepidermal water loss (TEWL) measurements. A report from the Standardization Group of the European Society of Contact Dermatitis. Contact Dermatitis **22** (3): 164-178, 1990.

Pope, I. M., Poston, G. J., and Kinsella, A. R.: The role of the bystander effect in suicide gene therapy. European Journal of Cancer **33** (7): 1005-1016, 1997.

Prausnitz, M. R.: Microneedles for transdermal drug delivery. Advanced Drug Delivery Reviews **56** (5): 581-587, 2004.

Prausnitz, M. R., Bose, V. G., Langer, R., and Weaver, J. C.: Electroporation of mammalian skin: a mechanism to enhance transdermal drug delivery. Proceedings of the National Academy of Sciences USA **90** (22): 10504-1058, 1993.

Prausnitz, M. R., Mitragotri, S., and Langer, R.: Current status and future potential of transdermal drug delivery. Nature Reviews: Drug Discovery **3** (2): 115-124, 2004.

Puissant, C., and Houdebine, L. M.: An improvement of the single-step method of RNA isolation by acid guanidinium thiocyanate-phenol-cholorform extraction. Biotechniques **8** (2): 148-149, 1990.

Qiao, M., Chen, D., Xichen, M. A., and Liu, Y.: Injectable biodegradable temperature-responsive PLGA-PEG-PLGA copolymers: Synthesis and effect of copolymer composition on the drug release from the copolymer-based hydrogels. International Journal of Pharmaceutics **294:** 103-112, 2005.

Raghavachari, N., and Fahl, W. E.: Targeted gene delivery to skin cells in vivo: a comparative study of liposomes and polymers as delivery vehicles. Journal of Pharmaceutical Science **91** (3): 615-22, 2002.

Rainov, N. G.: A phase III clinical trail evaluation of Herpes simplex virus type I thymidine kinase and ganciclovir gene therapy as an adjuvant to surgical and radiation in adults with previousley untreated glioblastoma mulitforms. Human Gene Therapy **11:** 2389-2401, 2000.

Raju, P. A., McSloy, N., Troung, N. K., and Kendall, M. A.: Assessment of epidermal cell viability by near infrared multi-photon microscopy following ballistic delivery of gold micro-particles. Vaccine **24** (21): 4644-4647, 2006.

Raz, E., Carson, D. A., Parker, S. E., Parr, T. B., Abai, A. M., Aichinger, G., Gromkowski, S. H., Singh, M., Lew, D., Yankauckas, M. A., and et al.: Intradermal gene immunization: the possible role of DNA uptake in the induction of cellular immunity to viruses. Proceeding of the National Academy of Sciences USA **91** (20): 9519-23, 1994.

Rengarajan, K., Cristol, S. M., Mehta, M., and Nickerson, J. M.: Quantifying DNA concentrations using fluorometry: A comparision of fluorophores. Molecular Vision **8:** 416-421, 2002.

Rogers, S.: Shope papilloma virus: A passenger in man and its significance to the poential control of the host genome. Nature **212:** 1220-1222, 1966.

Ruponen, M., Honkakoski, P., Ronkko, S., Pelkonen, J., Tammi, M., and Urtti, A.: Extracellular and intracellular barriers in non-viral gene delivery. Journal of Controlled Release **93** (2): 213-217, 2003.

Ruponen, M., Ronkko, S., Honkakoski, P., Pelkonen, J. Tammi, M., and Urtti, A.: Extracellular Glycosaminoglycans Modify Cellular Trafficking of Lipoplexes. Journal of Biological Chemistry **276:** 33875-33880, 2001.

Sawamura, D., Akiyama, M., and Shimizu, H.: Direct injection of naked DNA and cytokine transgene expression: implications for keratinocyte gene therapy. Clinical Experimental Dermatology **27** (6): 480-484, 2002.

Selkirk, S. M.: Gene therapy in clinical medicine. Postgraduate Medical Journal **80:** 560-570, 2004.

Shaefer, S.: Hepatitis B virus: significance of genotypes. Journal of Viral Hepatitis **12:** 111-124, 2005.

Shapiro, J., MacHattie, L., Eron, L., Ihler, G., Ippen, K., Beckwith, J. R., Reznikoff, W., and MacGillivray, R.: Isolation of pure *lac* operon DNA. Nature **244:** 768-774, 1969.

Shim, M. S., Lee, H. T., Shim, W. S., Park, I., Lee, H., Chang, T., Kim, S. W., and Lee, D. S.: Poly(D,L-lactic acid-co-glycolic acid)-b-poly(ethylene glycol)-b-poly (D,L-lactic acid-co-glycolic acid) triblock copolymer and thermoreversible phase transition in water. Journal of Biomedical Materials Research **61** (2): 188-196, 2002.

Shimohira-Yamasaki, M., Toda, S., Narisawa, Y., and Sugihara, H.: Merkel cell-nerve cell interaction undergoes formation of a synapse-like structure in a primary culture. Cell Structure and Functions **31** (1): 39-45, 2006.

Sikes, M. L., O'Malley, B. W., Finegold, M. J., and Ledley, F. D.: In vivo gene transfer into rabbit thyroid follicular cells by direct DNA injection. Human Gene Therapy **5** (7): 837-844, 1994.

Sivamani, R. K., Liepmann, D., and Maibach, H. I.: Microneedles and transdermal applications. Expert Opinions in Drug Delivery **4** (1): 19-25, 2007.

Sivamani, R. K., Stoeber, B., Wu, G. C., Zhai, H., Liepmann, D., and Maibach, H.: Clinical microneedle injection of methyl nicotinate: stratum corneum penetration. Skin Research and Technology **11** (2): 152-156, 2005.

Soumelis, V., Reche, P. A., Kanzler, H., Yuan, W., Edward, G., Homey, B., Gilliet, M., Ho, S., Antonenko, S., Lauerma, A., Smith, K., Gorman, D., Zurawski, S., Abrams, J., Menon, S., McClanahan, T., de Waal-Malefyt, R. D. R., Bazan, F., Kastelein, R. A., and Liu, Y. J.: Human epithelial cells trigger dendritic cell mediated allergic inflammation by producing TSLP. Nature Immunology **3** (7): 673-680, 2002.

Spradling, A. C., and Rubin, G. M.: Transposition of cloned P elements into Drosophila germ line chromosomes. Science **218** (4570): 341-347, 1982.

Spruit, D., and Malten, K. E.: The regeneration rate of the water vapor loss of heavily damaged skin. Dermatologica **132:** 115-123, 1966.

Steinert, P. M., and Marekov, L. N.: The protein elafin, filaggrin, keratin intermediate filiments, loricrin, and small proline-rich proteins 1 and 2 are isodipeptide cross-linked components of the human epidermal cornified cell envelope. Journal of Biological Chemistry **270** (30): 17702-17711, 1995.

Sterne, G. D., Titley, O. G., and Christie, J. L.: A qualitative histological assessment of various storage conditions on short term preservation of human split skin grafts. British Journal of Plastic Surgery **53** (4): 331-336, 2000.

Teichmann, A., Jacobi, U., Ossadnik, M., Richter, H., Koch, S., Wolfram, S., and Lademann, J.: Differential Stripping: Determination of the Amount of Topically Applied Substances Penetrated into the Hair Follicles. Journal of Investigative Dermatology **125:** 264-269, 2005.

Terheggen, H. G., Lowenthal, A., Lavinha, F., Colombo, J. P., and Rogers, S.: Unseccessful trail of gene replacement in arginase deficiency. Zeitschrift für Kinderheilkunde **119:** 1-3, 1975.

Tomita, Y., Nihira, M., Ohno, Y., and Sato, S.: Ultrastructural changes during in situ early postmortem autolysis in kidney, pancreas, liver, heart and skeletal muscle of rats. Legal Medicine (Tokyo) **6** (1): 25-31, 2004.

Tranchant, I., Thompson, B., Nicolazzi, C., Mignet, N., and Scherman, D.: Physicochemical optimisation of plasmid delivery by cationic lipids. Journal of Gene Medicine **6 Supplement 1:** S24-35, 2004.

Trommer, H., and Neubert, R. H.: Overcoming the stratum corneum: the modulation of skin penetration. A review. Skin Pharmacology and Physiology **19** (2): 106-121, 2006.

Trowell, O. A.: A modified technique for organ culture *in vitro*. Experimental Cell Research **6:** 118-147, 1954.

Uwiera, R. R. E.: Plasmid DNA induces increased lymphocyte trafficking: A specific role for CpG motifs. Cellular Immunology **214** (2): 155-164, 2001.

Varani, J.: Preservation of human skin structure and function in organ culture. Histology and Histopathology **13:** 775-783, 1998.

Verdier-Sévrain, S., and Bonté, F.: Skin hydration: a reveiw on its molecular mechanisms. Journal of Cosmetic Dermatology **6** (2): 75-82, 2007.

Wang, P. M., Cornwell, M., and Prausnitz, M. R.: Minimally invasive extraction of dermal interstitial fluid for glucose monitoring using microneedles. Diabetes Technology and Therapeutics **7** (1): 131-41, 2005.

Watson, J. D., and Crick, F. H. C.: A structure for deoxyribonucleic acid. Nature **171** (4356): 737-738, 1953.

Webb, A., Li, A., and Kaur, P.: Location and phenotype of human adult keratinocyte stem cells of the skin. Differentiation **72** (8): 387-395, 2004.

Wen, W. H., Liu, J. Y., Qin, W. J., Zhao, J., Wang, T., Jia, L. T., Meng, Y. L., Gao, H., Xue, C. F., Jin, B. Q., Yao, L. B., Chen, S. Y., and Yang, A. G.: Targeted inhibition of HBV gene expression by single-chain antibody mediated small interfering RNA delivery. Hepatology **46** (1): 84-94, 2007.

Wilke, N., Mulcahy, A., Ye, S.-R., and Morrissey, A.: Process optimisation and characterisation of silicon microneedles fabricated by wet etch technology. Microelectronics Journal 36: 650-656, 2005.

Wilkinson, E.: Evaluating the risk of gene therapy. The Lancet oncology **4:** 196, 2003.

Williams, A. C.: Transdermal and Topical Drug Delivery, Pharmaceutical Press, Padstow, 2003.

Williams, A. C., and Barry, B. W.: Penetration enhancers. Advanced Drug Delivery Reviews **56** (5): 603-618, 2004.

Wilson, J. M., Grossman, M. A., and Raper, S. E.: *Ex vivo* gene therapy of familial hypercholesterolemia. Human Gene Therapy **3:** 179-222, 1992.

Wolff, J. A., Malone, R. W., Williams, P., Chong, W., Acsadi, G., Jani, A., and Felgner, P. L.: Direct gene transfer into mouse muscle in vivo. Science **247:** 1465-1468, 1990.

Wu, J., Chappelow, J., Yang, J., and Weimann, L.: Defects generated in human stratum corneum specimens by ultrasound. Ultrasound in Medicine and Biology **24** (5): 705-710, 1998.

Yovandich, J., O'Malley, B., Sikes, M., and Ledley, F. D.: Gene transfer to synovial cells by intra-articular administration of plasmid DNA. Human Gene Therapy **6** (5): 603-610, 1995.

Zentner, G. M., Rathi, R., Shih, J., McRea, J. C., Seo, M., Oh, H., Rhee, B. G., Mestecky, J., Moldoveanu, Z., Morgan, M., and Weitman, S.: Biodegradable block copolymers for delivery of proteins and water-insoluble drugs. Journal of Controlled Release **72:** 203-215, 2001.

Zhang, X., Divangahi, M., Nqai, P., Santosuosso, M., Millar, J., Zqaniacz, A., Wang, J., Bramson, J., and Xiang, Z.: Intramuscular immunization with a mongenic plasmid DNA tubeculosis vaccine: Enhanced immunogenicity by electroporation and co-expression of GM-CSF transgene. Vaccine **25** (7): 1342-1352, 2007.

Zuckerman, J. N., and Zuckerman, A. J.: Journal of Infection **41** (2): 130-136, 2000.

Zweers, M. L. T., Engbers, G. H. M., Grijpma, D. W., and Feijen, J.: In vitro degradation of nanoparticles prepared from polymers based on DL-lactide, glycolide and poly (ethylene oxide). Jjournal of Controlled Release **100** (3): 347-356, 2004.

Appendix I

(Conferences and meetings)

Appendix

My postgraduate studies provided me with the opportunities to present my work at the following conferences:-

Perspectives in Percutaneous Penetration 10th International Conference, La Grande Motte, France 2006
Poster presentation

British Pharmaceutical Conference (BPC), Manchester 2006
Oral and poster presentation

A Biochemical Society Focused Meeting: Cellular delivery of therapeutic macromolecules. In association with the Royal Society of Chemistry, the Royal Pharmaceutical Society of Great Britain and the Academy of Pharmaceutical Sciences, Cardiff, 2006
Poster presentation

British Pharmaceutical Conference (BPC), Manchester 2005
Oral and poster presentation (**prize winner for oral presentation**)

British Society of Investigative Dermatologists, Cambridge 2005
Oral presentation

Ultra sound and standing wave (USW) network meeting, Wales College of Medicine, Cardiff, 2005
Oral presentation

United Kingdom and Ireland controlled release society (UKICRS), Birmingham 2005
Poster presentation

Postgraduate research day, Welsh School of Pharmacy, Cardiff University 2005
Poster presentation (**prize winner for poster presentation**)

Academy of Pharmaceutical Scientists Genes as Medicines Conference, London, 2004
Poster presentation

Appendix

Perspectives in Percutaneous Penetration 9th International Conference, La Grande Motte, France 2004
Poster presentation

Appendix II

(Publications)

Appendix

Journal Publications

Pearton, M., Allender, C., Brain, K., Anstey, A., Gately, C., Wilke, N., Morrissey, A., and Birchall, J. (2007) Gene delivery to the epidermal cells of human skin explants using microfabricated microneedles and hydrogel formulations. *Submitted to Pharmaceutical Research*

Birchall, J., Coulman, S., Pearton, M., Allender, C., Brain, K., Anstay, A., Gateley, C., Wilke, N., and Morrissey, A. (2005) Cutaneous DNA delivery and gene expression in ex vivo human skin explants via wet-etch microfabricated microneedles. *Journal of Drug Targeting* 13(7):415-21

Conference Publications

Pearton, M., Allender, C., Brain, K., Anstey, A., Gately, C., Wilke, N., Morrissey, A., and Birchall, J.C. (2006) Microneedle facilitated delivery of pDNA encoding HBsAg to human skin: potential for genetic vaccination. *British Pharmaceutical Conference 2006*, Manchester, UK

Pearton, M., Allender, C., Brain, K., Anstey, A., Gately, C., Wilke, N., Morrissey, A., and Birchall, J.C. (2006) Microneedle facilitated delivery of pDNA loaded hydrogels to the epidermis. *10th International Conference on Perspectives in Percutaneous Penetration, PPP2004*, La Grande Motte, France.

Wilke, N., Pearton, M., Coulman, S.A., Allender, C., Brian, K., Birchall, J. and Morrissey, A. (2006) Assesment of penetration efficiency of microneedle arrays applied to human skin. *10th International Conference on Perspectives in Percutaneous Penetration, PPP2004*, La Grande Motte, France.

Morrissey, A., Wilke, N., Coulman, S.A., Pearton, M., Anstey, A., Gately, C., Allender, C., Brain, K., Birchall, J.C. (2005) Determination of mechanical properties of silicon and polymer microneedles. *3rd European Medical & Biological Engineering Conference, EBEC'05*, Prague, Czech Republic

Pearton, M., Barrow, D., Anstey, A., Gately, C., Morrissey, A., Wilke, N., Allender, C., Brain, K., and Birchall, J.C. (2005) Hydrogels based on PLGA-PEG-PLGA triblock co-polymers as sustained release reservoirs for the delivery of pDNA to microneedle treated human skin. *British Pharmaceutical Conference 2005*, Manchester, UK

Birchall, J.C., Coulman, S.A., Pearton, M., Allender, C., Brain, K., barrow, D., Gately, C., Anstey, A., Sweetland, H., Wilke, N., and Morrissey, A. (2005) Cutaneous gene delivery and localised expression using microfabricated microneedle arrays. *2nd Annual Meeting, British Society for gene therapy*, Manchester, UK

Pearton, M., Barrow, D., Anstey, A., Gately, C., Morrissey, A., Wilke, N., Allender, C., Brain, K., and Birchall, J.C. (2005) Disruption of stratum corneum by microfabricated

microneedles for gene delivery from hydrogels. *British Society for Investigative Dermatology BSID Annual Meeting*, University of Cambridge, Cambridge, UK

Coulman, S.A., Allender, C., Pearton, M., Barrow, D., Wilke, N., Morressey, A., Gately, C., Anstey, A., Sweetland, H., Birchall, J.C. (2004) Minimally invasive gene delivery to viable human skin. *12th Annual Conference of European Society for Gene Therapy ESGT04*, Tampere, Finland.

Pearton, M., Gately, C., Anstay, A., Allender, C., Brain, K., and Birchall, J. (2004) Microfabricated microneedle channels provide "pathways" for the sustained release of plasmid DNA from Carbopol-940 hydrogels. *9th International Conference on Perspectives in Percutaneous Penetration, PPP2004*, La Grande Motte, France.

Pharmaceutical Research (© 2007)
DOI: 10.1007/s11095-007-9360-y

Research Paper

Gene Delivery to the Epidermal Cells of Human Skin Explants Using Microfabricated Microneedles and Hydrogel Formulations

Marc Pearton,[1] Chris Allender,[1] Keith Brain,[1] Alexander Anstey,[2] Chris Gateley,[2] Nicolle Wilke,[3] Anthony Morrissey,[3] and James Birchall[1,4]

Received February 23, 2007; accepted May 25, 2007

Purpose. Microneedles disrupt the stratum corneum barrier layer of skin creating transient pathways for the enhanced permeation of therapeutics into viable skin regions without stimulating pain receptors or causing vascular damage. The cutaneous delivery of nucleic acids has a number of therapeutic applications; most notably genetic vaccination. Unfortunately non-viral gene expression in skin is generally inefficient and transient. This study investigated the potential for improved delivery of plasmid DNA (pDNA) in skin by combining the microneedle delivery system with sustained release pDNA hydrogel formulations.
Materials and Methods. Microneedles were fabricated by wet etching silicon in potassium hydroxide. Hydrogels based on Carbopol polymers and thermosensitive PLGA-PEG-PLGA triblock copolymers were prepared. Freshly excised human skin was used to characterise microneedle penetration (microscopy and skin water loss), gel residence in microchannels, pDNA diffusion and reporter gene (β-galactosidase) expression.
Results. Following microneedle treatment, channels of approximately 150–200 μm depth increased trans-epidermal water loss in skin. pDNA hydrogels were shown to harbour and gradually release pDNA. Following microneedle-assisted delivery of pDNA hydrogels to human skin expression of the pCMVβ reporter gene was demonstrated in the viable epidermis proximal to microchannels.
Conclusions. pDNA hydrogels can be successfully targeted to the viable epidermis to potentially provide sustained gene expression therein.

KEY WORDS: DNA; human skin; hydrogel; microneedles; thermosensitive.

INTRODUCTION

A rapidly increasing body of evidence has shown that microfabricated microneedles are effective in disrupting the primary physical barrier of the skin, the stratum corneum (SC), to affect the intra- and trans-cutaneous delivery of both low molecular weight drugs and macromolecules (1–7). As a consequence, microneedles are also being investigated as a method for delivering plasmid DNA (pDNA) to the viable epidermis of the skin with potential applications in the gene based treatment of cancers or genetic diseases, and for DNA vaccination (8,9). Cutaneous DNA vaccination is a particularly attractive proposition since immune surveillance is a primary function of the skin (10). Epidermal dendritic cells (DCs) called Langerhans cells (LCs) are primarily responsible for antigen presentation and the consequential T-cell mediated immune responses and therefore this cell population represents an attractive target for antigenic stimulation following the cellular expression of a genetic vaccine (11). Microneedles transiently create microscopic channels that penetrate through the SC and extend into the epidermis (2) but do not stimulate pain receptors that are located within the underlying dermis. Therefore microneedle delivery of medicaments and vaccines to the epidermal strata is potentially pain free (12). In addition to the clinical benefit of minimally invasive strategies for vaccination, the manufacturing and stability advantages of genetic constructs potentially offers a more efficient, lower cost and mass-distributable means of vaccination compared to conventional approaches (13). This is of particular relevance for third world countries requiring mass vaccination programs, western countries recently immersed in a climate of threats from bioterrorism and globally, with the recent concern of a new influenza pandemic.

Previously, devices consisting of an array of microprojections have been shown to be capable of facilitating the delivery of pDNA based vaccines to animal models (14). In addition, in our laboratories, we have recently demonstrated that microneedles can facilitate the delivery of pDNA to the epidermis of human skin where it is taken up by viable epidermal cells and subsequently expressed (8,9). In this study we aimed to investigate whether microneedles could be used

[1] Gene Delivery Research Group, Welsh School of Pharmacy, Cardiff University, Cardiff, CF10 3XF, UK.
[2] Gwent Healthcare NHS Trust, Royal Gwent Hospital, Cardiff Road, Newport, South Wales, NP20 2UB, UK.
[3] Biomedical Microsystems Team, Tyndall National Institute, Prospect Row, Cork, Ireland.
[4] To whom correspondence should be addressed. (e-mail: birchalljc@cardiff.ac.uk)

the microneedles were surface coated with titanium, as an adhesive layer, and then platinum by evaporation.

Microneedle Characterisation

Individual microneedle arrays were mounted onto metal stubs with double-sided carbon tape and visualised using a Philips XL-200 scanning electron microscope (SEM) (FEI Company, Eindhoven, The Netherlands).

Microneedle Treatment of Heat Separated Epidermal Membrane

A sample of human breast tissue (female donor aged 63) was obtained following surgery with full ethical committee approval and informed patient consent. The subcutaneous fat was removed and the excised skin dissected into areas of approximately 2 cm^2. The skin samples were then placed into a 60°C water bath for 55 s and the epidermal sheet (SC and viable epidermis) carefully removed using blunt forceps. The heat separated epidermal sheets were placed back onto the dermis and the microneedle array applied using a single rolling motion. Subsequently, the heat separated epidermal sheets were fixed in 2% glutaraldehyde and dehydrated in an alcohol gradient (70, 80, 90 and 100% each for 30 min). The sheets were then mounted onto a metal stub with double-sided carbon tape and sputter coated with gold prior to SEM.

Determination of Trans-epidermal Water Loss (TEWL)

A frozen (−20°C) human breast skin sample (female donor aged 56) was allowed to defrost for 2 h, blotted dry and equilibrated for a further 30 min. Trans-epidermal water loss (TEWL) measurements were performed on untreated skin, skin treated with a single application of a 26 G hypodermic needle and skin treated with a frustum tipped microneedle array using an opened chamber TEWL probe connected to a DERMA-LAB meter (Cortex Technology, Hadsund, Denmark).

Preparation of Loaded and Control Carbopol-940 Hydrogel

Stock solutions of pDNA were diluted to an appropriate concentration in a specified volume, typically 0.5 ml. This solution was added to a pre-weighed quantity of Carbopol-940 polymer, mixed with a glass rod for 2 min, and allowed to fully swell for approximately 1 h to yield a hydrogel. Typically a 1% w/v polymer solution was prepared. Fluorescent nanoparticle (100 nm) loaded Carbopol-940 hydrogels were also prepared in the absence of pDNA using the same procedure. All Carbopol-940 hydrogels were neutralised (pH 6.5–7) with triethylamine (TEA).

Synthesis of PLGA-PEG-PLGA Tri-block Co-polymers and Preparation of Hydrogels

Synthesis of the PLGA-PEG-PLGA tri-block co-polymer was performed by ring opening polymerisation of lactide and glycolide using a stannous 2-ethylhexanoate catalyst (30). Briefly, Polyethylene glycol 1000 (7.5 g) was dried in a three-neck flask under vacuum at 150°C for 3 h. DL-lactide (14.1 g) and glycolide (3.8 g) were added (3:1 molar ratio), and the flask heated at 150°C for a further 30 min. To the reaction 50 μg of stannous 2-ethylhexanoate was then added and the temperature increased to 155°C where it was maintained for 5 h. The resulting crude polymer mix was dissolved in 500 ml of ice cold water and precipitated by heating at 80°C (this step was repeated a total of three times). Subsequently, the polymer was dehydrated by freeze drying and stored in a dried state at 4°C.

Stock solutions of pDNA were diluted to an appropriate concentration in a specified volume, typically 1 ml. This solution was added to a pre-weighed quantity of PLGA-PEG-PLGA polymer and mixed. The polymer was then incubated at 4°C overnight to yield a polymer solution. Typically a 23% w/w polymer solution was used during this study. The sol-gel transition temperature of the polymer solution was determined by a tube inversion test based on a method described by Jeong *et al.* (31).

^1H Nuclear Magnetic Resonance (NMR) Analysis

Approximately 10 mg of PLGA-PEG-PLGA tri-block co-polymer was dissolved in $CDCl_3$. NMR spectra were obtained using a Bruker 300 MHz NMR spectrometer (Bruker, Coventry, UK).

Gel Permeation Chromatography (GPC) Analysis

Approximately 10 mg of PLGA-PEG-PLGA tri-block co-polymer was dissolved in 1 ml of tetrahydrofuran (THF) containing 20 μl of toluene by stirring at room temperature for approximately 30 min. Samples were analyzed at ambient temperature using an integrated PL-GPC 20 GPC system (Polymer Laboratories Ltd, Shropshire, UK) with two ResiPore columns (particle size 3 μm, both 7.5 mm×300 mm) in series (Polymer Laboratories Ltd, Shropshire, UK) with detection via a deflection refractive index detector. THF was employed as a mobile phase with a flow rate of 1 ml/min and molecular weight of the polymer was determined relative to polystyrene standards.

Microneedle Facilitated Delivery of Fluorescent Nanoparticle Loaded Hydrogels to Skin

A human breast skin sample (female donor aged 62) was removed from −20°C storage and allowed to defrost and equilibrate to room temperature for ~2 h. Approximately 20 μl of nanoparticle loaded hydrogel (Carbopol 1% w/v and PLGA-PEG-PLGA 23% w/w in 1 ml of 0.5% aqueous nanoparticle stock solution) was applied to the surface of the excised human skin. A frustum-tipped microneedle device was applied to the hydrogel treated area using a single rolling motion whereby the needles were positioned at an angle of approximately 45° to the skin surface and rotated forward through an angle of approximately 90°, finishing at a 45° angle to the skin surface in the opposing direction. Consistent downward pressure was maintained throughout the application. Following treatment, the skin samples were incubated at 37°C for 15 min before the surface was washed in PBS, for 30 min, and then fixed in 2% glutaraldehyde for 2 h at 4°C. Residual fixative was removed by washing with PBS. Samples were subsequently embedded in OCT medium and stored at −80°C.

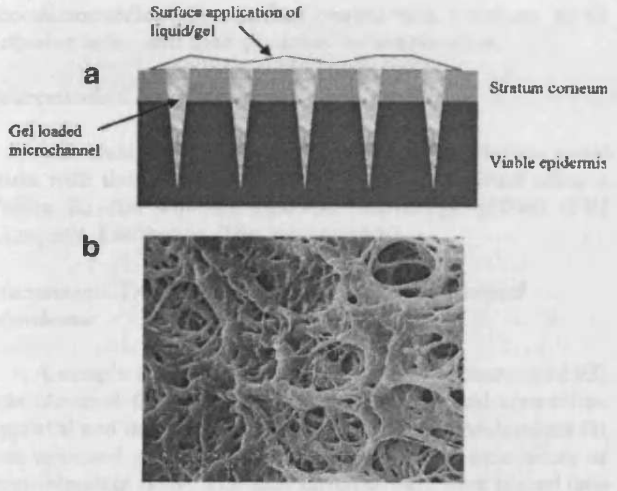

Fig. 1. **a** A schematic illustrating microneedle delivery of a pDNA loaded hydrogel to the epidermis. In the case of Carbopol the skin will be surface treated with gel, whereas for the thermosensitive gel the skin will be surface treated with a liquid which will form a gel in individual microchannels at increased temperature. **b** A dehydrated Carbopol-940 hydrogel observed by SEM.

in conjunction with a sustained release hydrogel formulation of pDNA to address the low gene expression efficiency often associated with non-viral gene delivery. In principle, the hydrogel provides a reservoir of pDNA, enabling migration and release over time, supplying fresh pDNA for cellular transfection. It was proposed that the micro-channels created by the microneedle device could be loaded with the pDNA hydrogel, which would act as a sustained release depot (Fig. 1a) (15,16). In this study, two distinct hydrogels were investigated, the first based on polyacrylic Carbopol-940 polymers and the second on a triblock copolymer of poly (lactide-co-glycolide) (PLGA) and poly (ethylene glycol) (PEG), i.e. poly (ethylene glycol-b-[DL-lactic acid-co-glycolic acid]-b-ethylene glycol) (PLGA-PEG-PLGA).

Carbopol is available commercially as a dehydrated powder. In this form the polymer consist of tightly coiled acrylic acid homopolymeric chains. Upon hydration, the polyacrylic acid polymers begin to uncoil and, once neutralized, form extended structures with a mesh-like appearance (Fig. 1b). Carbopol hydrogels have been shown to harbour and release low molecular weight drugs (17,18) as well as macromolecules including DNA (19). PLGA-PEG-PLGA triblock copolymers are particular useful materials since they can demonstrate thermosensitive behaviour. Specifically, they can be designed to undergo a liquid to gel change in physical state with increasing temperature (20,21). Thus polymer solutions that are low viscosity liquids at room temperature (~25°C) rapidly form a gel when the temperature is elevated to physiological temperatures (22). As an example, liquid formulations have been prepared that can be delivered hypodermically (20), but form a semi-solid gel reservoir following injection. A further benefit of these materials is that they are biodegradable, or bioeliminable, so that release of a therapeutic agent and subsequent elimination of the polymer can be controlled (23–25). Such polymer based hydrogels have previously been shown to be able to house and release pDNA over an extended period. Our novel approach was to produce an array of polymeric micro-reservoirs located at an appropriate level in the skin.

Microfabricated needles can be manufactured from a range of materials, including silicon (1,2), glass (26), metal (26) and polymers (27). The microneedles used in this study were manufactured from silicon wafers using the relatively simple and cost-effective method of wet-etching with potassium hydroxide. This reproducible process results in the formation of extremely uniform and robust arrays of microneedles that are ideally suited for application to human skin. Additionally, the process can be manipulated so that needles can be prepared with variant tip morphologies. Needle-tips were manufactured with different degrees of sharpness, from extremely sharp to a flat tipped "frustum" design. Previous studies showed that the frustum type needles create more discernable microchannels through the SC than sharp tipped needles (8) and therefore frustum tipped microneedles were used throughout this study.

MATERIALS AND METHODS

Materials

Amplification and purification of the pCMVβ reporter plasmid were as described previously (28). DL-Lactide (3, 6-dimethyl-1, 4-dioxane-2, 5-dione), stannous 2-ethylhexanoate, poly (ethylene glycol) (PEG) 1000, amine modified fluorescent nanoparticle suspension (L-1280), Hoechst 33258 (Bisbenzimide), deuterated chloroform ($CDCl_3$), TRI reagent® and constituents of the X-gal staining solution were from Sigma-Aldrich Chemical Company (Poole, UK). Triethanolamine (TEA) and Carbopol-940 were from Acros Organics (Geel, Belgium). Glycolide (1, 4-dioxane-2, 5-dione) was received as a gift from Purac (Gorinchem The Netherlands). All culture plastics were from Corning-Costar (High Wycombe, UK). Dulbecco's Modified Eagle's Medium (DMEM), foetal bovine serum (FBS), penicillin-streptomycin solution were from Invitrogen Corporation (Paisley, UK). Histological materials were from RA Lamb Ltd (Eastbourne, UK). DNA-free™ kit was from Ambion (Cambridgeshire, UK) and the one step RT-PCR kit from Qiagen Ltd (Crawley, UK). Other materials were of analytical grade and from Fisher Scientific UK (Loughborough, UK).

Methods

Microneedle Manufacture

Silicon microneedles were prepared using a previously reported approach (8, 29). Briefly, a silicon wafer was coated with a nitride and oxide layer using low pressure chemical vapour deposition (LPCVD). This layer was then lithographically patterned using plasma etching. The patterned wafer was subsequently etched using a 29% potassium hydroxide solution at a temperature of 79°C in a water bath with constant agitation. The aspect ratio of the resulting microneedles was 3:2 (height:base diameter). In a final step,

Diffusion of pDNA from Hydrogel Systems Through Heat Separated Epidermal Sheet

1% w/v Carbopol-940 and a 23% w/w PLGA-PEG-PLGA hydrogels were prepared, each containing 1 mg/ml pCMVβ. The donor compartment of a static Franz type diffusion cell was loaded with 1 ml of hydrogel and occluded with foil. The diffusive membrane was a heat separated epidermal sheet (prepared as described previously and treated once with the microneedle array) clamped between the donor and receptor phase and sealed with silicon grease. The receptor phase of each diffusion cell was filled with ~3 ml of TNE buffer (100 mM Tris; 2.0 M NaCl; 10 mM EDTA; pH 7.4) and magnetically stirred for 72 h in a 37°C water bath. At pre-determined time intervals, 200 µl samples were removed from the receptor phase which was replenished with an equal volume of TNE buffer. Plasmid permeation was monitored by measuring the total amount of DNA in each sample using Hoeschst DNA quantification (32). Fluorescence was measured using a FLUOstar Optima fluorimeter (BMG Labtechnologies, Offenberg, Germany).

Demonstration of Organ Culture Viability Over 24 H

Immediately following surgical removal, human breast tissue from a 64 year old female patient was transferred into full culture media at 4°C and transported to the laboratory where the subcutaneous fat and the majority of the dermis were removed by careful dissection, resulting in 'split-thickness' skin. The SC was disrupted in two distinct regions, and each subsequently received 20 µg of pCMVβ. One region was immediately placed in RNA*later*® and stored at −20°C. The other sample was cultured as reported previously (8) for 24 h before being immersed in RNA*later*® and stored at −20°C. Total RNA was isolated from each sample using TRI Reagent® and contaminating genomic DNA removed by treatment with DNA-free™ kit as described previously (REF). RT-PCR reactions were performed, using 2 µg of total RNA, on both samples using primers specific for a 400 bp fragment of the β-gal transcript (5'-TTC ACT GGC CGT CGT TTT ACA ACG TCG TGA-3' and 5'-ATG TGA GCG AGT AAC CCG TCG GAT TCT-3'). Reaction products were run on a 1% agarose gel, containing eithidium bromide, at 100 V for 1 h before observation with a UV gel doc (8).

Skin Organ Culture and pDNA Delivery

All gene delivery studies were performed on recently excised human breast skin from a 62 year old female donor. Each hydrogel formulation (100 µl containing 100 µg of pCMVβ reporter pDNA) was then applied and spread over a limited surface (~1 cm^2) of the split-thickness skin prior to application of the frustum-tipped microneedle device in a single rolling motion, i.e. the array is applied at an acute angle of 45° to the skin, rolled through an angle of 180° continuing to an obtuse angle of approximately 135° (n=4 for both types of hydrogel) on the same area. Other regions of the skin also received 100 µl of each hydrogel formulation spread over the surface but spread over an area ~1 cm×2 cm. The microneedle array was applied directly to the skin surface and dragged in a lateral scrap for ~2 cm, through the hydrogel formulation (n=2 for each hydrogel). The treated areas of the skin were dissected and cultured in full culture media (94% DMEM : 5% FBS : 1% penicillin/streptomycin) at 37°C and 5% CO_2 for 24 h using a previously validated organ culture system (8).

After 24 h, all samples were rinsed in PBS/$MgCl_2$ for 30 min, and fixed in 2% glutaraldehyde/PBS/$MgCl_2$ at 4°C for 2 h. Subsequently, each sample was rinsed three times in PBS/$MgCl_2$ for 2 h. Samples were then immersed in X-Gal staining solution (0.2% X-Gal, 2 mM $MgCl_2$, 5 mM $K_4Fe(CN)_6$, 5 mM $K_3Fe(CN)_6$ prepared in PBS) for 24 h at 37°C. Points of expression were counted on each sample by observation en face using a Stemi 2000-C Stereomicroscope (Zeiss, Welwyn Garden City, UK) and a KL1500 electronic external light source (Schott UK Limited, Stafford, UK), prior to each sample being embedded in OCT medium and stored at −80°C.

Preparation of Skin Cryosections and H&E Staining

Samples embedded in OCT blocks were sectioned using a Leica CM3050S Cryostat (Leica Microsystems, Milton Keynes, UK). Skin sections (10 or 12 µm) were captured onto Superfrost Plus® microscope slides, dried overnight and observed with an Olympus BX50 microscope (Olympus, Middlesex, UK). Selected slides were further subjected to haematoxylin and eosin (H&E) staining to assist visualisation of skin architecture.

RESULTS AND DISCUSSION

The wet etched microneedle arrays used in this study had a surface area of ~3 mm^2 and contained 16 microneedles equally distributed in a 4×4 arrangement. These were initially characterised by SEM (Fig. 2a). Although the wet etching process is commonly prone to poor reproducibility, the microneedle arrays used in this study were shown to be regular and reproducible through effective process control (11,27). At increased magnification, the structure of individual needles was apparent (Fig. 2b). Each needle was ~260 µm in height, with a base diameter of ~200 µm, and a flattened tip (frustrum) ~100 µm in diameter. This type of

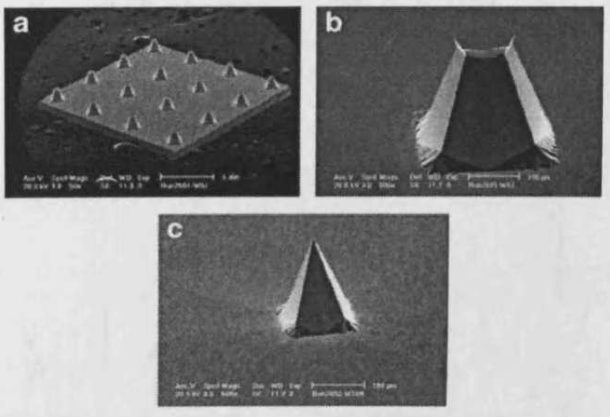

Fig. 2. SEM images of microneedle arrays at different magnifications. **a** The microneedle array used in the study (*bar* = 1 mm). **b** A frustum tipped microneedle array. **c** A sharp tipped microneedle (*bar* = 100 µm in both cases).

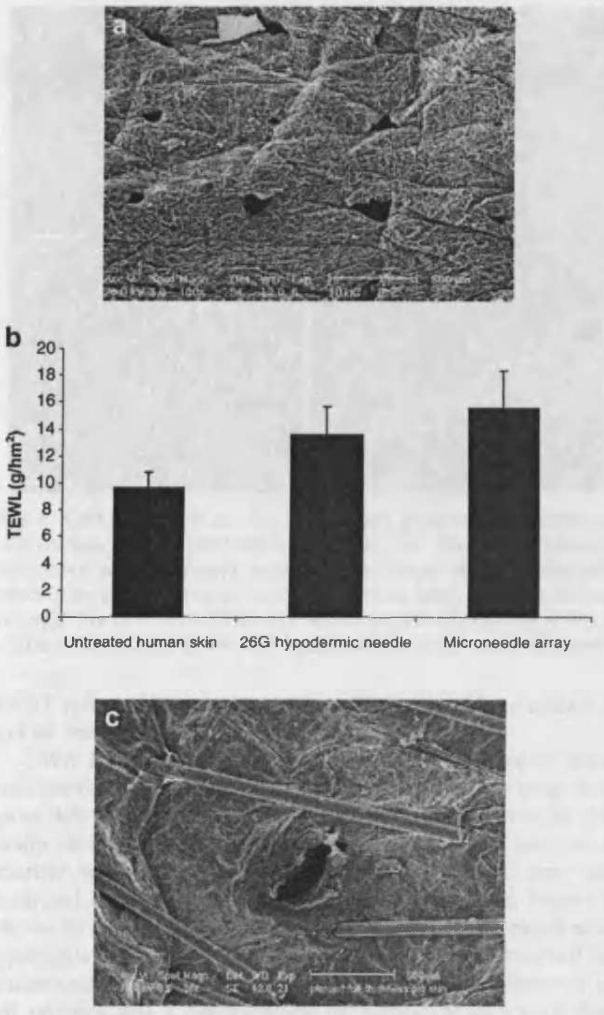

Fig. 3. **a** Disruption of the SC in a heat separated epidermal membrane resulting from microneedle application as observed by SEM (*bar* = 500 μm). **b** Loss of SC integrity in full thickness skin determined by TEWL. **c** An SEM image of porcine skin treated with a hypodermic needle (*bar* = 500 μm).

needle was used in preference to sharp tipped microneedles (Fig. 2c) as preliminary studies had indicated that this type of microneedle geometry resulted in improved gene expression due to increased transient disruption to the SC and possibly temporary compromise of keratinocyte membranes (8). Disruption of the SC, following frustum tipped microneedle treatment, was clearly visible when heat separated epidermal sheets, (SC and viable epidermis), were removed from treated skin (Fig. 3a). Membrane punctures, typically between 50–100 μm in diameter, corresponding to the spatial pattern of the microneedle array were clearly visible.

Microneedle induced disruption of full thickness skin was assessed by comparing the trans-epidermal water loss (TEWL) of treated skin with that of untreated control skin. It was predicted that microneedle treatment would result in a decrease in barrier function and a related increase in TEWL. A significant ($P<0.05$) increase in TEWL was observed for microneedle treated skin as compared to non-treated control skin (Fig. 3b). Skin samples that had received a single puncture with a 26 G hypodermic needle demonstrated statistically ($P<0.05$) comparable water loss to those samples treated with a single application of the 16-microneedle array. Interestingly, this observation directly correlates with the total area of punctures. Figure 3a shows that, although variable in dimensions, typically microneedle punctures have a diameter of 50–100 μm. Therefore, based on the assumption that one microneedle application creates 16 punctures, each of ~75 μm diameter, the total puncture area (or area of disruption) is $\sim 70\times10^3$ μm^2. When a similar calculation was carried out for the disruption to the skin surface (in this case porcine skin) caused by a 26 G hypodermic needle (Fig. 3c) (diameter of puncture ~300 μm) the total puncture area was essentially the same.

The PLGA-PEG-PLGA tri-block copolymer was initially characterised by ^{1}H-NMR spectroscopy and GPC. A typical ^{1}H-NMR spectrum is shown in Fig. 4. Spectra of peaks corresponding to the methine and methyl hydrogen of the DL lactide constituent (5.2 and 1.5 ppm, respectively), the methylene hydrogen of the glycolide component (4.8 ppm), and the methylene hydrogen of the PEG (3.6 ppm) were observed, which are consistent with the finding of Chen *et al.* (33). The ratio of DL Lactide to glycolide was determined, by ^{1}H-NMR, to be 1.74 (Table I) which suggests a relatively high glycolide component, a determinant of resultant release properties.

The molecular weight and polydispersity index of the PLGA-PEG-PLGA tri-block copolymer was determined by GPC as 3882 and 1.14, respectively (Table I). Polymers within this range have been shown to display thermoreversible sol-gel transitions when present in specific concentrations in aqueous solutions (33). Below the lower critical solution temperature (LCST) the gel reversibly returns to a fluid state and behaves as a Newtonian fluid (30), but when heated forms a gel. In this instance the gelation point was found to be ~32°C for a 23% w/w solution as determined by test tube inversion (data not shown). At temperatures above 40°C, the polymer precipitated, but when cooled below the

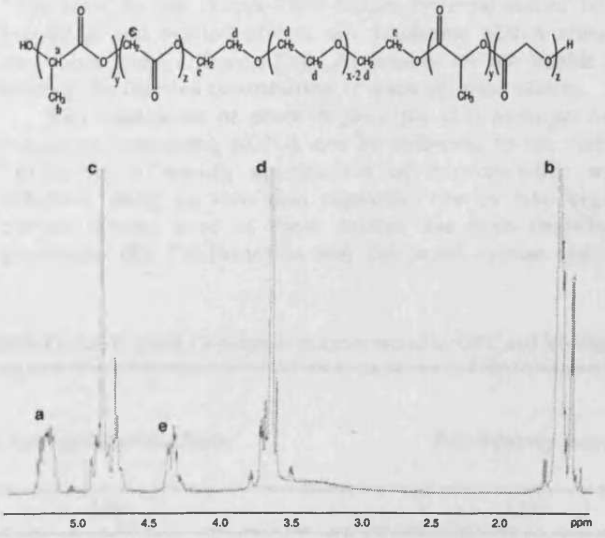

Fig. 4. A typical ^{1}H NMR spectra for PLGA-PEG-PLGA triblock copolymer.

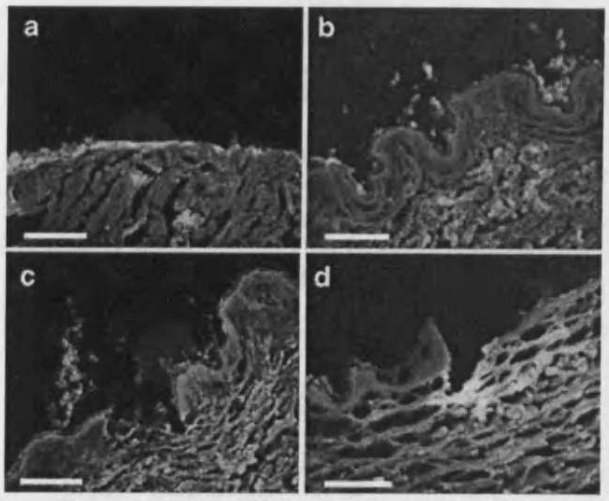

Fig. 5. Cryosections of *ex vivo* human skin observed by fluorescent microscopy. **a**, **b** Application of a 1% *w/v* Carbopol hydrogel containing red fluorescent nanobeads to intact skin. Microneedle application removes the SC integrity and the hydrogel formulations (**c** and **d**) are able to reach the epidermis: **c** a 1% *w/v* Carbopol-940; **d** a 23% *w/w* PLGA-PEG-PLGA hydrogel (*bar* = 100 μm in all cases).

LCST reverted back to a solution which was able to reform a gel on heating.

We have previously used 100 nm fluorescent latex nanoparticles as a readily identifiable model for non-viral gene delivery vectors, for example LPD (2). However, in this study these fluorescent latex nanoparticles were used as a marker within the hydrogel which demonstrated that the hydrogel resided within the formed microconduits. Figure 5 shows 10 μm cryosections of ex vivo human skin treated with hydrogels loaded with fluorescent nanoparticles observed by fluorescent microscopy. The green fluorescence observed in all sections was a consequence of autofluorescence of skin components and not the result of staining. Both types of hydrogels failed to penetrate the SC in regions where the microneedles were not applied, with the red fluorescent signal emitted from the nanoparticle loaded hydrogel restricted to the external surface of the SC (Fig. 5a,b). In some cases, the gel could be observed residing in skin ridges and other natural folds although the SC was still seen to be intact and no underlying red fluorescence was observed (Fig. 5b). However, when the hydrogel/nanoparticle formulations were applied to skin in conjunction with microneedles, nanoparticles were observed within the viable epidermis. Red fluorescence due to the nanoparticles was observed to be localised to microneedle created channels. This demonstrated that the application of the microneedles to the surface of the skin had penetrated the skin surface and pushed the nanoparticle containing hydrogel formulations into the resulting microchannels. (Fig. 5c,d). Significant disruption to the SC was clearly evident in these images, leading to the formation of conduits with typical depths of 150–200 μm and nanoparticles could clearly be observed as red or yellow (combination of red nanoparticle and green autofluorescence) against the green autofluorescent background within the viable epidermis.

The temporal release of pDNA from the hydrogel delivery systems was determined using Franz-type diffusion cells (Fig. 6). Hydrogels (23% w/w PLGA-PEG-PLGA; 1% Carbopol-940) containing pDNA 1 mg/ml were loaded into the donor compartment of diffusion cells with heat separated epidermal sheets, treated with a single application of the microneedle array, as the diffusive membrane. Release of pDNA from the hydrogel and the resulting diffusion into the receptor phase was determined over 5 days at 37°C. The migration of a control formulation of aqueous pDNA across the microneedle treated epidermal sheet was generally observed to be lower than the hypothetically expected values. This suggested that the channels were either becoming obstructed by debris released from the epidermal sheet or possibly that the channels were closing, due to hydration of the epidermal sheet which resulted in swelling and subsequent constriction of the channels. Nevertheless, the diffusion of pDNA was retarded when incorporated into both types of hydrogel. Release and subsequent diffusion was significantly greater from the PLGA-PEG-PLGA based hydrogel; with release and diffusion from the Carbopol hydrogel being negligible in comparison over this time period using this detection system. The mechanism of pDNA release would be expected to be different for the two types of hydrogel. In both hydrogels, migration of pDNA through the gel matrix would determine release rate. However, in the thermosensitive hydrogel, the PLGA-PEG-PLGA polymers are prone to hydrolysis of their ester bonds so that the integrity of the polymer matrix is lost relatively quickly (compared to Carbopol) at physiological temperatures. Therefore, for the PLGA-PEG-PLGA hydrogel matrix, both migration and erosion effects will determine pDNA release and subsequent diffusion (34). At present we are unable to predict the relative contribution of each of these effects.

Demonstration of proof-of-principle that hydrogel formulations containing pDNA can be delivered to the viable epidermis following application of microneedles was achieved using ex vivo skin explants. The ex vivo organ culture system used in these studies has been described previously (8). Confirmation that the organ culture system

Table I. Molecular Weight and PL/GA Ratio of the Synthesised PLGA-PEG-PLGA Triblock Copolymer as Determined by GPC and ^{1}H-NMR

Molecular Weight of PLGA-PEG-PLGA Polymers		DL-Lactide/Glycolide Ratio[a]	Polydispersity Index[b]
M_w^a	M_n^a		
3,882	2,986	1.24	1.139

[a] Determined by ^{1}H-NMR
[b] Determined by GPC

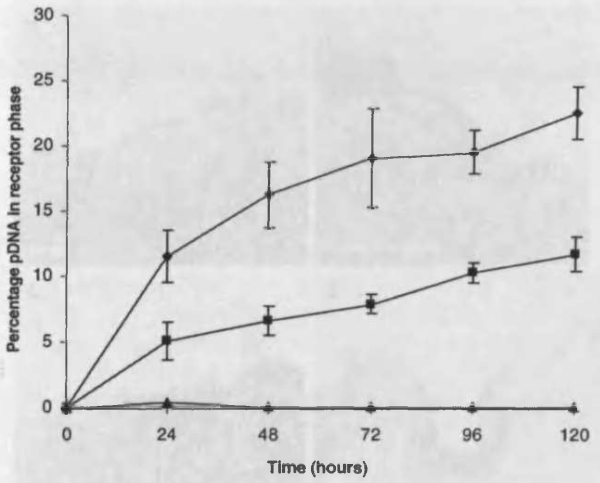

Fig. 6. The migration of pDNA through a microneedle treated human heat separated epidermal sheet: a solution of pDNA (*filled diamond*), a 1% *w/v* Carbopol hydrogel (*filled triangle*) and a 23% *w/w* PLGA-PEG-PLGA triblock copolymer hydrogel (*filled square*).

retains skin viability over the incubation period was demonstrated using RT-PCR specific for a 400 bp fragment of the β-galactosidase transcript. Figure 7 shows RT-PCR products of skin samples treated with pCMVβ and processed either immediately after treatment and following 24 h incubation in organ culture. The results show that the skin is still genetically viable at 24 h. Beyond this timepoint decreasing cellular viability becomes an issue, therefore to date all gene delivery studies performed in ex vivo human skin are performed over 24 h. Figure 8a,b shows en face images of *ex vivo* human skin treated with pCMVβ loaded hydrogel formulations, Carbopol-940 (a) and PLGA-PEG-PLGA (b), and wet-etch silicon microneedles with subsequent immersion in X-Gal staining solution. Figure 8c shows the total number of microchannels positive for gene expression following a single treatment with the hydrogels or a solution of pDNA. Both the 1% w/v Carbopol-940 and 23% w/w PLGA-PEG-PLGA tri-block copolymer hydrogels were shown to release functional pDNA which was able to transfect skin cells and express the gene product; β-galactosidase converting a substrate to reveal blue colouration. In control experiments, where pDNA hydrogels were applied to skin which had not been treated with microneedles, expression was not observed (data not shown).

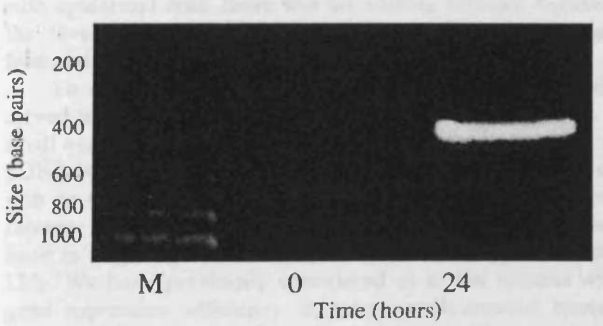

Fig. 7. RT-PCR analysis of β-galactosidase expression in *ex vivo* human skin. When RNA was isolated from samples immediately after the plasmid application (time 0) then no expression is observed. However, following culturing for 24 h, a clear signal indicating expression form the plasmid was observed, confirming that the skin remains genetically viable during the culturing period.

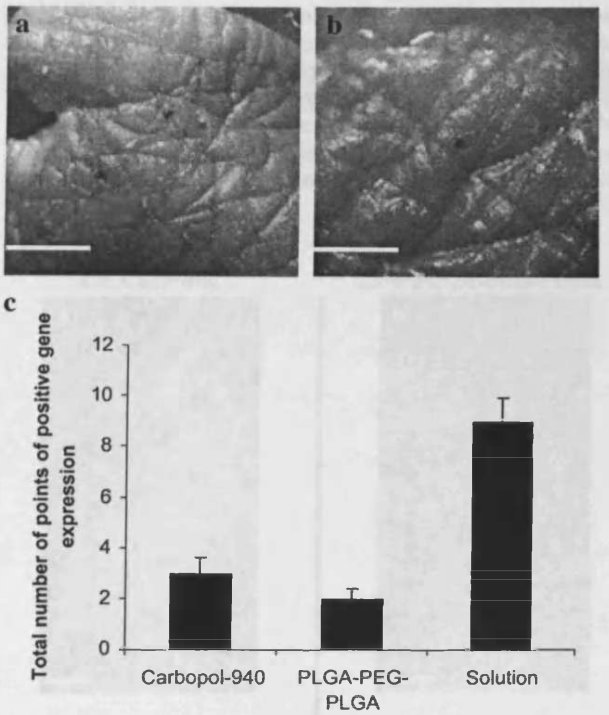

Fig. 8. Positive expression from microneedle assisted delivery of pCMVβ to *ex vivo* human skin (microneedles applied in a single rolling motion). *En face* image of skin treated with a 1% Carbopol-940 hydrogel (**a**) and 23% *w/w* PLGA-PEG-PLGA triblock copolymer hydrogel (**b**) each containing pDNA with subsequent application of microneedles (*bar* = 1 mm in both cases). **c** The total number of points of positive expression observed in samples treated with pDNA loaded hydrogels contrasted with pDNA delivered in solution.

It was noted that overall levels of gene expression were low and not significantly different between the hydrogel formulations (Fig. 8c) despite the aforementioned increase in pDNA release from PLGA-PEG-PLGA hydrogels (Fig. 6). It is possible that during hydrolysis of the PLGA-PEG-PLGA polymer hydrogel the constituent breakdown products could be reducing uptake and/or expression of pDNA either by direct physical hindrance or by chemically modifying the extracellular or intracellular environment, for example altering pH. Also, both hydrogel formulations will be gradually delivering pDNA over time and the human organ culture system that is currently employed only permits gene expression experiments to be performed for 24 h, due to restrictions of cellular viability. Clearly this may lead to an underestimation of gene expression from sustained release matrices and is currently being addressed using alternative biological models.

To determine the primary location of β-galactosidase expression in skin layers 12 μm cryosections were taken from the same samples and observed using light microscopy revealed that reporter gene expression following application of pDNA loaded hydrogels and microneedles were proximal

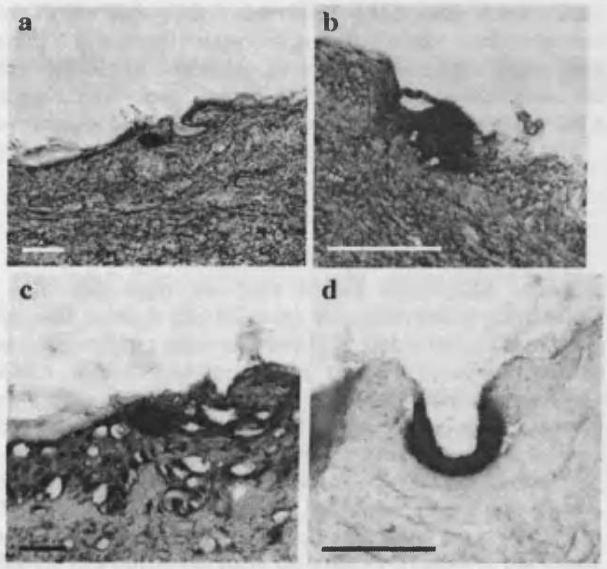

Fig. 9. Cryosections (12 μm) prepared from skin samples treated initially with either 1% Carbopol-940 (**a**, **c**) or 23% *w/w* PLGA-PEG-PLGA triblock copolymer hydrogel (**b**, **d**) and subsequently with wet-etch microneedles (*bar* = 150 μm in all cases).

to a microconduit (typically between150–200 μmin depth) and limited to cells of the epidermis, Fig. 9. The image shown in Fig. 9d, not stained with H&E, shows a micro-channel created using the frustum-tipped microneedles and loaded with thermosensitive gel. It is interesting to note that both the structural integrity of this individual microchannel, possibly a result of the loaded gel restricting tissue regress, and intensity of gene expression are more pronounced than that observed with the Carbopol gel (Fig. 9a,c) and aqueous formulations (11). Gene expression was also observed when the hydrogel formulations were applied to skin prior to lateral application of microneedles (Fig. 10a–d). The points of expression were exclusively associated with the barrier disruption caused by microneedle application (Fig. 10, arrows). While more points of expression were observed following this method of application, presumably as a result of enhanced disruption of SC and increased contact of pDNA with epidermal cells, there was no notable variance between the levels of gene expression arising from the hydrogel formulations Fig. 10e.

To date, the gene expression efficiency we have observed in microneedle treated skin has been restricted to a small number of microchannels. Typically, when a solution of pDNA was pre-applied to the surface of microneedle treated skin up to 30% of the microchannels demonstrated positive reporter gene expression (8). When the pDNA was formulated in a hydrogel this value was reduced to approximately 12%. We have previously speculated as to the reasons why gene expression efficiency in microneedle-treated human skin is relatively low. These include limited entry of the pDNA into the microchannel, inefficient cellular uptake of the pDNA, cell damage caused by the infiltrating microneedles and unreliable detection of reporter gene product due to restricted access of the staining solution to the transfected cells (8). By using a gel formulation we may be further restricting the access of pDNA to cellular targets over the initial 24 hr incubation period (as suggested in Fig. 6). As a corollary, whilst pDNA hydrogels provide potential for sustained release, such formulations may indeed *initially* result in lower levels of gene expression than would be observed with liquid systems. Whilst our organ culture system provides a valuable method for testing gene expres-

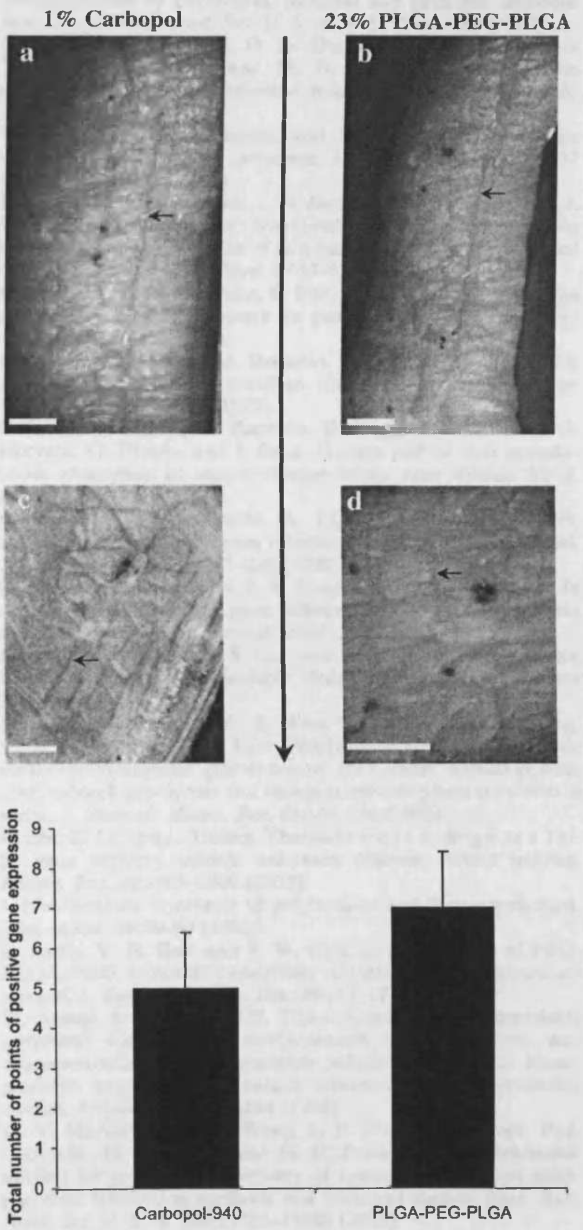

Fig. 10. Delivery of pDNA loaded hydrogels with microneedles applied in a single lateral scrape. The lines of disruption caused by the microneedles are indicated by *arrows*. Expression from pDNA loaded in 1% Carbopol-940 polymers (**a**, **c**) and 23% *w/w* PLGA-PEG-PLGA hydrogel (**b**, **d**). The *large black arrow* indicates the direction of microneedle lateral application; *bar* = 1 mm in all cases. **e** The total number of points of positive expression observed when microneedles were applied in a lateral motion ($n = 2$ in each instance).

sion in the biological and architectural human skin environment, it is currently impractical to guarantee excised human skin viability to determine gene expression over longer time periods. Further *in vivo* studies with these formulations will investigate the ability of these systems to control pDNA release for sustained gene expression.

CONCLUSIONS

In this study we have shown the ability to create channels through the SC using microfabricated needles and mediate reporter gene expression in viable human skin using pDNA loaded hydrogels. The frustum type microneedle array exploited in these studies was proficient in creating channels of sufficient dimensions for the passage of relatively large materials, such as macromolecular nanoparticles and pDNA, whilst being of sufficient robustness for repeated use. The hydrogel delivery systems were able to harbour pDNA in the microneedle-facilitated microchannel and release the plasmid in a functional form for gene expression in the viable epidermis. The combination of the microneedle physical delivery strategy and sustained release formulation could potentially be employed for clinical applications where it is an advantage for large molecules to enter the viable epidermis over prolonged periods, for instance in genetic vaccination.

ACKNOWLEDGEMENTS

The authors acknowledge the BBSRC for financial support of MP.

REFERENCES

1. S. Henry, D. V. McAllister, M. G. Allen, and M. R. Prausnitz. Microfabricated microneedles: a novel approach to transdermal drug delivery. *J. Pharm. Sci.* **87**:922–925 (1998).
2. F. Chabri, K. Bouris, T. Jones, D. Barrow, A. Hann, C. Allender, K. Brain, and J. Birchall. Microfabricated silicon microneedles for nonviral cutaneous gene delivery. *Br. J. Dermatol.* **150**:869–877 (2004).
3. W. Martanto, S. P. Davis, N. R. Holiday, J. Wang, H. S. Gill, and M. R. Prausnitz. Transdermal delivery of insulin using microneedles *in vivo*. *Pharm. Res.* **21**:947–952 (2004).
4. J. A. Matriano, M. Cormier, J. Johnson, W. A. Young, M. Buttery, K. Nyam, and P. E. Daddona. Macroflux® microprojection array patch technology: a new and efficient approach for intracutaneous immunization. *Pharm. Res.* **19**:63–70 (2002).
5. R. K. Sivamani, B. Stoeber, G. C. Wu, H. Zhai, D. Liepmann, and H. Maibach. Clinical microneedle injection of methyl nicotinate: stratum corneum penetration. *Skin Res. Technol.* **11**:152–156 (2005).
6. J. H. Park, M. G. Allen, and M. R. Prausnitz. Polymer microneedles for controlled-release drug delivery. *Pharm. Res.* **23**:1008–1019 (2006).
7. H. S. Gill and M. R. Prausnitz. Coated microneedles for transdermal delivery. *J. Control. Release* **117**:227–237 (2007).
8. J. C. Birchall, S. A. Coulman, M. Pearton, C. Allender, K. Brain, A. Anstey, C. Gateley, N. Wilke, and A. Morrissey. Cutaneous DNA delivery and gene expression in ex vivo human skin explants via wet-etch microfabricated microneedles. *J. Drug Target.* **13**:415–421 (2005).
9. S. A. Coulman, D. Barrow, A. Anstey, C. Gateley, A. Morrissey, N. Wilke, C. Allender, K. Brain, and J. C. Birchall. Minimally invasive cutaneous delivery of macromolecules and plasmid DNA via microneedles. *Curr. Drug Discov.* **3**:65–75 (2006).
10. I. R. Williams and T. S. Kupper. Immunity at the surface: homeostatic mechanisims of the skin immune system. *Life Sci.* **58**:1485–1507 (1996).
11. E. F. Fynan, R. G. Webster, D. H. Fuller, J. R. Haynes, J. C. Santoro, and H. L. Robinson. DNA vaccines: protective immunizations by parenteral, mucosal and gene-gun innoculations. *Proc. Natl. Acad. Sci. U. S. A.* **90**:11478–11482 (1993).
12. S. Kaushik, A. H. Hord, D. D. Denson, D. V. McAllister, S. Smitra, M. G. Allen, and M. R. Prausnitz. Lack of pain associated with microfabricated microneedles. *Anesth. Analg.* **92**:502–504 (2001).
13. M. T. S. Lin, L. Pulkkinen, and J. Uitto. Cutaneous gene therapy—principles and prospects. *Dermatol. Clin.* **18**:177–187 (2000).
14. J. A. Mikszta, J. B. Alarcon, J. M. Brittingham, D. E. Sutter, R. J. Pettis, and N. G. Harvey. Improved genetic immunization via micromechanical disruption of skin-barrier function and targetted epidermal delivery. *Nat. Med.* **8**:415–419 (2002).
15. D. W. Pack, A. S. Hoffman, S. Pun, and P. S. Stayton. Design and development of polymers for gene delivery. *Nat. Rev. Drug Discov.* **4**:581–593 (2005).
16. L. D. Shea, E. Smiley, J. Bonadio, and D. J. Mooney. DNA delivery from polymer matrices for tissue engineering. *Nat. Biotechnol.* **17**:551–554 (1999).
17. I. Csoka, E. Csanyi, G. Zapantis, E. Nagy, A. Feher-Kiss, G. Horvath, G. Blazso, and I. Eros. *In vitro* and *in vivo* percutaneous absorption of topical dosage forms: case studies. *Int. J. Pharm.* **291**:11–19 (2005).
18. P. Mura, G. P. Bettinetti, A. Liguori, and G. Bramanti. Improvement of clonazepam release from a Carbopol hydrogel. *Pharm. Acta Helv.* **67**:282–288 (1992).
19. F. A. Ismail, J. Napaporn, J. A. Hughes, and G. A. Brazeau. *In situ* gel formulations for gene delivery: release and myotoxicity studies. *Pharm. Dev. Technol.* **5**:391–397 (2000).
20. B. Jeong, Y. H. Bae, D. S. Lee, and S. W. Kim. Biodegradable block copolymers as injectable drug-delivery systems. *Nature* **388**:860–862 (1997).
21. M. S. Shim, H. T. Lee, W. S. Shim, I. Park, H. Lee, T. Chang, S. W. Kim, and D. S. Lee. Poly(D,L-lactic acid-co-glycolic acid)-b-poly(ethylene glycol)-b-poly (D,L-lactic acid-co-glycolic acid) triblock copolymer and thermoreversible phase transition in water. *J. Biomed. Materi. Res.* **61**:188–196 (2002).
22. P. Lee, Z. Li, and L. Huang. Thermosensitive hydrogel as a Tgf-β1 gene delivery vehicle enhances diabetic wound healing. *Pharm. Res.* **20**:1995–2000 (2003).
23. J. Nieuwenhuis. Synthesis of polylactides and their copolymers. *Clin. Mater.* **10**:59–67 (1992).
24. B. Jeong, Y. H. Bae, and S. W. Kim. *In situ* gelation of PEG-PLGA-PEG triblock copolymer solutions and degredation thereof. *J. Biomed. Materi. Res.* **50**:171–177 (2000).
25. W. Amass, A. Amass, and B. Tighe. A review of biodegradable polymers: uses, current developments in the synthesis and characterization of biodegradable polyesters, blends of biodegradable polymers and recent advances in biodegradation studies. *Polym. Int.* **47**:89–144 (1998).
26. D. V. McAllister, P. M. Wang, S. P. Davis, J. H. Park, P. J. Canatella, M. G. Allen, and M. R. Prausnitz. Microfabricated needles for transdermal delivery of macromolecules and nanoparticles: fabrication methods and transport studies. *Proc. Natl. Acad. Sci. U. S. A.* **100**:13755–13760 (2003).
27. J. H. Park, M. G. Allen, and M. R. Prausnitz. Biodegradable polymer microneedles: fabrication, mechanics and transdermal drug delivery. *J. Control. Release.* **104**:51–66 (2005).
28. J. C. Birchall, I. W. Kellaway, and M. Gumbleton. Physical stability and *in-vitro* gene expression efficiency of nebulised lipid-peptide-DNA complexes. *Int. J. Pharm.* **197**:221–231 (2000).
29. N. Wilke, A. Mulcahy, S.-R. Ye, and A. Morrissey. Process optimisation and characterisation of silicon microneedles fabri-

cated by wet etch technology. *Microelectron. J.* **36**:650–656 (2005).
30. G. M. Zentner, R. Rathi, J. Shih, J. C. McRea, M. Seo, H. Oh, B. G. Rhee, J. Mestecky, Z. Moldoveanu, M. Morgan, and S. Weitman. Biodegradable block copolymers for delivery of proteins and water-insoluble drugs. *J. Control. Release* **72**:203–215 (2001).
31. B. Jeong, Y. H. Bae, and S. W. Kim. Biodegradable Thermosensitive Micelles of PEG-PLGA-PEG Triblock Copolymers. *Colloids Surf., B Biointerfaces.* **16**:185–193 (1999).
32. K. Rengarajan, S. M. Cristol, M. Mehta, and J. M. Nickerson. Quantifying DNA concentrations using fluorometry: a comparision of fluorophores. *Mol. Vis.* **8**:416–421 (2002).
33. S. Chen, R. Pieper, D. C. Webster, and J. Singh. Triblock copolymers: synthesis, characterization, and delivery of a model protein. *Int. J. Pharm.* **288**:207–218 (2005).
34. Z. Li, W. Ning, J. Wang, A. Choi, P. Y. Lee, P. Tyagi, and L. Huang. Controlled gene delivery system based on thermosensitive biodegradable hydrogel. *Pharm. Res.* **20**:884–888 (2003).

Journal of Drug Targeting, August 2005; 13(7): 415–421

Taylor & Francis
Taylor & Francis Group

Cutaneous DNA delivery and gene expression in *ex vivo* human skin explants via wet-etch microfabricated microneedles

JAMES BIRCHALL[1], SION COULMAN[1], MARC PEARTON[1], CHRIS ALLENDER[1], KEITH BRAIN[1], ALEXANDER ANSTEY[2], CHRIS GATELEY[2], NICOLLE WILKE[3], & ANTHONY MORRISSEY[3]

[1]*Gene Delivery Research Group, Welsh School of Pharmacy, Cardiff University, Cardiff CF10 3XF, UK,* [2]*Gwent Healthcare NHS Trust, Royal Gwent Hospital, Cardiff Road, Newport, South Wales NP20 2UB, UK, and* [3]*Biomedical Microsystems Team, Tyndall National Institute, Prospect Row, Cork, Ireland*

(Received 9 September 2005; revised 22 September 2005; accepted 22 September 2005)

Abstract

Microneedle arrays increase skin permeability by forming channels through the outer physical barrier, without stimulating pain receptors populating the underlying dermis. It was postulated that microneedle arrays could facilitate transfer of DNA to human skin epidermis for cutaneous gene therapy applications. Platinum-coated "wet-etch" silicon microneedles were shown to be of appropriate dimensions to create microconduits, approximately 50 μm in diameter, extending through the stratum corneum (SC) and viable epidermis. Following optimisation of skin explant culturing techniques and confirmation of tissue viability, the ability of the microneedles to mediate gene expression was demonstrated using the β-galactosidase reporter gene. Preliminary studies confirmed localised delivery, cellular internalisation and subsequent gene expression of pDNA following microneedle disruption of skin. A combination of this innovative gene delivery platform and the *ex vivo* skin culture model will be further exploited to optimise cutaneous DNA delivery and address fundamental questions regarding gene expression in skin.

Keywords: *Microneedles, human skin, DNA, skin organ culture,* ex vivo, *gene expression*

Introduction

Microfabricated microneedle arrays offer a minimally invasive method for breaching the external barrier that prevents delivery of macromolecular therapeutics to the viable region of skin (Henry et al. 1998). Microneedles designed to increase skin permeability are generally $<400\,\mu m$ long, being of sufficient length to penetrate the stratum corneum (SC), the rate limiting barrier to diffusion, without stimulating the pain receptors that populate the underlying dermis. Their application is therefore free from pain or discomfort (Kaushik et al. 2001). Microneedle treatment results in the formation of transient micro-pores in the SC (Chabri et al. 2004) thereby facilitating the transfer of macromolecular nucleic acids, such as siRNA, anti-sense oligonucleotides and plasmid DNA (pDNA), to the viable epidermis or dermis. This in turn provides the opportunity for cutaneous gene therapy applications including the treatment of cutaneous malignancies (Hart and Vile 1994), hyperproliferative skin disorders (Menter 1998), alopecia (Li and Hoffman 1995, Ahamed et al. 1998), genodermatoses (Uitto and Pulkkinen 2000) and possible exploitation of the skin as a bioreactor for the production of pharmacologically relevant molecules (Lin et al. 2000). Genetic vaccination provides a method of immunizing patients by introducing DNA into cells, leading to expression of foreign antigen and the subsequent induction of an immune response (Fynan et al. 1993, Raz et al. 1994, Shi et al. 1999). Intracutaneous DNA vaccines take advantage of the excellent antigen-presenting capabilities of epidermal Langerhans

Correspondence: J. Birchall, Gene Delivery Research Group, Welsh School of Pharmacy, Cardiff University, Cardiff CF10 3XF, UK. Tel: 44 29 2087 5815. Fax: 44 29 2087 4149. E-mail: birchalljc@cardiff.ac.uk

ISSN 1061-186X print/ISSN 1029-2330 online © 2005 Taylor & Francis
DOI: 10.1080/10611860500383705

cells in eliciting a T-cell mediated immune reaction, leading to a more efficient and lower cost vaccination compared with the use of recombinant proteins (Lin et al. 2000).

It has been reported that microfabricated microneedle arrays, prepared from a range of substrate materials, including silicon (Henry et al. 1998, Chabri et al. 2004), various metals (McAllister et al. 2003), glass (McAllister et al. 2003) and polymers (McAllister et al. 2003, Park et al. 2005) can be used to enhance the transdermal penetration of a range of therapeutically active and representative model medicaments such as calcein (Henry et al. 1998), methylene blue (Chabri et al. 2004), trypan blue (McAllister et al. 2003), methyl nicotinate (Sivamani et al. 2005), insulin (Martanto et al. 2004), desmopressin (Cormier et al. 2004), protein antigens (Matriano et al. 2002) and 100 nm nanoparticles (Chabri et al. 2004). In addition, it has been demonstrated that microprojection structures can facilitate the delivery and functional expression of DNA vaccine in animal models (Mikszta et al. 2002). To date, however, the microneedle-assisted delivery of DNA to human skin resulting in gene expression in the viable epidermal layer has not been reported. Given that anatomical and biological differences between human skin and animal skin are well documented (Panchagnula et al. 1997), it is essential that microneedle arrays are designed appropriately for the delivery of pDNA to the appropriate cellular populations in human skin as well as the more commonly used animal models. In the present study, microneedles were used to facilitate localised delivery, cellular internalisation and subsequent gene expression of pDNA topically applied to *ex vivo* human skin. This will allow for future *ex vivo* investigations developing the optimum microneedle device composition and morphology, gene delivery vector and type of formulation to bring about optimal skin penetration, epidermal targeting and gene expression efficiency.

The microneedle arrays used in this study were prepared with high accuracy and excellent reproducibility from standard silicon wafers using a potassium hydroxide (KOH) "wet etching" approach. Wet etching is a commonly employed micromachining technique with advantages over dry-etch procedures, routinely used to make microneedles, including low processing and development costs (Wilke et al. in press). Wet etching of silicon to form microneedles can be a complex process but in our studies control of microneedle morphology was achieved by exploiting the crystal structure of silicon and its resulting etch characteristics in KOH.

Materials and methods

Materials

The plasmid pCMVβ (7.2 kb), containing the β-galactosidase reporter gene (Clontech, Palo Alto, USA), was propagated using a transformed DH5α strain of *Escherichia coli*, colonised onto an ampicillin selective Luria Bertani agar plate and cultured overnight at 37°C. The plasmid DNA was harvested and purified using a Qiagen Plasmid Mega Kit (Qiagen, Crawley, UK). All culture plastics were obtained from Corning-Costar (High Wycombe, UK). Dulbecco's Modified Eagle's Medium (DMEM), 25 mM HEPES, foetal bovine serum, penicillin–streptomycin solution and the β-galactosidase specific primers were from Invitrogen Corporation (Paisley, UK). Materials required for histological studies were from RA Lamb Limited (Eastbourne, UK). TRI reagent® and individual components of the X-gal staining solution were from Sigma-Aldrich Chemical Company (Poole, UK). The DNA-free™ kit was from Ambion (Cambridgeshire, UK) and the one step RT-PCR kit from Qiagen Ltd. (Crawley, UK). Other materials used during the course of these studies were of analytical grade and from Fisher Scientific UK (Loughborough, UK).

Microneedle fabrication

A wet etch process using KOH was used to fabricate arrays of silicon microneedles. A standard silicon wafer with crystal alignment marks is the starting material. The first process step is the deposition of 1000 Å of silicon nitride on a 350 Å silicon oxide layer using low pressure chemical vapour deposition (LPCVD). The oxide improves the adhesion of the nitride to the silicon. This double layer will act as an etching mask protecting designed/patterned areas of the silicon from the KOH solution during the etching step. To generate microneedles in the crystalline material, square shape patterns are transferred into the masking double layer by standard photolithography, where a positive photoresist on the wafer is exposed to UV light to achieve the required pattern in the resist layer. The resist pattern is transferred into the nitride layer using a plasma etch process. The resist is stripped off and the oxide layer is then removed in the open areas by a wet etch process in HF (hydrofluoric acid). After lithography, the wafer undergoes a wet etch fabrication process. The patterned silicon wafer is etched using a 29% w/v aqueous KOH solution at a temperature of 79°C. The needle formation is based on convex-corner undercut. This means that crystal planes will form on every side of the square. Silicon has anisotropic etch behaviour in KOH; the etched structures are therefore formed along the crystal planes. Every crystal plane group has a specific etch rate. Very fast etching crystal planes start etching on the corners of the squares. When etching around 1 μm into the silicon wafer, the lateral etch rate of these planes is twice as fast. Two planes on every corner move towards the square centre. The plane angle to the surface, which is almost 90°, decreases to 72° when the eight planes meet each other, forming the needle tip. Viewed from overhead, the etch process evolves (Figure 1) until one can see a very uniform octagon—the eight high index crystal planes which form the needle (Figure 2).

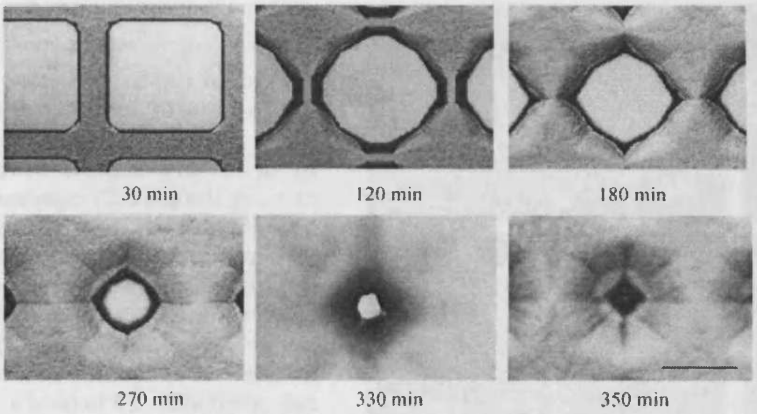

Figure 1. Top–down micrographs showing the evolution of microneedle formation through convex corner undercutting of a square mask. Needle shape is gradually formed when the eight high index crystal planes intersect on top of the frustum in a single point, generating a sharp needle tip. Bar = 500 μm.

Examination of morphological effects of microneedle treatment of human epidermal membranes

Skin from a 67-year-old female donor was immersed in heated deionised water (60°C) for 60 s to enable removal of the epidermal membrane from the underlying dermal tissue using forceps. The cooled epidermis was collected on aluminium foil and then placed on to the dermal layer before application of a microneedle array at a pressure of approximately 2 kg/cm^2 for 10 s. Following treatment the microneedle arrays and the epidermal membrane were air dried, mounted on an aluminium stub and gold sputter coated (EM Scope, Kent, UK) prior to being examined by scanning electron microscopy (SEM). In addition, epidermal membrane was also fixed in 2.5% glutaraldehyde and dehydrated in an increasing ethanol gradient (70, 90, 100%). A critical point dryer (Samdri 780, Maryland, USA) was used to completely dehydrate the specimen, which was mounted and gold sputter coated prior to SEM. Bar = 200 μm.

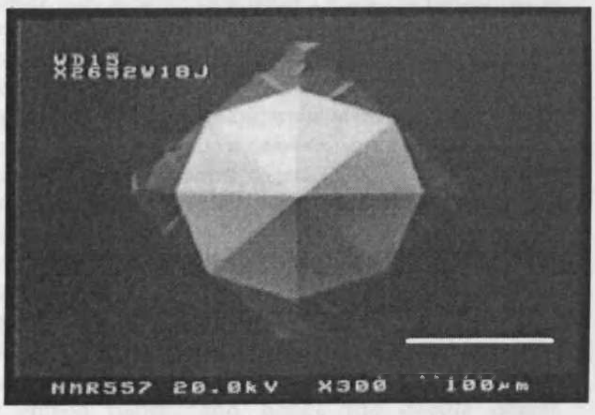

Figure 2. SEM image of an overhead view of a single octagonal wet-etch microneedle. Bar = 100 μm.

Preparation and maintenance of an ex vivo *human skin organ model*

Human breast skin from a 58-year-old female donor was collected immediately after excision, transported in media (DMEM 25 mM HEPES supplemented with 5% fetal bovine serum and 1% penicillin/streptomycin) on ice, and used within 2 h of surgical removal. Subcutaneous fat was removed using blunt dissection. The skin was separated using a scalpel blade to isolate the SC, viable epidermis and upper layers of the dermis (split-thickness skin).

Isolation and identification of β-galactosidase mRNA

Following disruption of the SC and application of 15 μg of pCMVβ plasmid DNA to the disrupted skin surface, approximately 1 cm^2 sections of skin were placed on lens tissue supported by metal gauze in a 6-well cell culture plate containing 3 ml media (DMEM 25 mM HEPES supplemented with 5% fetal bovine serum and 1% penicillin/streptomycin) per well (Figure 5A). The organ culture was maintained at an air–liquid interface for 24 h at 37°C. Subsequent to treatment, skin sections were snap frozen in liquid nitrogen and ground to a fine powder in a pre-cooled pestle and mortar. Total RNA was isolated from the *ex vivo* human skin and *E. coli* (control) using TRI Reagent® with contaminating genomic DNA removed using DNA-free™ kit. Two micrograms of isolated RNA was amplified using one step RT-PCR reaction containing primers specific for a 400 bp fragment of the β-gal transcript (5′-TTC ACT GGC CGT CGT TTT ACA ACG TCG TGA-3′ and 5′-ATG TGA GCG AGT AAC CCG TCG GAT TCT-3′). RT-PCR products were run on a 1% agarose gel, containing ethidium bromide, at 100 V for 1 h and visualized via a UV gel doc.

Determination of β-galactosidase expression in the ex vivo *human skin model*

Gene expression studies were carried out on human breast skin obtained from surgical procedures with full ethical approval and informed patient consent. Split-thickness skin was surface treated with 50 μl of pCMVβ plasmid DNA solution (2.5 mg/ml) prior to application of silicon microneedles. The skin, divided into approximate 1 cm^2 segments, was incubated for 24 h using the described organ culture conditions. Following one wash in PBS/$MgCl_2$ (30 min) the tissue was fixed for 2 h in 2% glutaraldehyde/$MgCl_2$ on ice. Subsequently, the tissue was rinsed in a series of PBS/$MgCl_2$ solutions for a total of 6 h. The tissue was stained for β-galactosidase expression using X-Gal staining solution. Selected tissue samples were counterstained with nuclear fast red (NFR); 5% solution applied topically to the treated area and removed after 30 min. Samples were then mounted between two microscope slides and visualised *en face* using a Zeiss Stemi 2000C Stereomicroscope with a 2,0X attachment and a Schott KL1500 electronic light source. For sectioning, tissue samples were embedded immediately (without NFR staining) in OCT and sectioned using a Leica CM3050S Cryostat. Tissue sections (12 μm) were collected onto Superfrost Plus® microscope slides and allowed to dry overnight before analysis using the Olympus BX50 microscope. Selected slides were stained with Harris' Haematoxylin and Gurr's Eosin and examined.

Results and discussion

The morphology of the wet-etched microneedles were initially characterised by SEM. The same technique was used to visualise the microchannels produced when the microneedle arrays were applied to human skin. Figure 3 shows the array pattern and structural dimensions of the two types of wet-etch microneedles used in this study. In the example presented, the microneedle arrays comprised 16 microprojections of silicon in a 4 × 4 array across a total array size of 3 mm^2. The array size, however, is totally at the discretion of the user, thus smaller or larger arrays can be produced as required. Larger arrays would provide the benefit of increased treatable tissue area; however, arrays with greater surface areas may cause handling problems due to the inherent brittleness of thin micro-structures. The pyramidal structures were approximately 280 μm in height with a width of 200 μm at the base and were prepared with either a sharp tip (Figure 3A and B) or a flattened tip, termed a frustrum (Figure 3C and D). Process variables, most notably etch time (but also mask pad size) determine the etched depth, and hence the needle height reported here. Needle heights up to 300 μm may be achieved given that the starting wafer thickness is approximately 525 μm, and sufficient material must remain non-etched to allow handling and process completion. We now have extremely accurate and reproducible process control over every step in the microneedle etching sequence. Traditionally, wet etching of microneedles has been viewed as being overly difficult to control and this is one of the primary reasons why dry etching techniques have replaced KOH etching for such micro-structures in silicon. But with the process control now achievable, benefits can be accrued from the lower costs and greater robustness of the needle arrays produced.

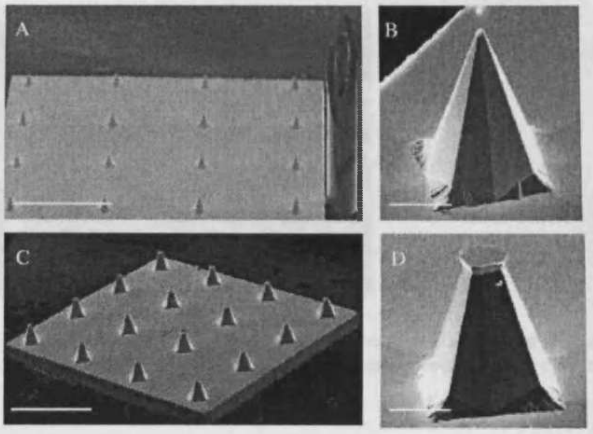

Figure 3. SEM images of wet-etch platinum coated microneedle arrays. (A) Sharp tipped microneedles; the tip of a 30 G hypodermic syringe providing a visual scale reference. Bar = 1 mm; (B) sharp tipped microneedles. Bar = 100 μm; (C, D) Frustum tipped microneedles. Bar = 1 mm (C) and 100 μm (D).

In order to assess microneedle skin penetration, full thickness human skin was heat separated to recover the epidermal membranes (SC and viable epidermis), replaced onto the dermal layer and treated with the microneedles prior to examination by SEM. Figure 4A depicts an electron micrograph showing an inverted view of the human epidermal sheet with the microneedle array still in position. The microneedle array pattern was transferred to the membrane creating an ordered arrangement of microconduits that extended through the SC and viable epidermis. At this magnification a number of microneedle tips can be observed penetrating through the sheet (see arrow). A critical point drying method was used to provide more detailed visualisation of the upper surface of heat-separated membrane. In this micro-graph, the dermatoglyphics of microneedle treated human skin are clearly defined (Figure 4B). Using the described SEM processing conditions the epidermal microchannels were apparent as 50 μm fissures piercing the skin corneocytes and underlying upper skin layers. Following topical skin application it was noted that the needle array remained intact, indicating good mechanical robustness.

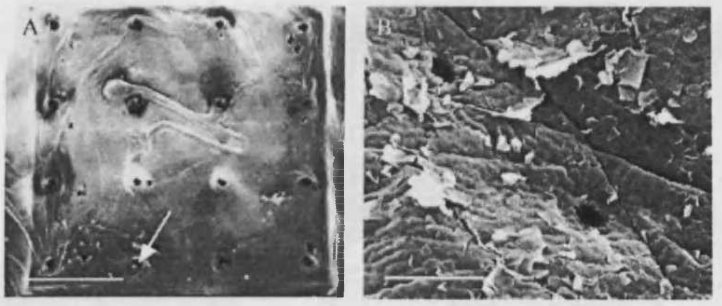

Figure 4. SEM images of heat separated epidermal membrane treated with the microneedle array. (A) Microneedles inserted into epidermal membrane (arrow denotes a microneedle penetrating through the epidermal sheet). Bar = 1 mm; (B) microneedle-treated epidermal membrane. Bar = 200 μm.

In order to maximise the cellular viability of the excised tissue, samples were immediately transferred from the patient into defined organ culture media at 0°C, transported to the laboratory and maintained at air–liquid-interface in growth media. Tissue viability was confirmed over a 24-hour-period through the continued production of endogenous epidermal mRNA and the transcription of β-galactosidase mRNA (Figure 5B) following intra-dermal application of the pCMVβ reporter plasmid.

Following confirmation of the presence of mRNA in the excised skin, the ability of the microneedles to facilitate gene expression was demonstrated using the β-galactosidase (pCMVβ) reporter gene. Figure 6 shows representative results of a skin transfection experiment. *En face* imaging, following topical application of reporter gene and microneedle puncturing, showed detectable reporter gene expression (Figure 6A and B). In control experiments, where pDNA was applied to skin, which had not been treated with microneedles, expression was not observed. Figure 6A shows the blue staining, arising from the reporter gene product, proximal to two microchannels created via application of the microneedle array, also shown in the figure for comparison. Figure 6B highlights the created microchannels by counterstaining with a low molecular weight red dye. As in Figure 6A, it is apparent that a minority of microchannels created in the skin stained positive for gene expression, despite the counterstain confirming that microconduits had been formed by each individual microneedle. The possible reasons for the variability in gene expression efficiency include limited access of the pDNA into the created microchannel, inefficient uptake of the pDNA into the cells located at the periphery of the microchannel, cell damage or death caused by the infiltrating microneedles, or simply unreliable detection of gene expression due to restricted access of the staining solution to the transfected cells. We are currently addressing these issues through the use of alternative microneedle materials and morphologies, different reporter pDNA constructs, improved detection methods and optimised pDNA delivery formulations. Clearly, for certain gene therapy applications, such as the correction or replacement of aberrant genes in genetic skin disorders and the treatment of cutaneous malignancies, such variable levels of expression would need to be addressed, although larger microneedle arrays could be utilised to increase surface coverage. In the case of genetic vaccination however, a sufficient number of cells may still be able to uptake and express the antigen gene to produce an appropriate quantity of antigen to stimulate an immune response. Indeed, in DNA vaccination, it may be more important to target appropriate loci within the skin rather than skin surface area in order to enhance antigen presentation to the immune responsive Langerhans cells. The depth and intensity of reporter gene expression in the underlying

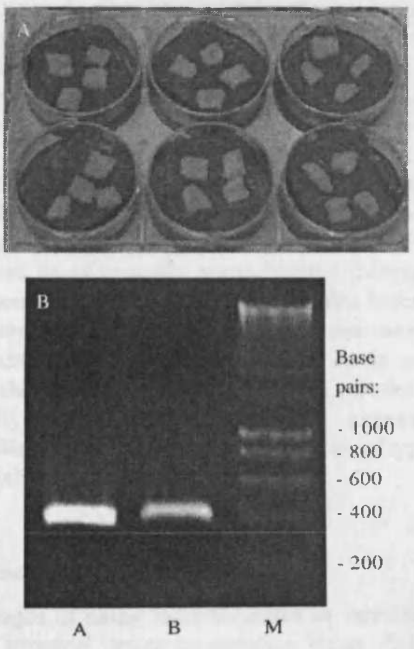

Figure 5. (A) The human skin organ culture procedure; (B) agarose gel showing presence of β-galactosidase mRNA isolated from viable human skin following 24 h incubation in organ culture [Lane A: β-galactosidase expression in *E. coli*; Lane B: β-galactosidase expression in *ex vivo* human skin; M: Molecular marker].

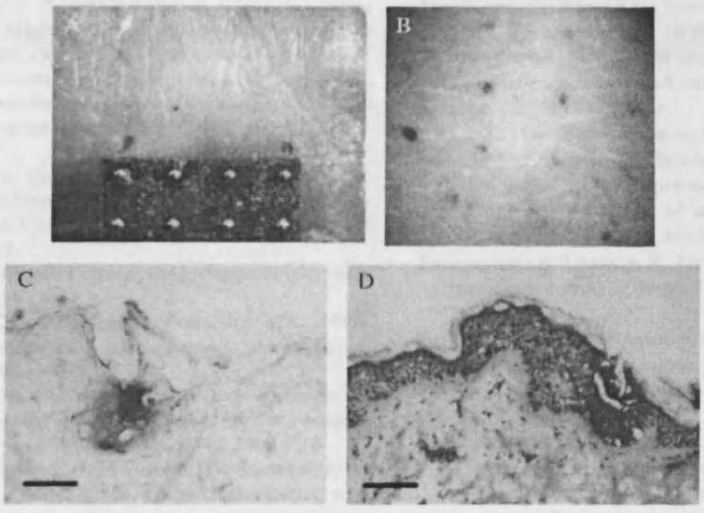

Figure 6. (A) *En face* image of β-galactosidase stained microchannels; the microneedle array providing a visual reference; (B) *En face* image of β-galactosidase stained microchannels with NFR counterstaining; (C) Unstained cryosection of β-galactosidase stained microchannel. Bar = 100 μm; (D) H&E stained cryosection of β-galactosidase stained microchannel. Bar = 100 μm.

skin strata was established by transversely sectioning the positively stained microchannels. Photomicrographs of 12 μm cryosections are presented in Figure 6C and D. Microchannels created in skin following application of the pyramidal microneedles appeared as 150 μm depth interruptions of the SC and epidermis. Figure 6C shows the intense level of reporter gene expression in cells proximal to the base of the microneedle channel. Haematoxylin and eosin staining of the sections revealed that the gene expression was restricted to the viable epidermal cells (Figure 6D).

During our studies, we observed that the extent of gene expression was unpredictable and somewhat difficult to control. However, we also observed that gene expression was more prevalent using microneedles with flattened as opposed to sharp points. We have tentatively attributed this to the likelihood that cells are more likely to suffer some limited damage to their cell membrane when perturbed by the insertion of the flattened microneedles, when compared to sharper microneedles. We suggest that such minor membrane damage may increase pDNA uptake and subsequently lead to enhanced gene expression efficiency. We are currently investigating this hypothesis in our laboratory.

Conclusions

The advantages of using microneedles as opposed to alternative physical trans-cutaneous drug delivery methodologies including biolistic particle bombardment (Kendall et al. 2004), jet injection (Sawamura et al. 1999), microscission (Herndon et al. 2004), tape stripping (Tregear and Dirnhuber 1962) and laser ablation (Lee et al. 2002) include: (i) direct and controlled delivery of the medicament; (ii) rapid exposure of large surface areas of skin to the delivery agents (microneedle arrays can be fabricated to contain over 1000 microneedles); (iii) effortless, convenient and painless delivery for the patient; (iv) ability to manipulate the therapeutic formulation, e.g. solution, suspension, emulsion, dry powder, gel; (v) enhancement of concomitant delivery methods such as transdermal patches and (vi) minimally invasive methodology not requiring complex machinery at time of application suited to patient self-administration without the need for medical supervision. We have confirmed the ability of solid silicon pyramidal microneedles, prepared using a low cost wet-etch microfabrication process, to penetrate the SC and create microchannels within human skin to facilitate the intra-epidermal delivery of pDNA. Further, in testing these devices we have developed an *ex vivo* human skin model with retained cellular viability.

The perceived importance of gene-based therapies in medicine is driving the development of novel and radical methods for delivering macromolecular drugs such as DNA. A combination of this innovative gene delivery system and the skin organ culture model can be further exploited to optimise cutaneous DNA delivery for clinical applications and importantly, can be used to answer more fundamental questions concerning the expression of genes in viable skin layers.

References

Ahmad W, Faiyaz ul Haque M, Brancolini V, Tsou HC, ul Haque S, Lam H, Aita VM, Owen J, deBlaquiere M, Frank J, et al. 1998. Alopecia universalis associated with a mutation in the human hairless gene. Science 279:720–724.

Chabri F, Bouris K, Jones T, Barrow D, Hann A, Allender C, Brain K, Birchall J. 2004. Microfabricated silicon microneedles for nonviral cutaneous gene delivery. Br J Dermatol 150:869–877.

Cormier M, Johnson B, Ameri M, Nyam K, Libiran L, Zhang DD, Daddona P. 2004. Transdermal delivery of desmopressin using a coated microneedle array patch system. J Control Release 97:503–511.

Fynan EF, Webster RG, Fuller DH, Haynes JR, Santoro JC, Robinson HL. 1993. DNA vaccines: Protective immunization by parenteral, mucosal and gene innoculation. Proc Nat Acad Sci USA 90:11478–11482.

Hart IR, Vile RG. 1994. Targeted therapy for malignant melanoma. Curr Opin Oncol 6:221–225.

Henry S, McAllister DV, Allen MG, Prausnitz MR. 1998. Microfabricated microneedles: A novel approach to transdermal drug delivery. J Pharm Sci 87:922–925.

Herndon TO, Gonzalez S, Gowrishankar TR, Rox Anderson R, Weaver JC. 2004. Transdermal microconduits by microscission for drug delivery and sample acquisition. BMC Med 2:12.

Kaushik S, Hord AH, Denson DD, McAllister DV, Smitra S, Allen MG, Prausnitz MR. 2001. Lack of pain associated with microfabricated microneedles. Anesth Analg 92:502–504.

Kendall M, Mitchell T, Wrighton-Smith P. 2004. Intradermal ballistic delivery of micro-particles into excised human skin for pharmaceutical applications. J Biomech 37:1733–1741.

Lee WR, Shen SC, Wang KH, Hu CH, Fang JY. 2002. The effect of laser treatment on skin to enhance and control transdermal delivery of 5-fluoruracil. J Pharm Sci 91:1613–1626.

Li L, Hoffman RM. 1995. The feasibility of targeted selective gene therapy of the hair follicle. Nat Med 1:705–706.

Lin MTS, Pulkkinen L, Uitto J. 2000. Cutaneous gene therapy: Principles and prospects. Dermatol Clin 18:177–188.

Martanto W, Davis SP, Holiday NR, Wang J, Gill HS, Prausnitz MR. 2004. Transdermal delivery of insulin using microneedles *in vivo*. Pharm Res 21:947–952.

Matriano JA, Cormier M, Johnson J, Young WA, Buttery M, Nyam K, Daddona PE. 2002. Macroflux® microprojection array patch technology: A new and efficient approach for intracutaneous immunization. Pharm Res 19:63–70.

McAllister DV, Wang PM, Davis SP, Park JH, Canatella PJ, Allen MG, Prausnitz MR. 2003. Microfabricated needles for transdermal delivery of macromolecules and nanoparticles: Fabrication methods and transport studies. Proc Nat Acad Sci USA 100:13755–13760.

Menter A. 1998. Pathogenesis and genetics of psoriasis. Cutis 61:8–10.

Mikszta JA, Alarcon JB, Brittingham JM, Sutter DE, Pettis RJ, Harvey NG. 2002. Improved genetic immunization via micromechanical disruption of skin-barrier function and targeted epidermal delivery. Nat Med 8:415–419.

Panchagnula R, Stemmer K, Ritschel WA. 1997. Animal models for transdermal drug delivery. Methods Find Exp Clin Pharmacol 19:335–341.

Park JH, Allen MG, Prausnitz MR. 2005. Biodegradable polymer microneedles: Fabrication, mechanics and transdermal drug delivery. J Control Release 104:51–66.

Raz E, Carson DA, Parker SE, Parr TB, Abai AM, Aichinger G, Gromkowski SH, Singh M, Lew D, Yankauckas MA, et al. 1994. Intradermal gene immunization: The possible role of DNA uptake in the induction of cellular immunity to viruses. Proc Nat Acad Sci USA 91:9519–9523.

Sawamura D, Ina S, Itai K, Meng X, Kon A, Tamai K, Hanada K, Hashimoto I. 1999. *In vivo* gene introduction into keratinocytes using jet injection. Gene Ther 6:1785–1787.

Shi Z, Curiel DT, Tang DC. 1999. DNA-based non-invasive vaccination onto the skin. Vaccine 17:2136–2141.

Sivamani RK, Stoeber B, Wu GC, Zhai H, Liepmann D, Maibach H. 2005. Clinical microneedle injection of methyl nicotinate: Stratum corneum penetration. Skin Res Technol 11:152–156.

Tregear RT, Dirnhuber P. 1962. The mass of keratin removed from the stratum corneum by stripping with adhesive tape. J Investig Dermatol 38:375–381.

Uitto J, Pulkkinen L. 2000. The genodermatoses: Candidate diseases for gene therapy. Hum gene ther 11:2267–2275.

Wilke N, Mulcahy A, Ye SR, Morrissey A, Process optimization and characterization of silicon microneedles fabricated by wet etch technology. Microelectronics J (in press).

Appendix III

(Experimental data)

Appendix

Linear Regression Y = mx +b

m	4.881E3
b	-5.987E2
r	0.999953

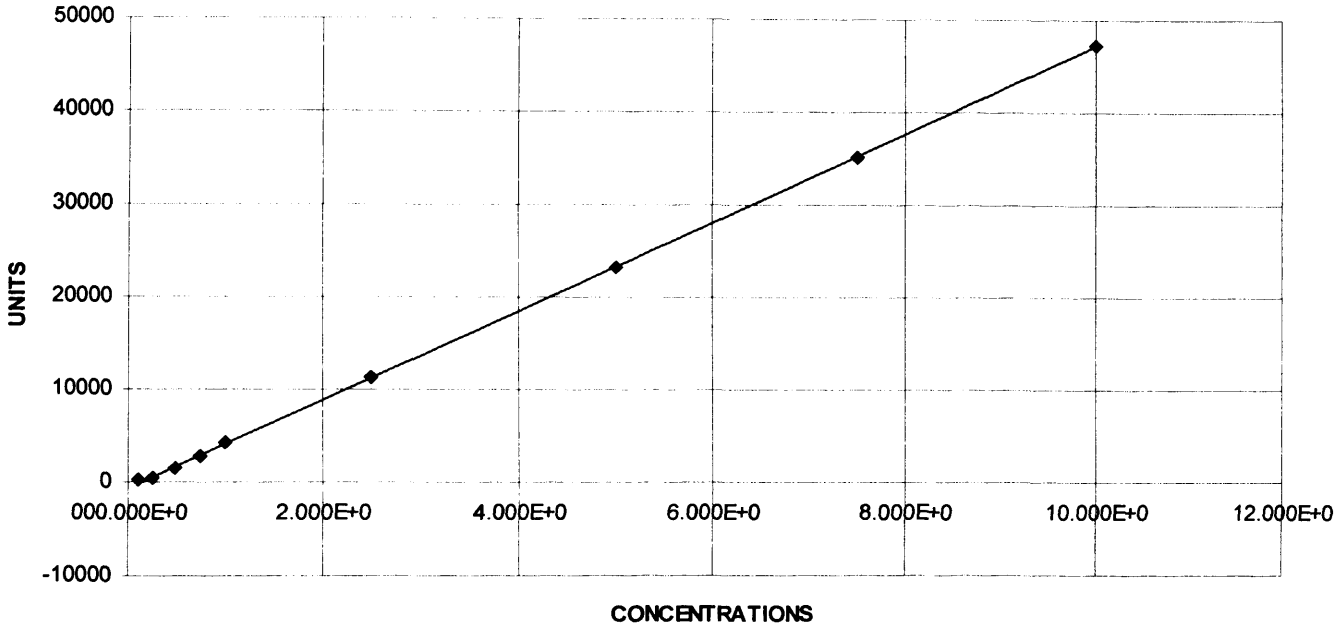

Standard curve for diffusion study involving fluorescent nanospheres

Appendix

Franz diffusion cell number	Cell Volume (ml)	Cell Area (cm2)
1	3.27	1.46
2	3.23	1.39
3	3.17	1.17
4	3.21	1.50
5	3.23	1.21
6	3.34	1.21
7	3.32	1.41
8	3.31	1.48
9	3.33	1.44
10	3.21	1.37
11	3.26	1.44
12	3.33	1.28
13	3.19	1.14
14	3.22	1.24
15	3.14	1.12

The cell volume and diffusive surface area of the Franz diffusion cells used during the course of these investigations.